

**STRIKE-SLIP FAULTING AND RESERVOIR DEVELOPMENT  
IN NEW YORK STATE**

**Task 4. Final Report**

Prepared for

**THE NEW YORK STATE  
ENERGY RESEARCH AND DEVELOPMENT AUTHORITY**

Albany, NY

Prepared by

**JAN C. RASMUSSEN**

Project Manager  
Jan Rasmussen Consulting

and

**STANLEY B. KEITH**

**MONTE M. SWAN**  
MagmaChem, L.L.C.

and

**DANIEL P. LAUX**

South Branch Resources

and

**JOHN CAPRARA**

EarthTechnics, Inc.

Contract Agreement No. 6984

## **NOTICE**

This report was prepared by Jan C. Rasmussen of Jan Rasmussen Consulting, Stanley B. Keith, Monte M. Swan and Daniel P. Laux of MagmaChem LLC, and John Caprara of EarthTechnics Inc. in the course of performing work contracted for and sponsored by the New York State Energy Research and Development Authority (hereafter “NYSERDA”). The opinions expressed in this report do not necessarily reflect those of NYSERDA or the State of New York, and reference to any specific product, service, process, or method does not constitute an implied or expressed recommendation or endorsement of it. Further, NYSERDA, the State of New York, and the contractor make no warranties or representations, expressed or implied, as to the fitness for particular purpose or merchantability of any product, apparatus, or service, or the usefulness, completeness, or accuracy of any processes, methods, or other information contained, described, disclosed, or referred to in this report. NYSERDA, the State of New York, and the contractor make no representation that the use of any product, apparatus, process, method, or other information will not infringe privately owned rights and will assume no liability for any loss, injury, or damage resulting from, or occurring in connection with, the use of information contained, described, disclosed, or referred to in this report.

## ABSTRACT

This study of tectonics and reservoir development at and near Glodes Corner, New York, has led to the development of an integrative hydrothermal dolomite (HTD) gas exploration model that not only has the potential to define gas or oil accumulations, but also may define important internal conduit features that are related to the hydrocarbon charge. The Glodes Corner field is characterized by a seismically defined sag structure that reflects a collapse feature associated with the formation of HTD at the Trenton-Black River level that is some 8,000 feet below the surface. Soil geochemistry interpreted according to this new fluid fractionation and shear-system kinematic model identifies well-developed, east-to-west asymmetrical patterns in redox potential ( $\text{CO}_2\text{:O}_2$  and ferrous:ferric ratios) and the distribution and compositional mixtures of hydrocarbon gases and a variety of trace metals.

**Zonal patterns identified within the field conform to an inferred reaction sequence that follows two earlier stages. Stage 1 is generation of methane/hydrocarbon-stable, metagenic fluids formed by serpentinization of peridotite in intracratonic failed rifts or collisional sutures in the basement as triggered by compressive, convergent orogenesis. Stage 2 is initial, low temperature, ‘passive’ dolomitization of the first replaceable, typically shelf carbonate in the overlying cratonic cover sequence. The following paragenetic stages occur at the reservoir site: Stage 3A (early saddle dolomitization at or near the depositional site), Stage 3B (late saddle dolomitization, anhydrite formation, carbon dioxide effervescence, hydrogen loss and methane unmixing), Stage 4 (sulfide and hydrocarbon deposition), and Stage 5 (deposition of late calcite at the depositional site and illite/smectite/kaolinite clays in and marginal to the depositional site).**

This paragenetic reaction series is the predicted fractionation pattern developed from an initially reduced, high-temperature fluid evolving toward a more oxidized, lower-temperature fluid. The within-reservoir, conduit architecture of permeability and dolomite permeability plugging can be identified by interpretation of hydrocarbon gas distribution ( $\text{C}_1\text{-C}_2$  high in conduits) and trace metal distribution (elevated along with  $\text{C}_5$  and  $\text{C}_6$  hydrocarbons away from the conduits). By integrating soil gas geochemistry, fluid fractionation, and shear-system kinematics, it may be possible to precisely detect permeable conduits inside the resolution from seismic imaging. This model has significant exploration implications for the geochemical identification of hydrocarbon-charged reservoirs where combined structural and stratigraphic features have produced geochemically zoned, three-dimensional geographic patterns during emplacement of the hydrocarbon charge.

The Glodes Corner field is located in the northeasternmost part of Steuben County in south-central New

York. Glodes Corner is the largest of a cluster of gas fields hosted in hydrothermal dolomites that have replaced shelf limestones in the Upper Ordovician Trenton-Black River Groups beneath south-central New York. Glodes Corner has sufficient hydrocarbons to be ranked as a 'significant' gas field in the U.S. Geological Survey classification. The field itself occurs beneath a seismically defined sag feature that is expressed at the current topographic surface as an east-northeast-striking synclinal fold in Devonian strata within the Catskill delta wedge. The Catskill wedge is the main sedimentological feature of the Acadian Orogeny of Devonian age and formed in its foreland.

During the Acadian Orogeny (350-400 Ma), large-scale, basement-derived, possibly hydrocarbon-stable, hydrothermal fluids are thought to have been derived from a serpentinized peridotite source in the Cambrian-age rift system beneath central Steuben County, New York. The inferred serpentine source is consistent with a prominent magnetic feature (resulting from magnetite formed during serpentinization) that coincides with a conspicuous gravity low in the middle of the magnetic high (resulting from low density serpentine). Serpentinization of the inferred peridotite is thought to have accompanied greenschist grade (~300°C at 5-8 km depth) metamorphism and the rift basement during the peak Acadian metamorphic event at about 360-375 Ma.

Hydrothermal fluids originating from the inferred peridotitic source are thought to have utilized a conduit system consisting of interconnected northwest- and northeast- to east-northeast-striking faults to travel from the serpentinized source to the Trenton-Black River shelf carbonate cover sequence. At Glodes Corner, potentially hydrocarbon-stable, hydrothermal, low-pH, carbonated alkali brines are thought to have laterally and vertically ascended along a N50W-striking feeder-conduit. Both vitrinite reflectance and conodont alteration index data indicate that the deep gas cluster in south-central New York could have formed in the uppermost part of or even above the thermogenic gas window, which is 200 to 300°C.

At Glodes Corner, the fluids migrated westward into an incipient riedel/tensile structural trap in highly reactive and replaceable calcitic limestones of the Trenton-Black River cratonic shelf cover. East-to-west flow is consistent with a gradual west-tapering within the field, which is about 5 km long in an east-west direction. The structural setting predicted an east-to-west chemical fractionation. A chemical zonation pattern resulted from fractionation of fluids that deposited a high-temperature, reduced chemical assemblage at the east end and deposited lower temperature, more oxidized distillates at its western end near the tip of the inferred fluid/alteration wedge. In particular, the zonal patterns at Glodes Corner strongly conform to the portion of the reaction sequence covered by stages 3A (early saddle dolomitization at and near depositional site) and 3B (late saddle dolomitization, anhydrite formation, carbon dioxide effervescence, hydrogen loss and methane unmixing), stage 4 (sulfide deposition and hydrocarbon



deposition), and stage 5 (deposition of late calcite at depositional site and illite/smectite/kaolinite clays in and marginal to depositional site).

Subsequent to the emplacement of the gas-bearing hydrothermal deposit, south-central New York was affected by the north-northwest – south-southeast shortening associated with the Alleghenian orogeny at about 260 to 300 Ma. At this time, the reservoir and the overlying Catskill sedimentary wedge were deformed around east-northeast – west-southwest-trending, broad, fold warps in the northern part of the Alleghenian fold-thrust deformational fan in the Pennsylvanian embayment/salient. Location of the fold features may have, in part, been controlled by the antecedent, Acadian-produced, riedel/tensile, graben/sag features, such as that at Glodes Corner.

Fluid migration patterns in strike-slip settings hosting hydrothermal metalliferous system (Carlin-type gold deposits) are analogous to hydrocarbon migration patterns, particularly in hydrothermal dolomite settings. Faults are not merely passive conduits and seals that statically receive and trap fluid sometime after their formation. Rather, fluid formation, movement, and deposition within any fault system characterize an active process that co-dynamically conjoins fault kinematics with fluid generation, flow, and deposition.

Porphyry metal deposit analogs (Carlin/North Trend of Nevada) indicate a synkinematic relationship between strike-slip fault movements, the emplacement of pluton gold sources, and the release of gold-bearing fluids into riedel/tensile splays and/or wedge-like stratigraphic traps. The most economic traps involve the intersection of favorable stratigraphy with the footwall of P-shear conduits. Where this stratigraphy is blocked in its updip portions by other faults that mark changes in dip domain or juxtapositions with unfavorable stratigraphy, a wedge-like ‘trap’ can be associated with especially high grade gold accumulations (e.g., Meikle mine). The fluid migration path is identified through geochemistry. As fluids migrate from a high pressure source to low pressure deposition sites, they fractionate, resulting in a systematic paragenetic chemical dispersal sequence. Increase in oxidation state during the process is a first order control on the fractionation.

Similar strike-slip configurations trap accumulations of petroleum in strike-slip fault environments (Jonas and Cave Creek gas fields in Wyoming and Glodes Corner, Steuben County, New York). In both mineral deposit and petroleum systems, the paths of the economic fluids utilized a curved trajectory in moving from the P-shear conduit to the stratigraphic wedge. This curved trajectory appears to be characteristic of fluid migration in both porphyry metal and petroleum accumulations related to wrench-fault tectonism.

Recent geochemical data from Glodes Corner, New York, may define fluid migration pathways that are analogous to the fluid migration pathways in Carlin gold systems. Carbon geochemistry fractionates from west to east along the riedel/tensile conduit. This fluid pathway is inferred from the presence of a more H-rich, reduced assemblage of higher  $\text{CO}_2/\text{O}_2$  ratios, C-1 to C-4 gases on the east (near the intersection with an inferred northwest-trending 'feeder' structure) to a more oxidized, H-poor environment on the west, characterized by and assemblage of higher C-number gases (especially C-5 and C-6) and more oxidized, O-rich assemblage characterized by lower  $\text{CO}_2/\text{O}_2$  ratios on the west. The inferred feeder structure appears to have been undergoing active, left-slip kinematics at the time of the gas introduction, which is inferred to have entered the hydrothermal dolomite reservoir in the underlying Trenton/Black River section from the southeast. Fluid movement and its fractionation are necessary products of interactively coordinated kinematics within the strike-slip fault system and, more importantly, specifically predict economic targets.

## Table of Contents

1. INTRODUCTION .....	1 - 1
PURPOSE AND SCOPE OF WORK.....	1 - 1
DATA COLLECTION .....	1 - 1
DATA INTEGRATION .....	1 - 2
GEOCHEMICAL VALIDATION .....	1 - 3
2. SADDLE DOLOMITES AND FLUID MIGRATION .....	2 - 3
HISTORICAL SADDLE DOLOMITE MODELS .....	2 - 3
<u>Saddle Dolomite Formation and Petroleum</u> .....	<u>2 - 3</u>
<u>Structures and Saddle Dolomite</u> .....	<u>2 - 3</u>
<u>Chemistry and Saddle Dolomite</u> .....	<u>2 - 4</u>
<u>Timing of Saddle Dolomite Formation</u> .....	<u>2 - 5</u>
HYDROTHERMAL DOLOMITE AND MISSISSIPPI VALLEY TYPE (MVT) ORE DEPOSITS .....	2 - 5
<u>Structures and MVT ore deposits</u> .....	<u>2 - 6</u>
<u>Chemistry of MVT ore deposits</u> .....	<u>2 - 6</u>
<u>Timing of MVT ore deposits</u> .....	<u>2 - 7</u>
HYDROTHERMAL DOLOMITE, PETROLEUM, AND MVT ORE DEPOSITS.....	2 - 7
<u>Common Model for Hydrothermal Saddle Dolomite and Petroleum and MVT Zinc-Lead Deposits</u> .....	<u>2 - 7</u>
3. REGIONAL GEOTECTONIC MODEL AND FLUID FLOW.....	3 - 1
GENERAL CONCEPTS OF GEOTECTONICS AND FLUID FLOW .....	3 - 1
<u>Fluid Flow in Strike-Slip Fault Settings</u> .....	<u>3 - 1</u>
<u>Porphyry Metal Fluid Flow</u> .....	<u>3 - 1</u>
<u>Hydrothermal Oil and Gas Fluid Flow</u> .....	<u>3 - 12</u>
<u>Dynamic Interpretation</u> .....	<u>3 - 12</u>
<u>Application to Wrench Fault Settings in New York State</u> .....	<u>3 - 15</u>
<u>Relationship to Hydrothermal Dolomite Model and Continental Basement Structure</u>	<u>3 - 22</u>
4. MODEL OF THE SOURCE, NATURE, AND MIGRATION OF HYDROTHERMAL PETROLEUM FLUIDS ...	4 - 1
CHEMISTRY OF HYDROTHERMAL DOLOMITE GAS MODEL .....	4 - 1
INTEGRATIVE MODEL FOR GENERATION, MIGRATION, AND DEPOSITION OF PETROLEUM FLUIDS .....	4 - 3
<u>Conceptual contrasts with existing models</u> .....	<u>4 - 3</u>
<u>Hydrothermal dolomite model design</u> .....	<u>4 - 4</u>
<u>Stage 1. Generation of Fluids in Peridotitic Basement Source Region</u> .....	<u>4 - 5</u>

<u>Fluid Source</u> .....	4 - 5
<u>Geophysical signatures of possible peridotitic basement sources</u> .....	4 - 6
<u>Stage 1 to Stage 2 Fluid Migration from Source to Trap</u> .....	4 - 6
<u>An example from the Northern Appalachian Basin</u> .....	4 - 7
<u>Evidence for Taconic timing (450-420 Ma)</u> .....	4 - 7
<u>Evidence for Acadian timing (400-350 Ma)</u> .....	4 - 8
<u>Evidence for Alleghenian timing (320-260 Ma)</u> .....	4 - 12
<u>Evidence for Mesozoic timing</u> .....	4 - 16
<u>Tectonic trigger for migration</u> .....	4 - 16
<u>Tectonic driver for migration</u> .....	4 - 17
<u>Conduit architecture</u> .....	4 - 17
<u>Constraints imposed by crustal oxidation state</u> .....	4 - 17
<u>Stage 2. Initial Dolomitization (Sucrosic) of Shelf Limestone Near Depositional Site4 - 18</u>	
<u>General considerations</u> .....	4 - 18
<u>Initial sucrosic dolomitization</u> .....	4 - 18
<u>Isotopic mixing</u> .....	4 - 22
<u>Stage 3. Early and Late Saddle Dolomite Formation At and Near Depositional Site4 - 24</u>	
<u>Stage 4. Sulfide Deposition and Hydrocarbons Development</u> .....	4 - 24
<u>Stage 5. Deposition of Late Calcite at Depositional Site and Illite/Smectite/Kaolinite Clays At and Near Depositional Site</u> .....	4 - 24
<b>5. EXPLORATION IMPLICATIONS AND APPLICATIONS OF STRIKE-SLIP FAULT KINEMATICS AND HYDROTHERMAL PETROLEUM FLUID CHEMISTRY</b> .....	5 - 1
<b>STAGE 1 - SOURCE – STAGE 1 SERPENTINIZATION OF MAFIC OCEANIC CRUSTAL MATERIAL UNDER REDUCED CONDITIONS</b> .....	5 - 1
<u>Tectonic Setting and Drivers of Stage 1 - Source</u> .....	5 - 1
<u>Geophysical Features of Stage 1 - Source</u> .....	5 - 1
<b>STAGE 1 TO 2 – MIGRATION – STAGE 1 TO STAGE 2 FLUID MIGRATION FROM SOURCE TO TRAP</b> .....	5 - 2
<u>Tectonic Setting and Drivers of Stage 1 to 2 - Migration</u> .....	5 - 2
<u>Conduit System of Stage 1 to 2 - Migration</u> .....	5 - 2
<u>Geophysical Features of Stage 1 to 2 - Migration</u> .....	5 - 3
<u>Tectonic Setting of Stage 2 - Sucrosic Dolomitization</u> .....	5 - 3
<u>Chemical Features of Stage 2 - Sucrosic Dolomitization</u> .....	5 - 4
<b>STAGE 3 - TRAP – STAGE 3A “HIGH” TEMPERATURE FERROAN HYDROTHERMAL DOLOMITIZATION IN IMMEDIATE VICINITY OF RIEDEL-TENSILE STRUCTURAL TRAPS OR REVERSE</b>	

FAULT/ANTICLINAL STRUCTURAL TRAPS.....	5 - 4
<u>Tectonic Setting of Stage 3A - Hydrothermal Dolomite (HTD)</u> .....	<u>5 - 4</u>
<u>Chemical Features of Stage 3A - Hydrothermal Dolomite (HTD)</u> .....	<u>5 - 5</u>
<u>Geophysical Features of Stage 3A - Hydrothermal Dolomite (HTD)</u> .....	<u>5 - 5</u>
STAGE 3B - TRAP – CARBON DIOXIDE EFFERVESCENCE AND ANHYDRITE FORMATION IN THE RIEDEL-TENSILE TRAP SITE. ....	5 - 6
<u>Tectonic Setting of Stage 3B - CO<sub>2</sub>-Anhydrite Formation</u> .....	<u>5 - 6</u>
<u>Chemical Features of Stage 3B - CO<sub>2</sub>-Anhydrite Formation</u> .....	<u>5 - 6</u>
STAGE 4 - TRAP - SULFIDE DEPOSITION AND HIGHER RANK HYDROTHERMAL PETROLEUM PRODUCTION.....	5 - 6
<u>Tectonic Setting and Structural Features of Stage 4 - Sulfide and Petroleum Production</u> .....	<u>5 - 6</u>
<u>Chemical Features of Stage 4 - Sulfide and Petroleum Production</u> .....	<u>5 - 7</u>
STAGE 5 - TRAP – LATE DISTAL CALCITE-CLAY-FELDSPAR-HIGH C-NUMBER HYDROCARBON FORMATION.....	5 - 7
<u>Tectonic Setting and Structural Features of Stage 5 - Late Distal Calcite-Clay- Feldspar-Hydrocarbon Formation</u> .....	<u>5 - 7</u>
<u>Chemical Features of Stage 5 - Late Distal Calcite-Clay-Feldspar-Hydrocarbon Formation</u> .....	<u>5 - 8</u>
6. APPLICATION TO GAS POTENTIAL IN NEW YORK.....	6 - 1
STAGE 1 - SOURCE(S) IN AND NEAR NEW YORK.....	6 - 1
<u>Regional Sources in the Appalachian Basin</u> .....	<u>6 - 1</u>
<u>Steuben County Sources</u> .....	<u>6 - 3</u>
<u>Cambrian Rift System and Overmatured Cover Rocks in New York</u> .....	<u>6 - 4</u>
<u>Possible Composition of the Peridotitic Source Rocks in the Rome Trough</u> .....	<u>6 - 6</u>
<u>Overmatured Cover Rocks and Timing of Fluid Migration in New York</u> .....	<u>6 - 6</u>
STAGE 1 TO 2 – MIGRATION – STAGE 1 TO STAGE 2 FLUID MIGRATION FROM SOURCE TO TRAP IN NEW YORK.....	6 - 8
<u>Introduction</u> .....	<u>6 - 8</u>
<u>Stage 1 to Stage 2 Conduit System in southern New York</u> .....	<u>6 - 9</u>
<u>Northwest-striking structural elements in New York</u> .....	<u>6 - 9</u>
<u>Northeast-striking structural elements in New York</u> .....	<u>6 - 11</u>
<u>West-northwest-striking structural elements in New York</u> .....	<u>6 - 11</u>
<u>Possible Reservoirs Between the Peridotite Source and the Trenton-Black River Horizon</u> .....	<u>6 - 12</u>

STAGE 3 TO STAGE 5 - TRAP – “HIGH” TEMPERATURE FERROAN HYDROTHERMAL DOLOMITIZATION, ANHYDRITE AND SULFIDE DEPOSITION, AND ABIOGENIC HYDROCARBON GENERATION IN THE TRAP SITE .....	6 - 14
<u>Application to the Glodes Corner HTD Gas Deposit in Steuben County, New York.</u>	<u>6 - 14</u>
<u>Geographic patterns of the geochemical data</u> .....	<u>6 - 15</u>
<u>Oxidation state zonation</u> .....	<u>6 - 15</u>
<u>Metal Zonation</u> .....	<u>6 - 15</u>
<u>Hydrocarbon Gas Zonation</u> .....	<u>6 - 16</u>
<u>Integration with Hydrothermal Dolomite (HTD) Hydrocarbon Conceptual Model</u> .....	<u>6 - 17</u>
<u>Electro-chemical processes for vertical transfer of the geochemical signature of the underlying resource to the surface</u> .....	<u>6 - 18</u>
<u>Physical processes for vertical transfer of the geochemical signature of the underlying resource to the surface</u> .....	<u>6 - 19</u>
<u>Economic implications</u> .....	<u>6 - 20</u>
<u>Summary of the Glodes Corner geochemistry</u> .....	<u>6 - 21</u>
<u>Stage 6. Possible ascension of HTD fluid plumes and deposition of gas in sandstones at higher stratigraphic levels.</u> .....	<u>6 - 22</u>
7. REFERENCE LIST .....	7 - 1
APPENDIX A: MAGMA-METAL SERIES MODELS USED IN THIS REPORT .....	1 - 1







## List of Figures

Figure 3.1. Fluid flow model for Carlin-type gold deposits.....	3 - 2
Figure 3.2. Model for multi-staged Porgera-Goldstrike type gold porphyry system. ....	3 - 3
Figure 3.3. Metal dispersion/fractionation at the Meikle mine, Carlin/North Trend, Nevada. ....	3 - 5
Figure 3.4. Schematic, stepped evolution of rock and metalliferous fluid phases in an oxidized iron-titanium-poor (hydrous), calc-alkalic, metaluminous magma series (MCA14C).....	3 - 6
Figure 3.5. Staged magma-metal fluid systems for meso-epizonal oxidized (magnetite-sphene stable) hydrous (hornblende-bearing, calc-alkalic, metaluminous magma series (MCA14M, Stage 2; MCA14C, Stage 3; MCA14J, Stage 4).....	3 - 7
Figure 3.6. Generalized differentiation hook sequence for hornblende-stable porphyry metal series. ....	3 - 8
Figure 3.7. Stress-strain diagram and four possible magmatic fluid flow (differentiation) paths. ....	3 - 9
Figure 3.8. Jurassic-Cretaceous magma-hydrothermal fluid flow in the North Carlin Trend deep ‘crack’ strike-slip fault systems. ....	3 - 10
Figure 3.9. Eocene magma- hydrothermal fluid flow in the North Carlin Trend deep ‘crack’ strike-slip fault systems. ....	3 - 11
Figure 3.10. Hydrocarbon plume fractionation in deep-seated strike-slip fault settings. ....	3 - 14
Figure 3.11. Structural interpretation of the Finger Lakes region of central New York. ....	3 - 16
Figure 3.12. CO <sub>2</sub> /O <sub>2</sub> ratios in soil gas chemistry in the Glodes Corner field, Steuben County, south central New York (from Jim Viellenave, Direct Geochemical).....	3 - 18
Figure 3.13. nPentane content (in ppbv) in soil gas chemistry in the Glodes Corner field, Steuben County, south central New York (from Jim Viellenave, Direct Geochemical). ....	3 - 19
Figure 3.14. Hexane content (in ppbv) in soil gas chemistry in the Glodes Corner field, Steuben County, south central New York (from Jim Viellenave, Direct Geochemical). ....	3 - 20
Figure 3.15. Trenton gas probability values in soil gas chemistry in the Glodes Corner field, Steuben County, south central New York (cumulative production in million cf in parentheses) (from Jim Viellenave, Direct Geochemical). ....	3 - 21
Figure 3.16. Model for metagenic fluid generation, migration, and deposition of hydrothermal dolomite, metals (Cu, Ag, Pb, Zn), and petroleum during convergent orogenic thickening episodes (see Appendix A for key to magma-metal series models).....	3 - 23
Figure 3.17. Oil and gas fields, MVT mineral deposits, and 1400 Ma transcurrent basement faults of the eastern U.S. ....	3 - 24

Figure 6.1. Map showing distribution of CO <sub>2</sub> /O <sub>2</sub> X 100 in soils. ....	6 - 24
Figure 6.2. Map showing distribution of percent ferrous iron in soils. ....	6 - 25
Figure 6.3. Map showing distribution of sodium in soils. ....	6 - 26
Figure 6.4. Map showing distribution of arsenic in soils. ....	6 - 27
Figures 6.5. Map showing distribution of zinc in soils. ....	6 - 28
Figure 6.6. Map showing distribution of potassium in soils. ....	6 - 29
Figure 6.7. Map showing distribution of vanadium in soils. ....	6 - 30
Figure 6.8. Northing versus zinc in soil for PIZ profile. ....	6 - 31
Figure 6.9. Northing versus nickel in soil for PIZ profile. ....	6 - 32
Figure 6.10. Northing versus potassium in soil for PIZ profile. ....	6 - 33
Figure 6.11. Northing versus magnesium in soil for PIZ profile. ....	6 - 34
Figure 6.12. Northing versus vanadium in soil for PIZ profile. ....	6 - 35
Figure 6.13. Northing versus ferric iron (Fe <sup>+3</sup> ) in soil for PIZ profile. ....	6 - 36
Figure 6.14. Northing versus ferric/ferrous ratio in soils for PIZ profile. ....	6 - 37
Figure 6.15. Northing versus methane in soils for PIZ profile. ....	6 - 38
Figure 6.16. Northing versus ethane in soils for PIZ profile. ....	6 - 39
Figure 6.17. Northing versus propane in soils for PIZ profile. ....	6 - 40
Figure 6.18. Northing versus nButane in soils for PIZ profile. ....	6 - 41
Figure 6.19. Northing versus iPentane in soil for PIZ profile. ....	6 - 42
Figure 6.20. Northing versus nPentane in soil for PIZ profile. ....	6 - 43
Figure 6.21. Northing versus iHexane in soil for PIZ profile. ....	6 - 44
Figure 6.22. Northing versus nHexane in soil for PIZ profile. ....	6 - 45
Figure 6.23. Map showing interpreted conduits and paragenetic stages of HTD conceptual model. ....	6 - 46
Figure 6.24. Northing versus total gases (C1+) in soils for PIZ profile. ....	6 - 47

**List of Tables**

Table 4.1. Alleghenian-age radiometric dates for MVT deposits in the central U.S. ....	4 - 13
Table 4.2. Isotope mixing calculation. ....	4 - 23

**List of Appendices**

Appendix A: Magma-Metal Series Models Used in This Report .....	1 - 1
---	-------

**List of Plates**

- Plate 1. Structural Interpretation of the Finger Lakes region .....In pocket
- Plate 2. Oil and Gas Fields, MVT Mineral Deposits, and 1400 Ma Transcurrent Basement Faults of the Eastern U.S. . ....In pocket
- Plate 3. Model for Metagenic Fluid Generation, Migration, and Deposition of Hydrothermal Dolomite, Metals (Cu, Ag; Pb, Zn), and Petroleum During Convergent Orogenic Thickening Episodes .....In pocket

**STRIKE-SLIP FAULTING AND RESERVOIR DEVELOPMENT  
IN NEW YORK STATE: FINAL REPORT**

**1. INTRODUCTION**

**PURPOSE AND SCOPE OF WORK**

The purpose of this study was to integrate new exploration technologies developed in the minerals industry and apply them to gas exploration in New York. The goal has been to better define the relationship between strike-slip faulting and reservoir development. The project has focused on the source, nature and migration of petroleum fluids related to hydrothermal saddle dolomites. Another purpose was to establish criteria to differentiate prospective seismically-defined faults from those that are not prospective. The final result is a model synthesizing strike-slip fault kinematics and hydrothermal petroleum fluid chemistry and movement and a synthesis of the information into an interpretation of natural gas potential in New York.

The scope of work included project management (research meetings and interim report preparation), data collection (data survey, hydrothermal dolomite research, Mississippi Valley-type deposit research, and interim report preparation), data integration (data integration meeting and interim report preparation), digital map construction and preparation of the final report, and technology transfer (AAPG annual meeting poster session and IOGANY presentation).

**DATA COLLECTION**

Data collection was carried out at local libraries (University of Arizona, Arizona State University, and Rice University); these sources and the internet were accessed for information on hydrothermal dolomite and geology and oil and gas occurrences in New York State and related areas. GeoRef and other bibliographic data sources were searched for hydrothermal dolomite and New York geology, tectonics, age dates, petrology, ore deposits, and related subjects. Data were also gathered from our own company libraries and files for hydrothermal dolomite occurrences in New York, geology of New York, Mississippi Valley Type (MVT) ore deposits, and strike-slip faulting. In addition, Monte Swan made contact with Jim Viellenave of Direct Geochemical regarding the results of geochemical surveys over hydrothermal dolomite-hosted oil and gas fields in New York

State (specifically the Glodes Corner field).

Data sources, such as New York institutions and individuals, U.S. Geological Survey, and computerized geologic databases, were surveyed. Also, Stan Keith, Dan Laux, and John Caprara flew to Albany, NY, February 4, 2002 on a data-gathering trip. Between February 4 and 8, they obtained technical data and met with experts in the New York hydrothermal dolomite-hosted oil and gas play and New York geology. Conversations with John Martin, Taury Smith, Rich Nyahay, Phil Whitney, Bill Kelley, Marion Squaw, Chuck Verstratten, Gerald Friedman, Bob Fickes, and others provided useful information and interpretations related to the 'state of the art' of hydrothermal oil and gas in New York, as well as access to samples and field outcrops.

Hydrothermal dolomite occurrences in New York State and associated geology of the New York region were researched by John Caprara of EarthTechnics using his existing 'data mining' capabilities, including the licensed use of AAPG data pages search engines and a proprietary exploration play database. The hydrothermal dolomite occurrences and their known relationship to igneous activity and MVT mineralization were documented.

The general characteristics of Mississippi Valley Type (MVT) deposits and their relationship to the geology and tectonic history of New York were researched by Stanley B. Keith. Numerous books and references, as well as files in the MagmaChem data bases, were researched for their application to New York geology and tectonic history. The possible relationship between MVT mineralization and hydrothermal dolomite has been clearly established.

## **DATA INTEGRATION**

Data integration consisted of three subtasks. Subtask 3.1 was data integration, subtask 3.2 was the data integration meeting in mid-February in Sonoita, AZ, and subtask 3.3 was the preparation of the Task 3 interim report. During late February and March, the interim report was prepared to summarize our research into saddle-dolomite and its relationship with strike-slip faulting, a deep gas reservoir model, and the gas potential in parts of New York.

Subtask 3.1 included integration of the research, which consisted of the preparation of maps summarizing strike-slip faulting in New York and development of a deep gas model. Preliminary results of this data integration were presented at an AAPG poster session and are described below. The AAPG presentation is also considered to be part of the Technology Transfer of Subtask 5.1.

The entire group (Jan Rasmussen, Stanley Keith, Monte Swan, Daniel Laux, and John Caprara) assembled in the Jan Rasmussen Consulting and MagmaChem LLC offices in Sonoita, Arizona, in mid-February, 2002. During this 4 day meeting, the participants integrated and consolidated the various data acquired and reviewed the current scientific models in order to develop an integrated model. These conclusions integrated hydrothermal dolomite-hosted oil and gas occurrences with what appear to be orogenically driven, strike-slip fault networks in the foreland of the Appalachian orogenic belts, specifically the Taconic or Acadian orogens. This information was consolidated into several posters, which were presented at the annual meeting of the American Association of Petroleum Geologists in Houston, TX, March 10-13, 2002.

### **GEOCHEMICAL VALIDATION**

A particularly exciting aspect of this research was realized during the 4-day integration meeting when geochemical data was obtained from Jim Viellenave of Direct Geochemical, who coincidentally was working on a geochemical characterization (via soil hydrocarbon gas analyses) of the Glodes Corner field in New York, funded by NYSERDA. Not only does the soil gas data ‘see’ the overall gas reservoir that is some 7,000 feet below the surface, but the data also displayed a fractionation pattern that was consistent with the strike-slip kinematic model derived during our integration meeting. The combined geochemical-tectonic model was presented at the poster session entitled “Pathways of Hydrocarbon Migration, Faults as Conduits or Seals” at AAPG. Jim Viellenave graciously allowed us to use his geochemical data and participated as a co-author at the poster session. An expanded version of the poster session is presented below.

The geochemical results were extremely important in validating our hydrothermal gas model. Until we examined the geochemical results from Jim Viellenave, we had a provocative conceptual approach to deep hydrothermal oil and gas exploration in New York. However, the acquisition of the geochemical data and our observation of its fractionation patterns (which had been predicted by our conceptual tectonic model derived for exploration for the mineral industry) now give us a validated model.

The integration of these geochemical results not only verifies our conceptual model, but also provides a predictive, practical tool that can validate surface targets predicted by the conceptual tectonic analysis. Both of these concepts provide important, relatively inexpensive, initial exploration tools that should precede more expensive seismic and drill follow-ups of the predicted deep, hydrothermal gas targets. The combined structural and geochemical mapping from surface data indicate flow paths that predict the most favorable hydrothermal

oil and gas occurrences. This integrated structural and geochemical approach is similar to the fluid-flow modeling that we have used to successfully predict deep, hydrothermal gold deposits concealed beneath the upper plate in the Carlin - North Trend of north central Nevada.

We had not anticipated the availability of the geochemical data. Originally, we had planned to investigate the geochemical aspects of the model in a later project. However, integration of the Glodes Corner geochemical information has allowed us to greatly accelerate development of an integrated, practical, hydrothermal oil and gas exploration tool for New York State in particular, and for a more generic hydrothermal oil and gas model in general. Consequently, NYSERDA is the beneficiary of what is now a much more sophisticated, more predictive model than we had originally anticipated.

## 2. SADDLE DOLOMITES AND FLUID MIGRATION

### **HISTORICAL SADDLE DOLOMITE MODELS**

Within the broader framework of the classical petroleum model of source → fluid generation → reservoir development → transport → deposition (trap), we have focused on the so-called 'hydrothermal oil' phenomena, which is a challenge to explain through conventional oil and gas generation models. Observational data that constrain interpretation of hydrothermal oil phenomena correlate well with observational data for the well-known Mississippi Valley-type (MVT) lead-zinc deposits.

With respect to New York geology, the higher temperature sources for possible oil generation and migration are still poorly understood. However, an important observation is that the lower Paleozoic Ordovician through Silurian section in central and western New York is literally 'soaked' in oil and gas occurrences. The challenge is not where the oil came from, but rather is to determine the 'sweet spots' within this 'cloud' of petroleum occurrences. In this regard, fault analysis has been an important focus in this project. We were especially interested in defining reservoir characteristics relative to hydrothermal activity and dolomitization on 'feeder faults'.

### **Saddle Dolomite Formation and Petroleum**

Most saddle dolomite literature has been written within the last 5 years -- from 1996-2001. Saddle dolomite, baroque dolomite, and hydrothermal dolomite are synonyms for which we will use the abbreviation HTD.

**Structures and Saddle Dolomite.** Saddle dolomite formation and deep gas occurrences have the following tectonic settings.

·Deep-seated, near-vertical fractures of variable kinematics commonly control and provide conduits for dolomitization (McKenzie, 1999; Barnes and Harrison, 2001; Cantrell and others, 2001; Kappler and Zeeh, 2000; Green and Mountjoy, 1999; Reinhold, 1998; White and Al Aasm, 1997; Belopolsky, 1996; White, 1995; Packard and others, 2001).

·Dolomitization and hot fluid circulation tend to coincide with crustal thrust thickening and/or burial (1-7 km) and orogenic events (e.g. Laramide orogeny, Variscan orogeny, and Ouachita orogeny) (Lewchuk and



others, 2000; Al Aasm, and others, 2000; Zeeh and Kappler, 2000; Boni and others, 2000; Torok, 2000; Wendte and others, 1999; Wendte and others, 1998; Chung and Land, 1997; Tobin and others, 1997) .

·Hydrothermal dolomitization is a globally widespread phenomena and is found in deeper stratigraphic reservoirs within most oil-field regions. Saddle dolomite precipitated coincident with oil migration (Green and Mountjoy, 1999).

·The fluids come from below and are associated with high-angle structures. Many of these high angle structures are associated with hydrothermal dolomitization in, adjacent to, and beneath hydrothermal dolomite reservoirs that contain oil and/or gas.

·The best reservoirs are the first permeable stratigraphy encountered above the basement.

**Chemistry and Saddle Dolomite.** Chemical settings of saddle dolomites have the following factors in common.

·Formation temperatures for saddle dolomites range from 70 to 220 degrees C, based on fluid inclusion data (Vandrey, 1991; Mountjoy and others, 1999; Yoo Chan, and others, 2000; Green and Mountjoy, 1999; Clarke, 1998; White and Al Aasm, 1997; White, 1995).

·The  $^{87/86}\text{Sr}$  initial ratios,  $\delta^{18}\text{O}$  and  $\delta^{13}\text{C}$ , and  $^{34}\text{S}$  data, generally indicate that the isotopic signatures of saddle dolomites are different from that of their host rocks (Dickson and others, 2001; Tritlla and others, 2001; Clarke, 1998; White and Al Aasm, 1997). Strontium isotopes of the saddle dolomites are typically more radiogenic than those of the wall rocks (Mountjoy and others, 1999; Clarke, 1998; White and Al Aasm, 1997; White, 1995).

·Moderate salinity dolomites (20-25%) typically postdate lower salinity dolomites (Yoo Chan and others, 2000; Clarke, 1998).

·Dolomite sequencing typically involves higher temperature, more ferroan, dolomites overprinting lower temperature, more magnesian dolomites (Yoo Chan and Gregg, 1997).

·Vanadium may accompany the high temperature, more ferroan dolomites.

·Accessory fluorite and sphalerite accompany saddle dolomite deposition in the Alberta basin, suggesting

dolomitization is accompanied by halogen metasomatism.

·Pyrite is the most common sulfide accessory in saddle dolomite deposits.

·Rare earth elements (Sm, Dy, Tb, Ho, and Eu occur in a saddle dolomite of hydrothermal veins (Habermann and others, 1996)

**Timing of Saddle Dolomite Formation.** Saddle dolomite formation and deep gas occurrences have the following timing constraints.

·Saddle dolomites are superimposed on normal diagenetic processes and in many cases may be much younger than the diagenetic event (Bradshaw, 1989; Colquhoun, 1991; Zeeh and Kappler, 2000).

·Moderate salinity dolomites typically postdate lower salinity dolomites.

·Porosity/permeability appears to coincide with the dolomitization (especially high-temperature dolomitization) (e.g. Bone Spring dolostone in Scharb Field, New Mexico (Bradshaw, 1989)).

·Dolomite sequencing typically involves higher temperature, more ferroan dolomites overprinting lower temperature, more magnesian dolomites (Vandrey, 1991).

·Oil and gas transport and deposition appear to accompany dolomitization in a number of cases (Colquhoun, 1991).

·Hydrothermal dolomite forms very rapidly, displays Mg-rich oscillatory zoning with increasing Mg-enrichment toward the edge of the dolomite grain, and implies rapid formation under non-equilibrium conditions (Searl, 1989). These observations are consistent with the process of precipitation from a hydrothermal fluid.

#### **HYDROTHERMAL DOLOMITE AND MISSISSIPPI VALLEY TYPE (MVT) ORE DEPOSITS**

Small amounts of petroleum products are characteristic of Mississippi Valley Type (MVT) lead-zinc-silver

deposits, where they generally occur in fluid inclusions.

**Structures and MVT ore deposits.** MVT deposits have the following tectonic settings.

·The fluids come from below and are typically associated with high angle feeder structures (Admiral Bay deposit, Canning Basin, WA: McCracken and others, 1996).

·Flower structures (pop-up structures) serve as fluid pathways (Admiral Bay deposit, McCracken and others, 1996) and compare with flower structures in the Cave Gulch gas field (Montgomery and others, 2001). High-angle feeder structures (riedel/tensile structures) branch upward as high-angle reverse structures (flower structures). The stratigraphy high over these structures is nearly flat; lower in the section there is very slight arching that becomes steeper arching closer to the flower structures.

·Mud or shale strata generally seal and stop the upward migration of fluids.

**Chemistry of MVT ore deposits.** Chemical settings of the saddle dolomites associated with MVT deposits have the following facts in common.

·Fluid inclusion data in sphalerite range from 60 to 120 degrees C with a modal peak of those in sphalerite and dolomite at 100°C and some in sphalerite ranging to 200 degrees C (Randell and Anderson, 1996).

·Isotopes of the wall rocks are different from those of the hydrothermal products (Randell and Anderson, 1996).

·Sulfide precipitation and hydrocarbon formation accompany a reduction (in oxidation state) event of the hydrothermal fluids following saddle dolomite formation.

·Salinities are greater than 15% in the MVT ore deposit in the Bowland Basin, UK (Gaunt and Gize, 1996).

·Fluid inclusions in sphalerite indicate 85 to 115 degrees C for Period I mineralization and 95 to 130 degrees C for Period II mineralization in the Bowland Basin, UK (Gaunt and Gize, 1996).

**Timing of MVT ore deposits.** Saddle dolomite formation and deep gas occurrences have the following timing constraints.

·The petroleum products generally form during and after sulfide precipitation and after saddle dolomite formation.

·Saddle dolomites occur early in the paragenetic sequence, before deposition of metal sulfides (and locally late) (Gaunt and Gize, 1996; Grobe and Machel, 1997). Relative timing of MVT mineralization and hydrocarbons generally shows the hydrocarbons are within fluid inclusions within the mineralization and postdate early vein carbonates. Bitumens are early, liquid hydrocarbons are intermediate, and hydrocarbon waxes are late in the paragenetic sequence.

·Radiometric and paleomagnetic dating indicate MVT formation coincides with major compressive orogenies, especially continental assemblies (such as, Ouachita and Alleghenian orogenies in North America).

## **HYDROTHERMAL DOLOMITE, PETROLEUM, AND MVT ORE DEPOSITS**

### **Common Model for Hydrothermal Saddle Dolomite and Petroleum and MVT Zinc-Lead Deposits**

Analysis of different literature source types (petroleum literature versus ore deposit literature) reveals a strong parallelism between observational data for petroleum occurrences hosted in hydrothermal (saddle) dolomite and/or chert reservoirs and observational data for certain low temperature types of hydrothermal metallogeny, especially the Mississippi Valley Type (MVT) zinc-lead deposits. Isotopic, fluid inclusion, paragenetic, structural, and stratigraphic data all indicate that the same types of physical and chemical controls attend deposition of both types of occurrences. The only real difference is the composition of the economically interesting materials (petroleum products versus zinc-lead products). Possible reasons for the compositional contrast include crustal oxidation state and composition of the source region from which the fluids were generated.

There is a strong correlation between the geologic processes that developed both petroleum and MVT types of systems. These processes appear to strongly coincide with generation of deep, possibly metagenic, fluids during compressively driven orogenesis (especially those that coincide with continental assembly events). These fluids,

then, are typically driven for long distances (in some cases, in excess of 300 km) towards the foreland basins - cratonward of the compressive orogen. In the case of west central New York, local downdip, lower Paleozoic sources could also be the source of petroleum generation under hydrothermal conditions (100 - 220 degrees C).

Specific controls at the emplacement site typically involve fluid flow into 'first permeability' carbonate reservoirs immediately above basement. These reservoirs are commonly 'sealed' by an overlying silici-clastic, shale-dominated 'cap'. The fluids arrive at these reservoirs via high-angle faults that are connected to the basement. The fluid arrival may coincide with transpressionally driven, flower structures and/or riedel/tensile faulting at the emplacement site.

In the case of New York, the 'first permeability' may be the Trenton/Black River groups above the Grenville basement. This study focused on known and possible faults that affect Trenton/Black River stratigraphy as well as Grenville basement. This study emphasized the kinematics of the fracture system during emplacement and how that fracture system was stressed during orogenic events that postdated deposition of the Trenton/Black River groups. In the New York region, emphasis has been placed on regional dynamics that attended the Acadian and Alleghenian orogenic episodes (based on a regional paleomagnetic and radiometric dating of what are probably related MVT deposits in the Appalachian to Ouachita regions).

The interpretations on timing and genesis of the petroleum product relative to the hydrothermal dolomite phenomenon in the petroleum literature contrast strongly with the timing and genesis interpretations in the ore deposit literature.

Articles on MVT deposits in the ore deposit literature invariably link saddle dolomite formation with ore paragenetic stages, emphasizing that the deposition of lead-zinc-bearing sulfides is part of a co-genetic reaction and depositional sequence in which sulfide deposition follows formation of the saddle dolomite stage. Opinion is more varied with respect to the petroleum products that commonly accompany and post-date sulfide deposition (for example, as petroleum-bearing fluid inclusions in sphalerite). Some interpretations suggest that the deposition of the petroleum in MVT deposits is part of the co-genetic paragenetic sequence that involves early stage, moderate temperature (above oil window) dolomitization (Gize, 1999). Other interpretations suggest that zinc-lead-Mg-rich basinal brines intersected pre-existing petroleum accumulations.

In the oil literature, the petroleum occurrences in saddle dolomite reservoirs are invariably portrayed as separate events. Either 1) petroleum was generated and migrated into hydrothermal dolomite permeability that had been created by an unrelated, earlier dolomitization event, or 2) an independent hydrothermal dolomitization event

was superimposed on pre-existing petroleum reservoirs that were created during early diagenesis and existing petroleum products were remobilized. Both of these independent fluid scenarios are consistent with conventional concepts whereby oil is generated from lower temperature sources. Because the hydrothermal dolomite is, in large part, deposited at temperatures above the oil window, it has been thought that such hydrothermal fluids could not be directly related to the petroleum-making events.

However, a third possibility emerges if the analogy between hydrothermal dolomites in both MVT deposits and deep gas deposits is valid: both sulfides and petroleum could have been products of the same process. In this third model, the carbon component is brought in with the hydrothermal fluid event that created the saddle dolomite. The hydrocarbons subsequently are formed and deposited in the context of sulfate/carbon dioxide reduction events that are superimposed on and induced by the earlier event of hydrothermal dolomitization. If this hypothesis holds true, a new class of hydrothermal oil and gas may emerge from this investigation. Obviously, this innovative genetic concept would open a wide-ranging array of new exploration possibilities for hydrothermal oil and gas deposits that have yet to be evaluated by more conventional approaches. The structural, geochemical, and genetic aspects of this new type of oil deposit will be the subject of our continued investigation, with the main emphasis focused on favorable structural habitats in the current project.



### 3. REGIONAL GEOTECTONIC MODEL AND FLUID FLOW

#### GENERAL CONCEPTS OF GEOTECTONICS AND FLUID FLOW

Results of the integration of the regional structural conceptual model for hydrothermal oil and gas accumulations as applied to New York State were presented in a poster session format at the AAPG annual meeting on March 10-13, 2002, in Houston, TX. Geochemical information provided by Jim Viellenave of Direct Geochemical provided an important, though unanticipated, corroboration of the geotectonic model, as well as a practical geochemical tool that can detect the surface manifestation of the deep petroleum resource. An expanded discussion of the poster session is provided below.

#### Fluid Flow in Strike-Slip Fault Settings

Fluid migration patterns in strike-slip settings that host hydrothermal metalliferous systems (such as the Carlin gold deposits) are analogous to hydrothermal hydrocarbon migration patterns, particularly in hydrothermal dolomite settings. Faults are not merely passive conduits and seals that statically receive and trap fluid sometime after their formation. Rather, fluid formation, movement, and deposition within any fault system are active processes that co-dynamically conjoin fault kinematics with fluid generation, flow, and deposition.

**Porphyry Metal Fluid Flow.** Porphyry metal deposit analogs (Carlin North Trend of Nevada) indicate a syn-kinematic relationship between strike-slip fault movements, the emplacement of plutonic gold sources, and the release of gold-bearing fluids into riedel/tensile splays and/or wedge-like stratigraphic traps. The most economic traps involve the intersection of favorable stratigraphy with the footwall of P-shear conduits (Figure 3.1). Where this stratigraphy is blocked in its updip portions by other faults that mark changes in dip domain or juxtapositions with unfavorable stratigraphy, a wedge-like 'trap' can be associated with especially high-grade gold accumulations (e.g., Meikle mine) (see Figure 3.2). The fluid migration path is identified through geochemistry. As fluids migrate from a high pressure source to low pressure deposition sites, they fractionate, resulting in a systematic paragenetic sequence and chemical assemblage pattern that reflects the dispersion of the hydrothermal fluids. Increase in oxidation state during the process is a first-order chemical control on the fractionation.



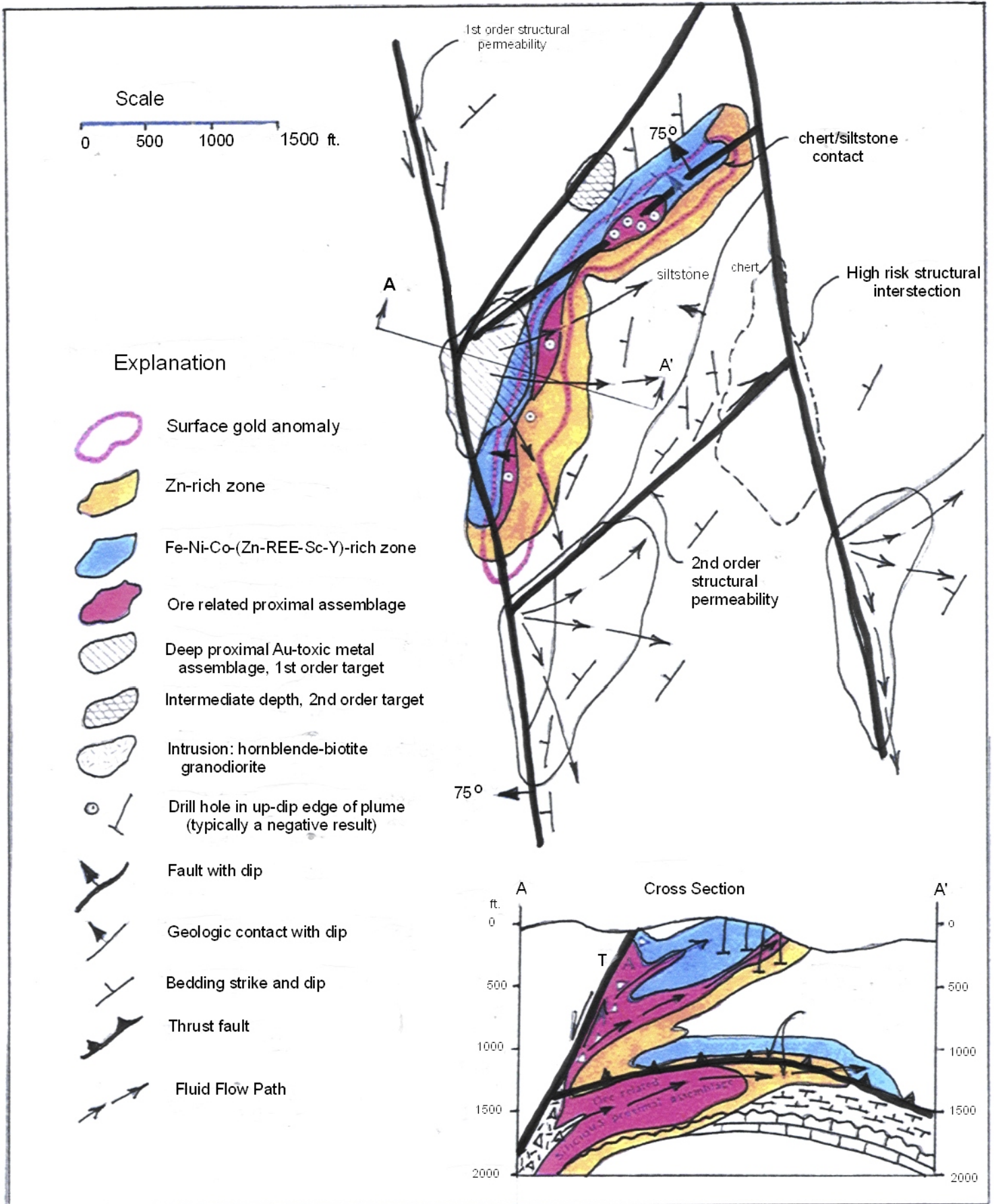
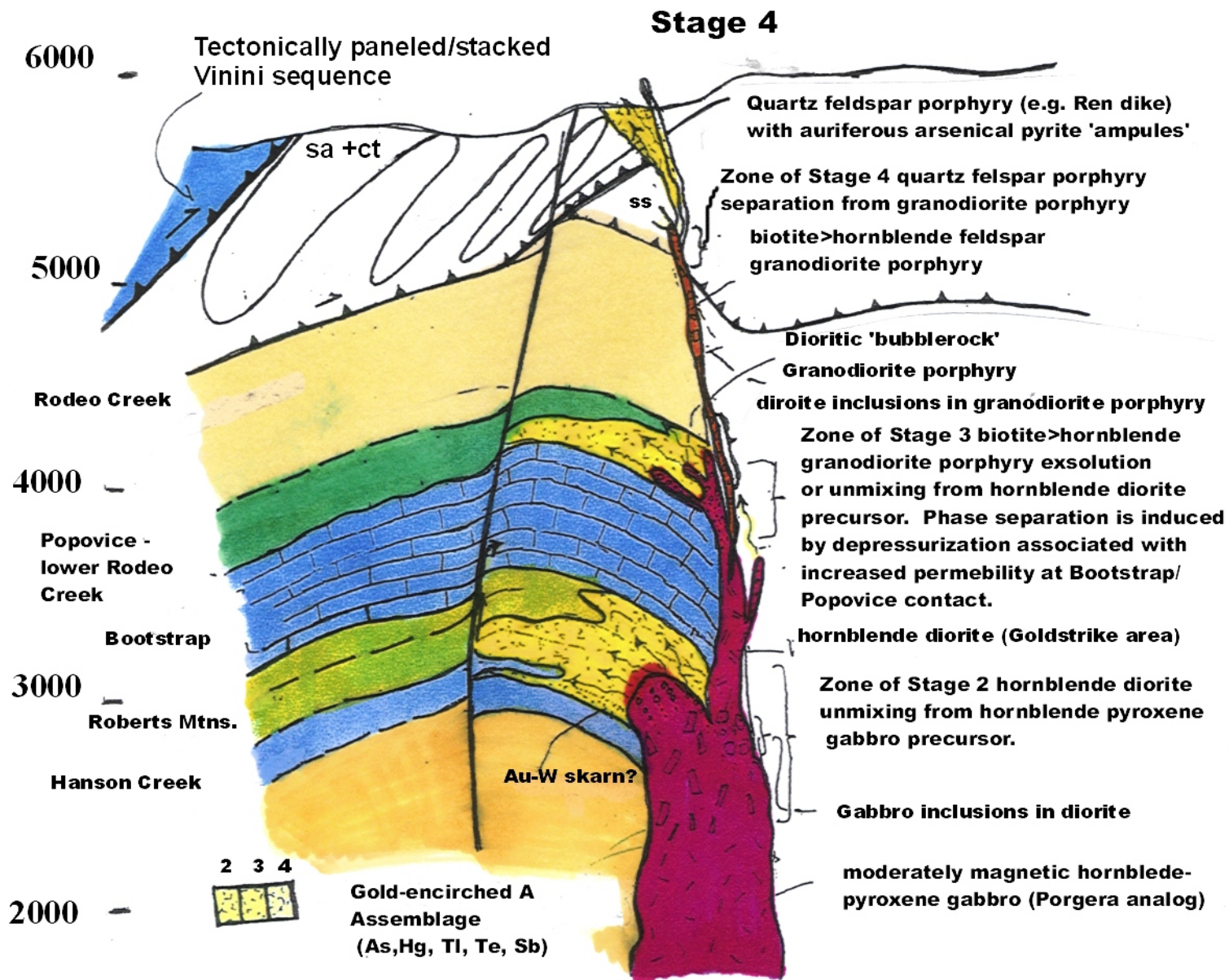


**Figure 3.1. Fluid Flow Model for Carlin-Type Gold Deposits**

Figure 3.1. Fluid flow model for Carlin-type gold deposits.

W

E



Model for multi-staged Porgera-Goldstrike type gold porphyry system. System is sourced to a reduced (early Ulvospinel -> titanomagnetite-later ilmenite), normal halogen, hydrous (hornblende bearing), calc-alkalic, metaluminous magma-fluid reaction sequence. Model is 'customized' to the geologic setting in the northern portion of the Carlin gold belt.

Figure 3.2. Model for multi-staged Porgera-Goldstrike type gold porphyry system.

Figure 3.2. Model for multi-staged Porgera-Goldstrike type gold porphyry system.

A ‘real-world’ case history involving fractionation of Carlin-type, gold-rich, hydrothermal plumes is demonstrated at the Meikle mine in the Carlin North Trend (Figure 3.3). Here, a proximal gold-thallium-tellurium assemblage that is associated with the main ore accumulation has fractionated into at least 6 distinct metal assemblages. The most distal of these assemblages is assemblage 6, which consists of anomalous Light Rare Earth Elements (LREE), thorium, scandium, and rubidium and is deposited in argillically altered, upper plate rocks. A series of intermediate assemblages is present between the outermost assemblage and the proximal assemblage (see Figure 3.3 for details).

Fractionation can also be documented in the pluton sources of the hydrothermal plumes (Figure 3.4 and 3.5). In this view, hydrothermal fluid plumes and their metal and alteration zoning represent hydrothermal fractionates of plutonic sources. The plutons, in turn, represent liquid fractionations of a mafic to felsic fractional differentiation sequence. This magmatic fractionation involves initial liquid-liquid magmatic fractionations, followed by crystal-liquid fractionations (fractional crystallization in the classic Bowen Reaction Series sense), and hydrothermal fluid releases from each igneous phase. Typically, four stages of igneous fractionation accompanied by hydrothermal fractionations attend each fractional differentiation sequence (see figures 3.4 and 3.5, which are applied to a typical porphyry copper fractionation sequence).

The above-described fractionation sequences are commonly emplaced in the context of a deep-seated, strike-slip fault framework. A simplified version of a magmatic and hydrothermal fractionation within a strike-slip fault setting is shown in plan view in Figure 3.6. The original gabbro portion in the sequence ascends through a deep-seated P-shear conduit and is typically ‘pulled’ asymmetrically in a lateral direction by the lateral kinematics related to the strike-slip faulting (the P-shear). In the diagram of Figure 3.6, the differentiation sequence is pulled left and differentiates leftward as it traverses through a network of left-slip shears. As the sequence crosses individual elements within the shear system that are generally pressure reduction zones associated with riedel/tensile splays (on Figure 3.6), various hydrothermal and magmatic unmixings may occur. With respect to a simplified conjugate shear model, a given differentiation sequence will display a hook-like pattern that reflects the lateral kinematics of the strike-slip fault system. In a typical conjugate shear model, four differentiation trajectories are possible (see Figure 3.7).

A ‘real-world’ case history application of the above logic is applied to the Carlin North Trend (Figures 3.8 and 3.9). Analysis of abundant map information, radiometric and geochemical data for both intrusions and gold mineralization reveals that two major periods of gold introduction are present in the Carlin North Trend deep crack system. Both of these gold mineralization events were accompanied by strike-slip faulting.





Figure 3.3. Metal dispersion/fractionation at the Meikle mine, Carlin/North Trend, Nevada.

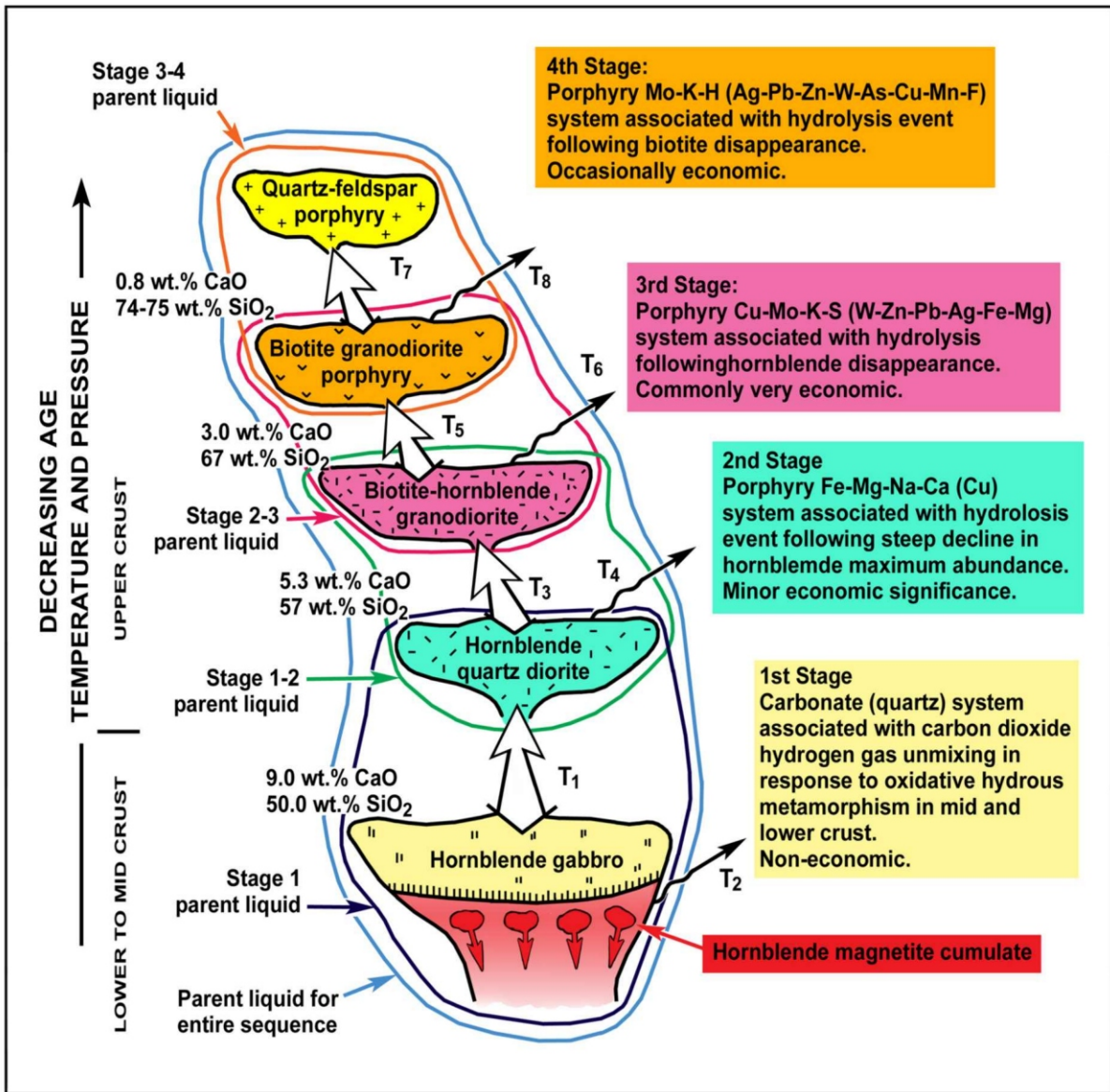


Figure 3.4. Schematic, stepped evolution of rock and metalliferous fluid phases in an oxidized iron-titanium-poor (hydrous), calc-alkalic, metaluminous magma series (MCA14C).



Figure 3.4. Schematic, stepped evolution of rock and metalliferous fluid phases in an oxidized iron-titanium-poor (hydrous), calc-alkalic, metaluminous magma series (MCA14C).

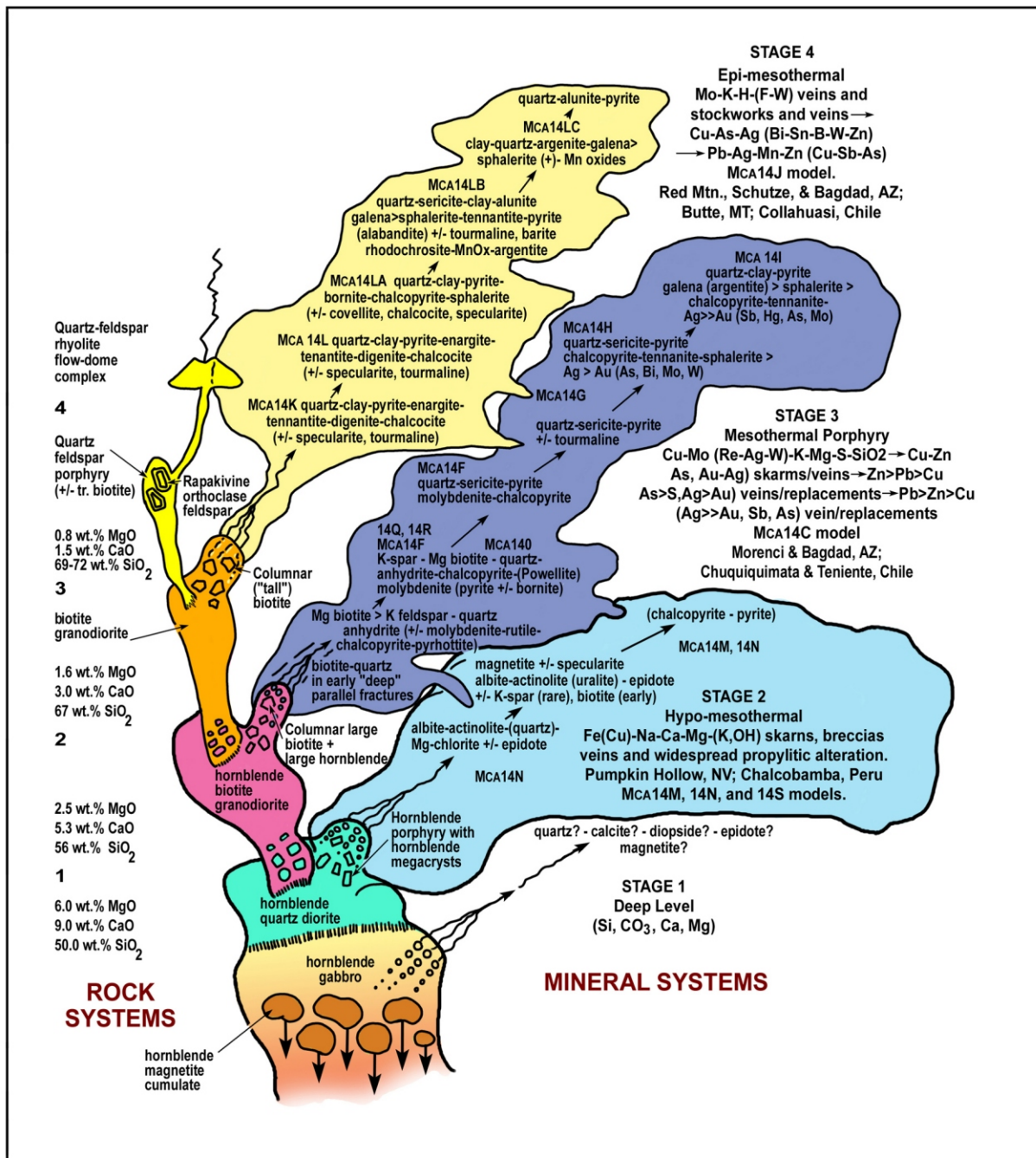


Figure 3.5. Staged magma-metal fluid systems for meso-epizonal oxidized (magnetite-sphene stable) hydrous (hornblende-bearing, calc-alkalic, metaluminous magma series (MCA14M, Stage 2; MCA14C, Stage 3; MCA14J, Stage 4).

Figure 3.5. Staged magma-metal fluid systems for meso-epizonal oxidized (magnetite-sphene stable) hydrous (hornblende-bearing, calc-alkalic, metaluminous magma series (MCA14M, Stage 2; MCA14C, Stage 3; MCA14J, Stage 4).

## Generalized Differentiation Hook Sequence for Hornblende Stable Porphyry Metal Series

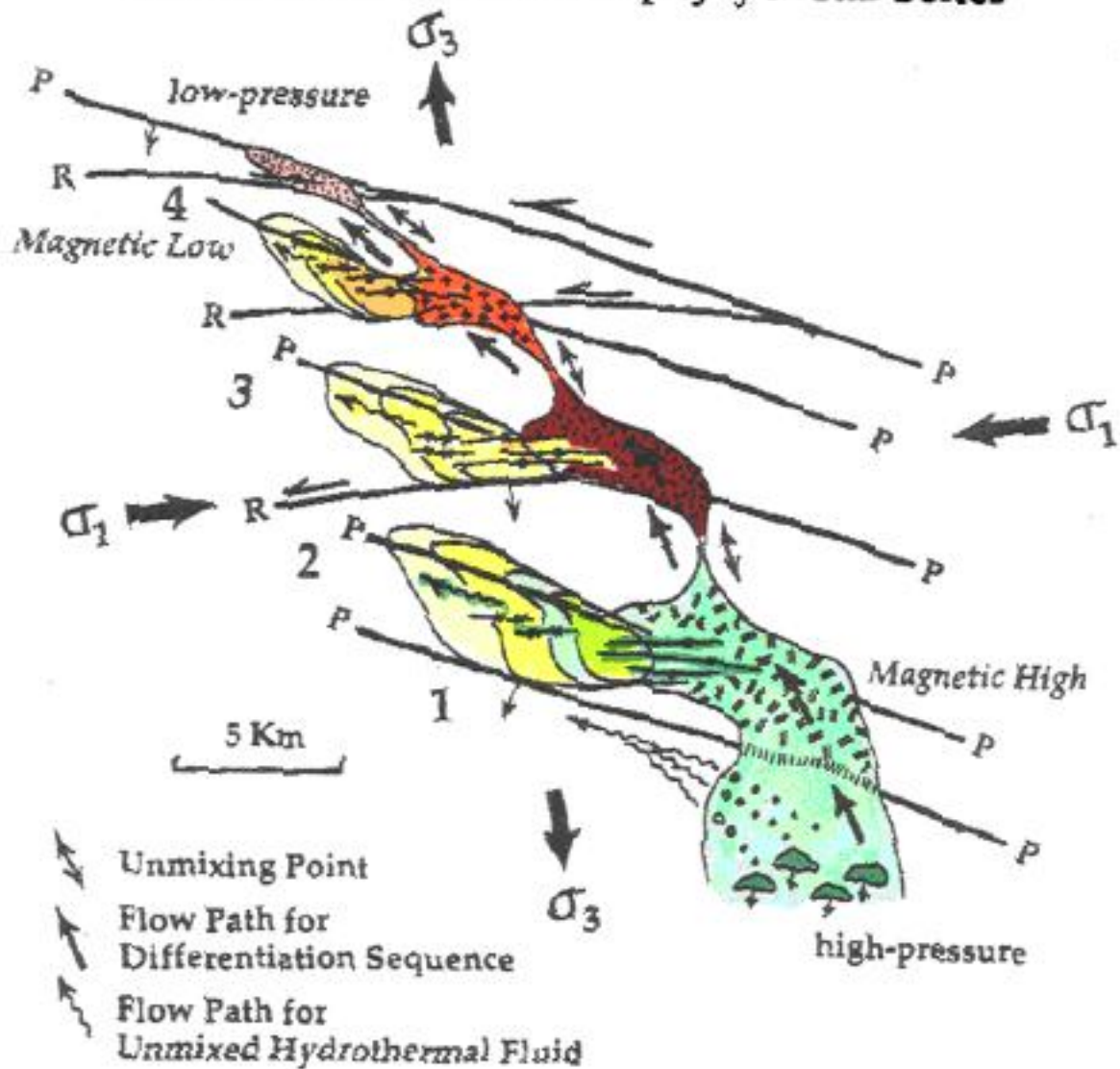
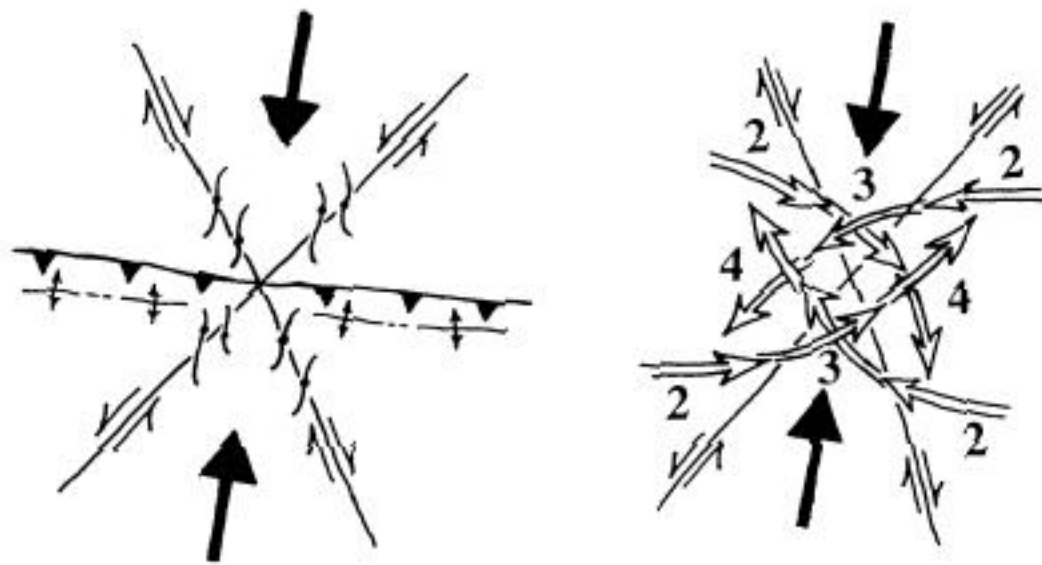


Figure 3.6. Generalized differentiation hook sequence for hornblende-stable porphyry metal series.

Figure 3.6. Generalized differentiation hook sequence for hornblende-stable porphyry metal series.



**Stress-Strain and Theoretical Fluid Flow Paths**

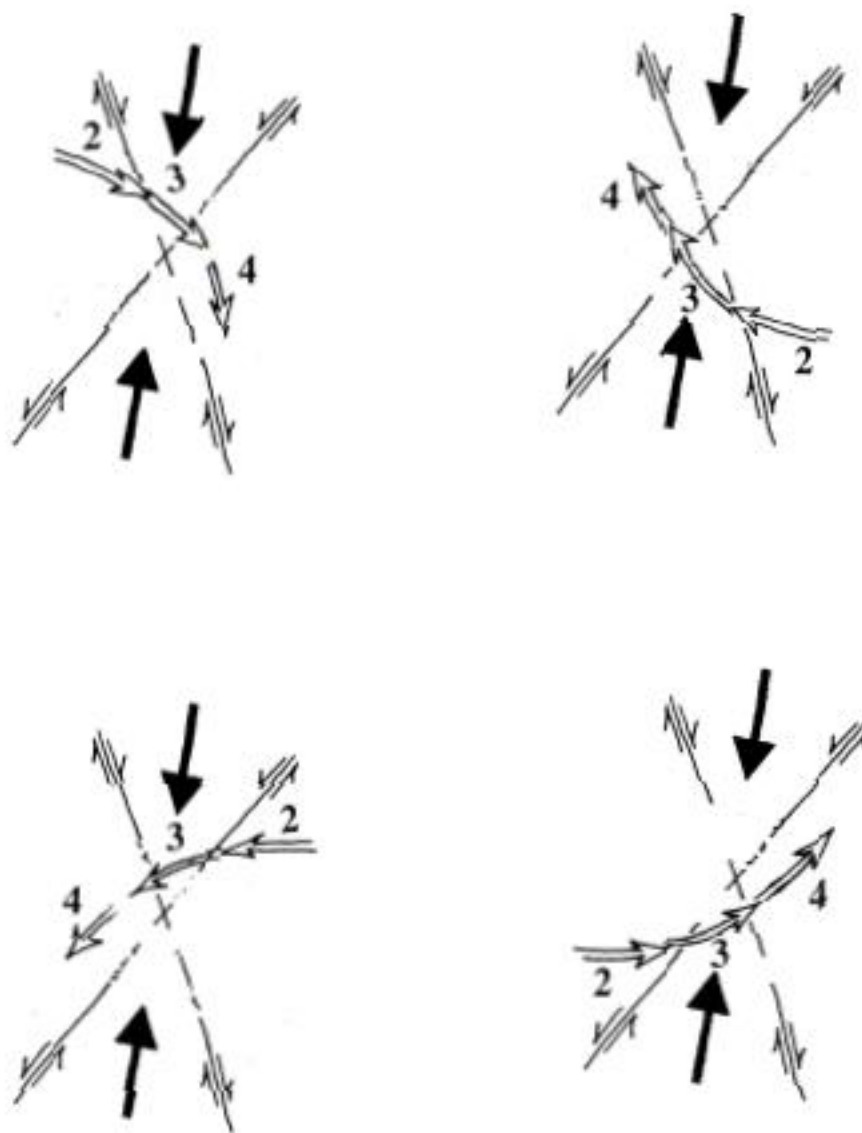


Figure 3.7. Stress-strain diagram and four possible magmatic fluid flow (differentiation) paths.

Figure 3.7. Stress-strain diagram and four possible magmatic fluid flow (differentiation) paths.



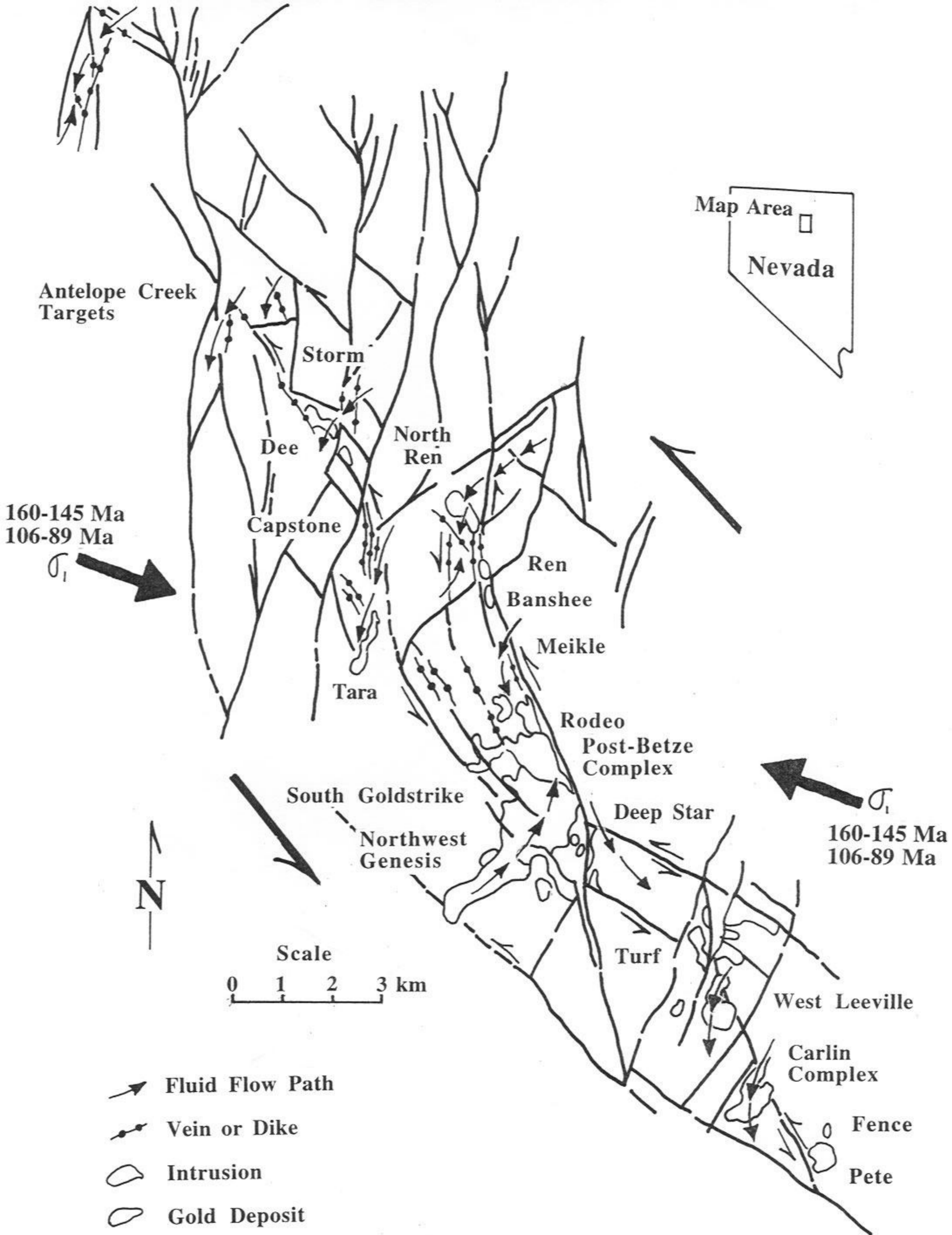
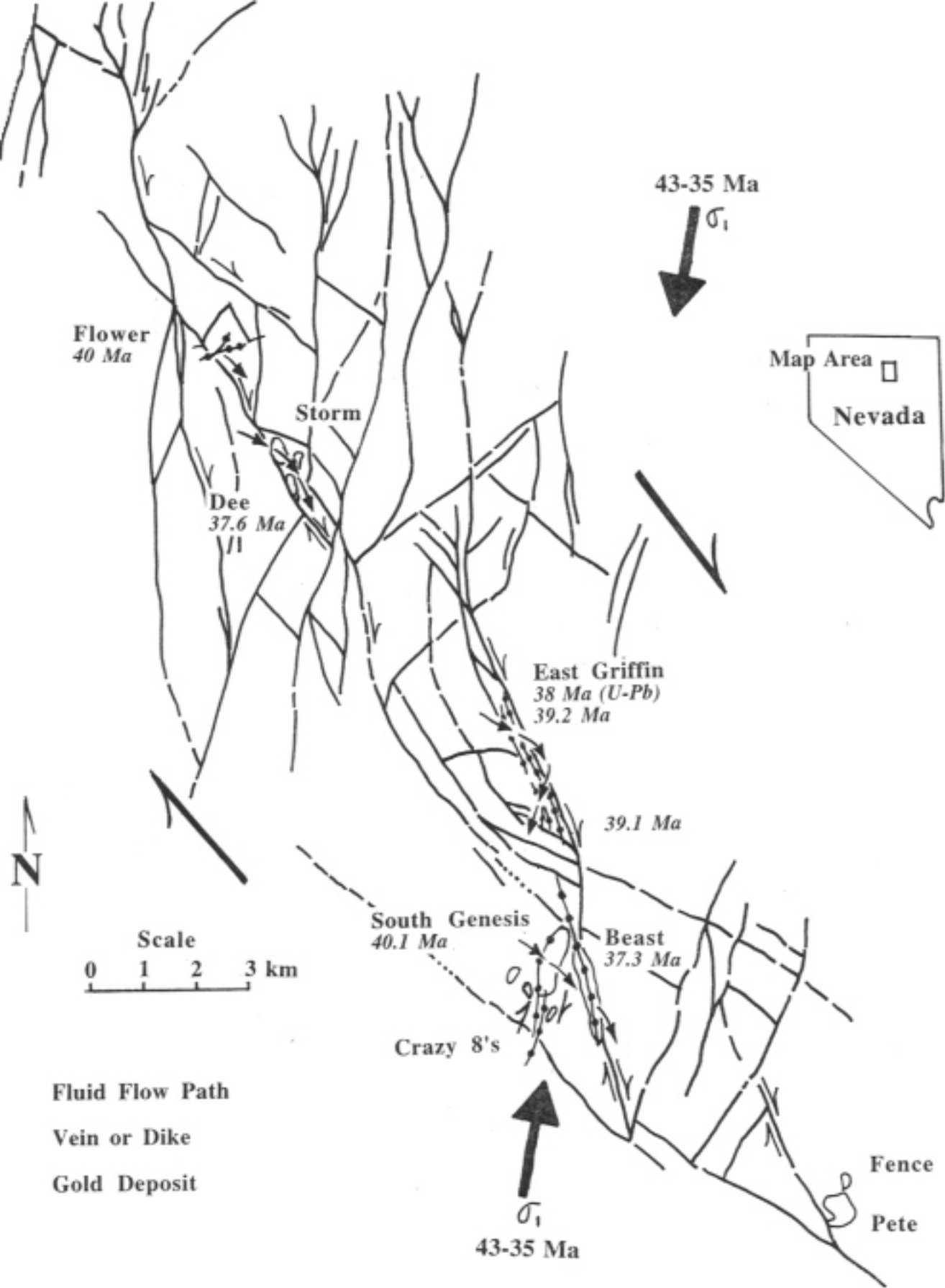


Figure 3.8. **Jurassic-Cretaceous Magma-Hydrothermal Fluid Flow in the North Carlin Trend Deep Crack System**



Figure 3.8. Jurassic-Cretaceous magma-hydrothermal fluid flow in the North Carlin Trend deep 'crack' strike-slip fault systems.





**Eocene Magma-Hydrothermal Fluid Flow  
 in the North Carlin Trend Deep Crack System**

Figure 3.9. Eocene magma- hydrothermal fluid flow in the North Carlin Trend deep 'crack' strike-slip fault systems.

The main period of gold introduction seems to be associated with a series of intrusions that display left differentiation hooks into a network of faults that were moving in a left-slip kinematic sense. The left slip was induced by regional, WNW-ESE-directed compression associated with the Nevadan (160-140 Ma) and Sevier (125-89 Ma) orogenic episodes. A major plate tectonic reorganization event occurred in the Eocene that orthogonally reoriented the regional stress field to NNE-SSW-directed regional compression. At this point, the fault net in the Carlin North Trend reversed its main slip sense to a right-slip kinematic sense. During this episode of right slip, a differentiation sequence of intrusions fractionated through a broad hook pattern from Dee (a Stage 2 diorite system) to Beast (a Stage 4 rhyolite system) some 10 miles to the south-southeast. This period of lower volume intrusions was associated with a suite of hydrothermal fractionation events with lower gold volumes. The Mesozoic gold introductions are estimated to be responsible for about 80% of the total gold introduced into the Carlin North Trend, whereas the Eocene intrusions are probably associated with about 20% of the volume of gold introduced.

**Hydrothermal Oil and Gas Fluid Flow.** The logic that was outlined above for fluid flow in porphyry metal situations can be applied, by analogy, to fluid flow of hydrothermal oil and gas associated with strike-slip faults. An idealized hydrothermal hydrocarbon plume associated with a deep-seated strike-slip fault setting is shown in Figure 3.10. Here, hydrocarbons are envisioned to have been produced in association with orogenic tectonism and burial of source rocks and in association with metamorphic dewatering events in the basement. Ascension of these fluids through a basement-connected, strike-slip fault conduit produces a water-oil-gas fractionation sequence as the plume migrates from high pressure to low pressure environments within the strike-slip fault setting (see Figure 3.10 for details).

Similar strike-slip configurations are associated with trap accumulations of petroleum in strike-slip fault environments, such as the Jonas and Cave Creek gas fields in Wyoming, the Albion-Scipio field in Michigan, and the Glodes Corner (or Pultney) and other fields in Steuben County, New York. In both porphyry metal and petroleum systems, the paths that the economic fluids utilized are characterized by a curved trajectory in moving from the P-shear conduit to the stratigraphic wedge. This curved or 'hook-shaped' trajectory appears to be characteristic of fluid migration in both porphyry metal and hydrothermal petroleum accumulations related to wrench fault tectonism.

**Dynamic Interpretation.** The fluid flow models outlined above, not only indicate flow caused by thermal buoyancy and lithostatic decompression, but also suggest flow caused by lateral pressure gradients due to lateral strain. Kinematic analysis begins with an assessment of pre-existing basement structures that provide conduits for fluids and that influence the nature of the lateral strain to which the fluids are reacting.

As rock strains, stress fields rotate into curved stress fields; this causes pressure gradients to also curve. The resulting  $\sigma_2$  ( $\sigma_2$ ) fluid paths are consequently curved. In this model, riedel-tensional structures (which are traditionally thought to be the primary pathways of fluid migration) lie at a high angle to the primary migration path. Fluid may locally flow along the riedel structures for short distances, but the total fluid pathway is at a high angle to them, along the P shear structures ( $\sigma_2$ ).

Although fluids flow along the high-to-low pressure gradient along the  $\sigma_2$  (P shear) "tunnel" for most of their journey, the destination – the reservoir site – is controlled by structural/stratigraphic traps in a "wedge"-shaped configuration. Here, the fluids move along local permeability and pressure gradients and are confined by stratigraphic or structural traps in the primary basement shear and the riedel/tensile splays, such as in the Jonas gas field of Wyoming.

In porphyry metal systems, the fluids (magmas and volatiles) are "frozen" in place and are thus still accessible for analysis. The precise chemical nature of fluids along the fluid migration path can thus be delineated. Chemical fractionation of magmas and hydrothermal volatile fluids along the fluid pathway is controlled not only by temperature and pressure, but also by oxidation state. Mineralogical and chemical partitioning and paragenesis exhibit gradients that follow the typically increasing oxidation state of a migrating fluid. This pattern allows chemical assemblages to be statistically modeled and provide oxidation state gradients that can be vectored into specific drill targets. This vectoring has contributed to a number of discoveries in the mineral deposit industry.

Compared to porphyry metal systems, oil and gas systems are more dynamic, volatile, and transitory. Unlike mineral systems, the main products of commercial interest do not necessarily remain at the deposition site as solidified precipitates. Rather, if the original deposition site is not effectively sealed, the hydrocarbon component may migrate or 'leak' out of deposition site. If the trap site contains oxidized wall rocks, the hydrocarbon accumulation may ultimately oxidize to water and carbon dioxide. Various intermediate degraded products of partial oxidation may include bitumens, resins, and/or sulfurous residues. The volatile nature of the various hydrocarbon products may produce various kinds

of hydrocarbon gases, which have a strong tendency to vertically diffuse through thousands of feet of overlying, pre- to post-depositional rock column. This volatile, diffusional characteristic may be utilized as an explorational opportunity, in terms of sampling (via soil gas chemistry) leakage from the underlying petroleum accumulation. The Glodes Corner case history in New York may be a spectacular example of such a leakage effect (see discussion below).







Figure 3.10. Hydrocarbon plume fractionation in deep-seated strike-slip fault settings.

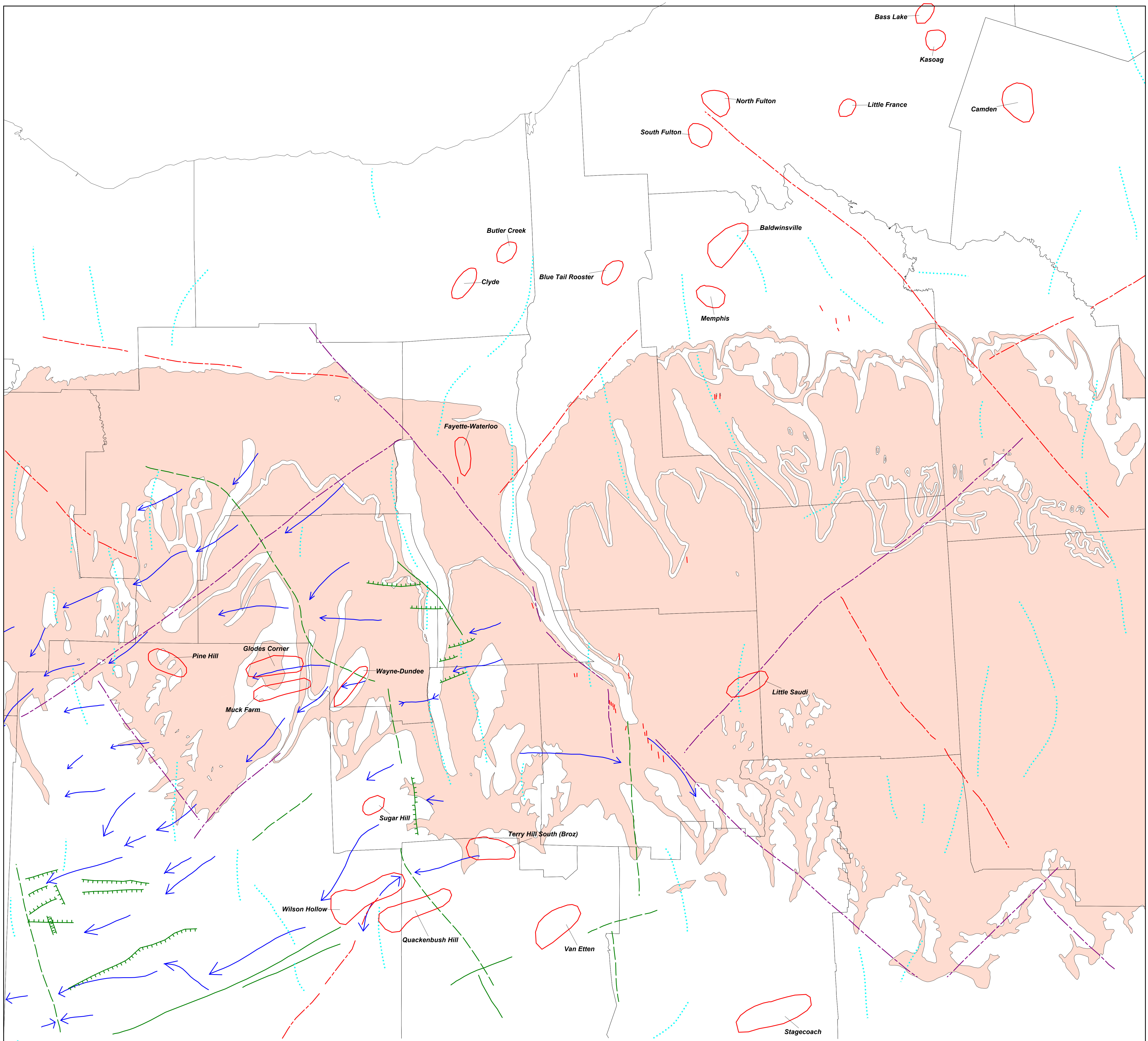
**Application to Wrench Fault Settings in New York State.** Regional tectonic elements that may be present in and near the gas accumulations in the Finger Lakes region of central New York State are shown in Figure 3.11. The structural elements were identified several ways. Obviously, the most direct evidence is from direct mapping of the structural element. Less direct methods utilized offsets in fold features that affected the Lower Devonian Oriskany Sandstone (especially the small-scale fold features identified by the detailed mapping of Bradley and Pepper (1938) in Steuben County, New York). Linearly aligned zones of *en echelon* kimberlitic dikes were also used to define potential, northwest-striking, deep-seated fault elements (such as the Ithaca line in Figure 3.11). Other potential basement structures were indicated by linear breaks between magnetic highs and lows, gravity highs and lows, radiometric highs and lows, as well as troughs. Offsets in the regional outcrop patterns could also be related to deep-seated faults. Alignments in the contour lines on the Conodont Alteration Indices (CAI) map were also used. The most likely structures based on all of the above indicators are shown on Figure 3.11.

With respect to deep-seated gas possibilities, one structure is particularly prominent. This structure is named the Glodes-Quackenbush Trend. The Glodes-Quackenbush Trend may be associated with gas reservoir development at Glodes Corner, Muck Farm, Wayne-Dundee, Sugar Hill, Wilson Hollow, and Quackenbush Hill. As currently delineated, the Glodes-Quackenbush Trend is about 100 km long, with an average strike of about N35W. The gas accumulations consistently occur on the southwest side of the trend and are associated with northeast- to east-west- (mainly east-northeast-) trending subzones that range up to about 10 km in length.

In terms of a dynamic model, the east-northeast-trending subzones are interpreted as riedel/tensile splays that curve east-southeastward into the Glodes-Quackenbush Trend. This trend is interpreted to be a basement-connected, P-shear, feeder zone that was operating in left slip during the time of gas introduction. Left slip on the Glodes-Quackenbush Trend is inferred to have been induced by regional, east-northeast--west-southwest compression that was operant in the foreland of either the Taconic or Acadian orogenies.

The best understood field, at this point in our investigation, is the Glodes Corner field in Steuben County, New York. The hydrothermal fluid flow model derived from the tectonic/dynamic model described above predicts that low carbon number, hydrogen-rich gases should have entered the riedel/tensile trap site from the basement structure on the east. As the hydrothermal fluids migrated west, according to the chemical fractionation models developed above, they would oxidize and produce higher carbon number gases in greater abundance towards the western part of the field.





**Structural Interpretation of the Finger Lakes region 1:250,000 scale**

**Explanation**

- |   |                          |   |   |
|---|--------------------------|---|---|
| * Drill Hole (Trenton/Black River test)         | ← Syncline               | ⋯ Potassium Low (trend of elongation)                   | - - - Fault (based on outcrop patterns) |
| ○ Gas Field with Trenton/Black River production | — Ordovician CAI isograd | — Fault (mapped on surface - teeth on downthrown block) | - - - Fault (based on magnetic data)    |
| ■ Middle Devonian Sedimentary rocks             | — Devonian CAI isograd   | - - - Fault (based on subsurface data)                  | — County boundary                       |
| Kimberlite dike                                 | ○ Magnetic High          |   |   |

Figure 3.11. Structural interpretation of the Finger Lakes region of central New York.

Fortunately, hydrocarbon gas chemistry was available from the NYSERDA-supported hydrocarbon gas study by Jim Viellenave and others of Direct Geochemical to test the above dynamic model. Indeed, the data shows that carbon geochemistry fractionated from east to west along the riedel/tensile conduit. The above fractionation pattern of hydrocarbon gases is shown in Figures 3.12 through 3.14. The east-to-west fluid pathway is indicated by the presence of a more hydrogen-rich, reduced assemblage with higher  $\text{CO}_2/\text{O}_2$  ratios (Figure 3.12) and C-1 to C-4 gases on the east, near the intersection with an inferred northwest-trending 'feeder' structure. The geochemical data indicate a more oxidized, H-poor environment on the west. This more oxidized environment is characterized by an assemblage of higher C-number gases (especially C-5 and C-6; Figures 3.13 and 3.14) and by a more oxidized, O-rich assemblage characterized by lower  $\text{CO}_2/\text{O}_2$  ratios on the west (Figure 3.12). The inferred feeder structure appears to have been undergoing active, left-slip kinematics at the time of the gas introduction, which is inferred to have entered the hydrothermal dolomite reservoir in the underlying Trenton/Black River section from the southeast. Significantly, the above patterns were not picked out during the initial study by Direct Geochemical, which focused on the use of soil gas chemistry to simply 'see' the underlying accumulation through discriminant function-determined probability values (see Figure 3.15). Consequently, Jim Viellenave was as intrigued by the results of our combined research as we were.

Indeed, the above surface fractionation pattern in the soil gas chemistry may have predictive qualities for indicating the producing gas field pay zone that is some 7,000 feet below the surface samples. Specifically, the pay zone should mirror the surface chemistry with more reduced, methane/ $\text{CO}_2$ -rich gases in the eastern part of the pay zone versus more oxygen-rich, heavy hydrocarbon gases in the western part of the field.

In summary, preliminary results of a recent soil geochemical survey at Glodes Corner by Direct Geochemical suggest that the analogy between fluid flow in mineral deposits and that in hydrothermal oil and gas is valid. The data exhibit chemical fractionation patterns analogous to mineral deposit chemical fractionation patterns. The fractionation patterns follow presumed oxidation state gradients and appear to be controlled by oxidation state. They are interpreted to define a hydrothermal fluid migration path from east (ENE) to west (SSW) with fluids originating in a relatively reduced state at the intersection of a NW-trending basement fault with ENE-trending riedel/tensile splays, and with fluids flowing in an arcuate path westward to a less reduced environment within the reservoir site.



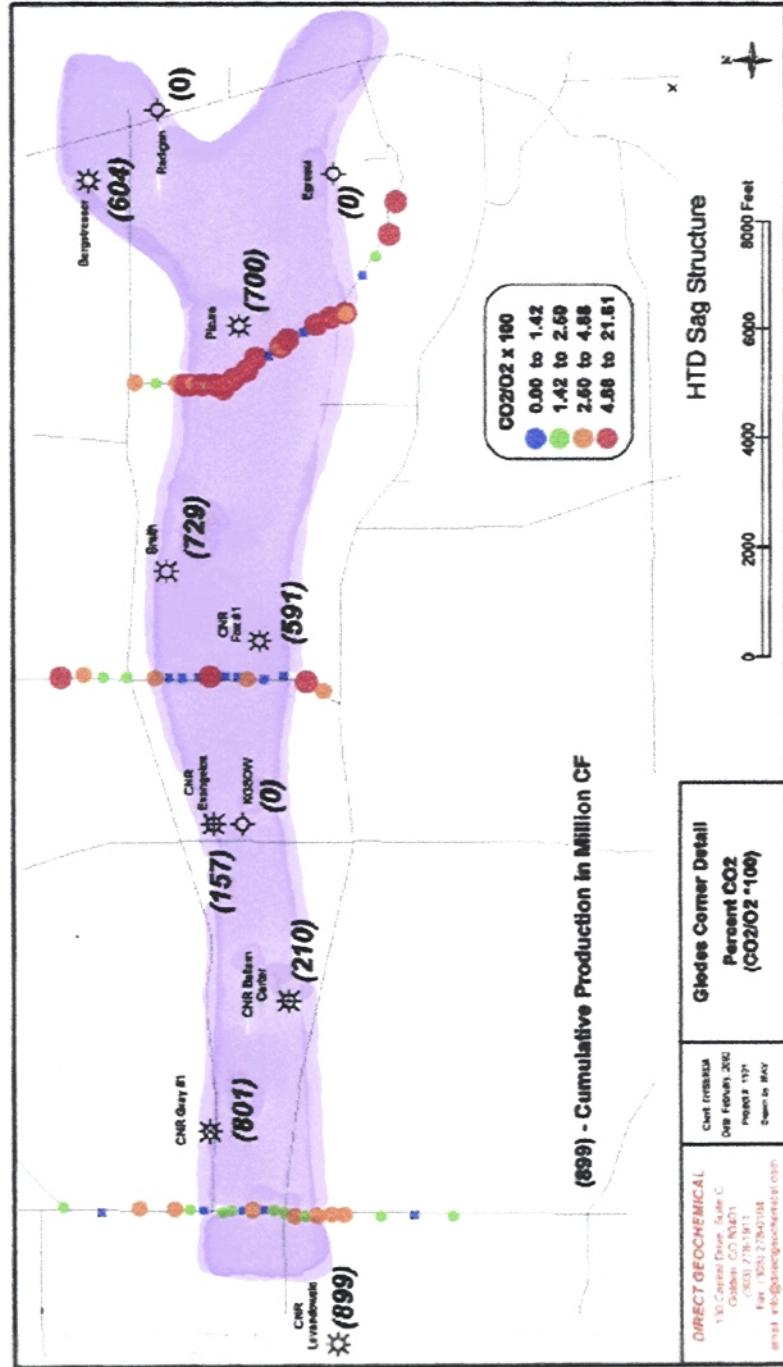


Figure 3.12. CO<sub>2</sub>/O<sub>2</sub> ratios in soil gas chemistry in the Glodes Corner field, Steuben County, south central New York (from Jim Viellenave, Direct Geochemical).

Figure 3.12. CO<sub>2</sub>/O<sub>2</sub> ratios in soil gas chemistry in the Glodes Corner field, Steuben County, south central New York (from Jim Viellenave, Direct Geochemical).

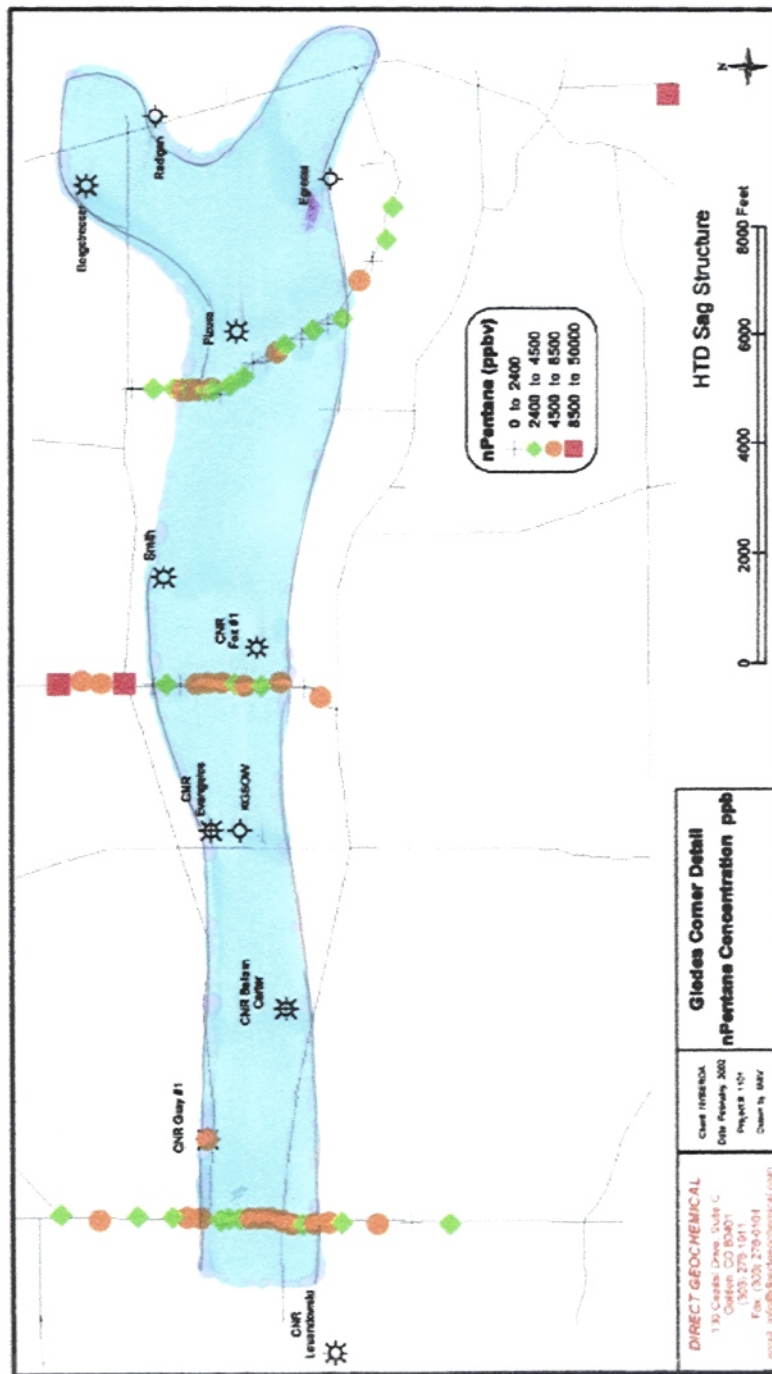


Figure 3.13. nPentane content (in ppbv) in soil gas chemistry in the Glodes Corner field, Steuben County, south central New York (from Jim Viellenave, Direct Geochemical).

Figure 3.13. nPentane content (in ppbv) in soil gas chemistry in the Glodes Corner field, Steuben County, south central New York (from Jim Viellenave, Direct Geochemical).



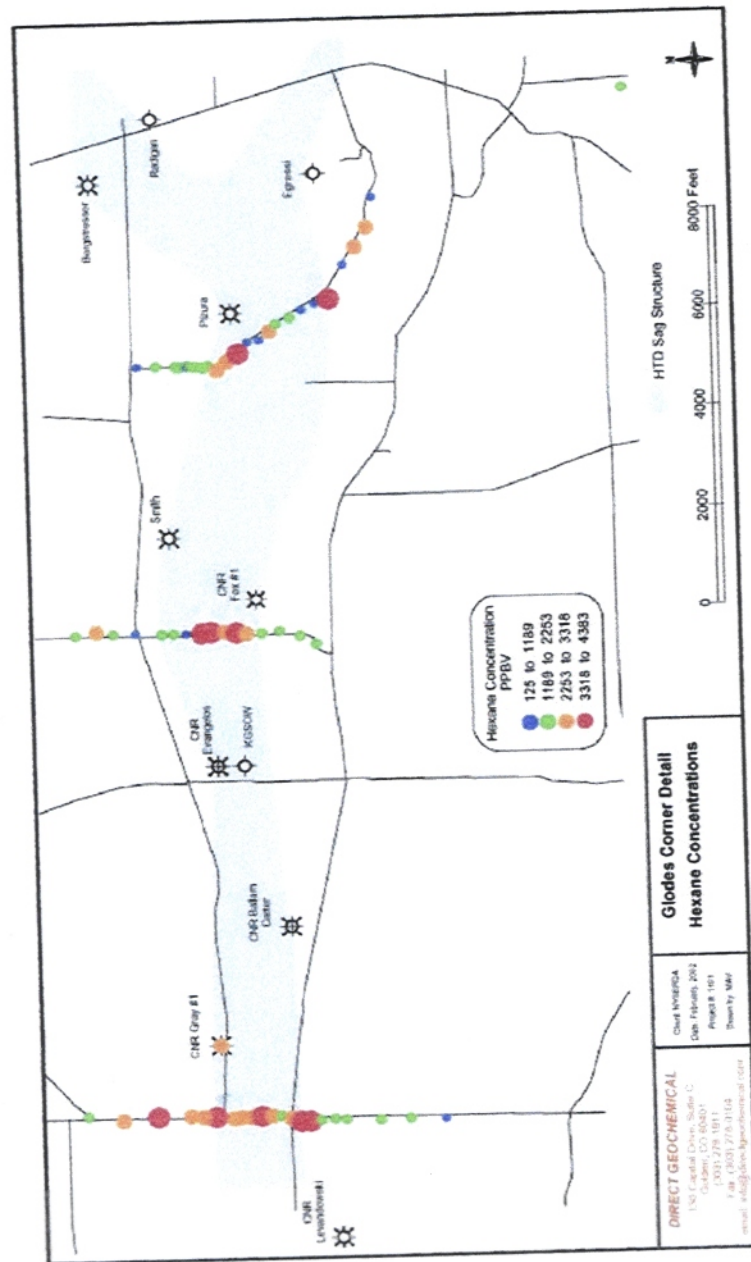


Figure 3.14. Hexane content (in ppbv) in soil gas chemistry in the Glodes Corner field, Steuben County, south central New York (from Jim Viellenave, Direct Geochemical).

Figure 3.14. Hexane content (in ppbv) in soil gas chemistry in the Glodes Corner field, Steuben County, south central New York (from Jim Viellenave, Direct Geochemical).

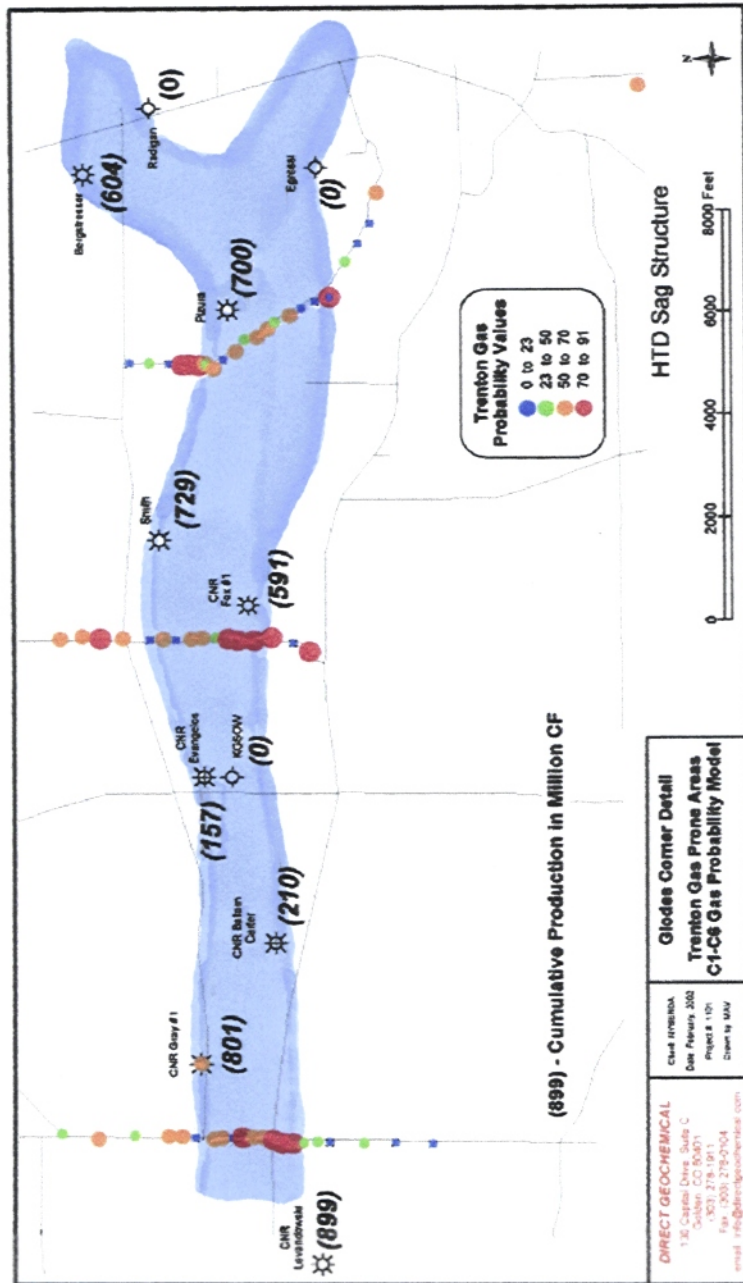


Figure 3.15. Trenton gas probability values in soil gas chemistry in the Glades Corner field, Steuben County, south central New York (cumulative production in million cf in parentheses) (from Jim Viellenave, Direct Geochemical).

Figure 3.15. Trenton gas probability values in soil gas chemistry in the Glodes Corner field,

Steuben County, south central New York (cumulative production in million cf in parentheses) (from Jim Viellenave, Direct Geochemical).

### **Relationship to Hydrothermal Dolomite Model and Continental Basement Structure**

The Glodes-Quackenbush Trend most probably represents a basement-connected structural conduit. Hydrocarbon-bearing, magnesium-rich fluids probably utilized this conduit while it was in left slip during the Taconic or Acadian orogenies. The fluids probably ascended through this conduit and migrated into riedel/tensile permeability, where they encountered the first replaceable carbonate sequence in the cover stratigraphy above basement (see Figure 3.16). In central New York State, the first replaceable carbonate unit above basement is the Trenton-Black River shelf carbonate sequence (mid-Upper Ordovician).

The magnesium-rich, hydrocarbon-bearing fluids (5P model in Figure 3.16) bear a strong resemblance to the Mississippi Valley type (MVT) fluids (34B model in Figure 3.16). See Appendix A for magma-metal series models and explanations. Other related, orogenically produced, metagenic fluids include the Kupferschiefer type (36A model) and the East Tennessee type (7Q model). All of these models have fluids that are derived from specific sources in the basement. In particular, the Trenton-Black River type (5P model) may possibly have been derived from serpentized, olivine-rich, magnesian, ultramafic rocks associated with failed rifts in the basement. In the New York case, one of these failed rifts may, in part, be represented by thickened Cambrian sediments, such as the Rose Run Sandstone. The possible failed rift coincides with basement magnetic high features beneath Steuben County, New York. This inferred failed rift feature may link into the more well-known Rome Trough and its allied elements, which are widespread in the basement beneath the Appalachian basin.




The Glodes-Quackenbush Trend is probably connected to a more extensive, continent-wide, basement fault network (Figure 3.17). The most prominent Precambrian basement structures of the U.S. developed during the 1400 Ma orogenic event, which extends from Scandinavia to Mexico. Although long thought to be anorogenic, recent work has shown that it is characterized by extensive intrusion of mantle- and crustally-derived granite that, in places, volumetrically comprise up to 75% of the mid- to upper crust. Structurally, these large volumes resulted in a relatively isotropic crust for much of the Precambrian in the U.S. Transcurrent, WNW-trending shears developed during the final stages of granite emplacement and appear to constitute the most significant anisotropy of the Precambrian basement (Swan and Keith, 1986).

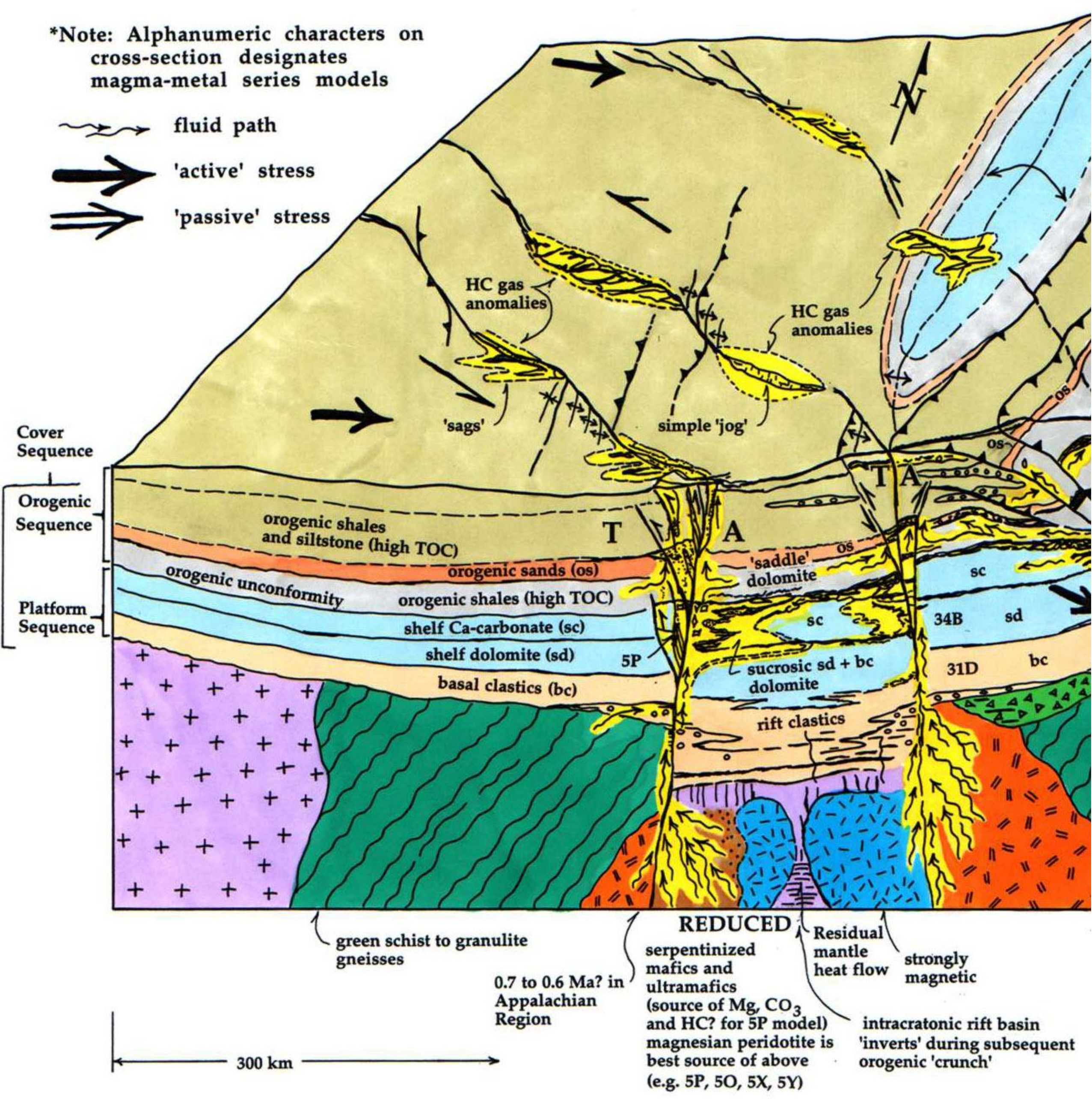
Subsequent tectonic events have been influenced by this WNW-trending basement structure. In common with

more recent subduction, the Devonian-Ordovician orogenic events of the Appalachian orogen are



\*Note: Alphanumeric characters on cross-section designates magma-metal series models

-  fluid path
-  'active' stress
-  'passive' stress



Cover Sequence

Orogenic Sequence

Platform Sequence

orogenic shales and siltstone (high TOC)

orogenic sands (os)

orogenic unconformity

orogenic shales (high TOC)

shelf Ca-carbonate (sc)

shelf dolomite (sd)

basal clastics (bc)

sucrosic sd + bc dolomite

rift clastics

green schist to granulite gneisses

0.7 to 0.6 Ma? in Appalachian Region

**REDUCED**

serpentinized mafics and ultramafics (source of Mg, CO<sub>3</sub> and HC? for 5P model) magnesian peridotite is best source of above (e.g. 5P, 5O, 5X, 5Y)

Residual mantle heat flow

strongly magnetic

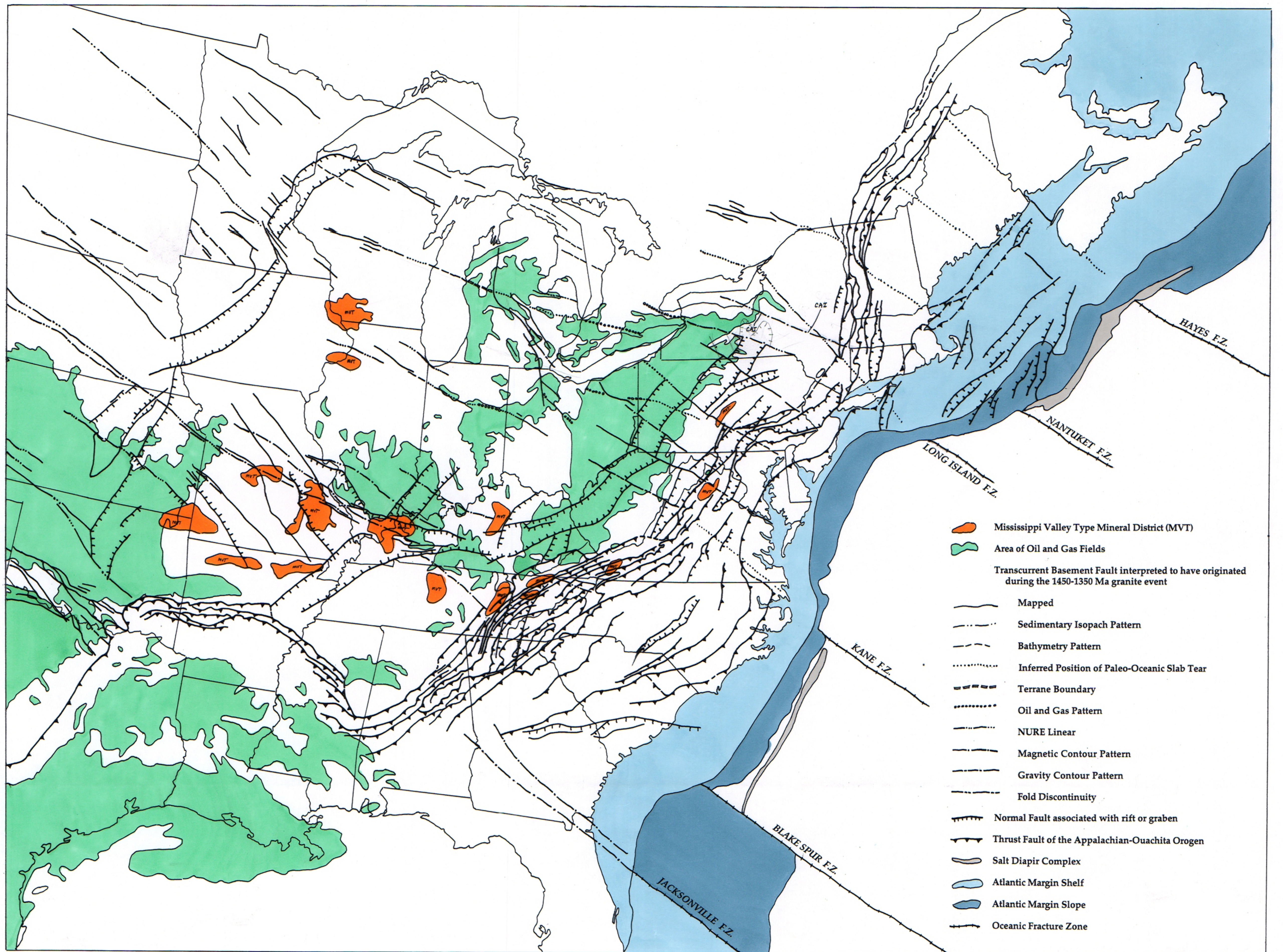
intracratonic rift basin 'inverts' during subsequent orogenic 'crunch'

300 km



Figure 3.16. Model for metagenic fluid generation, migration, and deposition of hydrothermal dolomite, metals (Cu, Ag, Pb, Zn), and petroleum during convergent orogenic thickening episodes (see Appendix A for key to magma-metal series models).





**Oil and Gas Fields, MVT Mineral Deposits, and  
1400 Ma Transcurrent Basement Faults of the Eastern U.S**



Figure 3.17. Oil and gas fields, MVT mineral deposits, and 1400 Ma transcurrent basement faults of the eastern U.S.

presumed to have involved periods of segmented subduction. The concept of segmentation of the plate tectonic slabs is an important aspect of the orogenies. The slab tears may coincide with the edges of well-known embayments that occur along the strike of the Appalachian orogen. The boundaries between embayments may mark slab tears in the Paleozoic subduction system that accompanied Cordilleran styles of Appalachian orogenic events. Along-strike changes in distribution of peraluminous versus metaluminous magmatism, basin geometry, uplift distribution, metamorphic grade patterns, transform faults, and salt on the continental slope may all be linked to slab segmentation. This segmentation, which is ultimately controlled by the basement fracture framework shown on Figure 3.17, may have re-propagated its pattern during the breakup of Pangea to produce the current oceanic fracture zone pattern of the Atlantic basin.

The basement faults have been mapped on the ground and can also be recognized in geophysical, remote sensing, and sedimentological data. Basement faults extend from zones such as the Lewis and Clark zone eastward across the continent. The regional distribution of oil fields and Mississippi Valley Type Zn-Pb deposits clearly reflects this basement structure.

Cambrian rifting (e.g. Rome Trough) has been modeled by previous workers as an idealized orthogonal rift/transform pattern (Schwochow, 2000; Thomas, 1977; and Hatcher and others, 1989). The actual pattern is probably more transtensional in nature due to the pre-existence of the WNW-trending basement faults at an angle less than 90 degrees (as Dewey has recently suggested). Strain usually occurred along the pre-existing WNW faults rather than along new transforms, which would have had northwest strikes. Some NW transforms apparently developed and linked the WNW faults and provided deep conduits for hydrothermal dolomite fluids and gas (e.g. Albion-Scipio Trend, Michigan, and Glodes-Quackenbush Trend, south central New York).

The prolific Albion-Scipio field of Michigan displays an obvious wrench fault-Riedel pattern that appears to have strongly influenced gas migration and reservoir formation (Hurley and Budros, 1990). This pattern is very similar to the pattern seen at Glodes Corner. Both WNW- and NW-trending basement faults are present and appear to have moved in a left-slip sense, causing EW- and ENE-trending riedel/tensile splays to form and providing a lateral pressure gradient that pulled the hydrothermal gas-bearing fluid into the riedel/tensile zones.



#### 4. MODEL OF THE SOURCE, NATURE, AND MIGRATION OF HYDROTHERMAL PETROLEUM FLUIDS

##### CHEMISTRY OF HYDROTHERMAL DOLOMITE GAS MODEL

Approaching the hydrothermal dolomite problem from an MVT point of view, the following scientific points are relevant to the HTD oil and gas model.

1. Fluid origination, transport, and deposition at the emplacement site all took place within a period of about 10 million years during orogenic contraction events that mobilize fluids from the underlying basement beneath the emplacement sites.
2. The early stage sucrosic dolomitization step, the main stage hydrothermal saddle dolomite step, the sulfide depositional step, and the late stage carbonate with peripheral clay alteration step are regarded as products of a single hydrothermal fluid event, which fractionated throughout its evolution.
3. The fluid generation events are part of standard, normal, dewatering processes that occur in the basement during regional prograde dynamic metamorphic events associated with orogenic thickening episodes. Fluids expelled from this basement are hydrocarbon-stable in terms of methane and other aliphatic hydrocarbon gases, as well as hydrogen. The fluids that emanate from the basement are radiogenic and highly carbon-charged (especially carbon dioxide- and carbonate-charged). Peridotitic sources may be involved in the production of magnesium-rich, chlorine-rich and carbonate-rich brines.
4. Metagenic waters expelled from the basement ascend into the cover via high-angle fault nets, which are being subjected to regional horizontal compression in the foreland of the orogenic belt. Consequently, the basement structural framework and its propagation into the overlying basin cover, such as that in New York, is a critical control for fluid ascension. Many of these fractures operate in a strike-slip manner during the fluid ascension. The fluids are deposited in low pressure dilatent zones, such as dilatent jogs, Riedel-tensile splays, and wedge fractures.
5. Porous, biohermal facies within limestone (calcium carbonate) units that intersect the structural scenario in point 4 provide an important stratigraphic and chemical control that strongly focuses the dolomitization events that precede and accompany hydrocarbon emplacement. Typically, the first shelf facies or shelf margin

facies (especially reef facies) stratigraphic unit above the basement is the unit that gets most extensively dolomitized and saturated with hydrocarbons. Hydrocarbons (both methane and petroleum fluids) are generated during chemical reactions within the dolomitizing fluid during the dolomitization, anhydrite formation, and sulfide deposition stages in the process. Chemical evolution of the fluids follows an orderly sequence whereby early sucrosic dolomitization occurs at salinities of 5 to 16% NaCl equivalent and temperatures of about 50 to 100°C. Main stage saddle dolomite formed in association with fluids at temperatures at about 90 to 200°C with salinities of about 10 to 30% and a global mean of about 20% NaCl equivalent. CO<sub>2</sub> contents were high and the fluids are consistently more radiogenic than seawater-equilibrated host rocks for a given time period.

6. A number of compositionally specialized sources in the basement are believed to be sources of metagenic fluids: 1) MVT lead-zinc fluids, 2) Cu-[petroleum] fluids, Kupferschiefer copper-silver (also Pb-Zn-PGE-Au-U-petroleum) fluids, and 3) HTD type petroleum and gas (also Zn-Fe[Zn > Pb]) fluids. In particular, Mg-rich peridotitic sources are believed to be the sources of HTD-type fluids (3), metaluminous alkali-calcic granitic basement may be the source of MVT-type fluids (1), and metaluminous quartz alkalic shoshonitic volcanic arc complexes may be the source of Kupferschiefer-type fluids (2).

7. Oxidation state of the fluids, which in part govern hydrocarbon stability, is initially controlled by the oxidation state of the basement sources. Peridotitic complexes within oceanic basements (such as buried failed rifts like the Rome Trough and its extensions beneath the Appalachian basement) are believed to produce more reduced fluids. Granitic basements, such as those in the St. Francis Mountains adjacent to the Reelfoot Rift in the North American mid-continent, produce weakly oxidized fluids. Shoshonitic volcanic complexes, such as the Eastern Creek Volcanics beneath Mt. Isa, Australia, produce weakly oxidized fluids.

8. Oxidation state of the fluids during their transport is also critical as the hydrocarbon generation process and stability require reduced conditions (typified by ferroan wall rock ferric/ferrous ratios of less than 0.6).

The visual aspects of the model are provided the block diagram of Figure 3.16 and are specifically applied to the south-central New York state gas region in Figure 3.17.

## **INTEGRATIVE MODEL FOR GENERATION, MIGRATION, AND DEPOSITION OF PETROLEUM FLUIDS**

### **Conceptual contrasts with existing models**

Aspects of this hydrothermal model are controversial with respect to current interpretations of HTD genesis, which commonly rely on conventional basin evolution paradigms. In the basin evolution concept, petroleum is generated from biogenic sources within the basin during burial stages. The fluids then migrate to the reservoir site represented by the porosity of the hydrothermal dolomite rocks, commonly long after the hydrothermal dolomite reservoir was created. For example, hydrothermal dolomite reservoirs created in the foreland of the Rocky Mountain fold-thrust belt presumably during the Mississippian-age Antler orogenic event are conventionally thought to have been subsequently charged by Cretaceous petroleum fluids generated during burial and maturation of organic sources in Cretaceous rocks during the Laramide orogeny of Late Cretaceous to Early Tertiary age (89-43 Ma). Similar conventional scenarios in the Appalachian basin form the HTD reservoirs during the Taconic or Acadian orogenies and then subsequently generate and migrate hydrocarbon fluid into the HTD reservoirs during the Alleghenian orogeny/basin burial episode.

In much of the petroleum literature, as well as the economic geology literature, fluid sources are largely believed to have originated in the basins and the term 'basinal brine' is in widespread current usage in both literatures. The hydrothermal model is more consistent with the term 'basement brine' and is also compatible with some recent interpretations of the hydrothermal dolomite problem that look at basin processes from the 'bottom up' (Smith and others, 2002). We would prefer the term 'basement up'. In effect, petroleum materials can be made during the reaction sequence that produces the reservoir-hosting hydrothermal dolomite. Oils made in this context can be accurately referred to as hydrothermal oil, hydrothermal petroleum, or hydrothermal gas.

If one looks at MVT/HTD portrayals in the metals economic geology literature versus the petroleum geology literature (for example, portrayals in Economic Geology magazine and related publications versus portrayals in AAPG Bulletin and related publications), a number of interesting 'disconnects' also emerge. In the

economic geology literature (for example, Gize, 1999), petroleum formation commonly is observed or interpreted to accompany hydrothermal reaction sequences that coincide with ore deposition of various metals. Fluid generation, migration, and deposition are generally portrayed within one, relatively short-lived, hydrothermal/tectonic episode. In this view, HTD-hosted petroleum accumulations can be alternatively viewed as hydrothermal petroleum mineral deposits in which petroleum formation is simply part of the mineral deposit process and is analogous to the formation of gold or tin deposits in association with reduced hydrothermal conditions.

In contrast, although recognized as locally accompanying and forming during hydrothermal events (specifically the saddle dolomite stages), most of the petroleum generation, migration, and deposition is interpreted in the conventional petroleum literature to be associated with much later events than the hydrothermal events that made the reservoir. In accord with sedimentary petrology and carbonate petrology in particular, hydrothermal dolomites are regarded as ‘facies’ (for example, the compendium entitled ‘Hydrothermal Dolomite Reservoir Facies’ by Davies, 2000). The dolomitization and petroleum phenomena are generally interpreted within the context of an ongoing, long-lived, ‘diagenetic’ process and the term ‘diagenetic fluids’ is in widespread usage. The term hydrothermal fluid is preferred where the petroleum formed during the ‘short-lived’ hydrothermal event.

The above conceptual contrasts are economically significant. If one takes the ‘hydrothermal oil’ point of view, the economically prospective locations are completely different in terms of source, migration, and trap. Typically in our ‘unconventional petroleum’ paradigm, the source is beneath the trap and the transport of petroleum materials involves an up-structure, fluid ascension mechanism with oil abiogenically produced in the context of a cooling, reduction reaction step. The oil window is approached from high temperatures in a cooling reaction rather than in a heating up of biogenically sourced kerogens from a lower temperature, biological source. Importantly, we do not disagree with the basin burial model as a viable geologic mechanism for oil generation, migration, and deposition within a given sedimentary basin. Rather, we argue that, because these HTD phenomena occur at the bottom of basins in close structural connection with an underlying basement, other models of petroleum formation and migration may be applicable. The detailed model developed below follows this ‘hydrothermal oil’ paradigm.

### **Hydrothermal dolomite model design**

The main features of the ‘hydrothermal oil’ model detailed below were constructed to explain what initially appear to be disparate features attributed to different fluids present at the occurrence site over a protracted period



of geologic time. To argue for a 'short-lived', single fluid evolution scenario, we have developed a staged fluid fractionation model that features five major steps:

- 1 Fluid generation in basement under reduced conditions which are hydrocarbon stable;
- 2 Expulsion and ascension of this fluid out of this basement and its reaction with the first replaceable limestone unit to form extensive early sucrosic dolomite, methane, and hydrocarbon;
- 3 Deposition of additional, high-temperature dolomite (including the well-known 'saddle' dolomite and later anhydrite) accompanied by continued methane and hydrocarbon production;
- 4 Deposition of metal sulfides (mainly pyrite and subordinate marcasite) concurrent with hydrocarbon (bitumen and oil); and
- 5 Migration of 'spent', reacted fluid and gases laterally and vertically into the 'distal', 'caprock' to produce extensive illite-mica- trace metal, possibly methane-chlorine-bearing halos or coronas.

In order to assess what kind of material and how much product are deposited during each major fractionation step, we modeled an empirically constrained brine that was derived metagenically by devolatilization of oceanic crust material. The devolatilization/'dewatering' of the oceanic crust source is interpreted to have accompanied the first major assembly-style orogenic event after the deposition of the shelf carbonate host. In the New York region this event would have been the Taconic or Acadian orogeny. In this model, the brine evolves through a series of five steps which are compositionally modeled by a series of mass-balanced chemical reactions that constrain what and how much of a given material is produced or reacted. Each reaction was ultimately constrained by how well it fit the large data base of experimental and observational empirical data.

With respect to the conventional petroleum system approach, the first step in the process characterizes what happens in the source region. The second step refers to the migration and initial reservoir preparation steps at the depositional/trap site. The third and fourth steps refer to key depositional reactions and events at the emplacement/trap site. The fifth step is perhaps the most unconventional with respect to the traditional petroleum system model. Here, fluids leave the immediate trap site, continue into the cover sequence where they react with it and may acquire additional petroleum material/potential via hydrogenation of kerogen-rich biogenic source material in the cover sequence. Some of the fluids then continue to ascend/migrate into the cover sequence after having acquired petroleum materials from this secondary/biogenic source. In effect, it now may be possible to view a given petroleum system as a broader, more open type of fluid system with connections into broader, planetary processes and systems.

### **Stage 1. Generation of Fluids in Peridotitic Basement Source Region**

**Fluid Source.** The fluid source for hydrothermal dolomite-hosted oil and gas accumulations (HTD) is thought

to be of basement origin. An analysis of the size of the hydrothermal dolomitized areas and mass balance calculations of the magnesium - CO<sub>2</sub> metasomatic component probably preclude 'basinal' fluid sources, as there is not enough pore-space volume and not enough easily mobilized Mg constituent. Timing, based on analog MVT radiometric dates, suggests that hydrothermal dolomites were deposited from hot brines early in basin evolution when most of the 'basin fill' was not yet there!. Radiometric data (Sr on dolomite and Pb on galena in analog MVT) suggest a radiogenic source in the basement. The strong association of hydrothermal dolomite deposits with high-angle faults that are connected to basement indicate that these faults may act as fluid conduits for ascension of hot CO<sub>2</sub>-Cl brines that were sourced in the basement. Occurrence of these HTD in the bottom of the basins makes derivation from hydrocarbon sources located higher in basin difficult. Brine compositions for HTD fluids are consistent with origination in basaltic oceanic crust within intracratonic, failed oceanic rifts. The process of serpentinization creates a void-space reduction in the basement that greatly enhances tectonically guided expulsion of fluids into overlying sedimentary cover sequences. Similar processes involving serpentinization of underthrust peridotitic basement by fluids derived from footwall carbonate-rich rocks have been previously suggested by Szatmari (1989).

**Geophysical signatures of possible peridotitic basement sources.** The chemical reactions involved in serpentinization of peridotites in the basement have major implications for geophysical expressions (especially gravity and magnetic) of possible hydrothermal oil sources in the basement. The high density of unaltered, unreacted peridotite in Stage 1 suggest that zones of unaltered peridotite in failed rift or orogenic suture basements should be manifested by high density or high gravity anomalies. Conversion of this peridotite, however, to serpentinite during the Stage 1 reactions will produce a much lower density, higher volume rock material.

In the Stage 1 chemical reactions, significant amounts of magnetite are also produced. Consequently, serpentinite reaction products are much more magnetic than their original peridotite reactants. As a function of serpentinization, the magnetic and gravity signatures of peridotitic material are, in effect, 'flipped'.

That is, peridotite parents are dense and nonmagnetic, whereas serpentinitic reaction products have lower density and are more magnetic. With respect to possible basement-derived methane-rich gases, gas fields in the cover sequence should show a geographic relationship to magnetized, low density, mafic/serpentinitic basements.

### **Stage 1 to Stage 2 Fluid Migration from Source to Trap**

Fluid migration from mafic oceanic sources in the basement to the trap environment in the overlying cover

sequence occurs during 'hard crunch' orogenic events. 'Hard crunch' orogenic events typically involve tectonic thickening where regional dynamic metamorphism of the basement is associated with dewatering and devolatilization of the basement and concomitant fluid expulsion from the basement. In terms of timing, the fluid expulsion event probably coincides with the time of peak metamorphism within the basement. Consequently, in terms of assessment of the regional geologic record for the possibility of HTD formation, one must look for periods of peak metamorphism associated with 'hard crunch' style orogenies. Because HTD formation has a strong geologic analogy with MVT formation, the fates of both deposit types can be related to the above-summarized geologic setting. The MVT analogy is especially important because most of the radiometric data that directly dates the fluid deposition events comes from MVT data sets.

**An example from the Northern Appalachian Basin.** The northern Appalachian Basin of New York and Pennsylvania offers an interesting laboratory within which to apply the timing aspects of the herein-developed hydrothermal oil and gas model. One of the major conundrums regarding the formation of the deep, Ordovician-hosted, HTD's in the northern Appalachian Basin has been the timing of fluid formation and migration. Within this part of the Appalachian orogen, three orogenic events are candidates for HTD fluid formation and migration: the Taconic orogeny (450-420 Ma), the Acadian orogeny (400-350 Ma), and the Alleghenian orogeny (320-260 Ma). MVT mineralization is also recognized in this part of the orogen in east Tennessee, Virginia, New York, and Ohio. All of these orogenic events post-date formation of the reservoir rocks (the Trenton-Black River group), which were emplaced in a continental shelf environment during the mid-Ordovician (about 470 to 450 Ma). The HTD and MVT deposits in the above region occur in the foreland of the above orogenies. With respect to the Taconic and Acadian orogenies, the HTDs in south central New York occur beneath the clastic wedge products of these orogenies. As such, burial associated with this sedimentation possibly could create the thermal maturation environment necessary to produce and migrate petroleum-rich fluids from hydrocarbon-rich sources in the clastic wedges.

Another anomalous problem concerning the geologic setting of the HTD deposits in south central New York is their occurrence within thermally over-matured host rocks that exceed the thermal constraints for the oil window and the gas window (Weary and others, 2000). Somehow, it is necessary to account for this overmaturation effect. Obviously, deposition in the context of cooling and condensation in the presence of an originally high temperature, hydrothermal fluid is a possible explanation. Examples are given below that constrain the timing possibilities for such hydrothermal events to intervals of limited duration during the presence of 'hard crunch' orogenesis.

**Evidence for Taconic timing (450-420 Ma).** The Taconic orogeny is associated with the emplacement

of the well-known Taconic allochthon in eastern New York State and Vermont during the Late Ordovician to Early Silurian (Drake and others, 1989). From a petroleum geology point of view, the HTD reservoirs occur in the foreland of the Taconic orogeny beneath its clastic wedge. A good account of this clastic wedge development as it relates to the hinterland of the Taconic orogen in New York and Pennsylvania is given by Zerrahn (1978). An important point about this sedimentary event that has serious implications for petroleum migration and maturation according to the conventional basin evolution model is that, in the area of HTD deposits in New York State, preserved sedimentation of this Taconic clastic wedge is only about 500-600 meters thick. This thickness is well below minimum thicknesses required for petroleum generation and migration (which typically involves sediment thicknesses of 3 to 6 km, using a geotherm of 25°C/km). Consequently, based on post-reservoir sediment thickness, the Taconic orogeny probably did not achieve the thermal maturity necessary to generate petroleum in the vicinity of the currently known HTD oil and gas deposits in south central New York.

Burial by the Taconic (or for that matter the Acadian) clastic wedge also does not explain the telescoped distribution of observed Conodont Alteration Index (CAI) isograds as documented by Weary and others (2000). If sediment thickness is causally related to thermal maturity as indicated by CAI's, then the geographic pattern of isopach lines should be similar to the CAI isograds.

If one wants to invoke Taconic orogeny as the time for HTD fluid formation and migration, then an anomalous regional isotherm or a hydrothermal fluid generation event must be invoked. The Taconic orogeny, however, has been widely characterized as produced by the collision of an offshore oceanic island arc with the proto-edge of eastern North America. These types of collisions can be characterized as 'soft crunch' orogenies, whereby the basement is not subjected to the extensive regional prograde dynamic metamorphism that induces widespread devolatilization of the basement. Consequently, the generation of regional hydrothermal fluid events in the context of 'soft crunch' orogenesis is considered to be unlikely.

The above lack of a regional hydrothermal fluid event is backed up by radiometric data for MVT deposits in this part of the Appalachian orogen. Compared to radiometric dates for MVT deposits in this part of the Appalachian orogen, which show a tendency for both Acadian and Alleghenian timing (see discussion below), MVT deposits here are characterized by a lack of Taconic ages. Consequently, we believe the Taconic orogeny is an unlikely candidate for regional generation of MVT and/or HTD fluids.

**Evidence for Acadian timing (400-350 Ma).** In contrast to a lack of evidence for Taconic timing, abundant radiometric, sedimentological, and tectonic evidence exists for Acadian timing for the HTD deposits in northern Appalachian Basin. Obviously, the best information relating to the timing of fluid migration would be in the form of well-constrained radiometric dates on materials that formed during the reaction sequence at the reservoir site. Minerals that can be dated include illite and/or sericitic mica ( $^{40}\text{K}/^{39}\text{Ar}$  incremental release ages on 2M [highly crystalline] illites), K-feldspar ( $^{40}\text{K}/^{39}\text{Ar}$  incremental release ages and lead isotope ages), sphalerite (Rb/Sr isochrons), or ferroan dolomite (characteristic remanent magnetization [ChRM]). At present, we are not aware of any such technologies applied to the *sensu stricto* HTD model. However, because of the strong geological analogy with hydrothermal dolomite-related MVT deposits, timing of the HTD deposits can be estimated by examining the very robust radiometric data base that has been applied to MVT timing (Symons and others, 1996).

Three main clusters of data emerge from the compilation of radiometric dates: 1) a 355-375 Ma cluster that is coincident with the later stages of the Acadian -Ellesmereian orogenic episode along the eastern margin of proto-North America (Laurentia-Baltica collision) in mid- to late Devonian, 2) a 265-290 Ma cluster that is coincident with the later stages of the Alleghenian orogeny (Laurentia-Gondwanaland collision), and 3) a 95-50 Ma cluster that is coincident with the Laramide orogeny of western North America (plate tectonic interpretations from Scotese and others, 1979). The Appalachian orogen deposits appear to mainly display timing associated with the Acadian event in Middle to Late Devonian. This includes the Polaris MVT deposit on Little Cornwallis Island in Nunavut (formerly Northwest Territories), which yielded a Late Devonian paleomagnetic age of  $367 \pm 7$  Ma (Symons and Sangster, 1991; 1992) and a well constrained Rb/Sr date on sphalerite of  $366 \pm 15$  Ma (Christensen and others, 1995). Newfoundland Zinc has yielded a Middle Devonian paleomagnetic age of  $380 \pm 7$  Ma (Pan and Symons, 1993), as well as a broadly constrained Rb/Sr isochron of  $375 \pm 75$  Ma on sphalerite (Nakai and others, 1993).  $^{40}\text{K}/^{39}\text{Ar}$  release spectra on secondary K-feldspar alteration from the Newfoundland Zinc mine indicate a thermochemical event  $360 \pm 10$  Ma (Hall and others, 1989). In the East Tennessee MVT district, Nakai and others (1993) have obtained Rb/Sr isochrons of  $347 \pm 20$  Ma and  $377 \pm 20$  Ma. Furthermore, Kesler (1996) noted that the area of most intense Devonian-age MVT mineralization in the Lower Ordovician rocks of the Tennessee Embayment is immediately adjacent to the area of Devonian metamorphism in the hinterland to the east.

Acadian-age MVT deposits may also be present in the western part of the North American craton, well to the southwest of the Acadian-Ellesmereian orogenic front. Pine Point in the Northwest Territories yielded fine-grained and colliform sphalerites; these had a wide range in Rb/Sr ratios and yielded a well-constrained age of  $361 \pm 13$  Ma. Incorporation of additional Rb-Sr data for the fluid inclusion fluids

yielded an indistinguishable age of  $362 \pm 9$  Ma with an Sr initial ratio of  $.7086 \pm .0005$  (Nakai and others, 1993). This initial ratio is similar to those of saddle dolomite cements at Pine Point (Qing and Mountjoy, 1994; Qing and others, 1995). In summary, the available radiometric data conclusively establish a significant MVT-related fluid event that affected much of the North American craton west of the Acadian-Ellesmereian orogen. The range of data spans from about 350 to 380 Ma. Significantly, the HTD-hosted gas plays in southern New York occur within the general area of Acadian-aged analog MVT deposits.

Additional evidence for Acadian timing and fluid expulsion from the basement is provided by Acadian sedimentary patterns and Acadian metamorphic ages within the Acadian orogen adjacent to the Appalachian MVT and HTD province. In particular, the Catskill clastic wedge or delta is the major sedimentological expression of the Acadian orogeny, where it was developed in the central Acadian orogen in the eastern United States. If the stratigraphy of the clastic wedge is calibrated to the absolute timescale, the major part of the wedge was developed between 375 and 360 Ma post-Tully Limestone after uppermost Middle Devonian (Isachsen and others, 1991).

The lower 20% or less of the wedge was built in the Middle Devonian, where it post-dated deposition of the Onondaga Limestone, which was the youngest pre-Acadian shelf carbonate (Early mid-Devonian - about 390 Ma). The first part of the wedge is represented by clastics of the Hamilton Group, after which ensued a period of quiescence represented by the Tully Limestone. During the first clastic wedge, the Acadian orogeny does not appear to be kinematically robust. In contrast, 80% of the Catskill delta is developed within a 15 million year interval above the Tully Limestone marker bed. Consequently, the evidence from the Catskill Delta suggests that the major deformation and basin development of Acadian age is Upper Devonian. Metagenic fluid development would most likely be associated with this strong orogenic pulse.

Significantly, the timing for the major portion of the Catskill Delta development (375-360 Ma) coincides with the better constrained dates for the Acadian-aged MVT deposits discussed above. It also coincides with the culminant phases of Acadian metamorphism, which in two areas have yielded ages of around 360 Ma (Dallmeyer and Van Breeman, 1981). Indeed, the orogenic sequence (as developed by Guidotti and others, 1983; Holdaway and others, 1982; and as summarized in Osberg and others, 1989) is impressively consistent with the sedimentological record contained in the Catskill Delta complex. The earliest pulse is related to fold deformation, which is truncated by plutons dated at approximately 394 Ma by Rb/Sr methods. Between 380 and 390 Ma, a number of plutons were emplaced in the core of the Acadian orogen. The plutonism and perhaps the earlier deformation are

associated with deposition of the Hamilton Group in the lower part of the Catskill clastic wedge.

A second pulse of deformation is associated with a younger folding event that deforms the earlier plutons. In two areas in north central Massachusetts and in Maine, hornblende closure temperatures dated by  $^{40}\text{Ar}/^{39}\text{Ar}$  methods are 360 Ma (Dallmeyer and Van Breeman, 1981). This second pulse of deformation coincides with the development of the main part of the Catskill clastic wedge between 375 and 360 Ma. It is the second episode of deformation that we associate with metagenic fluid generation in the Cambrian rifts during metamorphism/serpentinization to zeolite facies/greenschist facies during the Acadian peak orogenesis between 375 and 360 Ma. Migration of these basement-derived fluids during this time may have not only filled up Trenton-Black River HTD reservoirs, but also may have migrated further up-section to deposit gas (mainly) and petroleum within the Silurian Medina Sandstone and the Lower Devonian Oriskany Sandstone, as well as other favorable host rocks within the Catskill delta complex, such as the Upper Devonian West Falls and Canadaway Groups.

Additional tectonic evidence for Acadian age circulation of MVT and possibly related hydrocarbon fluids comes from hydrocarbon emplacements along the Ordovician age Knox unconformity in eastern Tennessee. Haynes and Kesler (1989) quantified the hydrocarbon occurrences at the Knox unconformity, which is penetrated by 794 drill holes. A map of these hydrocarbon occurrences (Haynes and Kesler, 1989, Figure 2) shows that, with respect to Alleghenian-age anticlines, the hydrocarbon-defined fields are at a high angle to the axes of the Alleghenian-age anticlines. This approximately orthogonal relationship suggests that hydrocarbon migration along the Knox unconformity appeared prior to deformation by the Alleghenian folding. If it occurred during Alleghenian folding, the expected hydrocarbon emplacement pattern should be approximately coaxial with the anticlinal axes. In addition, the distribution of organics displays a stronger correlation to paleohighs related to topography developed on the Knox unconformity (Haynes and Kesler, 1989, Figure 5). In terms of timing, Haynes and Kesler (1989) conclude that, "The apparent correlation of organic-rich zones with paleotopographic prefolding features and the lack of correlation with post-deformation structures suggest that hydrocarbon emplacement predated the Appalachian folding ... (Haynes and Kesler, 1989, Figure 7). ... Rather, the relationships are more consistent with earlier emplacement, perhaps in response to the dewatering of the shale-rich Sevier basin in the Devonian-Mississippian, as suggested by Grover and Read (1983), Haynes and Kesler (1987) and Haynes and others (1989)". We concur with the timing argument of Haynes and Kesler (1989), but would add that, based on the foregoing arguments, the fluid formation event occurred in the basement of the Rome trough during the Acadian orogeny.

Interestingly, the period of inferred hydrothermal petroleum-related and MVT-related fluid introduction

during the culminant tectonic pulse of the Acadian orogeny in the central Appalachian region also coincides with conventional basin thickening models for timing of petroleum expulsion and migration. In terms of a conventional sediment thickness versus time estimates for petroleum formation and migration coincide with the hydrothermal model timing presented here. In terms of time-thickness models, the maximum subsidence in the Appalachian basin would have occurred during deposition of the upper portion of the Catskill delta complex, where as much as 8,000 feet of sediment would have been rapidly accumulated during a 15 million year interval in the culminant phase of the Acadian orogeny from 375 to 360 Ma. Underlying organic-rich sources within the underlying section (especially the uppermost Ordovician Utica Shale) would have been matured and fluids expelled during the above orogenic pulse. Consequently, from a timing-migration point of view, there is no difference between the hydrothermal basement-derived and the conventional basin-sourced petroleum system model. The main difference is in the source, where orogenesis affecting basement sources beneath the basin mobilizes and expels hydrocarbon-stable fluids in the manner described above.

Tectonic evidence from the cluster of HTD deposit gas deposits in south central New York State is also consistent with Acadian timing. As can be seen on Figure 16, the known HTD reservoirs in Steuben County and vicinity display a distinct east-northeast or east-west orientation and are associated with synclinal 'sags' in overlying Devonian strata. This pattern is consistent with fluid migration into Riedel-tensile, low pressure environments adjacent to known and inferred northwest-striking faults that may be connected to the underlying basement. A dynamic interpretation of this pattern is consistent with a far-field maximum principal stress ( $\sigma_1$ ) oriented east-northeast to east-west. This orientation fits regional tectonic patterns known for the Acadian orogeny (see Osberg and others, 1989).

Significantly, the far-field maximum principal stress defined by the HTD gas fields is perpendicular to the local far field maximum principal stress indicated for the Alleghenian orogeny, based on the orientation of broad, open folds. These folds gently deform nearby Pennsylvanian coal-bearing strata to the immediate southwest in Pennsylvania. In south central New York, we infer that the graben-sags which host the HTD accumulations became the loci of later synclines that were formed during the Alleghenian deformation. In this regard, it is interesting that the detailed mapping work of Bradley and Pepper (1938), which focused on identification of subtle anticlinal folds in the Devonian sandstones, also identified synclinal features that ultimately coincide with the known HTD gas accumulations. The fact that the HTD gas accumulations coincide with synclinal features suggests that they may have formed in a non-Alleghenian tectonic environment. Alleghenian fluids should have migrated into Alleghenian structural traps, such as the anticlines mapped by Bradley and Pepper (1938). The current HTD gas distribution is consistent with the idea of Alleghenian structural modification of pre-existing



HTD deposits formed during the Acadian orogeny.

**Evidence for Alleghenian timing (320-260 Ma).** Within North America, a second major event of MVT mobilization, as well as attendant HTD emplacement, probably took place during the Pennsylvanian as alluded to above as part of Alleghenian and Ancestral Rocky Mountains orogenies. Abundant age dates in major MVT districts in the central United States have yielded paleomagnetic and radiometric dates that range between 300 and 250 Ma, with a maximum stratigraphic age of 303 Ma, and with a number of dates clustering at around 269 to 260 Ma. The maximum stratigraphic age is set by Pennsylvanian-hosted MVT style mineralization in the Cherokee Shale in the northern Arkansas and Tri-State MVT districts (Symons and others, 1996) and in the Southeast Missouri district, where paragenetically similar lead-zinc mineralization occurs in mid-Pennsylvanian rocks (Leach and Rowan, 1986; Leach, 1994, and Goldhaber and others, 1995 [from Symons and others, 1996]). As summarized in Table 1, a number of radiometric studies provide numerous radiometric dates that fall between 300 and 250 Ma.

**Table 4.1. Alleghenian-age radiometric dates for MVT deposits in the central U.S.**

location	date Ma	method	mineral	reference
central Tennessee	260 ± 42	<sup>232</sup> Th/ <sup>208</sup> Pb	ore stage calcite in Gordonsville mine	Brannon and others, 1996
central Tennessee	249 ± 9	paleomagnetic dating	hydrothermal ferroan dolomite	Lewchuk and Symons, 1996a
central Missouri	303 ± 17	paleomagnetic dating	barite ores	Symons and Sangster, 1991
southeast Missouri	< 297 ± 7	K-Ar	illites in clay pods	Hay and others, 1995
southeast Missouri	300 ± 60	<sup>40</sup> Ar/ <sup>39</sup> Ar incremental release age	authigenic orthoclase overgrowths on K-feldspar	Hearn and others, 1987
upper Mississippi Valley (Wisconsin)	269 ± 4	Rb-Sr isochron <i>Sr I ratio = .70933 ± 2</i>	sphalerite in West Hayden orebody, horizon 17 and 23 (includes fluid inclusion material)	Brannon and others, 1992; Brannon and others, 1996
upper Mississippi Valley (Wisconsin)	277 ± 20	Rb-Sr isochron <i>Sr I ratio = .70958 ± 7</i>	sphalerite in McNulty horizon 6	Brannon and others, 1996
Illinois-Kentucky	277 ± 16	Sm-Nd	fluorite	Chesley and others,

<b>location</b>	<b>date Ma</b>	<b>method</b>	<b>mineral</b>	<b>reference</b>
fluorspar district		isochron age		1994
Tri-State district	251 ± 11	<sup>232</sup> Th/ <sup>208</sup> Pb	calcite in Jumbo mine	Brannon and others, 1996
northern Arkansas	265 ± 20	paleomagnetic dating	ore and host rocks	Pan and others, 1990
Austinville, VA	287	<sup>40</sup> Ar/ <sup>39</sup> Ar plateau age	on 92% authigenic K-feldspar in the Shady Dolomite (Cambrian)	Hearn and others, 1987
Austinville, VA	278	<sup>40</sup> Ar/ <sup>39</sup> Ar total gas age	on 92% authigenic K-feldspar in the Shady Dolomite (Cambrian)	Hearn and others, 1987
near Tyrone, PA	284	<sup>40</sup> Ar/ <sup>39</sup> Ar plateau age	60% authigenic K-feldspar in the Gatesburg Ls. (Cambrian)	Hearn and others, 1987
near Tyrone, PA	288	<sup>40</sup> Ar/ <sup>39</sup> Ar total gas age	60% authigenic K-feldspar in the Gatesburg Ls. (Cambrian)	Hearn and others, 1987
Clear Spring, MD	317	<sup>40</sup> Ar/ <sup>39</sup> Ar plateau age	55% authigenic K-feldspar in Conococheague Ls. (Cambrian)	Hearn and others, 1987
Clear Spring, MD	314	<sup>40</sup> Ar/ <sup>39</sup> Ar total gas age	55% authigenic K-feldspar in Conococheague Ls. (Cambrian)	Hearn and others, 1987
Jefferson City, TN	322	<sup>40</sup> Ar/ <sup>39</sup> Ar plateau age	56% authigenic K-feldspar in Maynardsville Ls. (Cambrian)	Hearn and others, 1987
Jefferson City, TN	315	<sup>40</sup> Ar/ <sup>39</sup> Ar total gas age	56% authigenic K-feldspar in Maynardsville Ls. (Cambrian)	Hearn and others, 1987

Significantly, the geographic distribution of Alleghenian dates places the dated MVT deposits within

the mid-continent region of the central United States largely within the Mississippi Valley drainage net. Geographically related HTD's that occur in the same area as Alleghenian age MVT deposits include the well-known Albion-Scipio field in southern Michigan and the geographically widespread hydrothermal dolomite mineralization in the Trenton-Black River section in northern Indiana, as well as Trenton-Black River-hosted dolomitization in northern Kentucky near the Kentucky-Illinois fluorspar district. Widespread hydrocarbon production along the Cincinnati Arch that is hosted in Cambrian-Lower Ordovician Knox Group may be related to distal fluids that originated from MVT sources in the Jessemine Dome and Nashville Dome of north central Tennessee and south central Kentucky.

Compared to the area of MVT's in cospatial HTD systems, the regional cluster of Alleghenian MVT's and HTD's occur west of the Acadian deposits. The westward displacement of the Alleghenian MVT-HTD province is in concert with the westward displacement of the Alleghenian orogenic front relative to the Acadian orogenic front. Consequently, the westward shift of Alleghenian orogenesis relative to Acadian orogenesis seems to be coupled with a westward shift of basement-related or basemen-derived metagenic fluids that formed Alleghenian age MVT's as well as nearby HTD's. Basement sources could be related to conduit systems beneath the Cincinnati Arch, the Kankakee Arch, the Michigan Basin, and the northeast-striking Reelfoot Rift in northeastern Arkansas, southeastern Missouri, and western Kentucky.

There is, however, evidence for Alleghenian fluid migration that geographically overlaps with the Acadian hydrothermal fluid events. Hearn and others (1987) have shown that authigenic feldspars in Cambro-Ordovician carbonate-dominated strata in the region affected by Acadian-age fluids have yielded Alleghenian ages between 278 and 322 Ma (Late Mississippian to Pennsylvanian) (Hearn and others, 1987, Figure 1). Some of these fluids may be responsible for forming additional ferroan dolomites of Alleghenian age. While there does seem to be evidence of a reintroduction of Alleghenian age hydrothermal fluid phenomena, most of the direct dates on ore deposit minerals in this region have yielded Acadian dates, as noted in the discussion above. The overall lack of thick Alleghenian clastic wedges (Hatcher and others, 1989) in the sense of the Upper Devonian Catskill clastic wedge also suggests that basin thickening and strong orogenic tectonism were less intense in this area compared to the Acadian event. While we strongly prefer Acadian timing for MVT and HTD deposits in the Appalachian Basin, the presence of authigenic, Alleghenian-age feldspar provides a caveat whereby we cannot exclude HTD formation in the Appalachian Basin during the Alleghenian orogeny.

It is interesting that the MVT dates and authigenic feldspar dates compiled in Table 1 cluster towards the old end of the Alleghenian orogeny (about 315 to 275 Ma), whereas the total span of the

Alleghenian orogeny occurs between about 330 to 250 Ma. These dates coincide with the main stage of the deposition of the main portion of the clastic wedges formed during Alleghenian orogeny, which occurred during the early portions of the orogeny during Late Mississippian to Early Pennsylvanian time. This is evidenced in the deposition of the Mauch Chunk - Pottsville clastic wedge in eastern Pennsylvania and the Pennington-Lee clastic wedge in the Tennessee salient (Hatcher and others, 1989). The MVT dates also coincide with timing of Alleghenian deformational phases in the metamorphic cores of the Appalachian orogen. For example, dates in the Kiokee Belt and adjacent lithotectonic belts in South Carolina-Georgia are dated between 315 and 292 Ma; in the Lake Murray area and on the Irmo shear zone, Late D-4 deformation occurred prior to 260 Ma, but after about 290 Ma (see discussion in Hatcher and others, 1989, for details). These events in the southern Appalachians generally lie directly east of the MVT province in the Mississippi River basin and, as such, could represent the thermogenic drivers for metagenic MVT- and HTD-related fluid generation within the basement in the foreland of the southern Appalachian orogen.

**Evidence for Mesozoic timing.** One other explanation has been recently proposed for the high thermal maturity pattern that may be associated with HTD gas formation -- heat flow associated with the emplacement of Mesozoic age, ultramafic intrusive complexes into the area of the Rome trough (Weary and others, 2000). Specifically, Weary and others (2000) cited the kimberlitic dikes in central and eastern New York (Kay and others, 1983) as possible manifestations of an elevated geothermal flux of Jurassic - Early Cretaceous age (140-150 Ma). We regard this as unlikely, due to the fact that kimberlitic ultramafic intrusions are invariably associated with small, low volume diapirs that would have limited thermal mass. No batholiths of kimberlite composition are known.

**Tectonic trigger for migration.** It is apparent from the timing discussions above that the orogenic context is one of strong compressive orogenesis where the basement becomes actively involved in deformation, where dynamic regional metamorphism is associated with devolatilization/dewatering steps at metamorphic grade changes and with crustally generated peraluminous magmatism. Fluid expulsion, ascension, and migration are controlled by far-field compressive stress field operant during peak orogenic phases of convergent, contractional orogenies (continental assemblies, arc accretions, and flat Cordilleran subductions).

There are at least two and possibly three 'hard crunch' styles of compressive orogenesis in which the continental basement actively participates in the orogenesis. All three involve low-angle tectonic fusion of various crustal-scale, tectonic plates. The first and most familiar is the tectonic setting of continent-continent collision. The second, somewhat familiar, tectonic setting is that of an island arc with tectonically matured basement (Japan-like)

colliding with another continent or tectonically mature island arc. The third, less familiar, 'hard crunch' basement-involved style is that of flat subduction of an oceanic plate beneath a continental plate (such as the latest part of the Laramide orogeny beneath southwestern North America or, less familiarly, the ancestral Rocky Mountains of southwestern North America as attributed to flat subduction by Wo and Burchfiel, 1996).

The above 'hard crunch' style of orogenesis can be contrasted with 'soft crunch' orogenesis that involves collisions of oceanic island arcs and adjacent Unit 1 and Unit 2 oceanic crust with the edges of continental cratons. In these 'soft crunch' events, stress is not transmitted into the craton. Instead, the craton typically passively underthrusts a highly crumpled upper plate of upper oceanic crust and shelf margin material. Almost all of the deformation is restricted to the upper plate, where the deformation locally consists of spectacular, large-scale, recumbent folds of nappe dimension, with intervening thrusts parallel to axial surfaces of the folds. The continental margins typically act as a buttress, which the oceanic material attempts to overthrust, but does not deform. Sedimentation and deformation within the continental interior typically do not respond to the 'soft crunches' at the margin. An excellent example of the above "hard crunch" versus 'soft crunch' scenarios that has lessons for HTD and MVT type metagenic fluid systems is the orogenic framework of North America during the Carboniferous.

**Tectonic driver for migration.** The dynamics of fluid flow, as in conventional petroleum models, is from high to low pressure. Two main contributing triggers for migration are regional compression and expulsion of fluids during metagenic dewatering. The typical tectonic setting of the fluid migration is one of transpression that is at an angle to major pre-existing structures, but not in thrust fault situations. The regional stresses are oriented at an angle to the basement anisotropy, so that tensional gaps open to allow fluid migration. Tectonic drivers are far-field compression with fluid flow from high to low pressures. The driving pressures include the static pressure of sediment load, tectonic pressures, and expulsion forces from the metagenic dewatering process. This is in contrast to hydrofracing where the fluid stays in the created pore space and is disseminated regionally

**Conduit architecture.** The conduit architecture consists of large, high-angle, through-going, strike-slip basement faults that connect the basement to cover sequences and of riedel/tensile shear zones splaying off of the main strike-slip fault features. In plan view, these strike-slip 'ascension zones' display curved trajectories from the basement source to the trap site. Dip-slip 'ascensions' display linear trajectories from basement to trap in plan view; they display curved or anveled trajectories in cross-section.

**Constraints imposed by crustal oxidation state.** During the development of the Magma-Metal Series

Classification, it was recognized that fluids in the crustal basements of tectonically matured cratons played an extremely important role in porphyry magma genesis (Keith and others, 1991; Wilt, 1993, 1995; Keith and Swan, 1996). In addition to hydrating magmas via implosion in the mid-crust into hornblende-bearing magmas that are hydrous enough to fractionate porphyry metal expressions, fluid metasomatism of the incoming magmas also controlled the oxidation state of the magma by equilibrating it with the oxidation state of the wall rocks with which the imploding fluids had been in oxidative equilibrium.

It was also observed that fluids in equilibrium with reduced crust seemed to be in equilibrium with reduced hydrocarbons, which also may have been imploded into the magma. More importantly, however, these reduced fluids prevented hydrogen loss from the magma (hydrogen loss is the principal mechanism of magmatic oxidation). Porphyry metal expressions expelled from reduced magmas, as a result, are much more hydrogen-rich. Significantly, a large number of hydrocarbon occurrences (mainly as methane, pyrobitumen, and locally hydrothermal oil) have been documented from gold and tin metal deposits that are spatially and temporally associated with reduced magmas of various types.

It also follows that in the context of production of metagenic fluids from various crusts at different oxidation states that hydrogen and reduced hydrocarbon speciation will be strongly controlled by the oxidation state of the crust. In effect, crustal oxidation state may represent an entirely new geologic control for the stability of the well-known 'oil window', in addition to temperature. Another important parameter that may allow petroleum occurrences to be stable under hydrothermal conditions at elevated temperature is pressure. Recent results (Berndt and others, 1996; Horita and Berndt, 1999; Apps and van de Camp, 1993; Burruss, 1993; Houseknecht and Spotl, 1993) have shown that experimentally and empirically, methane in particular is stable in mid- to deep crustal environments at elevated temperature and pressure. We add that in all of the above contexts, the stability of oil and gas is strongly dependent on reduced crustal oxidation states.

In terms of the multi-staged model proposed here, wall rock oxidation states in the immediate vicinity of all the processes (Stage 1 source, Stage 1 to 2 migration, and Stage 2 through 5 depositional sequences within the trap site), the wall rock oxidation state must be equal to or less than 0.6 as expressed by the ferric:ferrous iron (as calculated from  $\text{Fe}_2\text{O}_3/\text{FeO}$ ).

## **Stage 2. Initial Dolomitization (Sucrosic) of Shelf Limestone Near Depositional Site**

**General considerations.** Once the fluids have originated in the basement, they ascend into the cover sequence through high-angle faults that typically are operating in a transcurrent tectonic regime (strike-slip faults). Where

they encounter what is typically the first (earliest) major shelf carbonate stratigraphic permeability above the basement fluid sources, the fluids tend to utilize this stratigraphic permeability where it intersects the footwall of the propagating basement structure. Biohermal facies within these shelf carbonates (especially porous reef facies) are especially conducive to fluid ingress. Once the fluids encounter the limestone, a major process of dolomitization takes place. This initial dolomitization is modeled by the reactions which incorporates as much relevant empirical data (fluid inclusion composition, salinities, strontium isotopes as possible).

**Initial sucrosic dolomitization.** The obvious feature of the initial fluid ingress into and near the emplacement site is extensive dolomitization. Indeed the dolomitization effect may be subregional in scale. For example, the initial dolomitization in southern and southeastern Alberta of the original Wabamun Group carbonates covers an area of 188,000 sq. km., where some 290 billion metric tons of dolomite were produced from original Devonian-age carbonates (Packard and Al-Aasm, 2002). Of more relevance to New York State, drilling in northern Indiana indicates that the entire northern third of the state has experienced dolomitization at the Trenton-Black River stratigraphic level over an area of about 34,500 sq. km (Yoo and others, 2000). This area extends into the Michigan Basin to the north and into Illinois to the west. The early initial passive dolomitization affects about twice as much rock as the later high-temperature, typically ferroan dolomitization event, based on cross-sections in Yoo and others (2000). Consequently, we used a 2:1 mole ratio for early sucrosic dolomite:later hydrothermal saddle dolomite. Thus one mole of non-ferroan dolomite is reacted with bicarbonate components of the incoming bicarbonate-chloride brine.

A number of important chemical aspects of the dolomitization reactions constrain genetic interpretations of HTD petroleum deposits. The first point regards the crystal chemistry of the dolomitization. While virtually all of the literature points out that significant amounts of magnesium are added, not so emphasized is the fact that the stoichiometry of the reaction requires an additional carbonate ion for each calcite molecule reacted. Hence, the fluid component must not only be enriched in magnesium, but it also must contain a carbonate ion component in excess of that required to make dolomite. Consequently, dolomitization is a process of significant, massive, magnesium and carbonate metasomatism. Hence, dolomitization is more a process of metasomatism than it is of dissolution. Indeed, the calcium atoms are preserved during the dolomitization and are not removed. The ultimate point here is that void space is not created by dissolution and removal of some kind of atomic mass, but rather, it is ultimately created by the atomic properties of the metasomatizing agents. Probably the most important atomic property is that the ionic radius of the magnesium atom is less than three-fourths that of calcium (.74 for  $Mg^{+2}$  and 1.04 for Ca) (Bloss, 1971).

Thus, in terms of ionic radii of atomic constituents, unit cell lengths, and density, the dolomite molecule occupies

significantly less space than the calcite molecule. As Deer, Howie and Zussman (1992) put it, a good approximate comparison of dolomite versus calcite molecules is that the dolomite molecule consists of one layer of calcite and one layer of magnesite ( $\text{MgCO}_3$ ). In terms of a qualitative comparison, if the layers are assumed to be the thickness of the cation ionic radii, then the dolomite layered molecule is 1.17 times less thick than a corresponding calcite molecule. In terms of three-dimensional reconstructions, dolomite occupies 13 % less spatial volume compared to the calcite molecule. Magnesite occupies about 24% less spatial volume compared to the calcite molecule.

The mechanism of creating void space by metasomatic replacement is different than karstification, which refers to creation of void space by dissolution and removal of mass by either low temperature meteoric waters (meteoric karsting) or high-temperature waters (hydrothermal karsting). Because this metasomatic replacement is accompanied by active transpressional tectonics, which is imposing a dilational strain on the replaced volume and is intimately coupled with the metasomatic reaction described above, we refer to this space creating process as 'metasomatic dilation'. Correspondingly, we refer to the sucrosic planar dolomites as replacive/metasomatic 'epigenetic dolomites' to distinguish them from syn-sedimentary 'syngenetic dolomites', which are formed in the context of syn-chemical sedimentary processes that may involve a component of early diagenetic magnesium, lower temperature replacement of incompletely limy muds or direct chemical precipitation of dolomite in situ. These dolomites typically have a much finer grained, micritic texture, as contrasted with the coarser grained sucrosic texture of the metasomatic, epigenetic dolomites.

The metasomatic dilation process referred to above, in conjunction with tectonic dilational enhancements, are sufficient to create the void space needed to subsequently fill with MVT sulfides and high temperature saddle dolomites or HTD petroleum products and high-temperature saddle dolomites. No karstification is necessary; however, if dissolution processes are operative at this stage, they simply enhance the void creating process. It should be pointed out, however, that the concept of hydrothermal karstification is conceptually at odds with metasomatism, as it implies dissolution and removal of mass. In contrast, metasomatism necessarily implies the addition of chemical mass, accompanied by rearrangement of chemical components into crystal structures that are denser and stable at higher temperatures. The creation of void space via metasomatic reactions, like karstification, can subsequently lead to collapse structures, such as collapse breccias, collapse sags, and collapse caves. These features may show up as U-shaped seismic indentations in otherwise continuous planar seismic reflector horizons.

Two other important chemical features take place during dolomitization, in addition to the creation of void space. The first feature is an increase in salinity due to release of other metal ions, such as sodium from their bicarbonate



complexes. The second feature is that under reduced conditions, dolomitization can result in the production of significant methane and other high rank hydrocarbons.

Salinity data from fluid inclusions indicate that the early stage of sucrosic hydrothermal dolomite (HTD) evolution occurs at lower temperatures (50 - 110°C) and lower salinities (3 to 17 wt.% NaCl equivalent) in contrast to the higher temperature dolomites produced during stage 3. The stage 2 chemical reaction demonstrates that significant salinity increases can occur during stage 2 sucrosic dolomitization. The increase in salinity is produced by a release of metal ions from bicarbonate and/or hydroxyl complexes. The carbonate is generally used up making the extra carbonate anion radical in the dolomite. Throughout the reaction, chloride complexes are progressively made at the expense of HCl. Salinities correspondingly increase from a value of 6.7 to 14.5 %, at which point the temperature increase and the disappearance of available limestone reactant led to stage 3, high temperature, hydrothermal dolomites, which include saddle dolomites and other non-planar dolomites.

The above chemical fractionation model eliminates the requirement for two distinct fluids and two distinct episodes of hydrothermal fluid ingress. The chemical fractionation model is in much better accord with the worldwide consistency of the paragenetic relationship and ordering between initial, low-temperature sucrosic dolomite followed by a high-temperature saddle dolomite stage. If the two-fluid model were real, one would expect to see many cases of reversal, where the sucrosic dolomites replace high temperature dolomites as the fluid origins and histories would have been independent. The consistent paragenetic ordering, however, implies some dependent necessary chemical fractionation between the early sucrosic dolomites of stage 2 and the later saddle dolomites of stage 3.

The third byproduct of dolomitization has significant economic implications. The sub-reactions of the dolomitization and the increase in salinity/chlorinity both create hydrogen gas. This sub-reaction removes a significant amount of oxygen from the fluid as carbonate into dolomite. Consequently, the H:C ratio of the fluid component increases throughout the dolomititic reaction. Because the fluid is already hydrocarbon stable as it enters the depositional environment, the hydrogen gas is free to react with the carbon dioxide component. Reduction of the carbon dioxide component produces additional methane, using the Fischer-Tropsch reaction. Methane production occurs in the context of an increasingly reduced and neutralizing fluid component.

A considerable amount of methane is made during this reaction. When factored over rock volume, a truly enormous amount of methane can be generated by this inorganic reaction process. For example, in the case of the Wabamun Group in Alberta, 390 billion metric tons of metasomatic dolomite was produced (Packard and Al-Aasm, 2002). If this dolomite was produced by chemical reactions similar to that described above, then 37.1

billion tons of methane was also produced. It is important to point out that other high temperature petroleum products were probably generated during the methane production. Hydrocarbon material is common as carbon-rich zones in the sucrosic dolomites and is texturally demonstrated as zoned dolomite crystals containing dark hydrocarbon-rich zones. Bitumens commonly occur in the pore spaces as well.

The temperature range of this sub-reaction (50-110°C) places much of the hydrocarbon generation within the early oil window (88 - 123°C from Figure 13 of Hulen and others, 1999, with an application to hydrothermal oil in Carlin gold-type settings). Because the rocks were being progressively heated during this step, much of the initial oil generation may have been thermally degraded into pyrobitumens by the later stage 3, high-temperature dolomite step. However, in many occurrences as indicated by the fluid inclusion data, temperatures which accompanied the stage 2 higher temperature dolomite step do not exceed the high temperature end of the oil window, which is about 160 to 190°C. The 'bottom line' is that a considerable amount of oil can be made and migrated during this early stage heating event. Some of this oil may be tectonically pushed ahead of the high temperature portions of the thermal plume and could be trapped in up structure positions at the edges of the thermal anomaly. In stage 4 reactions where hydrocarbon deposition accompanies sulfide deposition, if CO<sub>2</sub> is reduced by hydrogen gas along Fischer-Tropsch reaction lines, four times as much HC component is generated compared to methane, because much less hydrogen is needed to reduce the carbon component to HC. Thus, the oil generating potential of this stage 2 event should not be underestimated.

In fact, the overall hydrocarbon generation modeled was fairly conservative. Hydrocarbon stability as methane and other higher C number gases was experimentally generated when the H<sub>2</sub>:CO<sub>2</sub> ratio equals 1. We consider the methane, and by implication overall hydrocarbon, generation potential achievable to be considerably greater than that modeled by the dolomitization reactions.

**Isotopic mixing.** An important aspect of our modeling incorporated an assessment of the virtually universal relationship between strontium isotopes and the dolomitization. In North America it has been documented in a multitude of case histories (for example, Yoo and others, 2000; and numerous examples cited in Davies, 2000) that the early stage dolomites of a given HTD occurrence exhibit strontium isotopes near and slightly greater than the seawater equivalent for the time period, whereas the later stage 3 higher temperature HTD exhibit strontium initial ratios noticeably more radiogenic than the stage 2 sucrosic dolomites. To test whether or not the strontium isotopic data fits the fluid fractionation model presented here, we incorporated data from a case history that is relevant to the New York region: the fluid inclusion and isotopic characterization of epigenetic dolomites for the Trenton and Black River limestones in northern Indiana by Yoo and others (2000). Specifically, we used a strontium initial ratio of .7083, which represents an end member mixing composition for both Ordovician seawater and the

strontium isotopic composition of planar, non-ferroan dolomite (sucrosic) as well as one sample of planar, ferroan dolomite and Type I dolomite cements associated with planar dolomites. We used a strontium initial ratio of .7098, which represents the upper end of strontium isotopic compositions for high-temperature, non-planar, ferroan hydrothermal dolomites within the Trenton-Black River section.

Based on the balanced reactions and a mixing calculation, a strontium initial ratio of .7090 was obtained for the stage 2 dolomite after all of the initial limestone had been reacted to dolomite. An intermediate compositions at 50% of the reaction completed (.70865) was also calculated between the initial seafloor equilibrated limestone and the final 100% reacted dolomite product. The intermediate initial strontium ratio indicates the progression of the process, whereby the buffering effect exerted by the wall rock systematically decreases throughout the reaction.. In any case, the .7083 to .7090 range strongly corresponds to the empirical data for 4 planar dolomite samples and one Type I dolomite cement sample reported by Yoo and others (2000), which ranged from .70833 to .70902. According to the chemical fractionation model presented here, the intermediate values reported by Yoo and others (2000) represent various intermediate compositions that indicate the degree of dolomitization towards the end member.

**Table 4.2. Isotope mixing calculation:**

<b>formula units (f.u.)</b>	<b>original Sr initial ratio</b>	<b>formula units x Sr I</b>
100 f.u. of calcite	.7083	70.83
50 % reacted (142 f.u. of dolomite)	.70865	65.23
184 f.u. of final dolomite product	.7090	$130.4 / 184 = .7090$
84 f.u. of fluid component reacted	.7098	59.62

In summary, the mixing calculation in the context of a chemically fractionating carbonate/chloride brine shows that a one-fluid model also explains the strontium isotopic data. Hence, two fluids of different origins are not required. When integrated with the paragenetic consistency over a globally applicable observation, the one-fluid model appears to be a simpler alternative explanation.

Another major observation that strongly argues for an evolving, chemically fractionating, single-fluid model, is the systematic geographic variations in both the strontium isotope data and the physical thickness data for both sucrosic and high-temperature non-planar dolomites in northern Indiana. Stratigraphic sections taken from Yoo and others (2000) show that physical thicknesses of both non-ferroan planar sucrosic dolomite and ferroan non-planar high-temperature dolomite increase towards the northwest. This northwestward thickening can be interpreted to imply that the fluid plume initiated in the northwest and migrated southeastward.

The above interpretation is supported by the strontium initial ratio data, with one exception (the planar, non-ferroan dolomite sample in drill hole 801). Eight Sr initial ratio determinations for both early planar and later non-planar dolomites show a consistent southeastward decrease in the radiogenic strontium component in Indiana (Yoo and others, 2000). We interpret the radiogenic strontium enrichment toward the northwest as evidence for increasing proximity to the radiogenic source of the strontium. In terms of the broader model, this radiogenic strontium would have been brought to the Trenton-Black River strata by a basement brine originating from a source to the northwest of the drillhole section. These fluids would have presumably utilized a high-angle fault connector between this more radiogenic basement and the Trenton-Black River replacement datum in the overlying Paleozoic cover sequence. The basement source may also be expressed by a magnetic anomaly as suggested by our modeling. Initial flow toward the southeast of the brine into the Trenton-Black River section in northern Indiana produced the low-temperature dolomites. Once the limestone was completely reacted, the high-temperature hydrothermal dolomites filled up pore space mainly in the Trenton section (especially at its contact with the Cincinnati age [Upper Ordovician] Maquoketa Shale unit) as will be developed in our discussion of stage 5. Substantial amounts of fluid may also have reacted with clay components of the Maquoketa Shale to produce an illitic halo effect in the stratigraphic hanging wall.

### **Stage 3. Early and Late Saddle Dolomite Formation At and Near Depositional Site**

Extensive methane gas (+/- dead oil [pyrobitumens]) is produced during hydrogen reduction during dolomitization (both during the early replacive sucrosic stage and during the later ferroan, high temperature, metasomatic dolomite stage). These reactions also generate anhydrite, carbon dioxide effervescence, hydrogen loss, and methane unmixing. The ferroan dolomite includes fracture cement and zebra fabrics, plus quartz (silica) and brines. During this stage, ferroan saddle dolomite is precipitated in void space, acid components are neutralized, carbon dioxide is reduced, methane is generated, water is generated, and salinity increases. The crustal oxidation state in reservoir sites must be reduced (wall rock oxidation states  $\leq 0.6$ ) to maintain hydrocarbon stability during depositional reactions and preserve hydrocarbon stability after the hydrocarbons are deposited.

#### **Stage 4. Sulfide Deposition and Hydrocarbons Development**

In Stage 4, deposition of sulfides is accompanied by sulfate reductions and hydrocarbon forms from carbon dioxide reduction in the Fischer-Tropsch reaction. An oxidized residual hydrothermal fluid is developed during this stage. Fluids 'cool' into the upper oil window during the anhydrite-sulfide depositional step where various amounts of live oil, dead oil, and gas condensate are produced by catalytic reactions across sulfide interfaces.

#### **Stage 5. Deposition of Late Calcite at Depositional Site and Illite/Smectite/Kaolinite Clays At and Near Depositional Site**

Stage 5 consists of deposition of late calcite at the depositional or trap site and of illite/smectite/kaolinite clays at and near the depositional site. These reactions are accompanied by development of low temperature, lower salinity fluids. The nontronite (smectite clay) plus kaolinite is the wall rock clay component in silici-clastics. These reactions are also accompanied by precipitation of hydrothermal quartz or silica (commonly mistaken for chert), deposition of marcasite plus native sulfur, production of calcite from the remaining CO<sub>2</sub>, and reaction of the wall rock component to produce sodium-illite, and the production of methane from reduction of HC by H<sub>2</sub> gas.

Fluids continue to ascend into the shale caprock 'seals', where extensive illitization of the diagenetic clay component (mainly montmorillonite-kaolinite) takes place. Here also, generation of oil and gas occurs in the middle range of the oil and gas window. These reactions are accompanied by salinity lowering due to loss of Na, Ca, and K fluid components into the illite-clay reaction products. Late calcite carbonate cement and void fills are also produced.

The overall geometry of the trap site may be stacked with a 'tight' oil-gas deposit trapped in overlying shale caprock and methane-CO<sub>2</sub> rich gas with minor oil and much pyrobitumen trapped in the lower HTD 'reservoir' rock. Ultimate 'stacking' is expressed by gas transfer of small quantities of anomalous hydrocarbon gas, carbon gas, water, hydrogen, metals, and halogens into the cover sequence above the reservoir areas. The original chemical fractionations in the reservoir sites are recorded by geographic zonation of the elements in surface soils. The duration of this geologic process is 'geologically short'. The entire petroleum system formation episode (generation at source, migration to trap, and accumulation in traps) takes place during culminant/peak orogenic intervals that typically occur over a ten million year time interval.



## **5. EXPLORATION IMPLICATIONS AND APPLICATIONS OF STRIKE-SLIP FAULT KINEMATICS AND HYDROTHERMAL PETROLEUM FLUID CHEMISTRY**

Practical exploration techniques result from the application of the science developed in the previous chapter in a practical, generic exploration model. Exploration implications of the model are summarized below under the same headings of the staged hydrothermal petroleum fractionation sequence developed in Chapter 4.

### **STAGE 1 - SOURCE – STAGE 1 SERPENTINIZATION OF MAFIC OCEANIC CRUSTAL MATERIAL UNDER REDUCED CONDITIONS.**

#### **Tectonic Setting and Drivers of Stage 1 - Source**

The tectonic setting of the source is serpentinitized, mafic oceanic materials (especially peridotite) located in failed rifts or orogenic sutures within basements of tectonically matured cratons. Serpentinization of peridotite at the zeolite-greenschist facies transition at about 300° C and 1.5 to 3 km depth during 'hard crunch' compressive orogenesis (continent-continent collision or flat Laramide-style subduction) induces metagenic, hydrothermal fluid generation from the basement.

Serpentinization reactions are caused by carbon dioxide- metal- chloride-charged, low pH brines derived from hydrolysis of zeolite facies minerals in formerly weathered (seafloor weathering), oceanic crust and interstitial oceanic waters trapped in layer 1 and layer 2 oceanic crust. Serpentine, brucite, magnetite are the main reaction products. Methane and hydrogen are stable species within the brine reaction products.

#### **Geophysical Features of Stage 1 - Source**

The geophysical signature of Stage 1 processes is a characteristic lateral and vertical relationship between gravity lows and magnetic highs that indicate a serpentinitized, former peridotite from an oceanic rift setting. Serpentinization causes a major increase in magnetic susceptibility and a major decrease in density. Serpentinized basement is geophysically expressed in cratonic areas as linear zones of low density and high magnetic expressions. Deposition of low density sediments within rift troughs may enhance the density contrast with higher density rift shoulders.

## **STAGE 1 TO 2 – MIGRATION – STAGE 1 TO STAGE 2 FLUID MIGRATION FROM SOURCE TO TRAP.**

### **Tectonic Setting and Drivers of Stage 1 to 2 - Migration**

Reactivation of suture/failed rift, high-angle, basement fracture systems typically forms within a transpressive context by far-field, horizontal compression. This compression affects the cratonic basement in the foreland of a hard-crunch collision or affects the cratonic basement above 'hard crunch', flat-subducting oceanic lithosphere. Partial basin inversion may occur in the case of intracratonic autochthens.

A decrease in density and expansion of rock volume is associated with conversion of peridotite and this promotes fluid expulsion from oceanic source material. This fluid is expelled into the conduit system that links the basement source with stratigraphic (first shelf limestones) and/or structural (commonly riedel-tensile permeability) traps in cratonic cover sequences above basement sources.

Pressure in the context of a regional, 'far-field' stress field is typically a transpressional, far-field, dynamic setting. Flow is from high pressure source to low pressure traps (commonly riedel-tensile permeability). Flow lines approximate regional or local  $\sigma_2$  axes.

### **Conduit System of Stage 1 to 2 - Migration**

High-angle faults connect the basement source to the reservoir site in the first shelf carbonate horizon in the cover sequence above the basement. Faults may be propagated upward into the cover sequence. Riedel-tensile permeability may propagate into carbonate reservoir sites via high fluid pressure, wedge-style, hydrofracturing within a transpressive domain that envelops the upward propagating basement fractures. Transcurrent or strike-slip faults that transect the basement suture/rift system at high angles may be especially important conduits.

Transcurrent faults which intersect rift/suture features at high angles will display variable amounts of gravity and magnetic contrast, depending on gravity and magnetic properties of the basement wall rocks. The conduit-system, high-angle fault net can also be identified by seismic imaging where intra-rift basin-fill sediments will typically display strong reflectors that are truncated by high-angle fault features against relatively unreflective, seismically isotropic, crystalline basement. High resolution gravity and magnetic techniques and data may be especially useful in identifying conduit architecture in the absence of more expensive but higher resolution seismic data.



Brines that ascend through the conduit system are bicarbonate-charged, low pH, moderate salinity brines. Under reduced conditions, these brines are methane- and hydrogen-rich. These fluids leave geochemical evidences of their passage.

### **Geophysical Features of Stage 1 to 2 - Migration**

The conduit system is parallel to rift/suture features in the craton and will typically display strong magnetic and gravity contrasts with adjacent cratonic basement. Rifts may be manifested as either elongate, low-density anomalies or elongate, high-density anomalies in areas where unaltered, high-density, mafic crust predominates. The low-density anomalies result from a combination of serpentized, mafic 'oceanic' crust or low-density, intra-rift basin fill; the high-density anomalies result from layered mafic intrusions. Elongate magnetic highs may be associated with zones of magnetite-rich, serpentized mafic materials in suture/rift zones or with elongate magnetic lows associated with unaltered, non-magnetic mafic crust (e.g. peridotites).

Petroleum accumulations are preferentially associated with reservoirs in cratonic cover sequences immediately above or adjacent to underlying suture/rifts where magnetic highs overlap gravity lows, which indicate strong serpentization of ultramafic crust in the underlying rift/suture basement.

### **STAGE 2 – REGIONAL SUCROSIC DOLOMITIZATION OF HOST LIMESTONES IN THE GENERAL VICINITY OF RIEDEL-TENSILE STRUCTURAL TRAPS.**

#### **Tectonic Setting of Stage 2 - Sucrosic Dolomitization**

The tectonic setting for the Stage 2 - sucrosic dolomitization/trap is in the first replaceable calcitic carbonate horizon in the cover sequence above buried rift/suture features in the cratonic basement. Unconformities between the limestone sequence and the overlying siliciclastic horizons are especially susceptible to dolomitization.

During dolomitization, about 13% more void- or open-space is created. In areas of high fluid pressure and/or hydrodynamic fracturing, extensive collapse and dissolution may take place. This process of creating void space is also termed hydrothermal karstification. Additional high-temperature dolomitization may occur at the sites of fracturing, collapse and dissolution.

Initial, low temperature, planar, sucrosic dolomitization is commonly of subregional extent and may occupy or affect areas from about 13,000 square kilometers to greater than 230,000 square kilometers.

### **Chemical Features of Stage 2 - Sucrosic Dolomitization**

Stage 2 dolomitization reflects the process of magnesium and calcium carbonate metasomatism. In this process, calcitic carbonate is reacted to dolomite in the presence of moderate salinity, low pH, bicarbonate brines of moderate temperature (200 to 300°C) and in stability fields that include hydrothermal hydrocarbon. Under reduced conditions, additional hydrocarbon reaction products are produced via bicarbonate breakdown, which liberates hydrogen to react with carbon dioxide to make methane and/or pyrobitumens via Fischer-Tropsch synthesis. Methane production during dolomitization is more than enough to account for the volume of hydrocarbon present in HTD reservoirs.

Release of metal cations during dolomitization and recombination with chlorine released during neutralization of the acid brine component results in a salinity increase during Stage 2 dolomitization. Progressive replacement of the limestone isotopic component by the isotopically spiked, basement isotopic component also occurs. The isotopes of radiogenic strontium and stable isotopes of oxygen, sulfur, and carbon are the best known examples. Basement isotopic components may become more prominent near conduit ‘feeder zones’ that are connected with the basement isotopic source(s).

### **STAGE 3 - TRAP – STAGE 3A “HIGH” TEMPERATURE FERROAN HYDROTHERMAL DOLOMITIZATION IN IMMEDIATE VICINITY OF RIEDEL-TENSILE STRUCTURAL TRAPS OR REVERSE FAULT/ANTICLINAL STRUCTURAL TRAPS**

#### **Tectonic Setting of Stage 3A - Hydrothermal Dolomite (HTD)**

The tectonic setting for Stage 3A formation of high-temperature, ferroan, hydrothermal dolomite is within the first limestone horizon above basement and in the immediate vicinity of ‘feeder’ conduits that propagate into the cover sequence. These settings are within typically transpressive subdomains that are associated with basement fractures oriented at oblique angles to the far-field regional compression. They are associated with ‘hard crunch’ style orogenesis (e.g. Albion-Scipio, Michigan). Less frequently, these settings occur within typically compressive,

reverse-fault/fold domains that are associated with upward propagation of basement faults. These faults are oriented perpendicular to far-field regional compression that is associated with 'hard crunch' style orogenesis (e.g. Ardmore Basin, Oklahoma).

High-temperature, ferroan dolomite tends to fill up void space created by early Stage 2 sucrosic dolomitization. However, dissolution and tectonic/hydrodynamic permeability created by wedge-style hydrofracturing creates additional open-space. Precipitation of ore minerals and hydrocarbon charge (initial gas and mid-stage pyrobitumens and other Stage 4 and 5 oils) are focused toward this additional open-space. Solution collapse and hydrothermal karsting are common in the vicinity of Stage 3A hydrothermal dolomitization.

Compared to the subregional extent of Stage 2 sucrosic dolomitization, Stages 3A, 3B, 4, and 5 are local in scale and occupy less than 5% of the area affected by the Stage 2 dolomitization.

#### **Chemical Features of Stage 3A - Hydrothermal Dolomite (HTD)**

Hydrothermal brines reach maximum salinity (20 to + 30 wt.% NaCl equivalent) during Stage 3A, due to continued metal cation release and chlorine release during acid neutralization. Fluid inclusion filling temperatures reach their maxima, due to lack of a 'buffering' effect by 'cooler' wall rock. Under reducing conditions, hydrocarbons continue to be produced due to hydrogen liberated from bicarbonate breakdown and acid neutralization to make hydrothermal dolomite. Stage 3A terminates when the magnesium supply becomes exhausted and calcium starts to combine with aqueous anion species, such as sulfate to make anhydrite; sometimes this termination is incremental.

Stage 3A chemical features can be transferred electrochemically to the surface. At the surface, they are expressed as low sodium, high CO<sub>2</sub>/O<sub>2</sub> ratios, low ferric:ferrous ratios, and high C1/C6 gas ratios. These ratios reflect the reduced portion of the depositional sequence that is proximal to the main conduit 'feeder'. The high CO<sub>2</sub> ratios commonly couple with elevated iron signatures, which indicate the presence of elevated amounts of ferroan dolomite near the main conduit 'feeder'.

#### **Geophysical Features of Stage 3A - Hydrothermal Dolomite (HTD)**

Dissolution and solution collapse due to void space creation by Stage 2 and Stage 3A dolomitization, coupled with tensile normal faulting, leads to sag features within the replaced stratigraphy. These sag features can be detected

by high resolution seismic methods. In seismic profile, the reflector associated with the replaced beds may display subtle downward bending or deflection. The sag features may be manifested by elongate reflector troughs in three-dimensional seismic cubes.

### **STAGE 3B - TRAP – CARBON DIOXIDE EFFERVESCENCE AND ANHYDRITE FORMATION IN THE RIEDEL-TENSILE TRAP SITE.**

#### **Tectonic Setting of Stage 3B - CO<sub>2</sub>-Anhydrite Formation**

The tectonic setting for Stage 3B is similar to that of Stage 3A, except reactions may take place later in the paragenetic sequence and are slightly more distal to the main feeder, which is the high-angle strike-slip fault. The structural features of Stage 3B are also similar to those in Stage 3A. However, hydrodynamic wedging continues to propagate into wall rock replacement horizons away from the main feeder conduit.

#### **Chemical Features of Stage 3B - CO<sub>2</sub>-Anhydrite Formation**

The exhaustion of the magnesium supply ‘shuts down’ dolomitization, sometimes incrementally. Calcium begins to combine with HCO<sub>3</sub><sup>-</sup> or H<sub>2</sub>SO<sub>4</sub> to produce anhydrite and/or calcite, which is usually subordinate to anhydrite. Continued depressurization associated with creation of tensile permeability may lead to unmixing or degassing of dissolved gas component, which is frequently noted as effervescence. Significant amounts of carbon dioxide-methane-hydrogen effervescence may occur in various proportions. Under reduced conditions, hydrogen and methane production may continue. Hydrogen may combine with sulfur, which is released from sulfuric acid breakdown, to produce H<sub>2</sub>S. Continued neutralization of fluids and breakdown of chloride complexes may initiate production of chlorine gas and lowering of salinity. Breakdown or neutralization of perchloric acid and sulfuric acid components releases oxygen, which may make water that dilutes the brine component of the hydrothermal fluid. Salinity begins to lower.

Fluid reaction products are still characterized by high CO<sub>2</sub>:O<sub>2</sub> ratios, Fe<sub>2</sub>O<sub>3</sub>:FeO ratios, and C-1:C-6 gas ratios. Electrochemical transfer of this ‘fingerprint’ to the surface results in a soil chemistry pattern similar to reactions in Stage 3A, with the possible addition of a sulfur anomaly that reflects sulfate deposition as anhydrite in the underlying reservoir area. The geophysical signature of the Stage 3B reaction is similar to that of reaction 3A.

## **STAGE 4 - TRAP - SULFIDE DEPOSITION AND HIGHER RANK HYDROTHERMAL PETROLEUM PRODUCTION**

### **Tectonic Setting and Structural Features of Stage 4 - Sulfide and Petroleum Production**

The tectonic setting of the Stage 4 sulfide and petroleum formation is similar to that in Stage 3, except that sulfide precipitation takes place later in the reaction sequence and more distal to the main feeder conduit. In Stage 4 production of sulfides and hydrothermal petroleum, hydrodynamic wedging begins to wane. Tensile permeability produced by tectono-dynamics may reach maximum efficiency.

### **Chemical Features of Stage 4 - Sulfide and Petroleum Production**

Metal cations released from chloride complexes combine with sulfur released from sulfuric acid or hydrogen sulfide/bisulfide breakdown to precipitate as sulfide solid-state mineral compounds (primarily sphalerite-pyrite, with very minor galena). Under reducing conditions, flux of hydrogen and methane across electron-rich sulfide or clay interfaces may result in catalytic reactions to higher rank hydrocarbons (especially C-5 to C-6 gases and, more speculatively, C-6 to C-12 alkane oils). Breakdown of chloride complexes results in a lowering of salinities and filling temperatures. Fluid inclusions contain low magnesium due to removal by dolomite formation earlier in the reaction sequence (Stages 2 and 3). Gas effervescence begins to wane. Sodium and potassium may be released from chloride complexes to react with wall rock clay component to produce illitic clays which, if present, may enhance hydrothermal catalytic hydrocarbon reactions discussed above.

Electrochemical transfer to soil profiles above the reservoir site results in pronounced metal enrichments away from the main conduits. These are the most metal-enriched locations in the geochemical anomaly above the reservoir site. Within the overall field, metal anomalies occur at an 'intermediate' distance with respect to the primary conduit feature. The geophysical features of Stage 4 are similar to those of Stage 3.

## **STAGE 5 - TRAP – LATE DISTAL CALCITE-CLAY-FELDSPAR-HIGH C-NUMBER HYDROCARBON FORMATION**

### **Tectonic Setting and Structural Features of Stage 5 - Late Distal Calcite-Clay-Feldspar-Hydrocarbon Formation**

The late and distal occurrences of calcite, clay, feldspar and high C-number hydrocarbons occur in favorable limestone horizons along riedel-tensile zones that are most distal to the main conduit system. They also occur in siliciclastic 'caprock' immediately above reservoir zones along riedel-tensile zones and for some distance above the reservoir horizon in the vicinity of the main conduit. Gas produced by this and earlier reactions may migrate further up-section and be deposited in overlying sandstone reservoirs (along with oil).

'Tight' riedel-tensile fracturing in caprock shales may host tight shale-gas in shales above the reservoir site in immediately underlying hydrothermally dolomitized limestones. Tight shale gas may be especially abundant in shear fractures related to main conduit shears. Gas charge in overlying sandstone reservoirs may be offset laterally with respect to underlying HTD reservoirs. Lateral offset may systematically relate to the lateral slip sense on the main conduit feeder. Sag features may also be associated with the gas accumulations.

#### **Chemical Features of Stage 5 - Late Distal Calcite-Clay-Feldspar-Hydrocarbon Formation**

Calcium release from calcium chloride complex and combination with remaining carbon dioxide from remaining bicarbonate breakdown results in late calcite formation, along with a calcium contribution to hydrothermal clay production. Principal hydrothermal phyllosilicate production may be in the form of higher temperature illitic micas (both sodium- and potassium-bearing). This results from chloride breakdown during reaction of the hydrothermal fluid with the diagenetic clay component of caprock siliciclastics (especially high TOC black shales). Under reducing conditions, formation of hydrothermal electrostatic illite at temperatures and salinities considerably lower than those in the underlying HTD reservoir (within the oil window) may produce large amounts of catalytic reaction products of higher carbon number alkane oils and gases that locally may form large hydrocarbon-rich halos above and lateral to petroleum-bearing HTD reservoirs.

Salinity of fluid inclusions and filling temperatures in Stage 5 products are about fifty percent as high as those associated with Stage 3 and Stage 4 within the reaction sequence. These lower salinities are due to alkali chloride breakdown during reactions with wall rock-early diagenetic clay components to make illitic micas. Chlorine gas may be a significant component of the Stage 5 distal environment. Higher mass halogen gases, such as bromine and even heavier iodine, may also be enriched in distal zones with the high-mass iodine occupying the most distal part of a fractionated halogen corona feature.

## **6. APPLICATION TO GAS POTENTIAL IN NEW YORK**

In Chapter 6, the exploration models developed in Chapter 5 and the chemical models of hydrothermal dolomite and gas deposition developed in Chapter 4 are specifically applied to the geology of New York. More specifically, these models are applied to the Finger Lakes region of central New York and to Steuben County and adjacent areas with HTD gas reservoirs at the Trenton/Black River horizons (See Plate 1).

### **STAGE 1 - SOURCE(S) IN AND NEAR NEW YORK**

A basement source containing oceanic crustal sources conducive to serpentinization and subsequent expulsion of hydrothermal hydrocarbon-bearing and hydrocarbon-stable metagenic fluids is present in the Appalachian Basin. The regional geology of the Appalachian Basin in the south-central New York region may be very conducive to basement-sourced oil and gas fluids.

#### **Regional Sources in the Appalachian Basin**

A principal feature in the basement of the Appalachian Basin is the well-known Rome Trough, which has been documented in northeastern Kentucky and surrounding regions by drilling (Rankin and others, 1989, Figures 12 and 13). As summarized by Rankin and others (1989), the Rome Trough developed in the Early to Middle Cambrian, during what is known sedimentationally as the Rome Interval. The Rome sedimentary interval features redbeds and other continental clastics from local uplifts that were deposited in a northeast-trending trough (Parrish and Lavin, 1982, Figure 1). Facies within the Rome sedimentary unit include tidal-supertidal redbeds, fenestral dolomite, and laminated fine-grained shale and sandstone, as well as lower intertidal, red to grey shale and sandstone, and shallow subtidal sandstone and local coarse channel fills. Evaporite-bearing beds occur in the subsurface, but only silicified evaporites occur in outcrop. The unit dramatically thins westward and is absent over the Nashville Dome, but is thick to the immediate east in the fault-bounded Rome Trough and is locally up to 1,000 meters (Rankin and others, 1989, Figures 7 and 13).

Rift-related sedimentation continued into Middle to early Late Cambrian, where isopachs of carbonate-dominated facies display a geographic correlation with the Rome Trough. In particular, the main basin-fill deposited at this time is referred to as the Conasauga basin fill (Rankin and others, 1989). This unit consists of quiet water, green to gray shale and storm-reworked siltstone, thin ooid and skeletal limestone, and flat-pebble conglomerate. The sequence coarsens to the west and becomes more clastic-rich westward (Rankin and others, 1989).



Within southern New York, Cambrian sedimentational patterns imply the presence of a Rome Trough-type feature that may extend northerly into at least the southern portion of the Rochester Trough discussed below. In southwestern Steuben County, isopach contours for the Rose Run Sandstone of the middle Upper Cambrian are permissively centered on the geophysical features that define the Rochester Trough (see below). Thicknesses of the Rose Run sandstone, as determined from drilling, reach maximum thicknesses (250 feet) in south central Steuben County (Kreidler, and others, 1972).

The underlying Galway Dolomite and Potsdam basal clastic units have considerably different isopach patterns than the Rose Run. These lower units rest unconformably on Precambrian Grenville basement and display isopach patterns characteristic of shelf/platform sedimentary sequences. Similar shelf/platform isopach patterns are displayed by the Early Cambrian shelf carbonate sequence to the south (the Shady-Tomstown-Dunham interval as described by Rankin and others, 1989). Regionally, these basal clastic units are 'paper thin', shelf-sediment units.

Additionally, the Galway carbonate unit is a sedimentary dolomite, possibly formed by precipitation from magnesium-rich seawater formed in the context of fast-spreading, Mg-rich, komatiitic magmatism. A similar example is the magmatism associated with the extensive Betts Cove Ophiolite Sequence of Early to Middle Cambrian age in Newfoundland. This dolomite would have been in equilibrium with Mg-rich brines generated from serpentinized, Mg-rich, oceanic crustal materials in the Rochester Trough beneath Steuben County. As such, the Galway Dolomite unit would have been much less reactive compared to the calcite-dominated limestones of the Trenton-Black River groups, which overlie the Galway Dolomite in southwest New York.

In summary, the sedimentary evidence in southern New York is similar to that elsewhere to the south in the pre-orogenic, Cambrian-Early Ordovician-aged, Appalachian Basin. Here, initial, thin, shelf sediments deposited in the latest Precambrian to Early Cambrian are followed by rift-related, clastic sedimentation in the Middle to Upper Cambrian units. Although not present in southern New York, the Cambrian rift-related sedimentation was positionally overlapped by latest Cambrian to Early Ordovician age, predominantly dolomitic, shelf sedimentation to the east and south (Knox Group to the south or Beekmantown interval to the northeast).

The Rome Trough and related features are additionally expressed geophysically as a northeast-trending gravity low, which presumably marks the location of low-density, basin-fill sediments (Parrish and Lavin, 1982, Figures 2 and 3). It may also mark the location of lower density, serpentinized, oceanic crust developed in a failed rift setting beneath the sediments. The serpentinization may also coincide with magnetic highs, which reflect

magnetite produced during the serpentinization reaction.

Geophysical features similar to the Rome Trough project into Pennsylvania and southern New York in the area east of Steuben County. Also, a north-northwest-trending rift arm may extend northwestward from the Rome Trough and connect with a northerly trending gravity low feature that extends beneath Rochester, New York and into the eastern part of Lake Ontario. This rift-arm feature, herein referred to as the Rochester Trough, may link to the main Rome Trough in the vicinity of a gravity high on the New York-Pennsylvania border (Parrish and Lavin, 1982, Figure 2). The Rochester Trough lies along the Lawrence-Attica lineament defined by Parrish and Lavin (1982). This lineament is close to and subparallel to a series of northwest-trending faults inferred from the disruption of the east-northeast- to northeast-trending folds that deform Middle Devonian sedimentary rocks of the Catskill Delta complex in Steuben County (Plate 1). The gravity high also appears to mark the northeasternmost extension of the Kane gravity high. The Kane gravity high is inferred to represent a rift shoulder composed of Grenville-aged basement that defines the northwestern boundary of the Rome Trough in northern Pennsylvania and southern New York (Parrish and Lavin, 1982, Figure 3).

### **Steuben County Sources**

Within Steuben County in particular, there appears to be a coincidence of geophysical features that may be relevant to the hydrocarbon distribution in Steuben County. A prominent aeromagnetic high occupies the entire south-central portion of Steuben County (Plate 1). The eastern part of the magnetic high coincides with a prominent -60 milligal gravity low. The known and possible hydrocarbon occurrences in Steuben County and immediately adjacent areas display a peripheral pattern with respect to the gravity low feature; these hydrocarbon occurrences are located in a halo around the gravity low.

The geophysical data and the distribution of hydrocarbons are consistent with the interpretation that the gravity-low / magnetic-high feature may represent serpentinized mafic or ultramafic oceanic crustal material that formed in the rift arm beneath Steuben County. The interpretation that the density anomaly at the New York-Pennsylvania border is a dense un-serpentinized peridotite intruded into the triple junction between the Rochester Rift Arm and the main northeast extension of the Rome Trough, also fits the geophysical data.

The correlation of hydrocarbon occurrences with inferred rifts described above is typical of what may be a much larger, regional pattern. The correlation between hydrocarbon occurrences and regional geology in the Appalachian Basin highlights the geographic correspondence between gas occurrences of the Appalachian Basin

with the Rome Trough. Comparison of the map of gas fields of the United States (Terra Graphics, 1977) with the gravity map of (Parrish and Lavin, 1982, Figure 2) reveals a strong correlation of the Rome Trough and related Middle to Upper Cambrian rift structures with Appalachian region oil and gas occurrences. These correlations are even more impressive when the gas and oil associated with the Trenton-Black River reservoirs is overlain on the position of the Rome Trough.

### **Cambrian Rift System and Overmatured Cover Rocks in New York**

The Rome Trough geographically coincides with Conodont Alteration Index (CAI) thermal maturity patterns. Recent augmentation and recontouring of conodont-based thermal maturity patterns in New York State by Weary and others (2000) shows a strong east-west flexure in geographic patterns of Conodont Alteration Index isograds from conodonts extracted from Middle and Upper Ordovician carbonate rocks [especially the Trenton-Black River intervals] (Weary and others, 2000, Figure 4). The telescoped area of CAI contours fits snugly around the northwestern corner of the Rome Trough projection into south-central New York State, based on interpretation of the gravity contours (comparing Figure 2 from Parrish and Lavin, 1982 with Figure 4 from Weary and others, 2000). A similar, but less pronounced, pattern with two distinct easterly flexures is apparent from CAI data obtained from Devonian sedimentary rocks (Weary and others, 2000, Figure 6).

As Weary and others (2000) point out, the geographic distribution of both CAI data sets suggests that the region is thermally overmature, assuming that the known thicknesses of overburden is accurate. Some 10,000 to 12,000 feet (3-3.7 km) of overburden would be required above the existing sediment pile to explain the thermal maturity of the conodonts. At the present time, we see no evidence for thick clastic wedge-type sedimentation of Pennsylvanian-Permian age in the New York region. For example, the 0 isopach for the Mauch Chunk - Pottsville clastic wedge in the Pennsylvania salient is shown to occur well south of the Pennsylvania-New York boundary (Hatcher and others, 1989, Figure 5).

A possible explanation for the overmature CAI data suggested by Weary and others (2000) is that the thermal maturation was produced by thermal input during the emplacement of Mesozoic mafic intrusions, such as the kimberlite dike swarm in the vicinity of Ithaca, New York. We are skeptical about this possibility because, throughout our world-wide data set, kimberlite diapirs and alkaline magmatic diapirs generally display small, point-source, thermal anomalies. We agree with Weary and others (2000) and Dorobek (1989) that flow of basin-derived fluids through the conodont-bearing strata would probably be too fast to produce a thermal equilibration with the conodont-bearing strata. In addition, the overall thermal mass of any basin-derived fluid would probably not have been high enough to heat up the surrounding limestone strata. Available heat flow also would have been

restricted to conduits and would have had a difficult time penetrating thermal insulators, such as limestone.

There is, however, a fourth possible heat source: regional circulation of hot (initially 300°C), basement-derived brines that were produced by metagenic processes acting on mafic, oceanic crustal material in the Rome Trough basement. These fluids, as discussed in Chapter 4, would be capable of producing hydrothermal hydrocarbon reaction products during cooling from 300°C to 150°C. This is the approximate median temperature for fluid inclusions associated with Stage 3 hydrothermal dolomite formation. As discussed in Chapter 4, the amount of fluid generated by metagenesis of basement material is capable of affecting huge volumes of rock, especially limestone via dolomitization. During dolomitization, the ambient temperatures of replaced limestones would certainly be raised above the 4.5 CAI isograd. It is possible that abundant, metagenic, hydrocarbon-stable fluids would be produced within the basement of the Rome Trough during peak Acadian metamorphism.

It is also extremely significant that recent discoveries of deep, HTD gas in the Trenton-Black River groups of New York occur in the thermally over-matured CAI zones. Since Weary and others (2000) published their revision of the CAI patterns [which fit the then-known patterns of oil and gas distribution in New York State], major new discoveries of deep gas have been found hosted within the hydrothermally dolomitized limestones of the Trenton-Black River groups. Most of these gas fields (see Plate 1) occur within the thermally matured zone where the CAI's exceed 4.5. This CAI is beyond conventional delimitations of the oil and gas windows and exceeds the window for dry, natural gas generation and preservation, in particular (Dow, 1977; Harris and others, 1978; and Tissot and Welte, 1984; Weary and others, 2000).

Thus, the occurrence of these HTD gas fields in southern New York poses a major conundrum for the conventional oil and gas model: they shouldn't exist! One possible explanation of this apparent paradox is to generate the thermal anomaly during the Acadian orogeny (along with the creation of the HTD reservoir) and later migrate oil and gas fluids to the reservoir sites, presumably during the Alleghenian orogeny. The problem with this explanation is that there is no documented basin-thickening or sediment-loading, which is required by the conventional, basin-centric, oil and gas model for maturation and migration of biogenic basin-derived, petroleum fluids. On the other hand, if the hydrocarbons were produced abiogenically during reactions associated with a cooling, regional, hydrothermal plume or plumes, then the above paradox is resolved.

Another independent data set demonstrates that the southern New York deep gas was emplaced into a thermally overmature setting. In addition, this data set can be used to date the influx of hot, basement-derived brines during the Acadian orogeny. The data set comes from a fission track study along an east-west traverse in central New York by Johnsson (1986). Fission tracks for the Middle Devonian Tioga metabentonite datum display a marked

step in apatite fission track cooling ages southwest of Syracuse, New York. (The metabentonite datum is a widespread Appalachian stratigraphic marker bed that occurs just below the first appearance of molasse sedimentation associated with the Acadian orogeny). East of this step, much younger cooling ages record a thermal disturbance within the northern Appalachian basin that rendered this part of the basin overmature with respect to the conventional oil and gas window (Johnsson, 1986, Figure 2). In addition, Johnsson (1986) reports fission track dates ( $354 \pm 29$  Ma on zircon and  $155 \pm 10$  Ma on apatite) for one other sample (#T01) from a metabentonite 750 meters below the Tioga, near the top of the Middle Ordovician Black River Group. Johnsson (1986) attributes the discrepancy between the mineral ages to partial annealing of fission tracks due to exposure of metabentonite to temperatures approaching  $175^{\circ}\text{C}$ .

### **Possible Composition of the Peridotitic Source Rocks in the Rome Trough**

Regionally, the possible composition of oceanic crustal material that may be present within the Rome Trough rift system can be inferred. The Upper Cambrian and Lower Ordovician shelf carbonates throughout continental shelves of the entire planet at that time were dominated by sedimentary (primary) dolomite. Consequently, the hydrosphere column can be inferred to have been more magnesium rich due to magnesium input from the emplacement of highly magnesian, komatiitic volcanism in the global oceanic rift system during fast spreading in the Middle to Late Cambrian. Thus, we can make an additional inference that magmatism that would have appeared in Cambrian-age failed rifts within the cratons (such as the Rome Trough system) would also have a magnesian aspect.

The magnesian aspect of peridotitic magmatism has important implications for amounts and types of hydrocarbons generated. Specifically, lower C-number hydrocarbons (such as methane) will be degassed from oceanic spreading centers or generated metagenically in greater amounts from magnesian peridotitic sources than from more calcic peridotitic sources.

### **Overmatured Cover Rocks and Timing of Fluid Migration in New York**

The fission track data ( $155 \pm 10$  Ma fission tracks from apatite and  $354 \pm 24$  Ma fission tracks from zircon; Johnsson, 1986) is especially relevant to the timing of late Acadian fluid introduction. The 155 Ma date represents later cooling, refrigeration, and annealing of the deeper stratigraphic level, Ordovician apatites. The 354 Ma date may represent resetting of the initial Middle Ordovician zircons by a late Devonian hydrothermal event, which reached temperatures near the zircon annealing temperature (about  $200^{\circ}\text{C}$ ). It was discussed above

that the timing of Acadian peak metamorphism and peak sedimentation ranged between about 350 and 375 Ma. In this context, the 354 Ma zircon fission track date could represent annealing of zircon in the metabentonite immediately after the introduction of Acadian-age hydrothermal metagenic fluids. It is significant that the zircon systems have not been affected by any post-Acadian annealing event, such as one that might be attributed to regional fluid circulation during the Alleghenian orogeny (circa 250 - 310 Ma).

In the above context, it is also significant that the metabentonite has been altered to well-ordered, high-percentage, illite-rich mica, which represents 'a very high diagenetic grade' according to Johnsson (1986). The alternative to 'diagenesis' as used in the passive burial model advocated by the standard petroleum paradigm is to reinterpret the presence of illite/clay to have been the result of the introduction of an active, high-temperature, epigenetic, hydrothermal brine that was exotic to the rock system it influenced. In this sense, the illite/clays constitute a secondary reaction product that accompanied the thermal event associated with the introduction of the hydrothermal brines.

This brine may have not only affected the Ordovician section, but may also have risen to higher levels, where it affected rocks within the Upper Devonian Catskill clastic wedge complex. Here, additional fission track data reported by Lakatos and Miller (1983) give similar results to those reported by Johnsson (1986). Four fission track determinations on zircon extracted from feldspathic sandstone of earliest Late Devonian age in the southern Catskill Mountains near the town of Monticello, New York, yielded ages ranging from 311 to  $333 \pm 13$  Ma (Lakatos and Miller, 1983). Fission track dates for apatite extracted from the same sandstone range from 113 to  $132 \pm 4$  Ma. Using a 200°C closing temperature for zircon annealing, the Late Devonian sandstone experienced a thermal event sometime between its deposition at about 360 Ma and about 320 Ma.

The conventional burial model would require 8 km of sedimentation above this rock, between 360 and 320 Ma to explain the annealing of the zircon at 200°C using a thermal gradient of 25°C/km. The problem with this hypothesized, extremely rapid burial is that there is simply no empirical sedimentological evidence that this burial event took place. Isopach maps in the vicinity of the Catskill Mountains in New York show that no more than 1.1 km of Upper Devonian and Mississippian sediments are preserved (Sevon, 1985; Ayrton, 1963; Hatcher and others, 1989; Cook and Bally, 1975). These sediments fall within normal isopach and sedimentological facies patterns that strongly suggest that the original section deposited during that key time interval is largely preserved. Consequently, the only other mechanism that can explain the high thermal maturity of the rocks in the southern New York region is the introduction of an Acadian-age, hydrothermal, metagenic fluid. The lack of late Paleozoic or Mesozoic intrusive bodies of large-enough size to regionally reset the fission track clocks has been discussed above. The zircon ages appear to preclude the regional introduction of any Alleghenian-age hydrothermal

metagenic fluids in the New York State region.

The temperature of the invading hydrothermal fluids may have been between about 250 and 200°C, based on the 354 Ma age, in the context of about 1.1 km of late Acadian sedimentation. The lithostratigraphic setting of the hydrothermal event suggests that this mineralization took place at relatively shallow levels within the earth's crust, generally within about 1 km of the paleosurface. The shallow depths of the fluid introduction are consistent with an epithermal depth and temperature zone, as defined by the classic Lindgren classification of ore deposits (Lindgren, 1919). Lindgren's original analysis has been confirmed a multitude of times by fluid inclusion and stratigraphic reconstructions of epithermal mineralization. Because these fluids are far-traveled from their serpentinite source regions, the term 'leptothermal' might be more appropriate. Nevertheless, maximum temperatures for leptothermal and epithermal epigenetic fluids do not exceed 250°C, which is consistent with the reported thicknesses of stratigraphic cover and with the fission track zircon data discussed above.

#### **STAGE 1 TO 2 – MIGRATION – STAGE 1 TO STAGE 2 FLUID MIGRATION FROM SOURCE TO TRAP IN NEW YORK.**

##### **Introduction**

The previous section described the setting in the northern Appalachian basin of potential source rocks (mafic, oceanic crustal materials) that, when affected by orogenically driven metagenesis, could subsequently generate a hydrocarbon-stable hydrothermal brine. In the case of the Appalachian Orogen, the Rome Trough and its extensions provide an ideal setting for such source rocks. Obviously, such a source is important only if a suitable tectonic event is imposed on the source to generate the hydrocarbon-stable brines and if a suitable conduit system is available to provide a pathway for transport from the source to a suitable trap in the cover sequence proximal to the trough.

Many stratigraphically constrained, permeable horizons were developed after the deposition of potential source rocks in the Rome Trough. All of the well-known stratigraphic reservoirs in New York State (Isachsen and others, 1991, Figure 15.7) were deposited before the Acadian orogenic period. During this period, hydrocarbon-stable, metagenic fluids were generated within the Rome Trough and migrated to at least the Trenton-Black River horizons via the conduit system described below. This regional migration was associated with the coincident development of base metal-rich brines, which deposited MVT-style, East Tennessee type zinc deposits derived from different basement sources at the southern end of the Rome Trough. There is ample evidence for the Acadian timing of this event (see Chapter 4), both in the form of radiometric dates, peak metamorphic ages in the

center of the orogen, and the development of the Catskill clastic wedge coevally with Acadian tectonism to the east. The 'hard-crunch' orogenic style of the Acadian orogeny, which is required to involve the basement in metagenic fluid generation, involved a collision with the Avalon microcontinental plate. The far-field stress field in southern New York was oriented with  $\sigma_1$  east-northeast. The area from which the fluids were expelled is centered on the gravity low.

### **Stage 1 to Stage 2 Conduit System in southern New York**

The Trenton-Black River datum in southern New York is less than 200 meters above the basement (Rankin and others, 1989, Figure 11). This highly productive oil and gas reservoir horizon is probably connected with the rift basement beneath Steuben County by a northwest-striking conduit system. Of the various basement-connected possibilities, the most important control appears to be associated with northwest-striking structural elements. Northeast- to east-west-striking structural controls are locally more important at the reservoir site, but are less important as conduits connecting basement sources with the stratigraphic traps. The most subtle basement control is probably related to northwest-striking structural elements. However, it is the WNW-striking structural fabric that may have the most important regional control in terms of defining regional structural and physiographic provinces (see Plate 2).

**Northwest-striking structural elements in New York.** Regional tectonic elements that may be present in and near the gas accumulations in the Finger Lakes region of central New York State are shown in Plate 1. The structural elements were identified by direct and indirect evidence. Obviously, the most direct evidence is physical mapping of the structural element. Less direct methods utilized offsets in fold features that affected the Lower Devonian Oriskany Sandstone. Especially useful were the small-scale fold features identified by the detailed mapping of Bradley and Pepper (1938) in Steuben County, New York. Linearly aligned zones of *en echelon* kimberlite dikes were also used to define potential, northwest-striking, deep-seated fault elements (such as the Ithaca line in Plate 1). Other potential basement structures were indicated by linear breaks between magnetic highs and lows, gravity highs and lows, radiometric highs and lows, as well as troughs. Offsets in the regional outcrop patterns could also be related to deep-seated faults. Alignments in the contour lines on the Conodont Alteration Indices (CAI) map were also used. The most likely structures, based on all of the above indicators, are shown on Plate 1.



Two northwest-striking main conduits may have been operative, based on the geophysical features discussed above. On the southwest side of the overlapping gravity low/magnetic high, a series of northwest-trending faults are inferred from the disruption of fold axes on Middle Devonian strata. These fault features may integrate downward into the N50W-trending basement feature referred to above as the Lawrenceville-Attica geophysical lineament (Parrish and Lavin, 1982, Figure 2). A series of en echelon, west-northwest-striking faults that separate en echelon fold features may be surface manifestations of the more deep-seated Lawrenceville-Attica geophysical lineament. Several small Devonian Oriskany Sandstone-hosted gas fields may be related to these fault systems.

However, with respect to deep-seated gas possibilities, one northwest-striking structure on the northeast side of the coincident magnetic high/gravity low is particularly important. Following the conventions of Chapter 3, this structure is named the Glodes-Quackenbush Trend (Plate 1). The Glodes-Quackenbush Trend may be associated with gas reservoir development at Glodes Corner, Muck Farm, Wayne-Dundee, Sugar Hill, Wilson Hollow, and Quackenbush Hill. As currently delineated, the Glodes-Quackenbush Trend is about 100 km long, with an average strike of about N35W. The gas accumulations consistently occur on the southwest side of the trend and are associated with northeast- to east-west-trending (but mainly east-northeast-trending) subzones that range up to about 10 km in length.

In terms of a dynamic model, the east-northeast-trending subzones are interpreted as riedel-tensile splays that curve east-southeastward into the Glodes-Quackenbush Trend. This trend is interpreted to be a basement-connected, P-shear, feeder zone that was operating in left slip during the time of gas introduction. Left slip on the Glodes-Quackenbush Trend is inferred to have been induced by regional, east-northeast--west-southwest compression that was operant in the foreland of the Acadian orogenies. It is important to point out that the Glodes-Quackenbush Trend originally may have been the principal bounding fault zone on the northeast side of what is referred to above as the Rochester Trough.

Farther to the northeast, another northwest-striking fault, referred to herein as the Ithaca Zone, was defined by the trace of a 50 km-long zone of north-south striking, en echelon, kimberlite dikes. The best known swarm of these dikes is a northwest-striking group of *en echelon* dikes centered on and within the town of Ithaca, New York. The southeast projection of the Ithaca Zone, in part marks the northern termination of the prominent gravity trough segment of the Rome Trough system to the south. The northwest projection of the Ithaca Zone may be associated with a prominent westerly bend in the -50 milligal gravity contour near Rochester, New York (Plate 1). At this point in our investigation, no hydrocarbon occurrences have been found on or near the main Ithaca Zone. However, the small Hamilton Shale-hosted gas field lies along the southeast projection of the Ithaca Zone and the

large Silurian-hosted Fayette-Waterloo field lies astride the northwestern segment of the Ithaca Zone and the deeper Trenton-Black River-hosted Fayette-Waterloo gas field lies to the immediate northeast of the Ithaca Zone.

It is interesting that no petroleum occurrences have been identified along the main segment of the Ithaca Zone, where the main kimberlite dikes occur. The lack of petroleum may correlate with the comparatively oxidized nature of the kimberlites, which more technically are termed micaceous peridotite or Type II non-diamondiferous kimberlite (MPA72 or 75 model in the Magma-Metal Series Classification in Appendix A).

**Northeast-striking structural elements in New York.** Northeast-trending structural zones may also be locally important as conduits connecting the reservoir sites with the ultimate basement sources. In the southern part of the aforementioned combined gravity low/magnetic high, a prominent northeast-striking zone is associated with known and potential hydrocarbon occurrences. The known occurrences are east-northeast-elongate gas reservoirs hosted in the Devonian Oriskany Sandstone. Deeper, Black-River-hosted reservoirs may occur to the northeast of the higher level Oriskany gas accumulations. At the northeast corner of the magnetic anomaly, another inferred northeast structural zone may have provided a conduit feeder for expulsion of hydrocarbon-bearing brines. Some of these may have accumulated in the northeast-trending Wayne-Dundee reservoir near its intersection with the Glodes-Quackenbush trend. The northeast structure above may continue farther northeastward where it is associated with a prominent northeasterly jog in what is generally an east-west-striking alignment of the Devonian sediments at the north edge of the Allegheny Plateau in the vicinity of the Fayette-Waterloo population centers.

**West-northwest-striking structural elements in New York.** The third major structural control may relate to west-northwest-striking structures that define the northern limits of the Allegheny Plateau physiographic feature in central New York. The northernmost of these west-northwest-striking structures coincides with the northern limit of Devonian outcrops as well as with a prominent, east-stepping deflection in the Devonian and Ordovician Conodont Alteration Index (CAI) isograds. The second, more southerly, west-northwest-striking feature is associated with a second, prominent easterly deflection in the Devonian Conodont Alteration Index isograds. The main kimberlite cluster associated with the northwest-striking Ithaca Zone also occurs at the intersection of the Ithaca Zone with the southerly west-northwest-striking, inferred, basement fault. These west-northwest structural elements may be components of a much larger, continent-wide network of west-northwest-striking structural elements that were formed during the mid-Proterozoic (1400 Ma) orogenic event (Plate 2), which includes the Glodes-Quackenbush Trend.

The most prominent Precambrian basement structures of the U.S. developed during the 1400 Ma orogenic event, which extends from Scandinavia to Mexico. Although long thought to be anorogenic, recent work has shown that it is characterized by extensive intrusion of mantle- and crustal-derived granite that, in places, volumetrically comprise up to 75% of the mid- to upper crust. Structurally, these large volumes resulted in a relatively isotropic crust for much of the Precambrian in the U.S. Transcurrent, WNW-trending shears developed during the final stages of granite emplacement and appear to constitute the most significant anisotropy in the Precambrian basement (Swan and Keith, 1986).

Subsequent tectonic events have been influenced by this WNW-trending basement structure. In common with more recent subduction, the Devonian-Ordovician orogenic events of the Appalachian orogen are presumed to have involved periods of segmented subduction. The concept of segmentation of the plate tectonic slabs is an important aspect of the orogenesis. The slab tears may coincide with the edges of well-known embayments that occur along the strike of the Appalachian orogen. The boundaries between embayments may mark slab tears in the Paleozoic subduction system that accompanied Cordilleran styles of Appalachian orogenic events. Along-strike changes in distribution of peraluminous versus metaluminous magmatism, basin geometry, uplift distribution, metamorphic grade patterns, transform faults, and salt on the continental slope may all be linked to slab segmentation. This segmentation, which is ultimately controlled by the basement fracture framework shown on Plate 2, may have re-propagated its pattern during the breakup of Pangea to produce the current oceanic fracture zone pattern of the Atlantic basin (Keith and others, 2003).

The basement faults have been mapped on the ground and can also be recognized in geophysical, remote sensing, and sedimentological data. Basement faults extend from zones such as the Lewis and Clark zone eastward across the continent. The regional distribution of oil fields and Mississippi Valley Type Zn-Pb deposits clearly reflects this basement structure.

Cambrian rifting, such as produced the Rome Trough, has been modeled by previous workers as an idealized orthogonal rift/transform pattern (Schwochow, 2000; Thomas, 1977, 1991; and Hatcher and others, 1989). The actual pattern is probably more transtensional in nature due to the pre-existence of the WNW basement faults at an angle less than 90 degrees. Strain usually occurred along the pre-existing WNW faults rather than along new transforms, which would have had northwest strikes. Some northwest transforms apparently developed and linked the WNW faults and provided deep conduits for hydrothermal dolomite fluids and gas (e.g. Albion-Scipio Trend, Michigan, and Glodes-Quackenbush Trend, south central New York).

The prolific Albion-Scipio field of Michigan displays an obvious wrench fault-riedel pattern that appears to have strongly influenced gas migration and reservoir formation. This pattern is very similar to the pattern seen at Glodes Corner. Both WNW- and NW-trending basement faults are present and appear to have moved in a left-slip sense, causing EW- and ENE-trending riedel/tensile splays to form and providing a lateral pressure gradient that pulled the hydrothermal gas-bearing fluid into the riedel/tensile zones.

### **Possible Reservoirs Between the Peridotite Source and the Trenton-Black River Horizon**

Whereas the Trenton-Black River productivity is now well known, the 'bottom-up' model developed in this report allows for deposition between the peridotite source, which would be at the bottom of any Cambrian sedimentary cover in the failed Cambrian rift system, and the productive Trenton-Black River carbonate horizons of Ordovician age above the regional Knox unconformity. Indeed, the Knox unconformity may have served as an important stratigraphic conduit for lateral migration of hydrocarbon-charged fluids. In western and central New York State, small amounts of gas production have been obtained from the Cambrian Galway Dolomite and Potsdam Sandstone below the Knox unconformity. In west central New York, the provocative possibility exists that significant gas resource might exist in the Rose Run Sandstone of Late Cambrian age. Isopachs for this sandstone were discussed above in connection with the possible extension of a rift arm extending northward through Steuben County from the main Rome Trough feature to the south in Pennsylvania. It is in this area that the Rose Run isopachs are the thickest, as reported in Pford (1981).

Elsewhere in the Appalachian Basin, the Rose Run Sandstone is a significant producer, especially in Ohio, where a 250 mile-long, northeast-trending, subcrop belt of Rose Run has been documented (Ryder and others, 1998, Figure 1). The description of Ryder and others (1998) for the Rose Run production are worth quoting here.

“In the 1980s and early 1990s most exploration for Knox unconformity hydrocarbon accumulations had moved to east-central Ohio along the 250-mi-long subcrop belt of the Upper Cambrian(?) Rose Run Sandstone and the overlying Lower Ordovician part of the Knox (Beekmantown) Dolomite (Riley and others, 1993) (Figures 1, 2). Natural gas is the dominant hydrocarbon type along this trend, but locally it is associated with condensate or oil. The largest gas fields found to date are concentrated in Coshocton, Holmes, and Tuscarawas counties. Traps for the Rose Run and Beekmantown fields consist of buried hills, truncation, and subtle anticlines (Coogan and Maki, 1986; Riley and others, 1993). Secondary intergranular porosity, caused by dissolution of feldspar grains and dolomite cement, is the dominant porosity type in the Rose Run Sandstone, whereas solution-enhanced vuggy porosity, intercrystalline porosity, and fracture

porosity are the dominant types in the Beekmantown Dolomite (Riley and others, 1993).”

Significantly, the Rose Run production (Riley and others, 1993, Figure 1) occurs in close proximity to a strong aeromagnetic high, coupled with sharply decreasing gravity gradients in the immediate vicinity. In this respect, it would be very interesting to prospect the Rose Run interval in the vicinity of the combined magnetic high/gravity low feature in central Steuben County, New York, where the Rose Run Sandstone apparently is relatively thick, according to the isopach maps of Pferd (1981) who, interestingly, was investigating the Rose Run interval as a reservoir for hot geothermal water.

### **STAGE 3 TO STAGE 5 - TRAP – “HIGH” TEMPERATURE FERROAN HYDROTHERMAL DOLOMITIZATION, ANHYDRITE AND SULFIDE DEPOSITION, AND ABIOGENIC HYDROCARBON GENERATION IN THE TRAP SITE**

Within the vicinity of the combined gravity low/magnetic high feature centered on Steuben County, New York, at least nine hydrothermal dolomite-hosted gas fields in the Trenton-Black River horizons have been discovered to date (since 2000). At least 21 sag-like features that could permissively host additional HTD gas fields occur in a annular pattern around the above-described geophysical feature.

Fortunately, we have had a chance to evaluate emerging geochemical data for one of these fields (the Glodes Corner field in northeastern Steuben County). Analysis of the geochemical data allowed us to test the exploration model and science developed in Chapters 4 and 5. It also allowed us to begin the development of a practical exploration tool to identify HTD exploration plays in southern New York and, indeed, elsewhere on the planet.

#### **Application to the Glodes Corner HTD Gas Deposit in Steuben County, New York.**

One of the exciting opportunities that occurred during the development of our conceptual model was the identification of a testable, producing gas situation. During the project, after the basic conceptual tool had been developed, we became aware of a study by Direct Geochemical at the Glodes Corner field in New York. Jim Viellenave, of Direct Geochemical, has graciously allowed us to incorporate some of his preliminary geochemical results into this study and in results that were reported at the AAPG conference in Houston in March, 2002. Indeed, new data and interpretations of that data are continuing beyond the scope and budget of the current

projects. In fact, we did not anticipate anything this advanced at this early stage. In effect, obtaining this data has allowed us to ‘leapfrog’ several steps ahead within the exploration science process. We are additionally pleased to report that interpretation of the geochemical data appears to confirm in specific detail aspects of the conceptual model.

A series of maps of the Glodes Corner field for selected elements and hydrocarbon gases are presented in Figures 6.1 through 6.7. The maps were constructed from three geochemical profiles taken across the east, central and west portions of the seismically defined sag feature. This sag feature presumably reflects development of a collapse feature associated with formation of hydrothermal dolomite at the Trenton-Black River level some 8,000 feet below the soil surface where the geochemical samples were collected. Gas wells shown in the field, together with production, are also shown for comparison with the seismic and geochemical data. In addition, we have provided profile characterizations of selected elements and hydrocarbon gases from the easternmost PIZ profile (Figures 6.8 through 6.14 for metals and Figures 6.15 through 6.22 for selected hydrocarbon gases).

It is particularly significant that the geochemical data are of an inexpensive, conventional nature in that conventional ICP analyses and conventional soil preparation procedures were used. However, it will be interesting to see what higher precision technologies, based on selective extraction, such as Enzyme Leach, will see. As it turns out, the conventional approach “sees a lot!”

### **Geographic patterns of the geochemical data**

**Oxidation state zonation.** Perhaps the most striking feature of the data is that it displays an overall asymmetry from east to west within the field. In addition to identifying the overall field, the data appear to see overall chemical fractionations within the field. These fractionations appear to be consistent with oxidation state of the volatiles. In the eastern part of the field, parameters sensitive to oxidation state, such as CO<sub>2</sub>:O<sub>2</sub> ratio (Figure 6.1) and percent ferrous iron (Figure 6.2), are highest in the eastern PIZ part of the field (PIZ profile), intermediate along the central profile (FOX), and lowest in the western part of the field (as shown by data on the GREY profile). Within each profile, there appears to be a smaller scale structure that identifies possible conduit architecture within the field. This is particularly evident on a map of ferrous iron where a distinct, high ferrous conduit may be identified on the northern part of the PIZ profile (easternmost profile), the central part of the FOX profile, and central to south central parts of the GREY profile in the western portion of the field.

**Metal Zonation** Metals may also show an overall zonation. Sodium and arsenic (Figures 6.3 and 6.4) are especially low in the eastern part of the field

(PIZ profile), appear to be highest in the central FOX profile, and are also elevated in the western GREY profile (especially arsenic). Elements such as zinc (Figure 6.5), potassium (Figure 6.6), appear to be most depleted in the eastern profile, most elevated in the central profile, and relatively depleted in the western profile. These elements also show enrichments away from the main conduit features identified by the high ferrous iron zones (Figure 6.2). Vanadium appears to identify the overall field as well or better than most of the other metals and gases and is generally enriched in all three profiles, especially the western (GREY) profile (Figure 6.7). Like the other metals, vanadium displays an apparent enrichment away from the main conduit features.

Element enrichment or depletion relative to apparent conduit features can be observed especially well on individual profile lines where element/gas contents versus line distance are plotted for the easternmost profile (PIZ). In terms of metallic elements, zinc (Figure 6.8), nickel (Figure 6.9), potassium (Figure 6.10), magnesium (Figure 6.11), and vanadium (Figure 6.12) display distinct highs away from what are inferred to be four main conduit features within the sag, which are ranked from 1 to 4 in terms of development of their chemical texture (1= best developed). The general coincidence of the other metals with elevated magnesium (Figure 6.11) suggests that the central part of the sag is occupied by higher amounts of hydrothermal dolomite. The main conduit features may occur immediately peripheral to a major CO<sub>2</sub> anomaly that largely coincides with the seismic sag feature where it is crossed by the PIZ profile in the eastern part of the field. This CO<sub>2</sub> anomaly coincides with the magnesium high and, as such, supports the presence of underlying hydrothermal dolomite in the sag feature.

The association of the conduits with reduced geochemical features along the profile lines is supported by ferric:ferrous iron data (Figures 6.13 and 6.14 together with the map of Plate 1). A profile of ferric iron on

the easternmost profile (PIZ) shows distinct troughs at each end of the line and three distinct breaks in the middle part of the line that coincides with an overall ferric iron high. The lows in ferric iron coincide with the metal depletion zones in four of the five cases (compare Figures 6.13 and 6.14 with Figures 6.8 through 6.12). The pattern is repeated by inspection of Figure 6.14 where five areas of ferrous-enriched ferric:ferrous ratio coincide with the above-described metal depletion zones and depletion in ferric iron. Significantly, the two most geochemically pronounced depletion zones (marked 1 and 2 on the figures) of ferric iron and metals coincide with the margins of the seismically defined sag feature, which has also been incorporated on all of the figures of profiles (Figures 6.8 to 6.14). Two smaller inferred conduit zones (marked 3 and 4 on the figures) consistently appear within the seismic sag feature on the PIZ line and can be observed as smaller depletions in metals and ferric iron on Figures 6.8 through 6.14.

**Hydrocarbon Gas Zonation.** Perhaps even more significantly, the depleted zones of metal and ferric iron coincide with marked highs in the low C-number hydrocarbon gas profiles (Figure 6.15 – on conduits 1 and 2 for methane, Figure 6.16 – on conduits 1 and 3 for ethane, Figure 6.17 – on conduit 2 for propane, and Figure 6.18 – on conduit 2 for butane). For the higher C-number hydrocarbon gases, the pattern shifts to the dolomitized wall rocks away from the conduits, although some of the data spikes in the vicinity of the conduits. I-Pentane, iHexane, and nHexane show maximum spikes at 4711800 N, which is halfway between inferred conduits 3 and 4 (see Figures 6.19, 6.21 and 6.22). I-Hexane shows the most distal pattern with respect to the conduits (see Figure 38), followed by nHexane (Figure 6.22). The pentanes show a mixed pattern with respect to their distribution to the inferred conduits.



In summary, there appears to be a fractionation pattern in the hydrocarbon gases with the lower C-number hydrocarbon gases (methane and ethane) distributed towards the conduits, especially conduit 1 at the northern end of the PIZ profile. In contrast, the intermediate C-number gases (propane [Figure 6.17] and nButane [Figure 6.22]) show a distinct preference for conduit 2 at the south end of the PIZ profile. However, pentane and hexane appear to be markedly distributed away from the northern conduit 1 and, in general, away from all of the conduits, with the exception of some pentane preference for conduit 2.

Thus, with respect to a fractionation pattern that is a function of oxidation state, both on maps and profiles, methane and ethane appear to be present in the most reduced parts of the system, which occurs in the eastern part of the field and in the immediate vicinity of conduit 1 throughout the field. Propane and butane occupy an intermediate position in the spectrum and appear to show a preference for conduit 2, whereas hexane and pentane are most enriched in the western part of the field and are displaced away from the main conduits. Hexane and pentane also show the most overall coincidence with the metals, which also occupy positions peripheral to the conduit features (see discussion above).

**Integration with Hydrothermal Dolomite (HTD) Hydrocarbon Conceptual Model.** The apparent geochemical zoning patterns in the Glodes Corner field that have been outlined above are impressively consistent with the conceptual model developed in the NYSERDA project Contract No. 6984. In particular, the zonal patterns at Glodes Corner strongly conform to the reaction sequence covered by stages 3A (early saddle dolomitization at and near depositional site) and 3B (late saddle dolomitization, anhydrite formation, carbon dioxide effervescence, hydrogen loss and methane unmixing), stage 4 (sulfide deposition and hydrocarbon deposition), and stage 5 (deposition of late calcite at depositional site and illite/smectite/kaolinite clays in and marginal to depositional site). The conceptual model is applied to the map of geochemical data in Figure 6.23, which also shows the geographic distribution of ferrous iron as does the unannotated version. The geochemical data line in the easternmost profile best conforms to the initial stages 3A and 3B chemical reactions that accompanied main stage, high temperature, hydrothermal dolomitization. The elevated magnesium anomaly and CO<sub>2</sub> anomaly, together with the abundance of methane and ethane and overall high ferrous iron content, suggest the earlier, less oxidized stage of the reaction paragenesis.

The preference of the base metals and potassium for the middle (FOX) profile suggest a reaction similar to Stage 4 sulfide deposition and higher C-number hydrocarbon synthesis occurred in the general vicinity of the FOX profile. The elevated potassium in this profile (Figure 6.6), as well as sodium (Figure 6.3), suggest that illitic clay developed in the vicinity of the FOX profile, where they possibly served as important catalytic agents, along with small amounts of pyrite and sphalerite in the formation of higher C-number hydrocarbon gases (especially pentane and hexane). The most distal and latest depositional reactions may

have taken place in the western part of the Glodes Corner field, where they are represented by geochemical signatures in the GREY profile in the western part of the field. This line contains the most elevated hexane and pentane, the highest overall ferric/ferrous ratios, and the most oxygen-biased CO<sub>2</sub> to O<sub>2</sub> ratios. It also contains the most elevated sodium (possibly in sodic illite or smectitic clays) and vanadium (possibly in vanadiferous illite [roscoelite]) and arsenic (possibly as small amounts of arsenian pyrite and/or low temperature marcasite). All of the previously described chemistry is consistent with the lower temperature, more oxidized part of the paragenesis. In turn, all of the above-described chemistry is consistent with and confirms the hydrothermal petroleum model developed in NYSERDA Contract 6984.

**Electro-chemical processes for vertical transfer of the geochemical signature of the underlying resource to the surface.** An interesting geochemical question concerns how what we have inferred to be an underlying primary chemical dispersion/fractionation footprint is transferred from the reservoir region some 8,000 feet vertically into the overlying B horizon of surface soils. In some cases, the geochemical 'footprint' has somehow been transferred some 20,000 feet vertically above certain kinds of hydrocarbon resources! (Bob Clark, personal communication, August 2002).

Just as the primary geochemical footprint relates to fractionation of hydrothermal fluids along oxidation state gradients, the vertical transfer of the geochemical signature from the source region is also primarily a function of redox state. In this case, very small amounts of chemical constituents are transferred by gas and/or electrochemical processes from the reservoir region to the surface. In the area of the more reduced conduits, element depletions are generally common, especially those elements that are directly a function of oxidation state. For example, ferric:ferrous iron ratios range from about 15:1 to over 1,000:1. Consequently, by far the greater amount of iron is in the form of ferric iron, which is arranged laterally to the more reduced ferrous iron, which occurs in much smaller amounts in the vicinity of the conduits.

The contrast in oxidation state of the conduit central zone and the wall rock peripheral zone can result in a dramatic transfer of ions. The ions include transition metals and halogens, and the pattern is, in part, a function of the redox state and structure of the underlying reservoir. Oxidation of this reservoir results in electrochemical transfer of ions from the reduced, oxidizing core to more oxidized peripheral setting in the more oxidized wall rocks. The ion transfer is electrochemical in nature and reflects, in part, oxidation of an electrochemical cell centered on reduced components, which also coincide where the main reduced hydrocarbon charge is likely to be present.

Hydrogen may play a key role in the electro-chemical process described above. In particular, hydrogen gas

may act as a carrier or bridge for electrons and charged ion species. Electron-rich areas in the central, conduit-related zones also coincide with zones that are rich in hydrogen, in contrast with metal- and halogen-rich coronas which reflect a progressive decrease in hydrogen content outward, especially in the more halogen-rich coronas.

However, it was also shown above that the underlying pattern, in part, reflects, and may indeed largely reflect the original geography and fractionation of elements in the original hydrocarbon plume, including the primary deposition of hydrogen and related compounds. Electrochemical oxidation of this multi-element, compounded plume subsequently results in the vertical gas/electrical transfer of very small amounts of charged ions vertically above the primary footprint. This electro-chemical flux, which is more or less constant, is trapped at the lithosphere/atmosphere interface in the B horizons of surface soils. Analytical technologies, such as Induction-Coupled Plasma (ICP) and Induction-Coupled Plasma/Mass Spectrometry (ICP/MS) have now achieved a precision and low enough detection limits to reliably measure the above-described, low-level, ionic flux. This ion-flux process obviously has the capacity to penetrate post-mineral/hydrocarbon emplacement cover sequences during the oxidation of the underlying resource.

**Physical processes for vertical transfer of the geochemical signature of the underlying resource to the surface.** The problem with the simple flux model discussed above is that, even though the flux involved relatively dissociated, relatively light gas species (with the exception of hydrogen), the molecular size of the above-described gas species is probably too large to simply diffuse through relatively impermeable horizons, such as black shale. Consequently, some kind of physical fracture framework is required to provide a conduit system for passive vertical transfer of ionically charged hydrogen gas and larger sized hydrocarbon molecules. The main physical conduits may be provided by steeply dipping to vertical joints that occupy the cover sequence above the reservoir site. After its emplacement, which involved a considerable lateral component due to the ambient transcurrent tectonic setting active at the time of field emplacement, the field passively oxidized and degassed into the near vertical joint network between the field and the surface. In the case of Glodes Corner field, the passive degassing may have begun after its emplacement during the Acadian Orogeny. This near vertical joint framework was the culmination of Paleozoic and Mesozoic tectonism that affected the area. The field probably continually degassed and oxidized at a very slow rate after its emplacement and continues to do so today.

Recent studies of geothermal fields suggest that the geochemical signature of the underlying field is continuously fluxed into the surface soil horizons. Indeed, in a geothermal case history in southwest New Mexico, recent agricultural disturbances appear to have been overridden by reestablishment of the underlying geochemical pattern since fields were tilled. The reestablishment appears to have taken place

within a period of several months and may even within a matter of weeks. Because the flux involves very low amounts of elemental materials (parts per billion and parts per trillion), it takes very recently developed analytical technologies to identify these low level elemental fluxes. Nevertheless, these fluxes are statistically real with respect to the data sets.

The geopressured environment in the original reservoirs may also be important to the establishment of various elemental and hydrocarbon gas anomalies in surface samples. Recent case histories suggest that geopressured reservoirs in the Rocky Mountain west are overlain by more concentrated hydrocarbon anomalies than nongeopressured, but still gas-saturated reservoir rocks immediately adjacent to the reservoir. One possibility is that the geopressure in the productive reservoir is an artifact of the original geopressure induced by the tectonic loads that accompanied the original reservoir emplacement (in this case the ambient geotectonic pressures associated with the Laramide Orogeny in the Rocky Mountain west). In effect, fields such as Glodes Corner are still depressurizing and 'leaking' at very slow rates since their emplacement. That is, even 'sealed in', pressurized reservoir environments still leak continuously, with the leakage being trapped at soil horizons where the leakage is transferred from the lithosphere to the atmosphere at the biosphere interface.

At boundaries (for example, faults) between pressure changes within the original geopressured fabric, significant contrasts in element and hydrocarbon assemblages, as well as in amounts, may be observed. At Glodes Corner, for example, the overall element in element and hydrocarbon dispersion anomalies all give way to background levels in rocks underlying soils on the north and south margins of the east-west-trending reservoir. This may reflect much lower pressure regimes that simply do not provide enough 'pressure head' to push gases vertically through the joints framework above the reservoir. It also may reflect a difference in fracture density between the reservoir environment and the wall rocks. This contrast in fracture density may allow greater gas flux in joints vertically situated above the reservoir, which can focus the passive rise of buoyant, low density, ionically charged gas molecules that are under higher pressure.

One might ask whether or not the biosphere hydrocarbon production obscures the deeper sourced hydrocarbon and element fluxes. In our experience to date, the biosphere 'noise overlay' is not significant enough to override the primary deeper sourced hydrocarbon and elemental fluxes. Even in the case of methane, conduit architecture and field definition of the underlying reservoir strongly correspond with methane geographic patterns in surface soils. Hence, microbial methane production, even though it is real, probably adds a constant background overlay that, despite seasonal variations, is still not large enough to obscure the underlying patterns, at least in temperate and desert climates where our case history examples have been gained to date. Tropical soil sample media have yet to be evaluated.

**Economic implications.** We have saved the best for last: the economic implications of the above narrative.

Figure 6.24 shows that in terms of total hydrocarbon gases along the PIZ profile, the total C-1 to C-6 hydrocarbon gas shows a strong preference for conduits 1 and 2 defined by the high ferrous zones. In particular, the northern conduit (#1) is strongly associated with the major producing gas wells (see Figure 6.23). In concert with reports we have heard about the field operation, this conduit may be more or less continuous throughout the field. In terms of the production history, most of the major producers appear to be linked to the same fracture system, as there appears to be considerable communication between the wells (personal communications to John Caprara from personnel associated with the production at Glodes Corner). This conduit is associated with the northern margin of the seismic sag feature in the east and central portions of the field and then may traverse at a low angle across the sag feature on a more WSW trend to connect with the important producers at the west end of the field.

The surface soil geochemistry confirmed a pattern that was identified in the field only by deep drilling. Deep drilling established that the central part of the field appeared to be 'plugged' by large amounts of hydrothermal dolomite that apparently filled up much of the pore space and available permeability. Remaining permeability associated with production appears to be restricted to fracture permeability around the edges of the field. The 'plugging' effect is associated with elevated CO<sub>2</sub> and base metals that consistently define low level anomalies in the center of the seismically defined sag feature.

Although not conclusive at this point, there may be some remaining drill targets. These targets may be associated with an interconnected conduit system that borders the southern margin of the seismically defined sag feature. One possible conduit configuration is shown on Figure 6.24. This conduit needs much more definition in the form of more profiles and square grids.

### **Summary of the Glodes Corner geochemistry**

In summary, geochemical data for three profiles at the Glodes Corner field in south central New York confirms the conceptual hydrothermal petroleum model developed in the final report of Contract 6984. It also preliminarily identifies a within-field conduit architecture that consistently explains the known production and may provide some additional exploration targets in the southern part of the field, where the conduits may be present in dolomitized wall rocks of the Trenton-Black River section immediately south of the seismic sag feature. Furthermore, the geochemical data have provided a semi-rigorous test of the above conceptual model and also preliminarily suggest that the practical geochemical tool may be imminent that would not only see the

overall field, but would also see internal conduit features that are related to the gas/oil charge within the field. This resolution appears to 'see' detail inside of the resolution obtainable from geophysical technologies, such as seismic and aeromagnetics.

The best understood field, at this point in our investigation, is the Glodes Corner field in Steuben County, New York. The hydrothermal fluid flow model derived from the tectonic/dynamic model described above predicts that low carbon number, hydrogen-rich gases should have entered the riedel/tensile trap site from the basement structure on the east. As the hydrothermal fluids migrated west, according to the chemical fractionation models developed above, they would oxidize and produce higher carbon number gases in greater abundance towards the western part of the field.

The current geochemical model at Glodes Corner can be extrapolated to other fields and field possibilities from an exploration point of view. This extrapolation is shown in Plate 3 together with a fluid flow model developed from the conduit architecture described in the Stage 1 to Stage 2 migration model for the Finger Lakes region. In terms of known Trenton-Black River gas production, 22 Trenton-Black River producers are presently known within the Finger Lakes region. Within the Steuben County area, at least 21 more sag features could be associated with potential Trenton-Black River resources. These potential fields should have similar geochemical signatures/characteristics and zonations as the Glodes Corner field. Obviously, the preliminary Glodes Corner geochemical study outlined above should be perfected and extended to other known producers (such as Muck Farm).

#### **Stage 6. Possible ascension of HTD fluid plumes and deposition of gas in sandstones at higher stratigraphic levels.**

One of the provocative implications of the 'bottom up' basement-sourced hydrocarbon model is that it is possible that the fluid plumes did not simply 'top out' at the Black River-Trenton horizons, but that these extremely large-volume fluid plumes inevitably found and utilized conduits to ascend to higher structural levels. These basement-derived fluids may have mixed with carbon sources in reduced, hydrogen- and carbon-rich shales, such as the Utica black shale and its equivalents. Gas deposits that are typically hosted in sandstone horizons in uppermost Ordovician through Devonian age rocks that predate to syn-date Acadian Orogeny (Isachsen and others, 1991, Figure 15.7). In this regard it is significant that no oil or gas accumulations have been reported in uppermost Devonian Conneaut and Conswango Groups or the Mississippian Pocono Group or the Pennsylvanian age Pottsville Group, despite the fact that these groups contain favorable sandstone horizons. One possibility is that

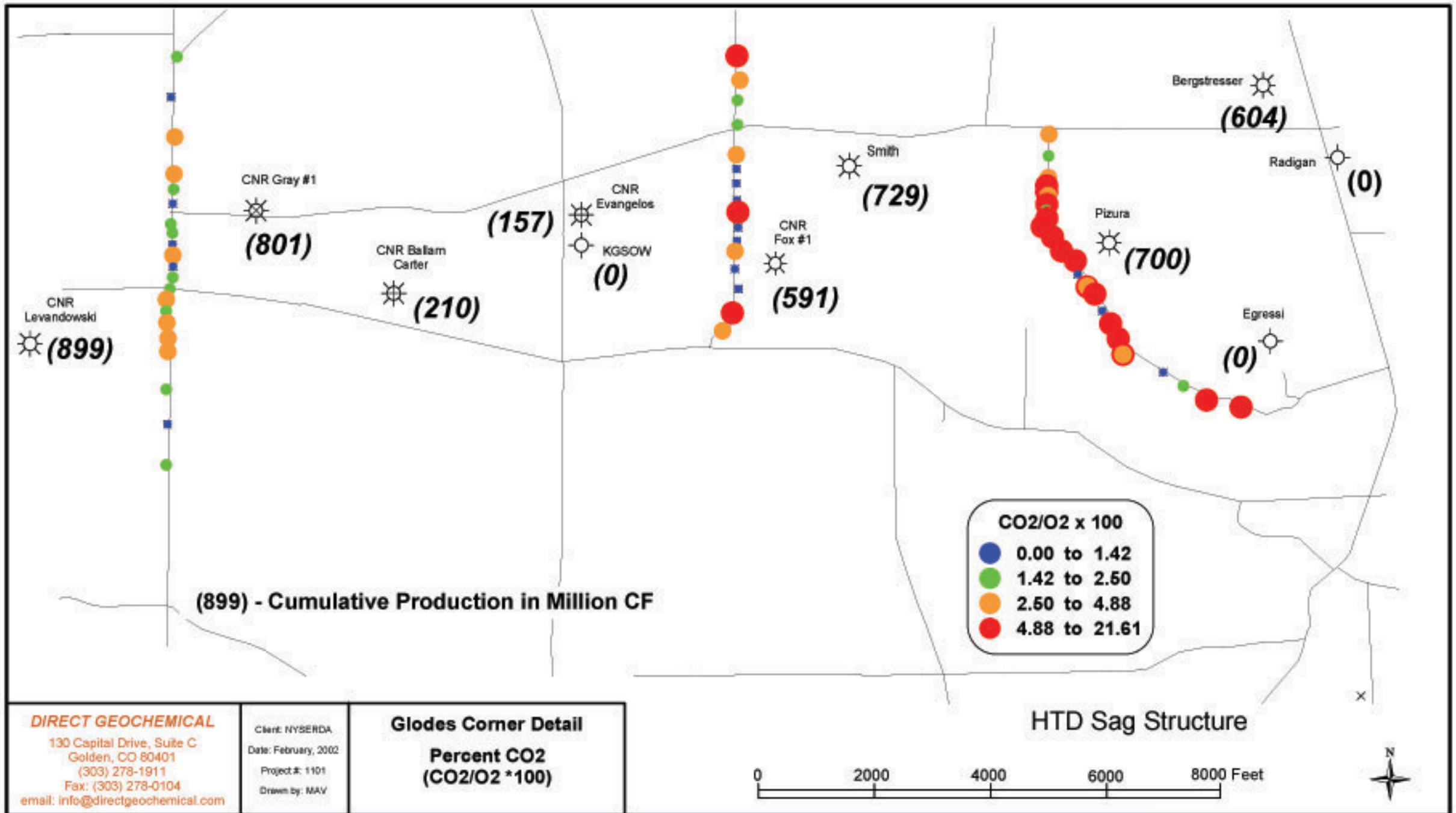
the highest Devonian unit with oil and gas (the Canadaway Group) in the upper portion of the Catskill Delta complex, may actually date the fluid generation event. Significantly, the age of this group is approximately the same as the 354 Ma fission track date that was discussed above.

The 'bottom-up' model for gas deposits throughout the Cambrian through Upper Devonian section in central and western New York is consistent with gas chemistry provided by Jenden and others (1993a, 1993b). The New York data is isotopically heavier, in terms of carbon 13 and deuterium isotopes  $\delta D$ , more helium rich, and more helium 3 biased. In addition to the mixing possibility model advocated by Jenden and others (1993), we would advocate the strong possibility of a 'bottom up'; isotopic fractionation model, whereby isotopically heavy gases at lower stratigraphic levels cool and are fractionated into isotopically lighter gases at higher stratigraphic levels. Again, it should be pointed out that cooler abiogenic gases generated during serpentinization experiments by Horita and Berndt (1999) are isotopically lighter (Horita and Berndt, 1999, Table 1). The chemical fractionation of the isotopic component may also be density related. Upon ascent, the heavier isotopic component in methane ( $^{13}C$  in the case of carbon isotopes or deuterium in the case of hydrogen isotopes)\* simply remains behind as the lighter isotopes separate and move with lower density methanes upward towards higher stratigraphic levels. {\* Note:  $^{13}C/^{12}C$  ratios are reported in d-notation as  $\delta^{13}C(\text{permil}) = 1000 \times [(^{13}C/^{12}C)_{\text{sample}} / (^{13}C/^{12}C)_{\text{PDB}} - 1]$  or deuterium is reported as  $\delta D = \{[(D/H)_{\text{sample}} - (D/H)_{\text{SMOW}}] / (D/H)_{\text{SMOW}}\} \times 1000$ }.

From an exploration point of view, the more well-known gas reservoirs hosted in the post-Trenton-Black River strata, such as the reservoirs in the Silurian Medina or the Lower Devonian Oriskany sandstones, may represent leakage features with respect to the large basement-sourced plume systems originating in the Cambrian rift basements. It may be possible to utilize the leakage concept to infer possible deeper targets associated with synclinal sag features offset laterally from a known field. For example, a Hamilton Shale-hosted (mid Devonian) tight gas field named the Naples field occurs to the northwest of Glodes Corner. Immediately east of this field, a synclinal sag feature potentially could host deeper Trenton-Black River gas resource that represents the down-plume extension of volatiles that migrated upwards into the middle Devonian Hamilton units. This type of fluid flow model may be applied to numerous other target possibilities in Steuben County and vicinity.





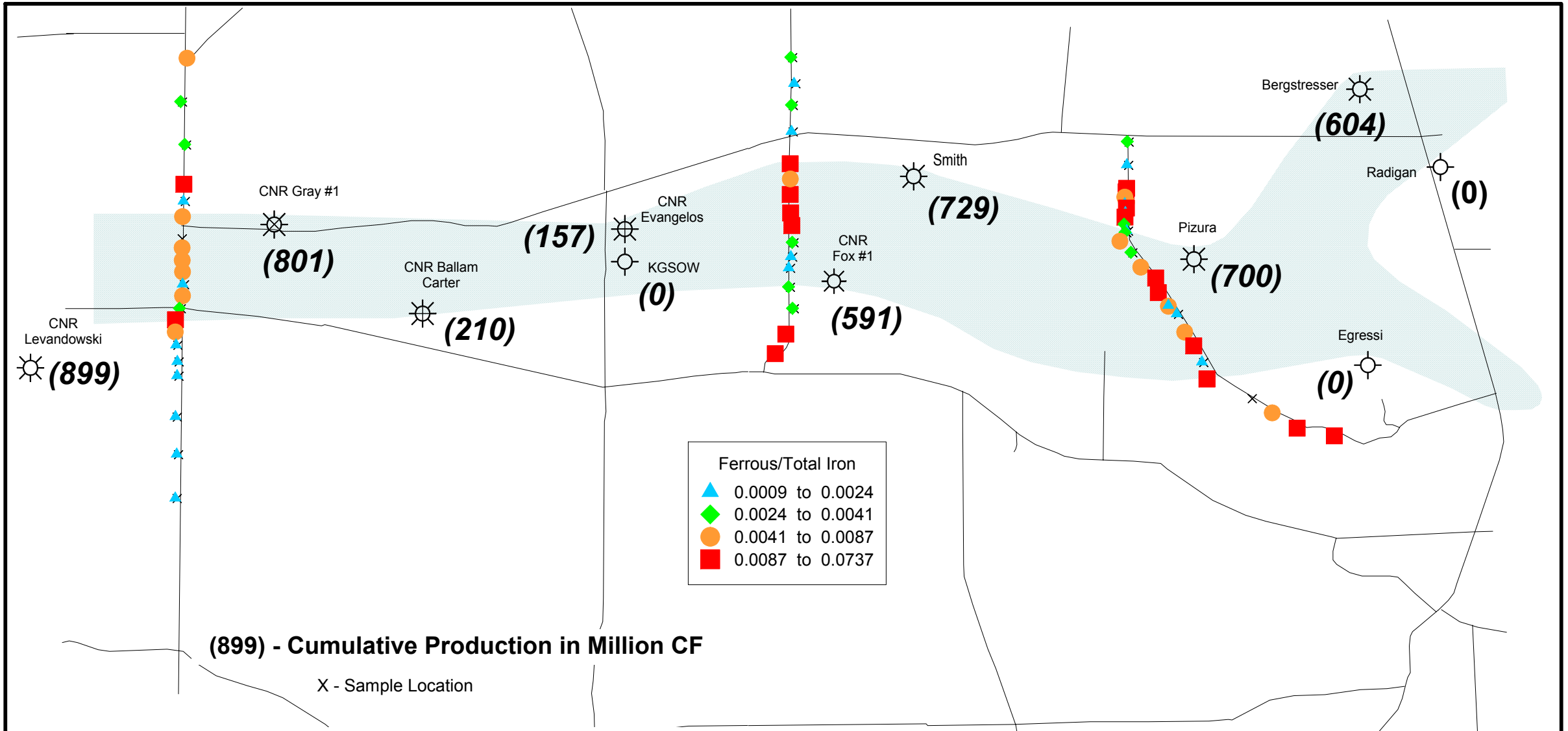


**DIRECT GEOCHEMICAL**  
 130 Capital Drive, Suite C  
 Golden, CO 80401  
 (303) 278-1911  
 Fax: (303) 278-0104  
 email: info@directgeochemical.com

Client: NYSERDA  
 Date: February, 2002  
 Project #: 1101  
 Drawn by: MAV

**Glodes Corner Detail**  
**Percent CO2**  
**(CO2/O2 \* 100)**

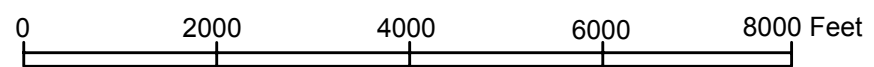
Figure 6.1. Map showing distribution of  $\text{CO}_2/\text{O}_2 \times 100$  in soils.



**(899) - Cumulative Production in Million CF**  
 X - Sample Location

Ferrous/Total Iron	
▲	0.0009 to 0.0024
◆	0.0024 to 0.0041
●	0.0041 to 0.0087
■	0.0087 to 0.0737

HTD Sag Structure

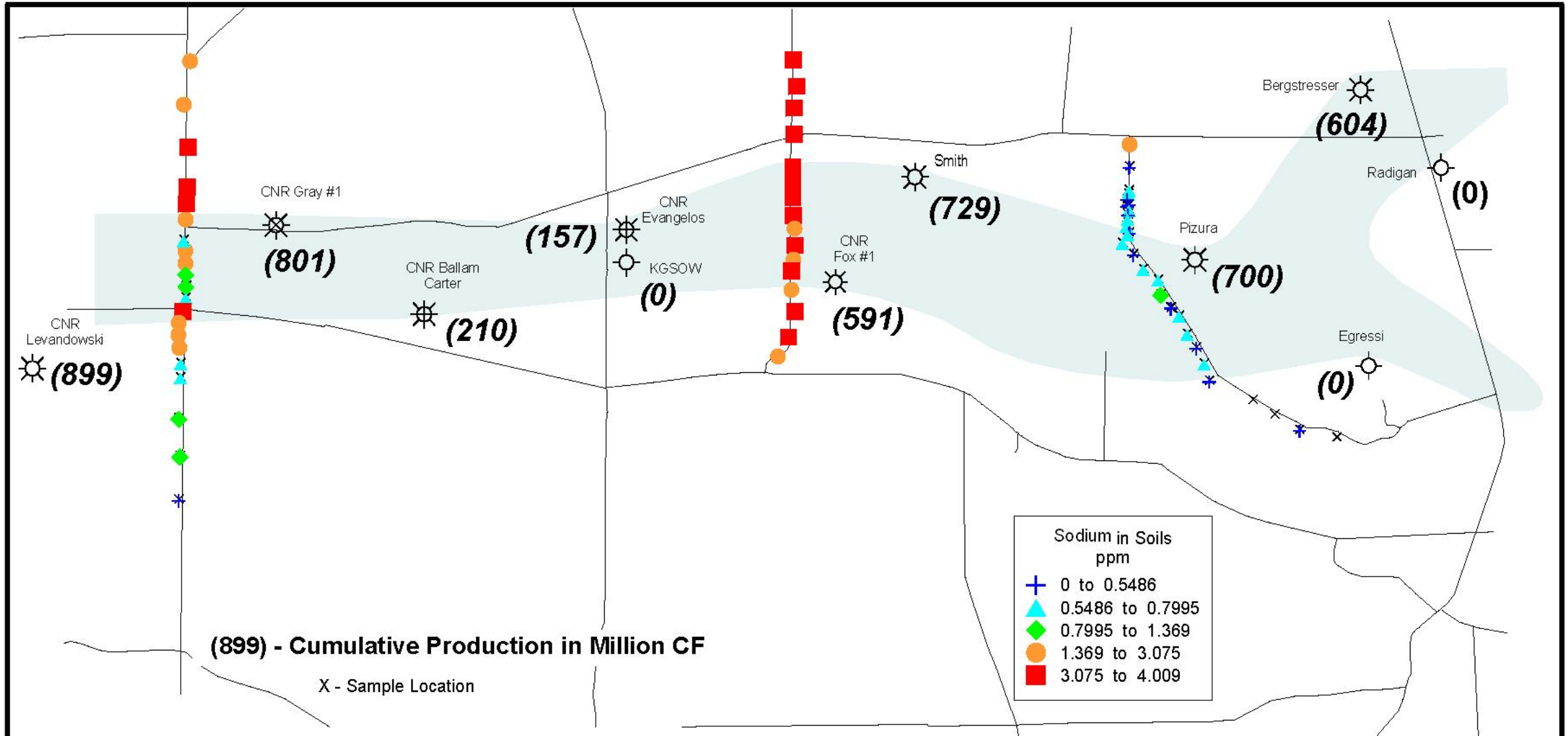


**DIRECT GEOCHEMICAL**  
 130 Capital Drive, Suite C  
 Golden, CO 80401  
 (303) 278-1911  
 Fax: (303) 278-0104  
 email: info@directgeochemical.com

Client: NYSERDA  
 Date: February, 2002  
 Project #: 1101  
 Drawn by: MAV

**Glodes Corner Detail  
 Percent Ferrous Iron**

Figure 6.2. Map showing distribution of percent ferrous iron in soils.

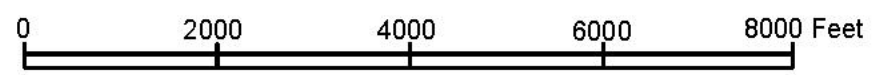


**(899) - Cumulative Production in Million CF**

X - Sample Location

Sodium in Soils ppm	
+	0 to 0.5486
▲	0.5486 to 0.7995
◆	0.7995 to 1.369
●	1.369 to 3.075
■	3.075 to 4.009

HTD Sag Structure

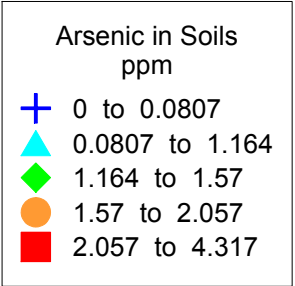
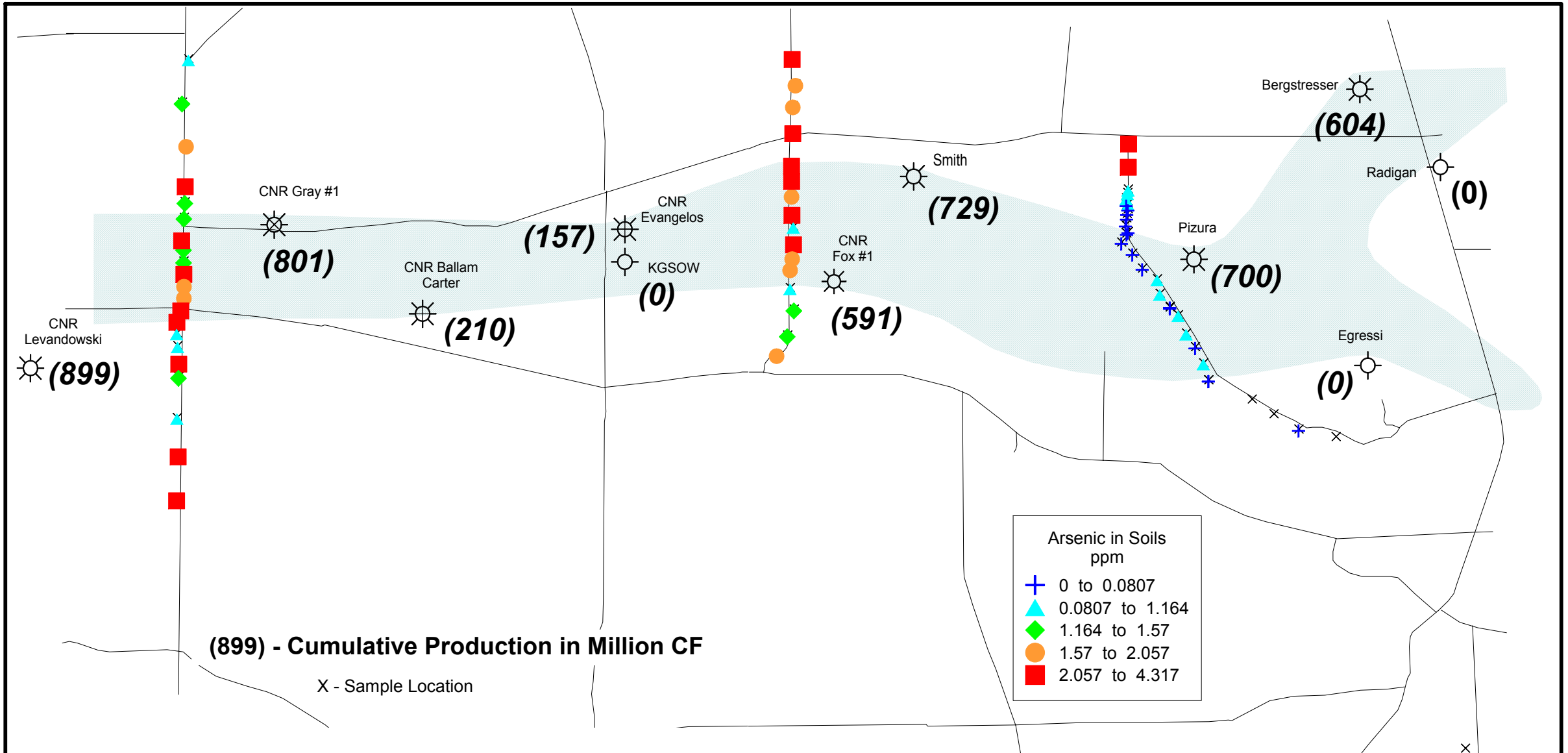


**DIRECT GEOCHEMICAL**  
 130 Capital Drive, Suite C  
 Golden, CO 80401  
 (303) 278-1911  
 Fax: (303) 278-0104  
 email: info@directgeochemical.com

Client: NYSERDA  
 Date: February, 2002  
 Project #: 1101  
 Drawn by: MAV

**Glodes Corner Detail  
 Arsenic Concentrations**

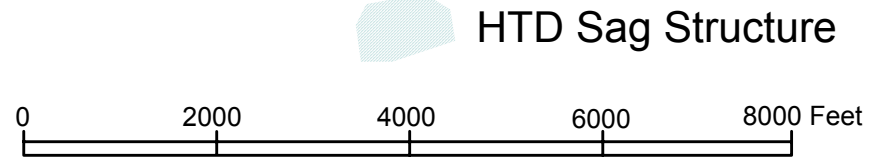
Figure 6.3. Map showing distribution of sodium in soils.



**DIRECT GEOCHEMICAL**  
 130 Capital Drive, Suite C  
 Golden, CO 80401  
 (303) 278-1911  
 Fax: (303) 278-0104  
 email: info@directgeochemical.com

Client: NYSERDA  
 Date: February, 2002  
 Project #: 1101  
 Drawn by: MAV

**Glodes Corner Detail  
 Arsenic Concentrations**

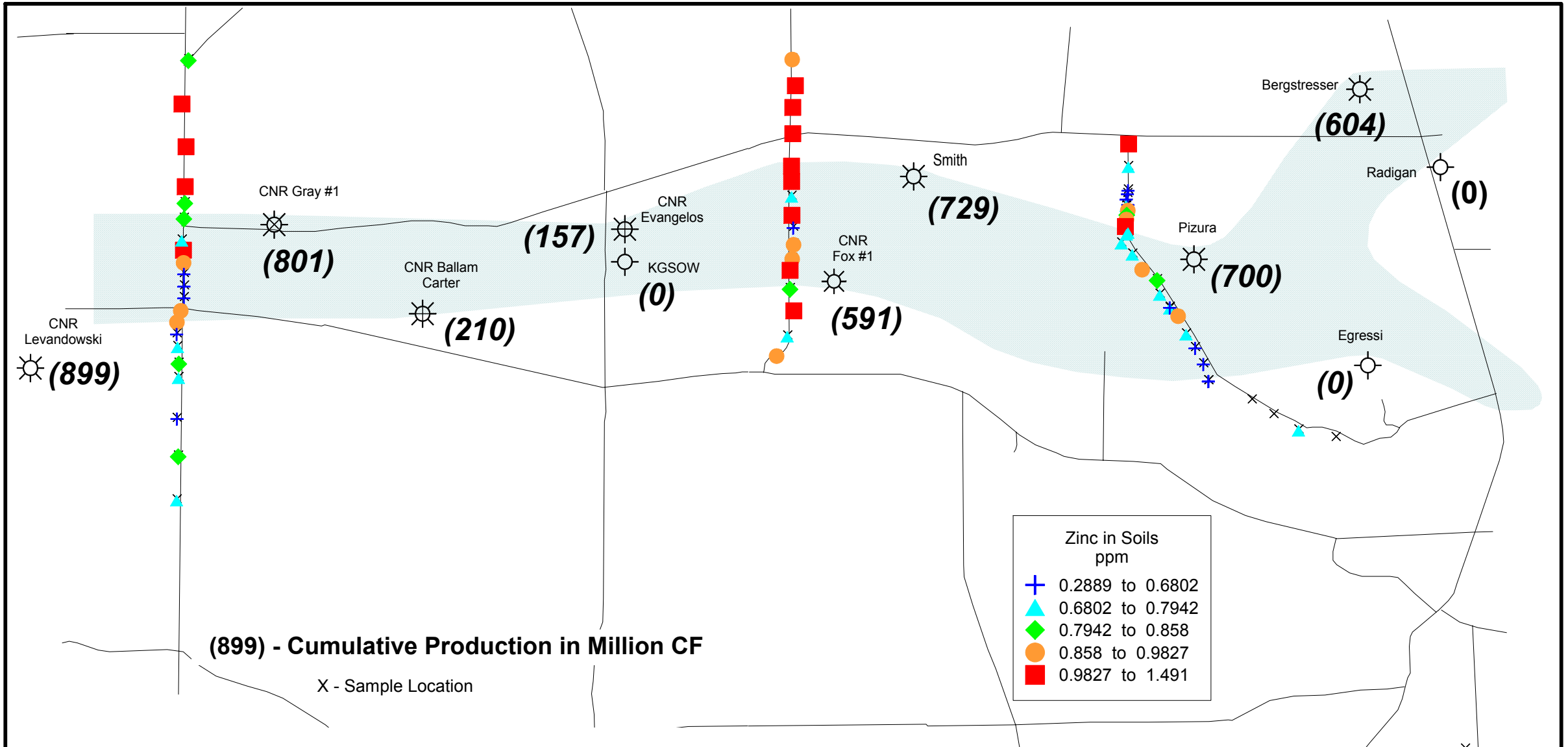


HTD Sag Structure



Figure 6.4. Map showing distribution of arsenic in soils.

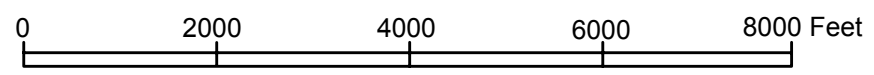




**(899) - Cumulative Production in Million CF**  
 X - Sample Location

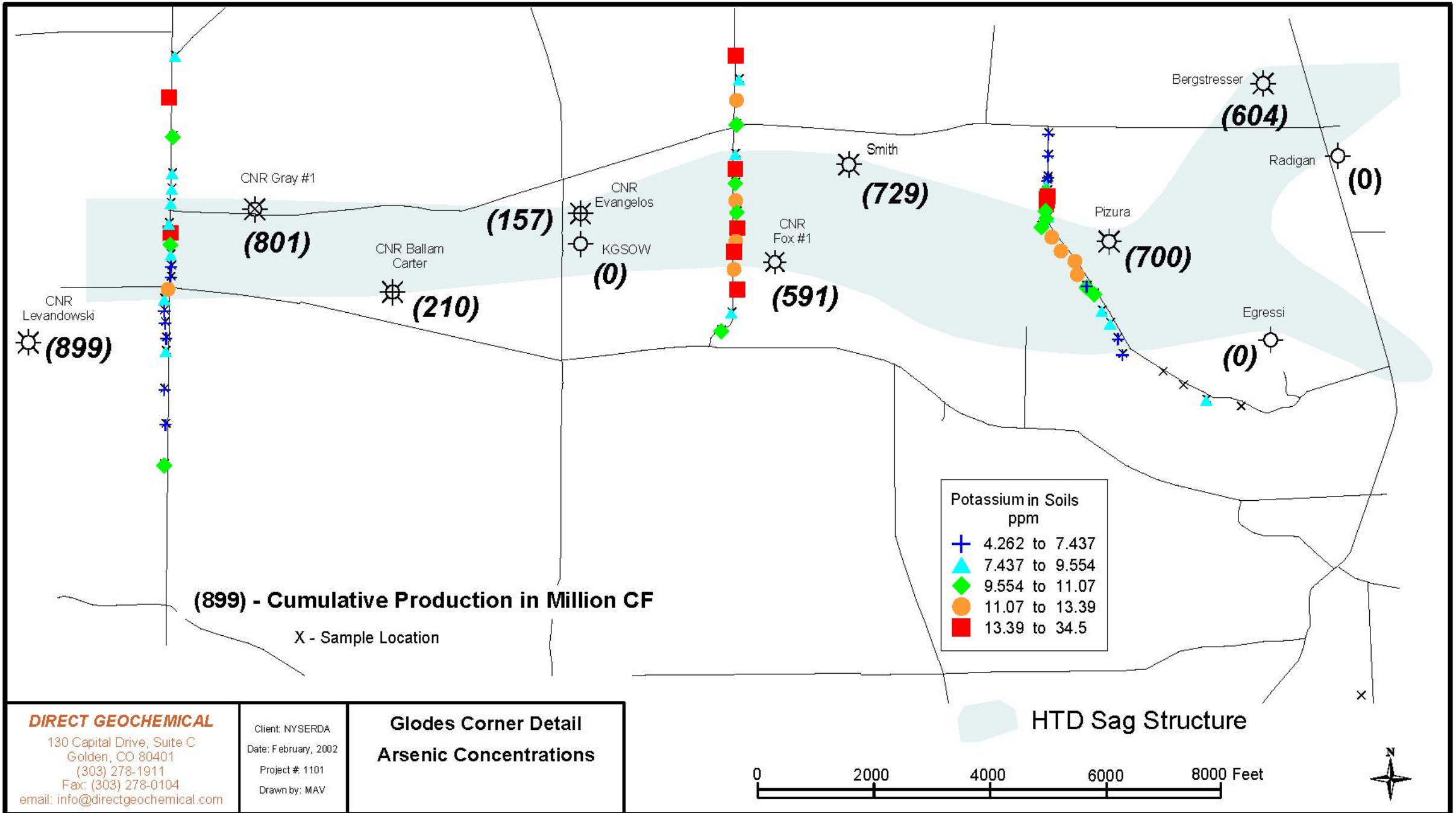
Zinc in Soils ppm	
+	0.2889 to 0.6802
▲	0.6802 to 0.7942
◆	0.7942 to 0.858
●	0.858 to 0.9827
■	0.9827 to 1.491

HTD Sag Structure



<p><b>DIRECT GEOCHEMICAL</b>          130 Capital Drive, Suite C          Golden, CO 80401          (303) 278-1911          Fax: (303) 278-0104          email: info@directgeochemical.com</p>	<p>Client: NYSERDA          Date: February, 2002          Project #: 1101          Drawn by: MAV</p>	<p><b>Glodes Corner Detail</b>  <b>Zinc Concentrations</b></p>
--	--	--

Figures 6.5. Map showing distribution of zinc in soils.



CNR Levandowski  
 ☀ (899)

CNR Gray #1  
 ☀ (801)

CNR Ballam Carter  
 ☀ (210)

(157)

CNR Evangelos  
 ☀ (0)

KGSOW  
 ☀ (0)

CNR Fox #1  
 ☀ (591)

Smith  
 ☀ (729)

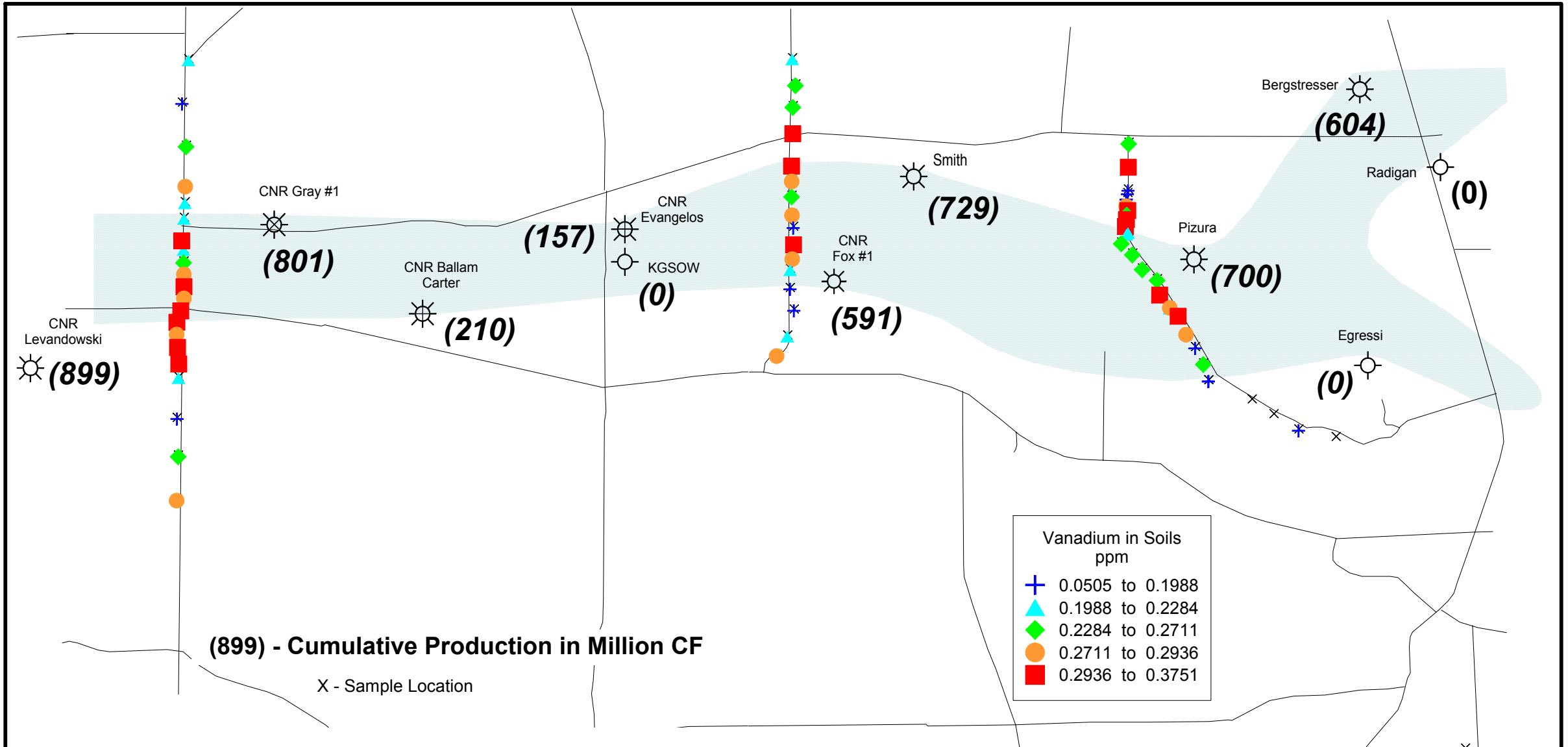
Pizura  
 ☀ (700)

Bergstresser  
 ☀ (604)

Radigan  
 ☀ (0)

Egressi  
 ☀ (0)

Figure 6.6. Map showing distribution of potassium in soils.



**DIRECT GEOCHEMICAL**  
 130 Capital Drive, Suite C  
 Golden, CO 80401  
 (303) 278-1911  
 Fax: (303) 278-0104  
 email: info@directgeochemical.com

Client: NYSERDA  
 Date: February, 2002  
 Project #: 1101  
 Drawn by: MAV

**Glodes Corner Detail  
 Vanadium Concentrations**

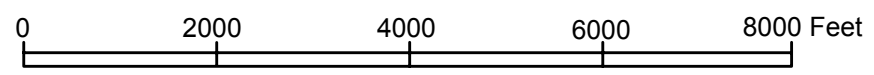


Figure 6.7. Map showing distribution of vanadium in soils.

Figure 6.8. Northing Versus Zinc in Soil for PZ Profile

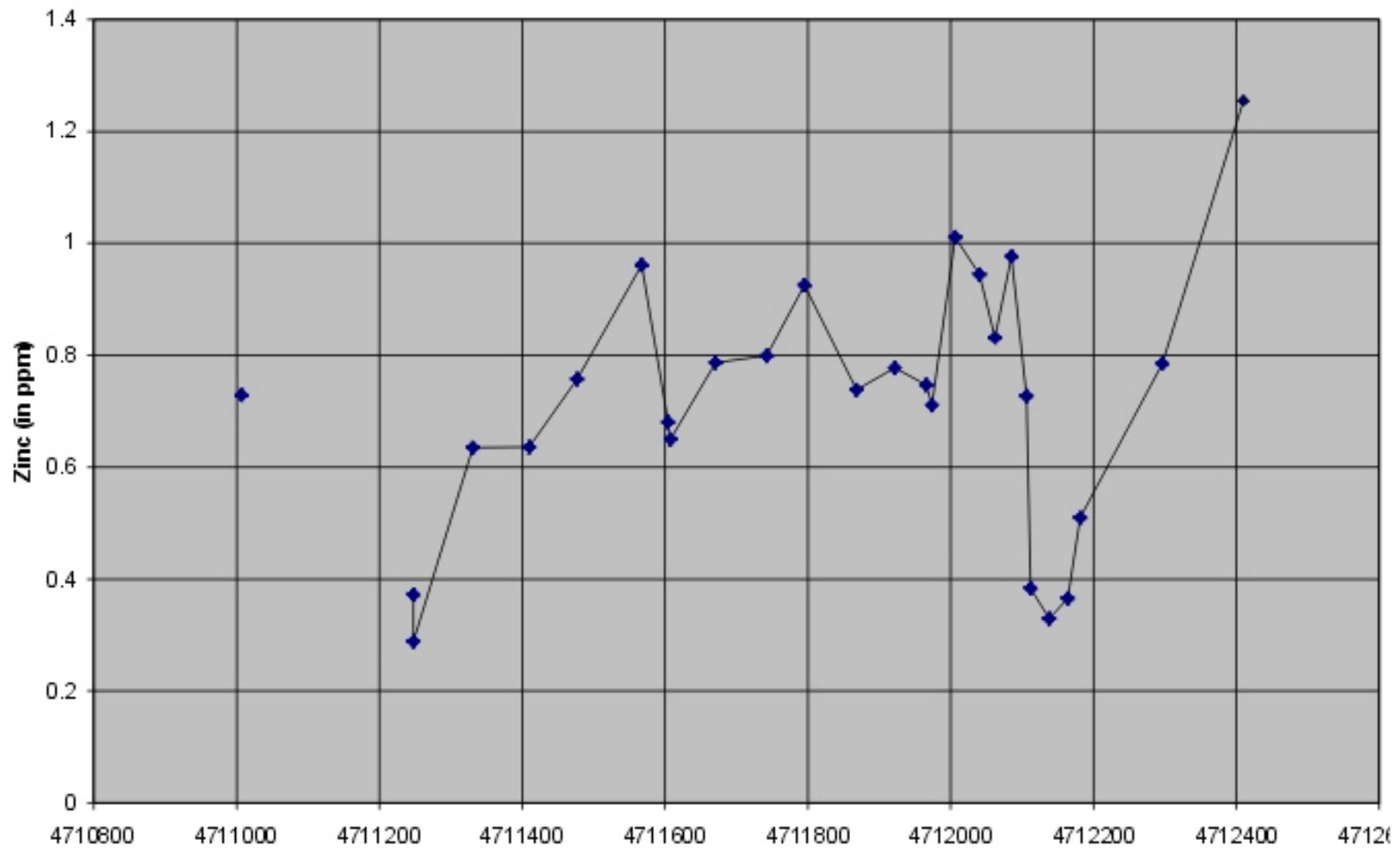


Figure 6.8. Northing versus zinc in soil for PIZ profile.



Figure 6.9. Northing Versus Nickel in Soil for PIZ Profile

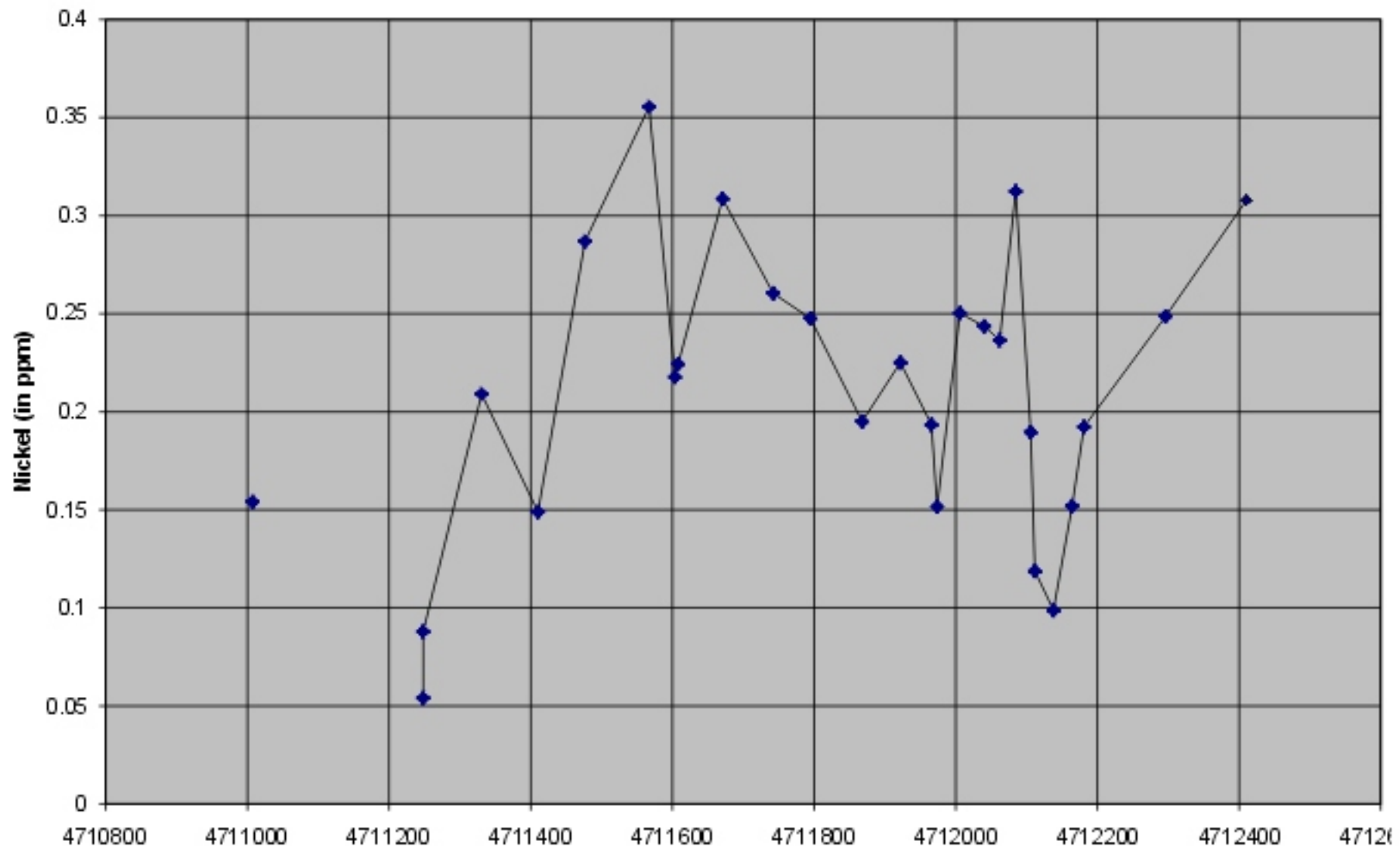


Figure 6.9. Northing versus nickel in soil for PIZ profile.

Figure 6.10. Northing Versus Potassium in Soil for PZ Profile

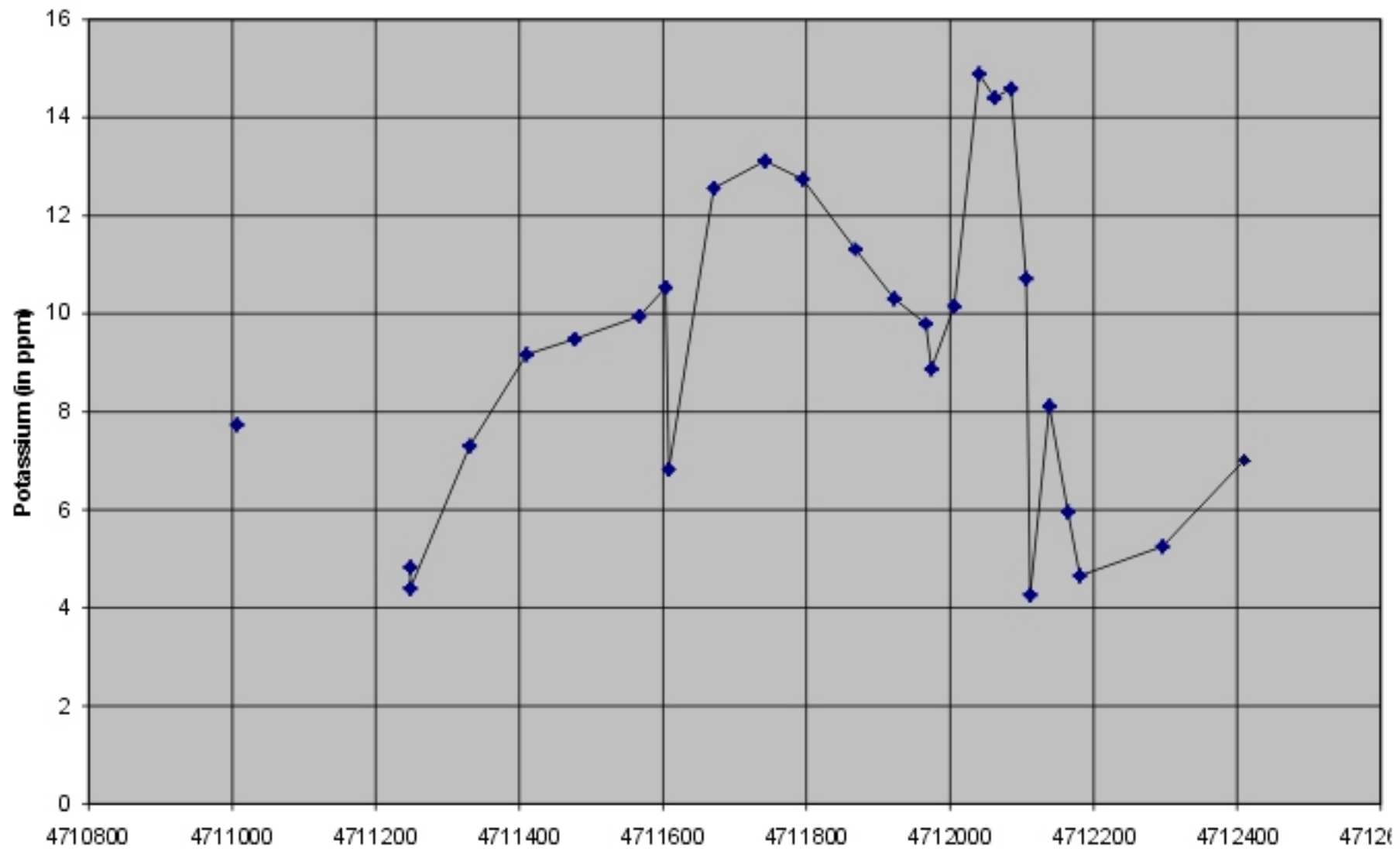


Figure 6.10. Northing versus potassium in soil for PIZ profile.

Figure 6.11. Northing Versus Magnesium in Soil for PIZ Profile

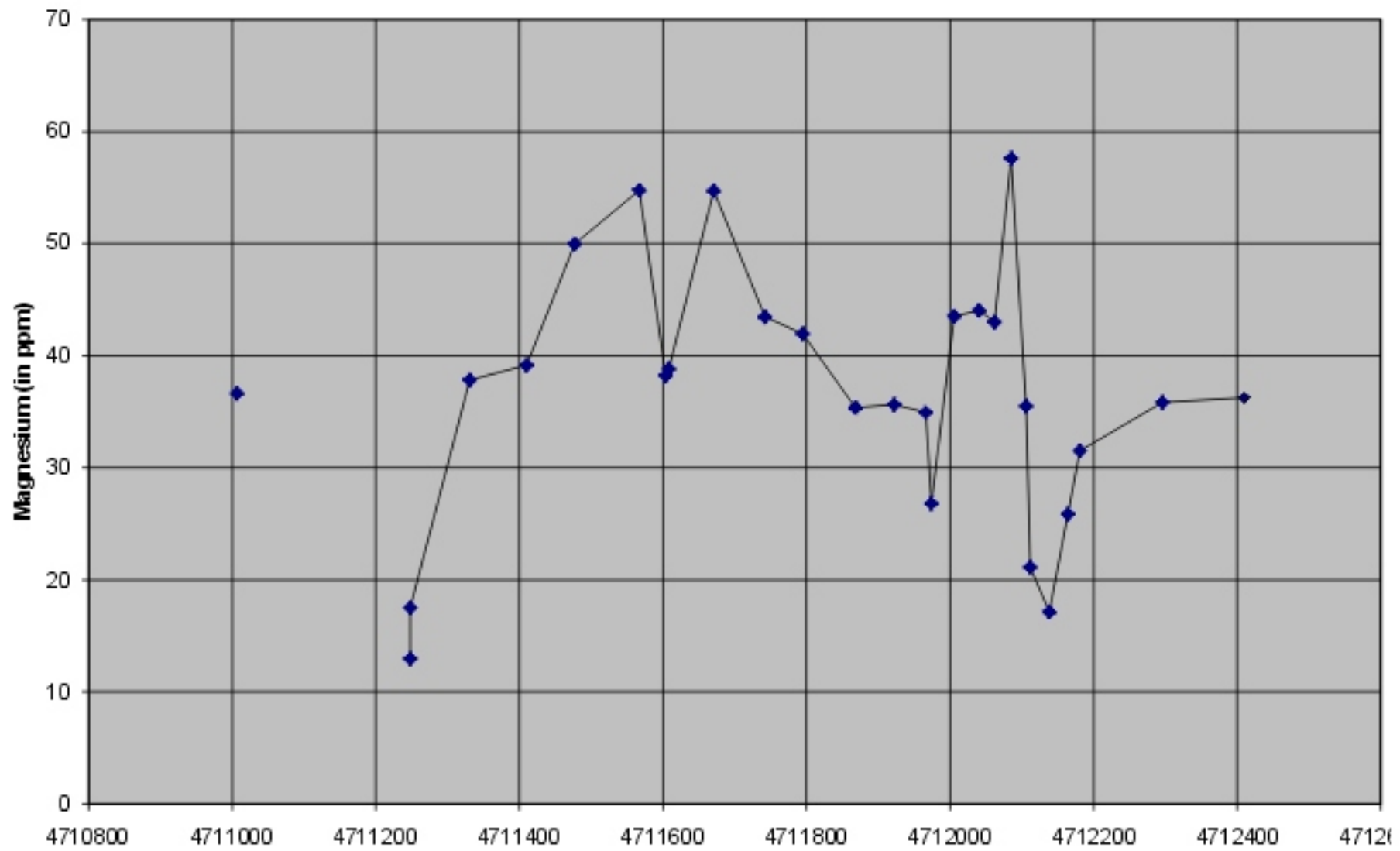


Figure 6.11. Northing versus magnesium in soil for PIZ profile.

Figure 6.12. Northing vs. Vanadium in Soils for PZ profile

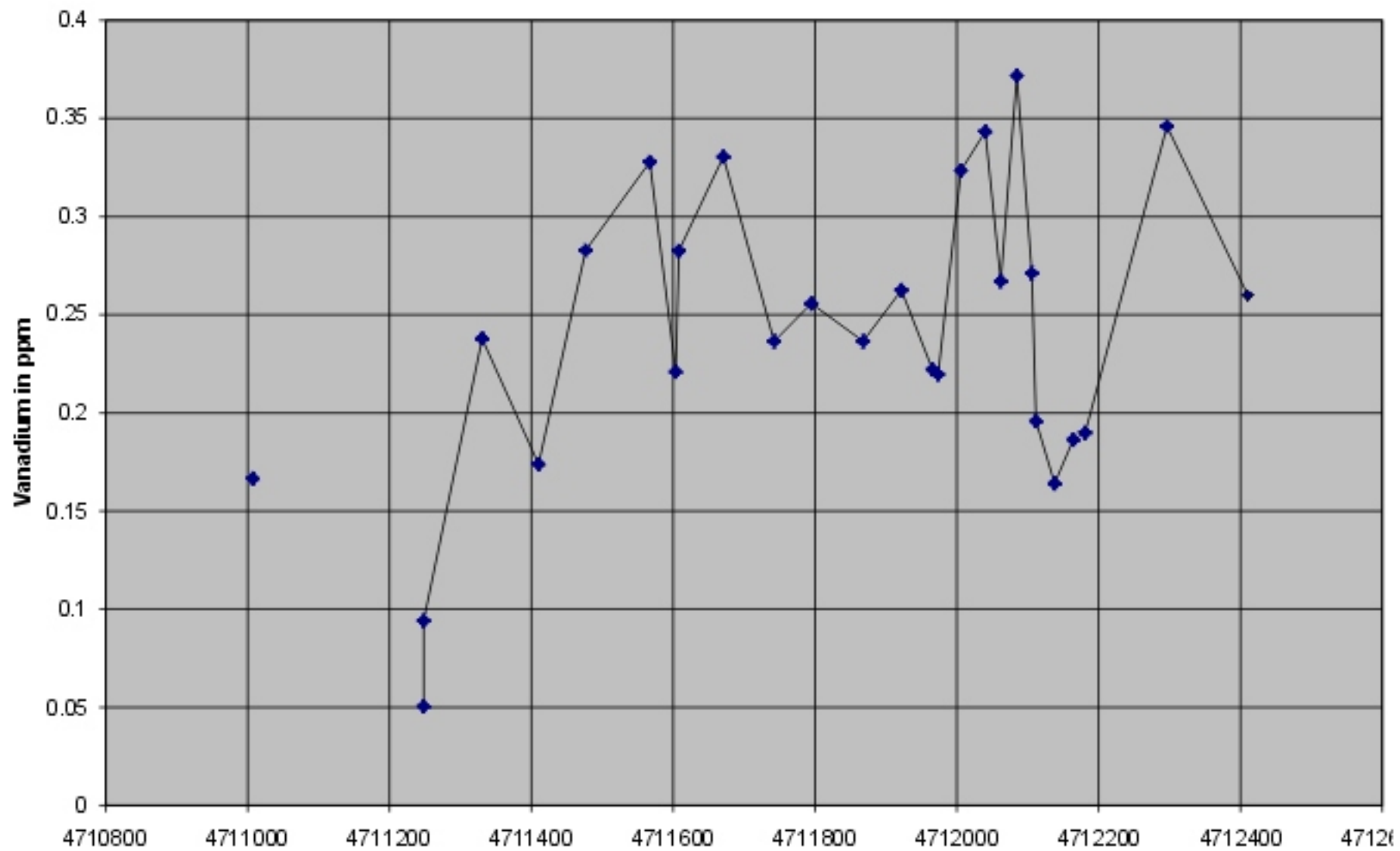


Figure 6.12. Northing versus vanadium in soil for PIZ profile.



Figure 6.13. Northing Versus Ferric Iron ( $\text{Fe}^{3+}$ ) in Soil for PIZ Profile

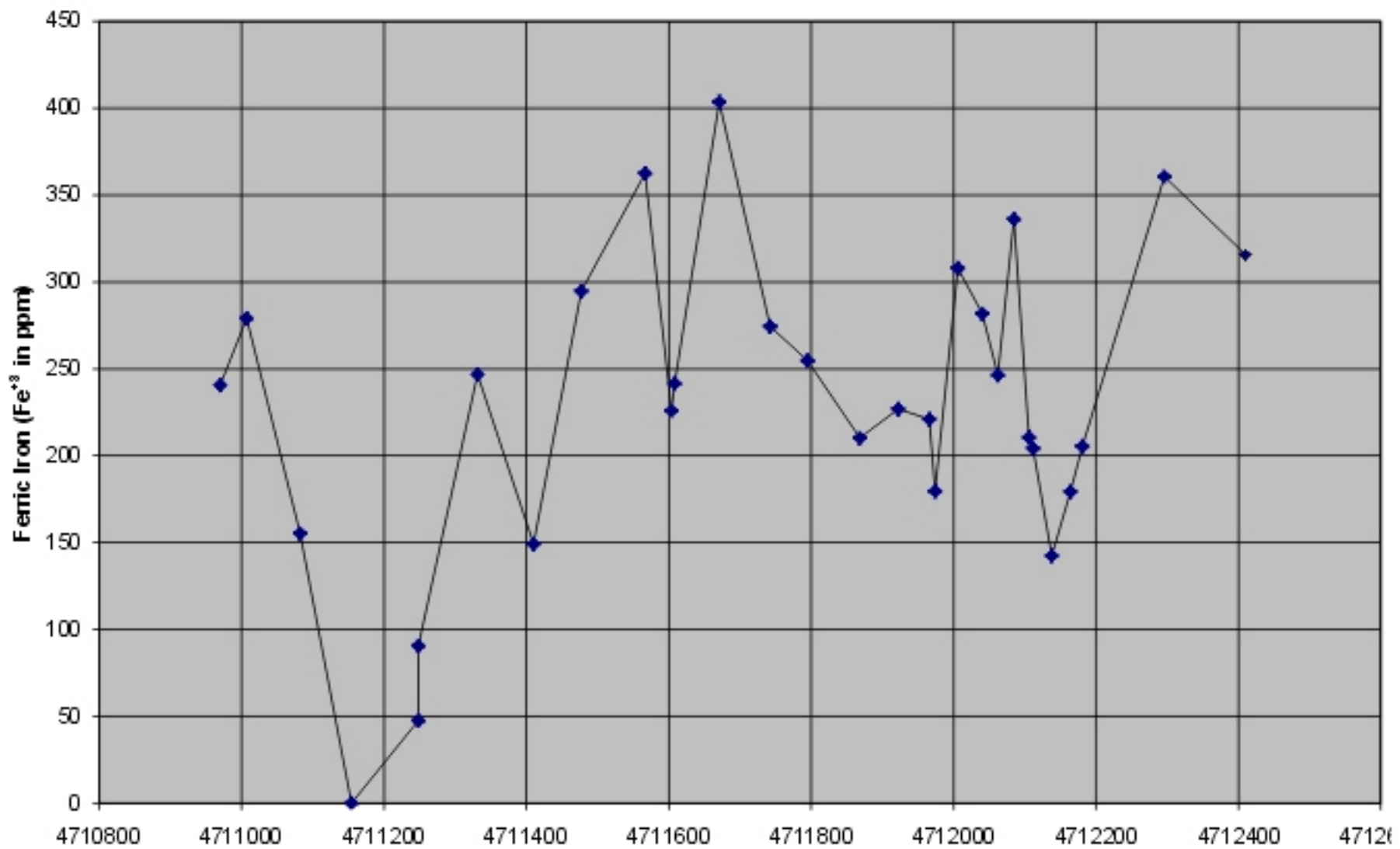


Figure 6.13. Northing versus ferric iron ( $\text{Fe}^{+3}$ ) in soil for PIZ profile.

Figure 6.14. Northing Versus Ferric/ferrous Ratio in Soils for PZ Profile

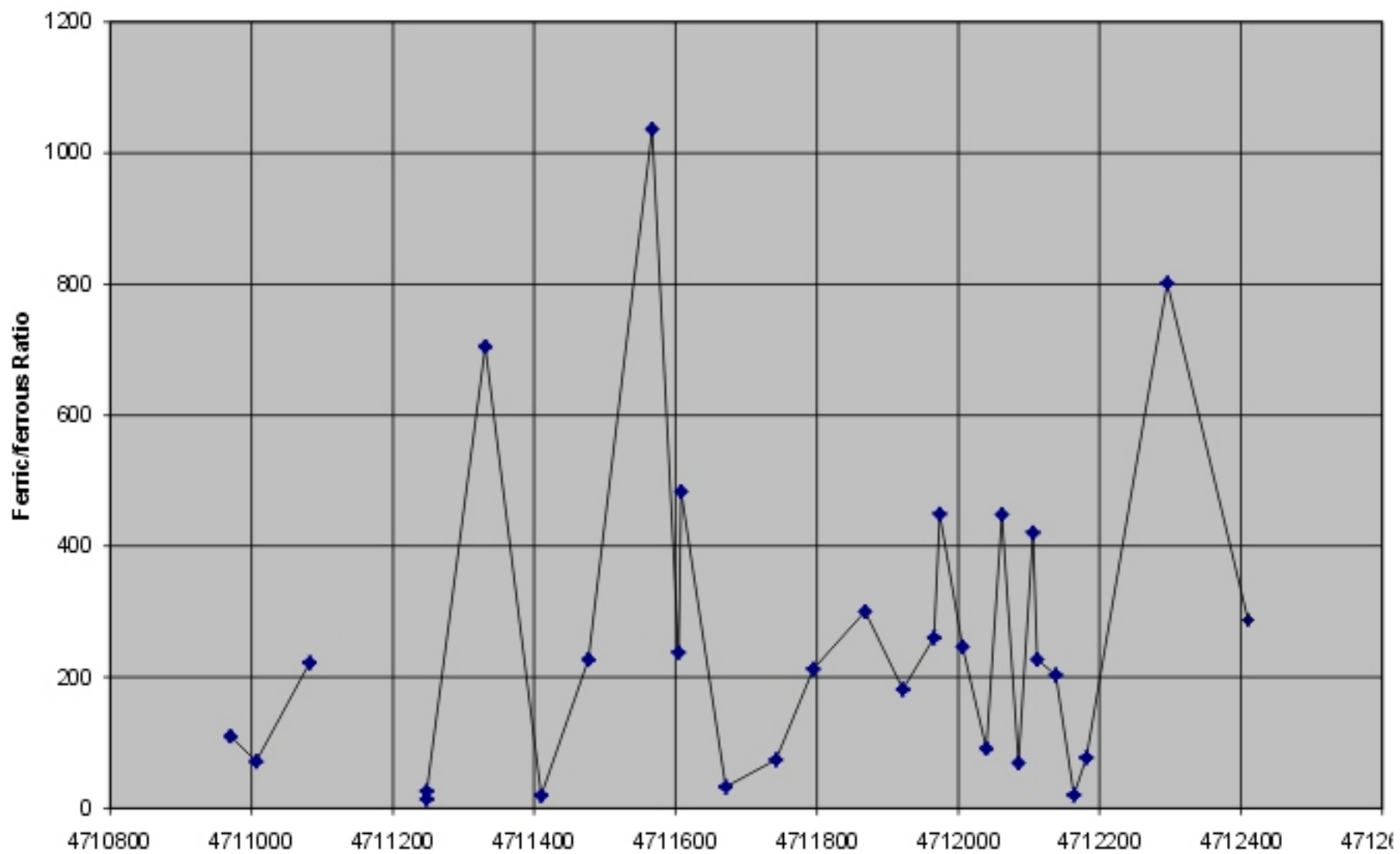


Figure 6.14. Northing versus ferric/ferrous ratio in soils for PIZ profile.

Figure 6.15. Northing Versus Methane in Soils for PIZ Profile.

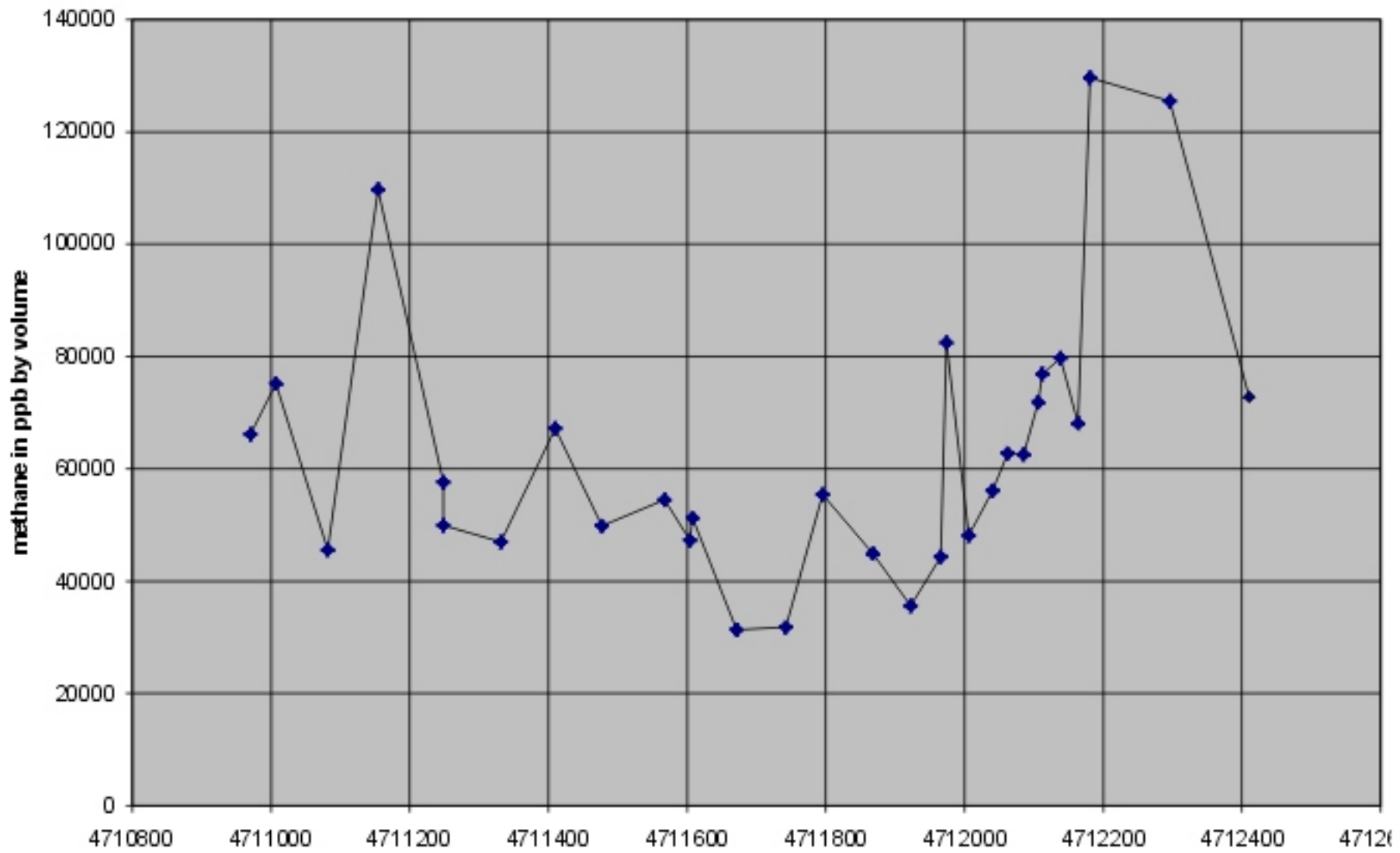


Figure 6.15. Northing versus methane in soils for PIZ profile.

Figure 6.16. Northing Versus Ethane in Soils for PZ Profile

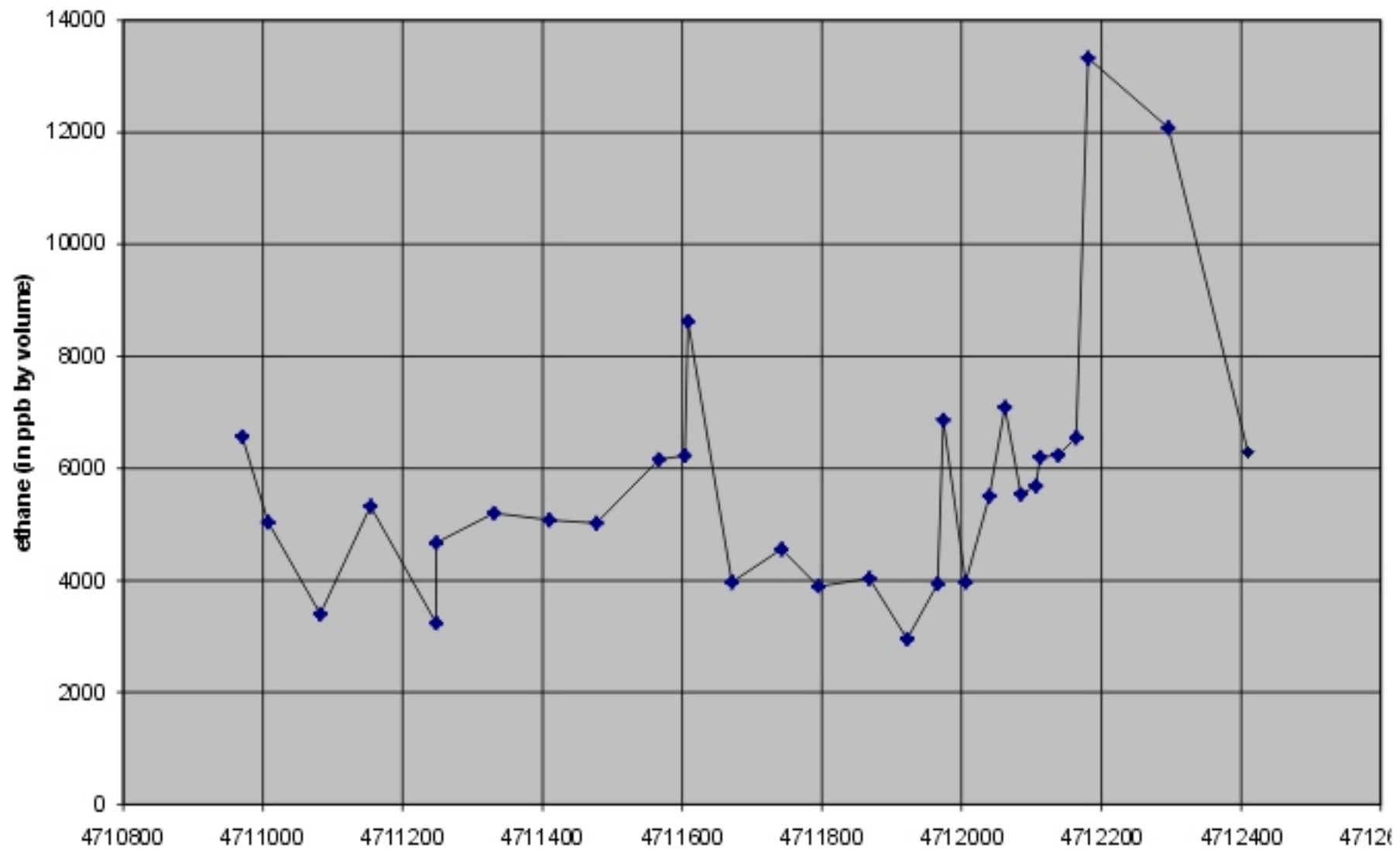


Figure 6.16. Northing versus ethane in soils for PIZ profile.



Figure 6.17. Northing Versus Propane in Soils for PZ Profile

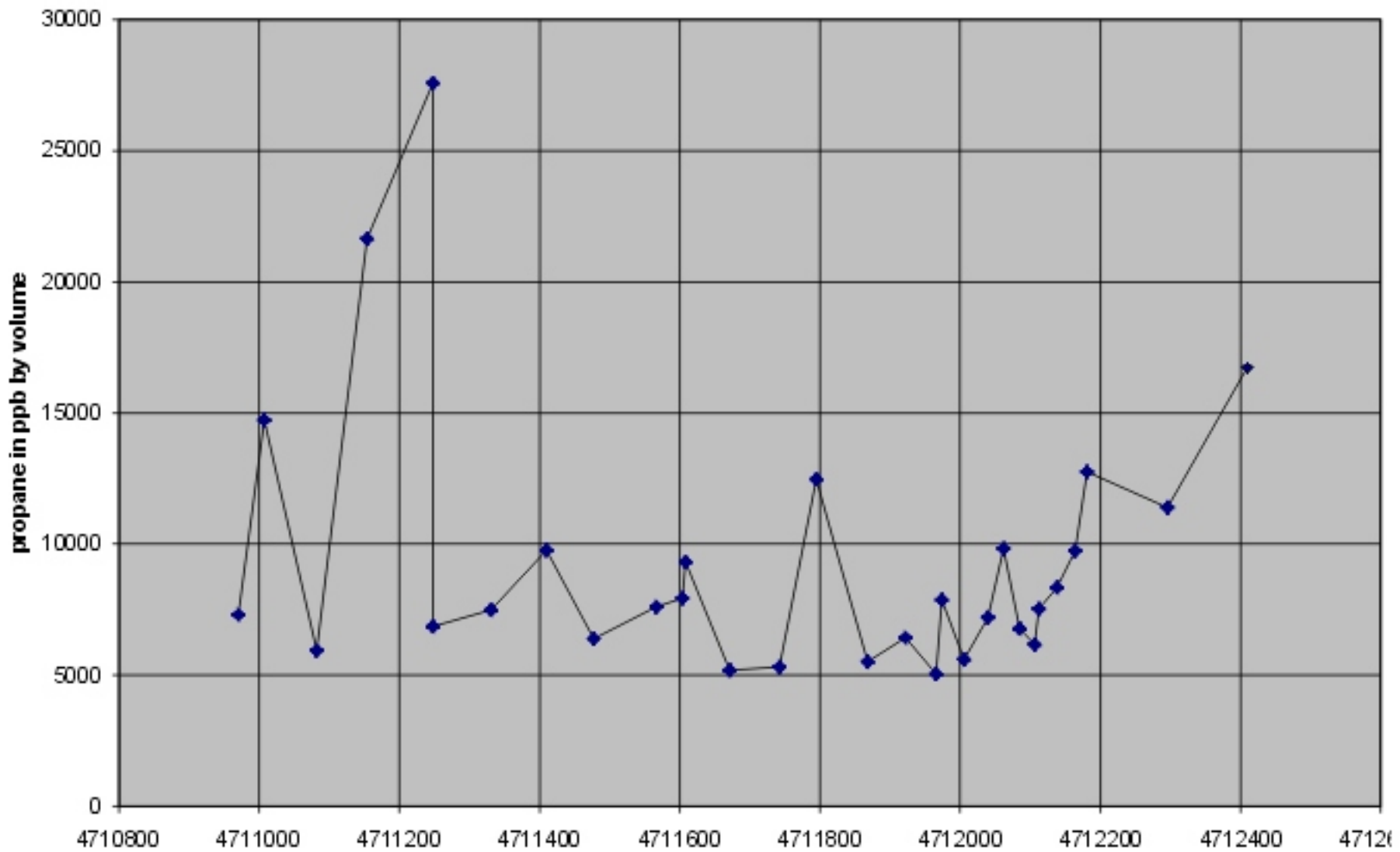


Figure 6.17. Northing versus propane in soils for PIZ profile.

Figure 6.18. Northing Versus nButane in Soils for PZ Profile

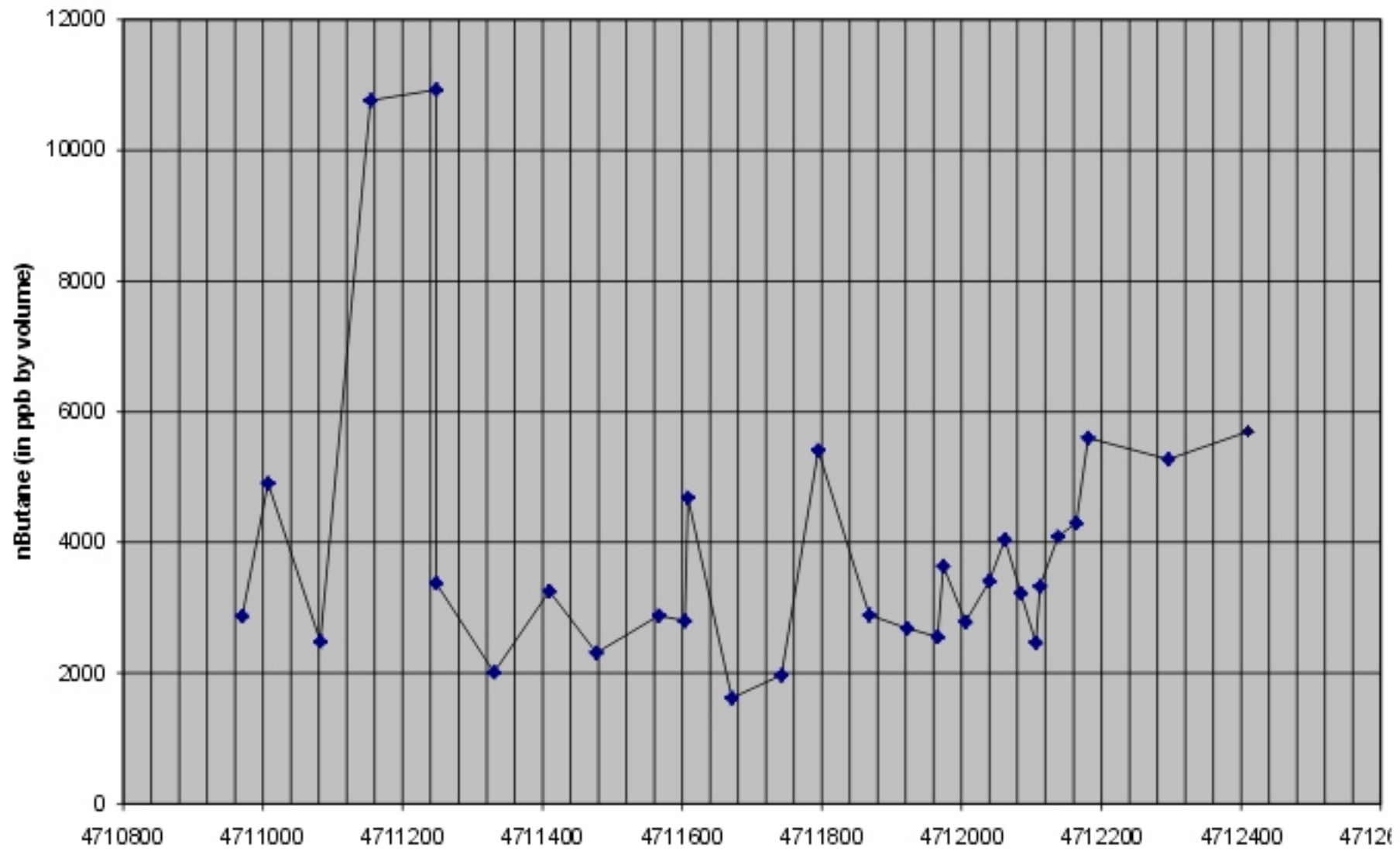


Figure 6.18. Northing versus nButane in soils for PIZ profile.

Figure 6.19. Northing Versus iPentane in Soil for PIZ Profile

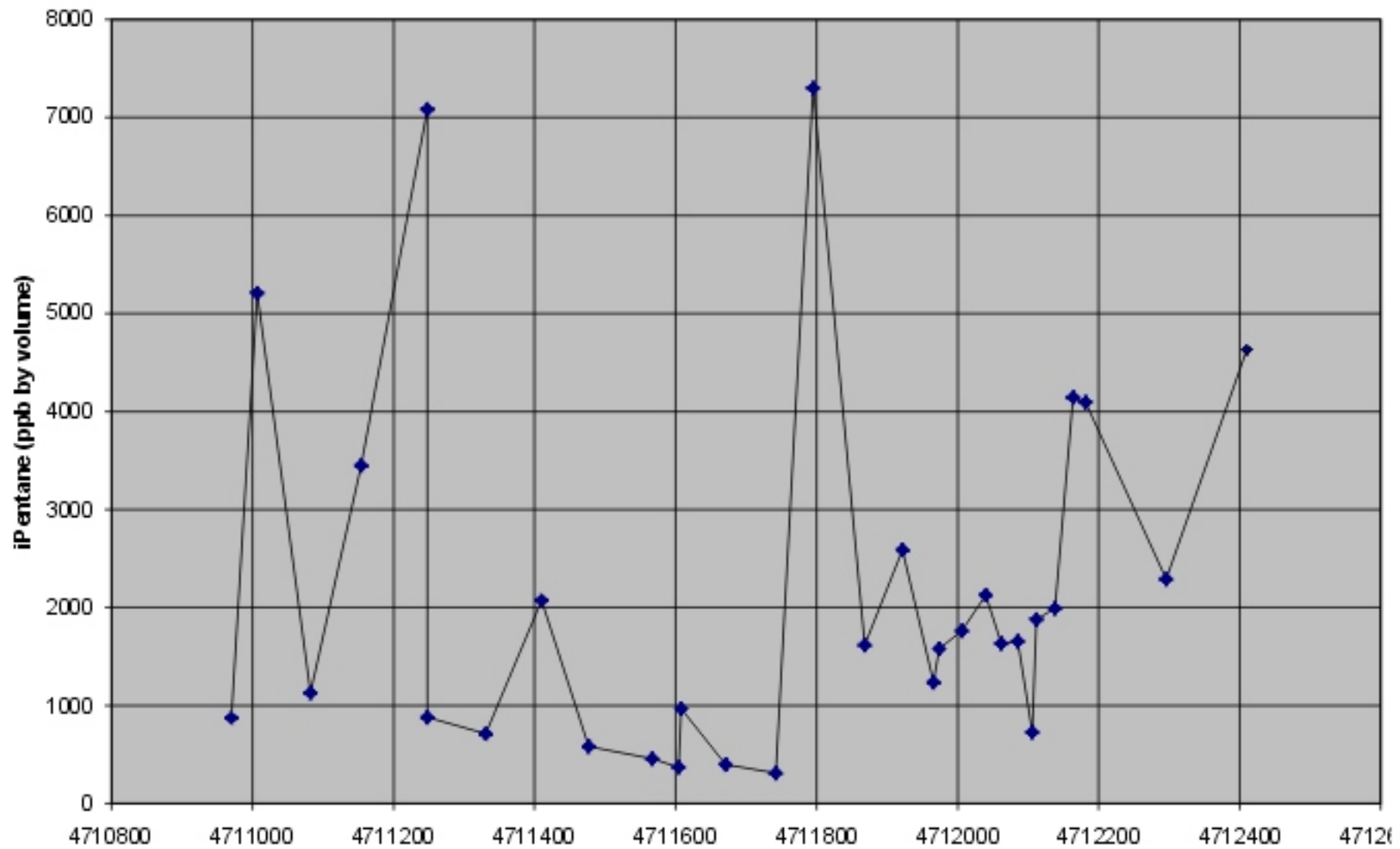


Figure 6.19. Northing versus iPentane in soil for PIZ profile.

Figure 6.20. Northing Versus nPentane of Soil for PZ Profile

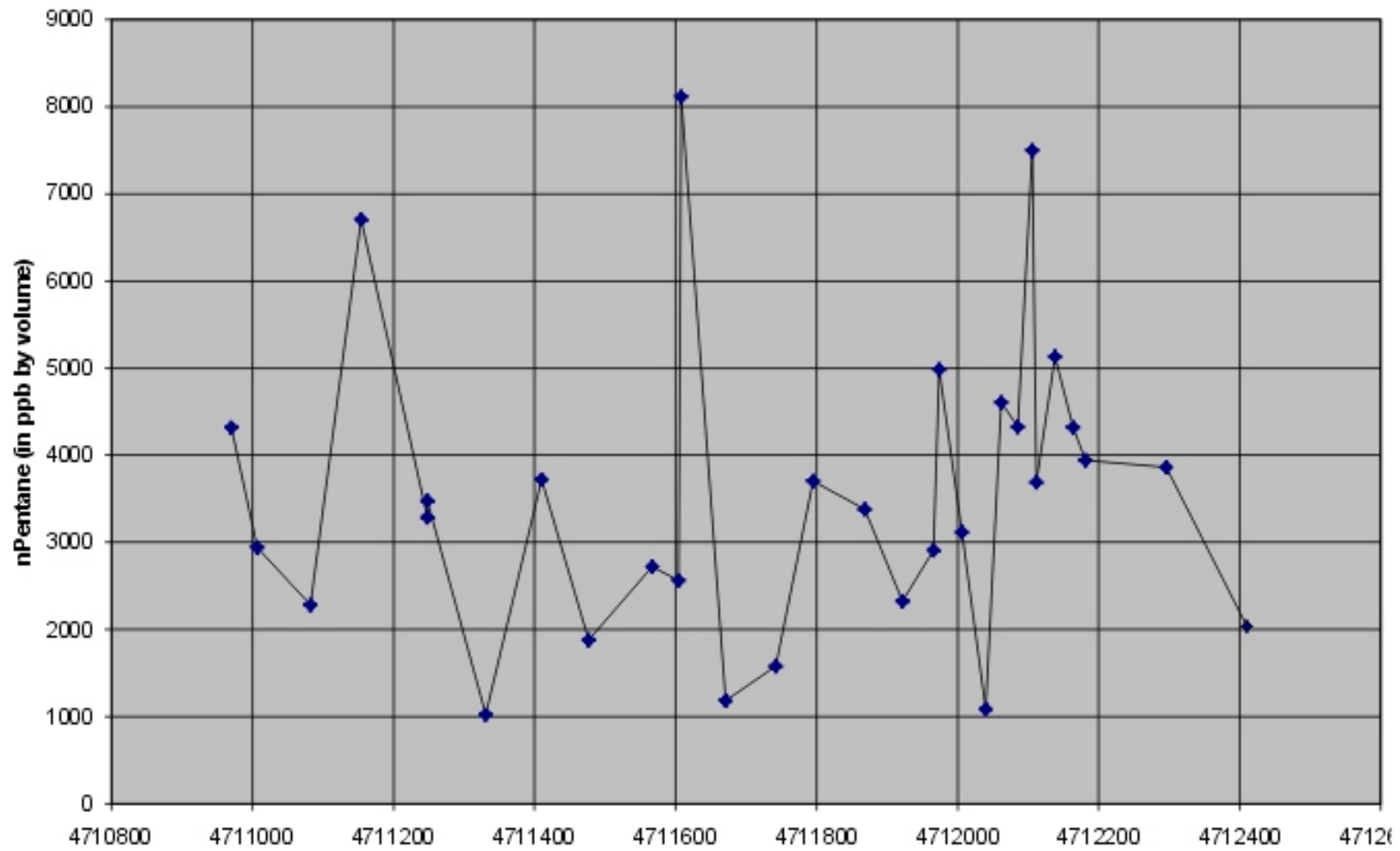


Figure 6.20. Northing versus nPentane in soil for PIZ profile.



Figure 6.21. Northing Versus iHexane in Soil for PIZ Profile

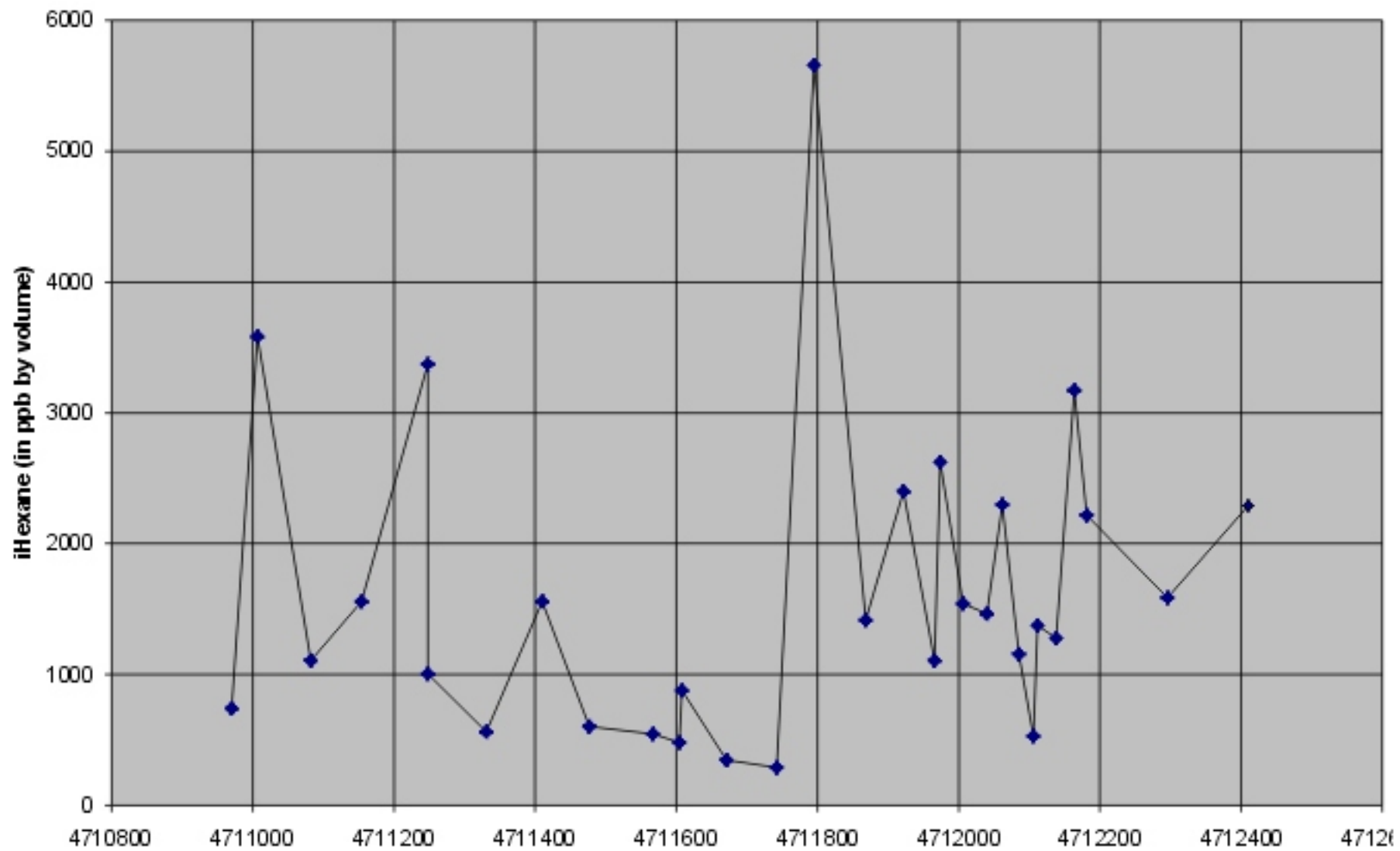


Figure 6.21. Northing versus iHexane in soil for PIZ profile.

Figure 6.22. Northing Versus nHexane in Soil for PIZ Profile

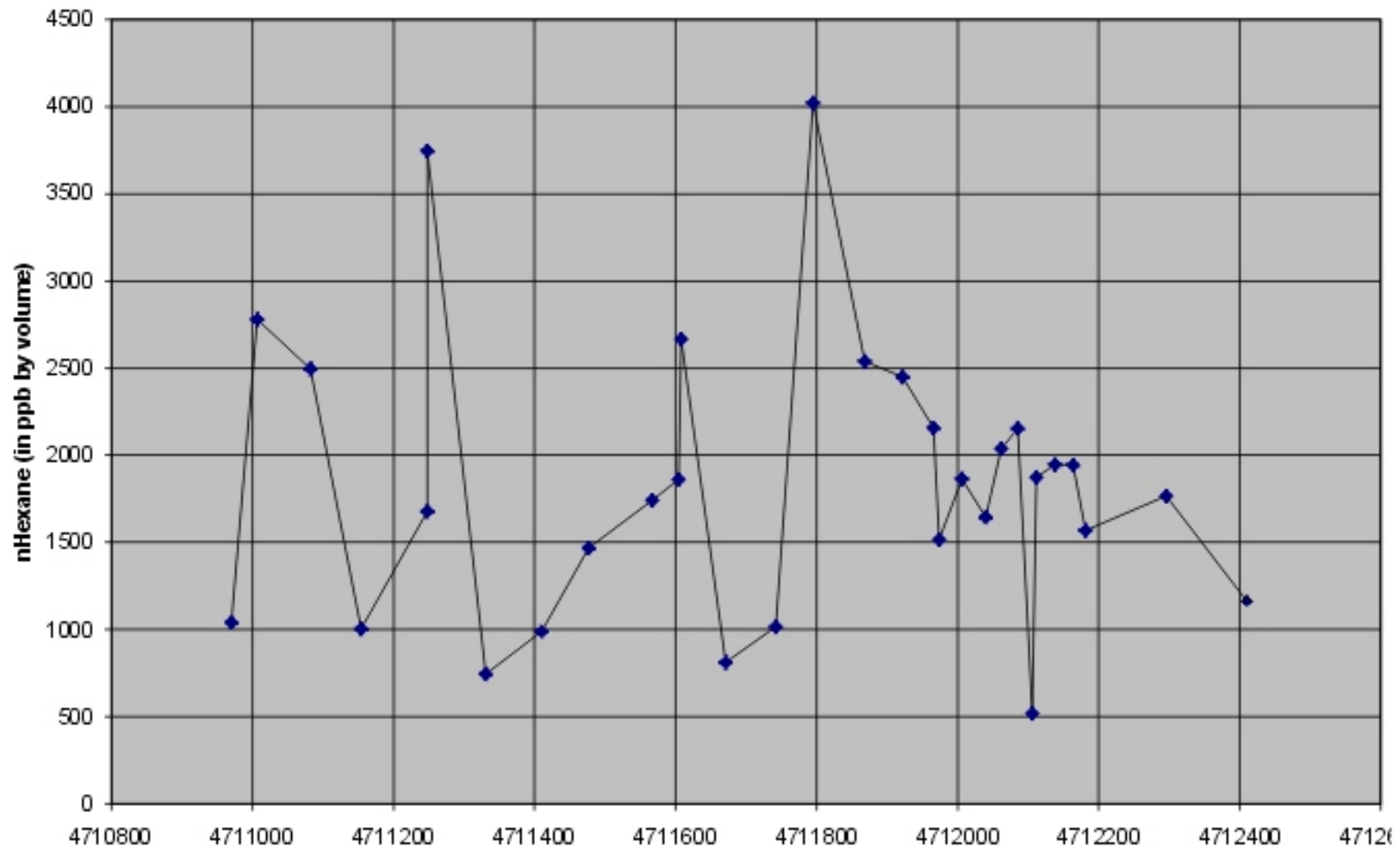


Figure 6.22. Northing versus nHexane in soil for PIZ profile.

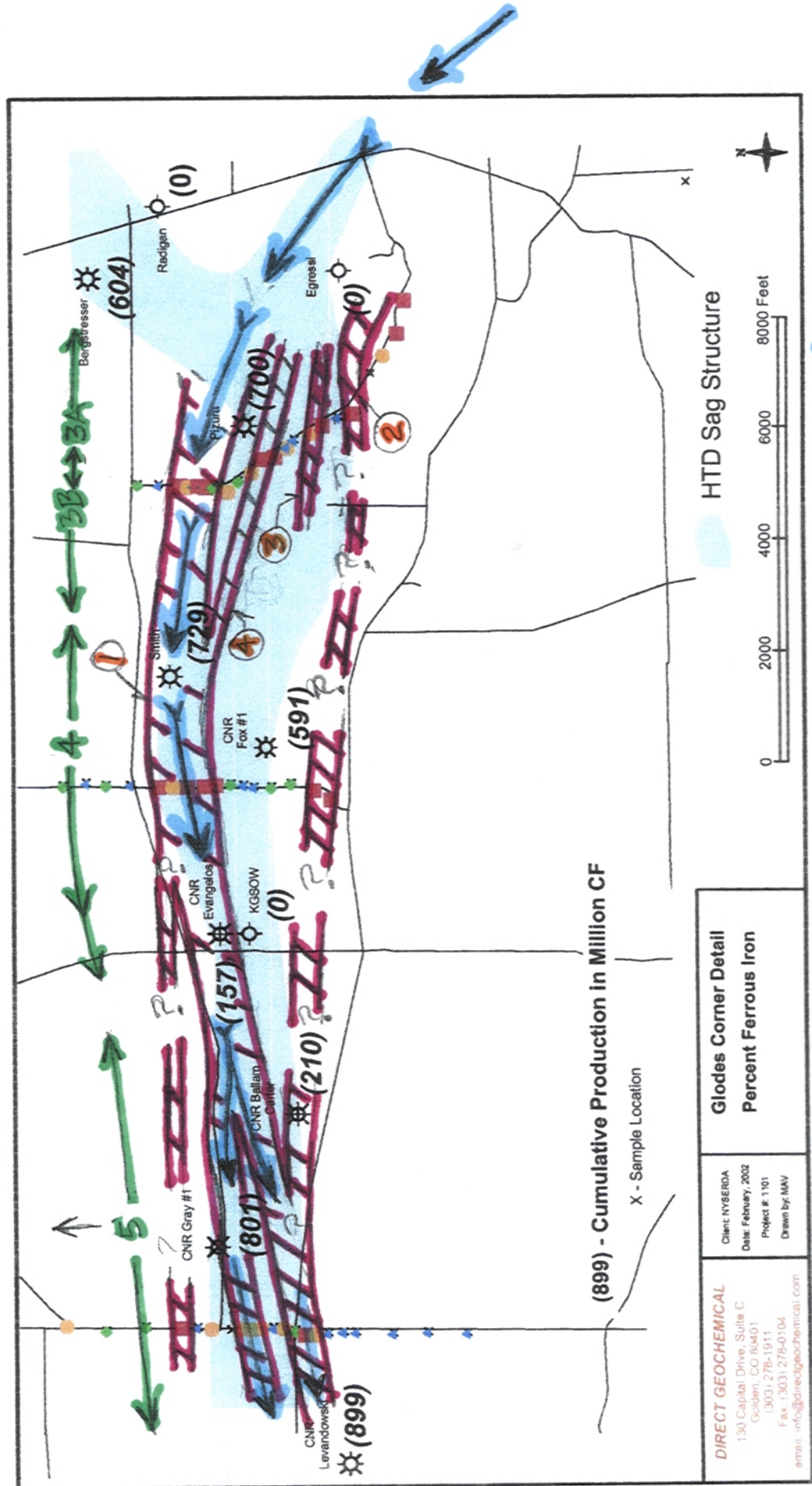


Figure 6.23. Map showing interpreted conduits and paragenetic stages of HTD conceptual model.

Figure 6.23. Map showing interpreted conduits and paragenetic stages of HTD conceptual model.

Figure 6.24. Northing Versus Total Gases (C1+) in Soils for PIZ Profile

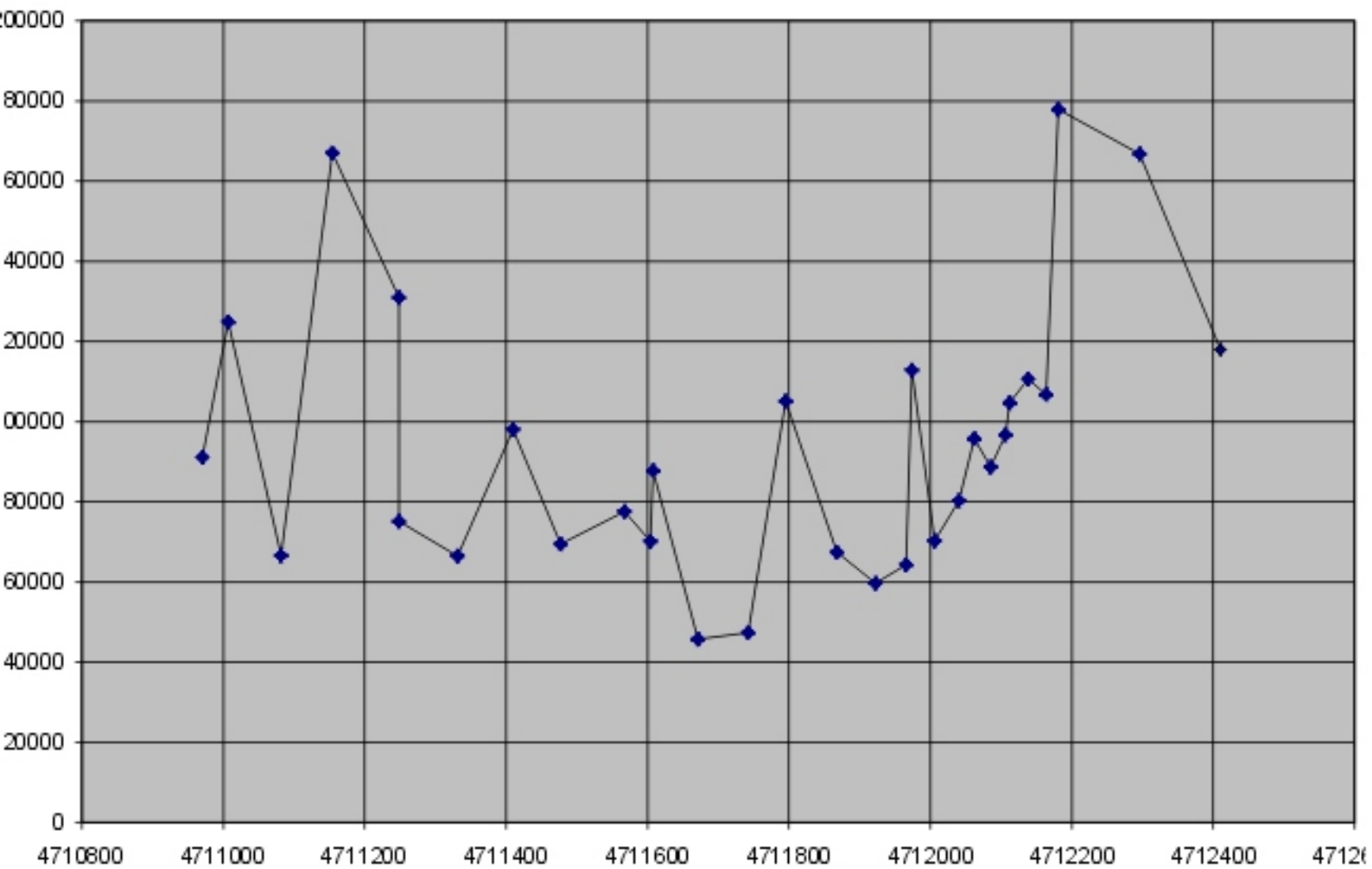


Figure 6.24. Northing versus total gases (C1+) in soils for PIZ profile.





## 7. Reference List

- Al Aasm, I., Lonnee, J., and Clarke, J., 2000, Multiple fluid flow events and the formation of saddle dolomite; examples from Middle Devonian carbonates of the Western Canada Sedimentary Basin.: In Pueyo, J.J., Cardellach, E., Bitzer, K., and Taberner, C., editors, Proceedings of Geofluids III; Third International Conference on Fluid Evolution, Migration and Interaction in Sedimentary Basins and Orogenic Belts: Journal of Geochemical Exploration, v. 69-70, p. 11-15.
- Apps, J.A., and van de Kamp, P.C., 1993, Energy gases of abiogenic origin in the earth's crust, , in Howell, D.G., editor, The future of energy gases: U.S. Geological Survey Professional Paper 1570, p. 81-132.
- Ayrton, W.G., 1963, Isopach and lithofacies map of the Upper Devonian of northeastern United States, in Symposium on Middle and Upper Devonian stratigraphy of Pennsylvania and adjacent states: Pennsylvania Geological Survey, 4th series, Bulletin (General Geology Rept.) G 39, p. 3-6.
- Barnes, D. A., and Harrison, W. B. III, 2001, Hydrothermal dolomite reservoir facies (HTDRF) in the Dundee Limestone, central Michigan Basin, USA.: American Association of Petroleum Geologists Bulletin, v. 85, no. 8, p. 1530.
- Belopolsky, A. V., 1996, Sedimentology and diagenesis of Famennian exposures, Timan Pechora Basin, Russia., Master's Thesis: Binghamton, NY, United States, SUNY at Binghamton.
- Berndt, M.E., Allen, D.E., Seyfried, W.E., Jr., 1996, Reduction of CO<sub>2</sub> during serpentinization of olivine at 300°C and 500 bar: Geology, v. 24, no. 4, p. 351-354.
- Bloss, F.D., 1971, Crystallography and crystal chemistry: New York, Holt, Rinehart and Winston, Inc., 545 p.
- Boni, M., Parente, G., Bechstaedt, Thilo, De Vivo, B., and Iannace, A., 2000, Hydrothermal dolomites in SW Sardinia (Italy); evidence for a widespread late-Variscan fluid flow event.: In Mucchez, P., and Bechstaedt, T., editors: Paleofluid Flow and Diagenesis During Basin Evolution: Sedimentary Geology. v. 131, no. 3-4, p. 181-200.
- Bouabdellah, M., Brown, A. C., and Sangster, D. F., 1996, Mechanisms of formation of internal sediments at the

Beddiane lead-zinc deposit, Touissit mining district, northeastern Morocco: Society of Economic Geologists Special Publication, v. 4, p. 356-363.

Bradley, W. H., and Pepper, J. F., 1938, Geologic structure and occurrence of gas in part of southwestern New York: Part 1. Structure and gas possibilities of the Oriskany Sandstone in Steuben, Yates, and parts of the adjacent counties: U. S. Geological Survey Bulletin 899-A, 68 p.

Bradshaw, W.A., 1989, Carbonate petrology and diagenesis of the Bone Spring Formation dolostones, Scharb Field, Lea County, New Mexico: West Texas State University, unpublished M.S. thesis.

Brannon, J.C., Podosek, F.A., and McLimans, R.K., 1992, Alleghenian age of the Upper Mississippi Valley zinc-lead deposit determined by Rb-Sr dating of sphalerite: *Nature*, v. 356, p. 509-511.

Brannon, J.C., Podosek, F.A., and Cole, S.C., 1996, Radiometric dating of Mississippi Valley-type ore deposits, in Sangster, D. F., editor, Carbonate-Hosted Lead-Zinc Deposits: Society of Economic Geologists Special Publication Number 4, 75<sup>th</sup> Anniversary Volume, p. 536-545.

Burruss, R.C., 1993, Stability and flux of methane in the deep crust – a review, *in* Howell, D.G., editor, The future of energy gases: U.S. Geological Survey Professional Paper 1570, p. 21-30.

Cantrell, D. L., Swart, P. K., Handford, R. C., Kendall, C. G., Westphal, H., 2001, Geology and production significance of dolomite, Arab-D Reservoir, Ghawar Field, Saudi Arabia.: *GeoArabia* (Manama), Gulf Petrolink in Bahrain. Manama, Bahrain, v. 6, no. 1, p. 45-60.

Chesley, J.T., Halliday, A.N., Kyser, T.K., and Spry, P.G., 1994, Direct dating of Mississippi Valley-type mineralization: use of Sm-Nd in fluorite: *Economic Geology*, v. 89, p. 1192-1199.

Christensen, J.N., Halliday, A.N., Kesler, S.E., Leigh, K.E., and Randell, R.N., 1995, Direct dating of sulfides by Rb-Sr – a critical test using the Polaris Mississippi Valley-type Zn-Pb deposit: *Geochimica et Cosmochimica Acta*, v. 59, p. 5191-5197.

Christensen, J.N., Halliday, A.N., and Kesler, S.E., 1996, Rb-Sr dating of sphalerite and the ages of Mississippi Valley-type Pb-Zn deposits, in Sangster, D. F., editor, Carbonate-Hosted Lead-Zinc Deposits: Society of Economic Geologists Special Publication Number 4, 75<sup>th</sup> Anniversary Volume, p. 527-535.

- Chung, Gong S., and Land, L. S., 1997, Dolomitization of the periplatform carbonate slope deposit, the Machari Formation (Middle to Late Cambrian), Korea.: Carbonates and Evaporites. Northeastern Science Foundation, Inc., Rensselaer Center of Applied Geology. Troy, NY, United States, v. 12, no. 2, p. 163-176.
- Clarke, J. D., 1998, Petrology, geochemistry and diagenesis of the Middle Devonian Slave Point Formation, Hamburg Field, northwestern Alberta, Master's Thesis: Windson, ON, Canada, University of Windsor.
- Colquhoun, I. M., 1991, Paragenetic history of the Ordovician Trenton Group carbonates, southwestern Ontario., Master's Thesis: Canada, Brock University, Canada.
- Coogan, A.H., and Maki, M.U., 1986, Trapping configurations for the Cambrian Rose Run production in Ohio: Society of Petroleum Engineers of AIME Eastern Region Conference Proceedings, Paper SPE-15922, p. 71-78.
- Cook, T.D., and Bally, A.W., editors, 1975, Stratigraphic atlas of North and Central America, prepared by the exploration department of Shell Oil Company, Houston, Texas: published by Princeton University Press, Princeton, New Jersey, 272 p.
- Dallmeyer, R.D., and Van Breeman, O., 1981, Rb-Sr whole rock and  $^{40}\text{Ar}/^{39}\text{Ar}$  mineral ages of the Togus and Hollowell quartz monzonite and Three Mile Pond granodiorite plutons, south-central Maine: their bearing on post-Acadian cooling history: Contributions to Mineralogy and Petrology, v. 78, p. 61-73.
- Davies, G.R., 2000, Hydrothermal dolomite reservoir facies: global and western Canadian perspectives: Graham Davies Geological Consultants, Ltd., Calgary, Alberta.
- Deer, W.A., Howie, R.A., and Zussman, J., 1992, An introduction to the rock-forming minerals, 2<sup>nd</sup> edition: Hong Kong, Longman Scientific & Technical, 696 p.
- Dickson, J.A.D., Montanez, I.P., and Saller, A.H., 2001, Hypersaline burial diagenesis delineated by component isotopic analysis, late Paleozoic limestones, West Texas: Journal of Sedimentary Research, v. 71, no. 3, p. 372-379.
- Dorobek, S., 1989, Migration of orogenic fluids through the Siluro-Devonian Helderberg Group during late Paleozoic deformation: constraints on fluid sources and implications for thermal histories of sedimentary

- basins: Tectonophysics, v. 159, p. 25-45.
- Dow, W.G., 1977, Kerogen studies and geological interpretations: *Journal of Geochemical Exploration*, v. 7, p. 79-99.
- Drake, A.A., Jr., Sinha, A.K., Laird, J., and Guy, R.E., 1989, The Taconic orogen, *in* Hatcher, R.D., Jr., Thomas, W.A., and Viele, G.W., editors, *The Appalachian-Ouachita Orogen in the United States: The Geological Society of America, Decade of North American Geology, The Geology of North America Volume F-2*, p. 101-178.
- Fennel, M.J., Hagni, R.D., and Bradley, M.F., 1996, Mineralogy, paragenetic sequence, mineral zoning, and genesis at the Magmont-West mine, southeast Missouri lead district, in Sangster, D. F., editor, *Carbonate-Hosted Lead-Zinc Deposits: Society of Economic Geologists Special Publication Number 4, 75<sup>th</sup> Anniversary Volume*, p. 597-610.
- Fraser, S. C., 1996, *Geology and geochemistry of the Prairie Creek Zn, Pb, Ag deposits, southern MacKenzie Mountains, N.W.T., Master's Thesis: Edmonton, AB, Canada, University of Alberta.*
- Gaunt, J. M., and Gize, A. P., 1996, *Application of basin evolution modeling to date ore deposition: an example: Society of Economic Geologists Special Publication*, v. 4, p. 546-554.
- Gize, A. P., 1999, Organic alteration in hydrothermal sulfide ore deposits: *Economic Geology*, v. 94, p. 967-980.
- Goldhaber, M.B., Church, S.E., Doe, B.R., Aleinikoff, J.N., Brannon, J.C., Podosek, F.A., Mosier, E.L., Taylor, C.D., and Gent, C.A., 1995, Lead- and sulfur-isotope investigation of Paleozoic sedimentary rocks from the southern midcontinent of the United States: implications for paleohydrology and ore genesis of the southeast Missouri lead belt: *Economic Geology*, v. 90, p. 1875-1910.
- Green, D. H., Nichols, I.A., Viljoen, M.J., Viljoen R.P., 1975, Experimental demonstration of the existence of peridotitic liquids in earliest Archean magmatism: *Geology*, v. , no. 1, p. 11-14
- Green, D., and Mountjoy, E., 1999, *Application of fluid inclusions and basin modeling to burial diagenesis and oil migration and maturation, Upper Devonian reservoirs, west-central Alberta.: Annual Meeting Expanded Abstracts - American Association of Petroleum Geologists*, p. A50.
- Grobe, M., and Machel, H. G., 1997, Petrographic and geochemical evidence for fault-controlled hydrothermal

mineralization of the Brilon reef complex, Germany.: In AAPG Foundation Grants-in-Aid Abstracts: American Association of Petroleum Geologists Bulletin., v. 81, no. 10, p. 1775.

Guidotti, C.V., Trzcienski, W.E., and Holdaway, M.J., 1983, A northern Appalachian metamorphic transect: eastern townships, Quebec to the central Maine coast, *in* Schenk, P.E., editor, Regional trends in the geology of the Appalachian-Caledonian-Hercynian-Mauritanide orogen: Dordrecht, D. Riedel Publishing Company, p. 235-247.

Habermann, D., Neuser, R. D., and Richter, D. K., 1996, REE-activated cathodoluminescence of calcite and dolomite; high-resolution spectrometric analysis of CL emission (HRS-CL): Sedimentary Geology. Elsevier. Amsterdam, Netherlands. v. 101, no. 1-2, p. 1-7.

Hagni, R.D., 1996, Mineralogy and significance of bornite ores in the Viburnum Trend, southeast Missouri lead district, in Sangster, D. F., editor, Carbonate-Hosted Lead-Zinc Deposits: Society of Economic Geologists Special Publication Number 4, 75<sup>th</sup> Anniversary Volume, p. 611-630.

Hall, C.M., York, D., Saunders, C.M., and Strong, D.F., 1989, Laser 40Ar/39Ar dating of Mississippi Valley-type mineralization from western Newfoundland: Proceedings, International Geological Congress, v. 2, p. 10-11.

Hanor, J.S., 1996, Controls on the solubilization of lead and zinc in basinal brines, in Sangster, D. F., editor, Carbonate-Hosted Lead-Zinc Deposits: Society of Economic Geologists Special Publication Number 4, 75<sup>th</sup> Anniversary Volume, p. 483-500.

Harris, A.G., Harris, L.D., and Epstein, J.B., 1978, Oil and gas data from Paleozoic rocks in the Appalachian basin: maps for assessing by hydrocarbon potential and thermal maturity (conodont color alteration isograds and overburden isopachs): U.S. Geological Survey Miscellaneous Investigation Series Map I-917-E, 4 sheets with text.

Hatcher, R.D., Jr., Thomas, W.A., Geiser, P.A., Snoke, A.W., Mosher, S., and Wiltschko, D.V., 1989, Alleghanian orogen, *in* Hatcher, R.D., Jr., Thomas, W.A., and Viele, G.W., editors, The Appalachian-Ouachita Orogen in the United States: The Geological Society of America, Decade of North American Geology, The Geology of North America Volume F-2, p. 233-318.

Hay, R.L., Liu, J., Barnstable, D.C., Deino, A., Kyser, T.K., Childers, G.A., and Walker, W.T., 1995, Dates and mineralogic results from clay pods of Mine 29 and the Sweetwater Mine, Viburnum Trend, Missouri:

Extended Abstracts, International Field Conference on Carbonate-Hosted Lead-Zinc Deposits, Society of Economic Geologists, St. Louis, Missouri, June 3-7, 1995, p. 124-126.

Haynes, F.M., and Kesler, S.E., 1987, Chemical evolution of brines during Mississippi Valley-type mineralization: evidence from East Tennessee and Pine Point: *Economic Geology*, v. 82, p. 53-71.

Haynes, F.M., and Kesler, S.E., 1989, Pre-Alleghenian (Pennsylvanian-Permian) hydrocarbon emplacement along Ordovician Knox unconformity, eastern Tennessee: *American Association of Petroleum Geologists Bulletin*, v. 73, p. 289-297.

Haynes, F.M., Beane, R.E., and Kesler, S.E., 1989, Simultaneous transport of metal and reduced sulfur, Mascot-Jefferson City zinc district, east Tennessee: geologic and fluid inclusions evidence: *American Journal of Science*, v. 289, p. 994-1038.

Hearn, P.P., Jr., Sutter, J.F., and Belkin, H.E., 1987, Evidence for Late-Paleozoic brine migration in Cambrian carbonate rocks of the central and southern Appalachians: implications for Mississippi Valley-type sulfide mineralization: *Geochimica et Cosmochimica Acta*, v. 51, p. 1323-1334.

Holdaway, M.J., Guidotti, C.V., Novak, J.M., and Henry, W.E., 1982, Polymetamorphism in medium- to high-grade pelitic metamorphic rocks, west-central Maine: *Geological Society of America Bulletin*, v. 93, p. 572-584.

Horita, J., and Berndt, M.E., 1999, Abiogenic methane formation and isotopic fractionation under hydrothermal conditions: *Science*, v. 285, p. 1055-1057.

Horrall, K.B., Farr, M.R., and Hagni, R.D., 1996, Evidence for focusing of Mississippi Valley-type fluids along the Bloomfield Lineament Zone, southeast Missouri, in Sangster, D. F., editor, *Carbonate-Hosted Lead-Zinc Deposits: Society of Economic Geologists Special Publication Number 4, 75<sup>th</sup> Anniversary Volume*, p. 400-412.

Houseknecht, D.W., and Spotl, C., 1993, Empirical observations regarding methane deadlines in deep basins and thrust belts, in Howell, D.G., editor, *The future of energy gases: U.S. Geological Survey Professional Paper 1570*, p. 217-232.

- Hulen, J.B., and Collister, J.W., 1999, The oil-bearing, Carlin-type gold deposits of Yankee basin, Alligator Ridge district, Nevada: *Economic Geology*, v. 94, p. 1029-1050.
- Hurley, N.F., and Budros, R., 1990, Albion-Scipio and Stoney Point fields, U.S.A., Michigan Basin, *in* Beaumont, Edward A., Foster, Norman H., editors, *Stratigraphic traps; I: American Association of Petroleum Geologists, Treatise of Petroleum Geology, Atlas of Oil and Gas Fields, A-018*, p. 1-37.
- Hutcher Jr. R.D. and others, Alleghanian Orogen (*in*) *The Appalachian-Ouachita Orogen in the United States, The Geology of North America, The Decade of North American Geology Project, Geological Society of America, Vol F-Z Page 244*, 1989.
- Isachsen, Y.W., Landing, E., Lauber, J.M., Rickard, L.V., and Rogers, W.B., editors, 1991, *Geology of New York, a simplified account: New York State Museum/Geological Survey, State Education Department, Educational Leaflet No. 28*, Albany, NY, 284 p.
- Jenden, P.D., Drazan, D.J., and Kaplan, I.R., 1993a, Mixing of thermogenic natural gases in northern Appalachian basin: *American Association of Petroleum Geologists Bulletin*, v. 77, p. 980-998.
- Jenden, P.D., Hilton, D.R., Kaplan, I.R., and Craig, H., 1993b, Abiogenic hydrocarbons and mantle helium in oil and gas fields, *in* Howell, D.G., editor, *The Future of Energy Gases: U.S. Geological Survey Professional Paper 1570*, p. 31-56.
- Johnsson, M.J., 1986, Distribution of maximum burial temperatures across northern Appalachian Basin and implications for Carboniferous sedimentation patterns: *Geology*, v. 14, p. 384-387.
- Kappler, P., and Zeeh S., 2000, Relationship between fluid flow and faulting in the Alpine realm (Austria, Germany, Italy): *In* Muecher, P., and Bechstaedt, T., editors, *Paleofluid Flow and Diagenesis During Basin Evolution: Sedimentary Geology*, Elsevier. Amsterdam, Netherlands., v. 131, no. 3-4, p. 147-162.
- Kay, S.M., Snedden, W.T., Foster, B.P., and Kay, R.W., 1983, Upper mantle and crustal fragments in the Ithaca kimberlites: *Journal of Geology*, v. 91, p. 277-290.
- Keith, S.B., Laux, D. P., Maughan, G., Schwab, K., Ruff, S., Swan, M. M., Abbott, E. W., and Friberg, S., 1991, Magma series and metallogeny; a case study from Nevada and environs *in* Buffa, Ruth H., and Coyner, Alan



R., editors, *Geology and ore deposits of the Great Basin; field trip guidebook compendium*: Geological Society of Nevada, Reno, NV, p.404-493.

Keith, S.B. and Swan, M.M., 1996, The Great Laramide Porphyry Copper Cluster of Arizona, Sonora, and New Mexico: the Tectonic setting, Petrology, and Genesis of a World Class Porphyry Metal Cluster, in Coyner, A.R., and Fahey, P.L., eds., *Geology and Ore Deposits of the American Cordillera: Geological Society of Nevada Symposium Proceedings*, Reno/Sparks, Nevada, April, 1995, p 1-80.

Keith, S.B., Rasmussen, J.C., Swan, M.M., and Laux, 2003, Cracks of the world: global strike-slip fault systems and giant resource accumulations: *Houston Geological Society bulletin*, March 2003.

Kesler, S. E., 1996, Appalachian Mississippi Valley-type deposits: paleoaquifers and brine provinces, in Sangster, D. F., editor, *Carbonate-Hosted Lead-Zinc Deposits: Society of Economic Geologists Special Publication Number 4, 75<sup>th</sup> Anniversary Volume*, p. 29-57.

Kriedler, W.L., Van Tyne, A.M., and Jorgensen, K.M., 1972, Deep wells in New York State: New York State Museum and Science Service, Bulletin no. 418S, 335 p.

Kyle, J.R., and Saunders, J.A., 1996, Metallic deposits of the Gulf Coast basin: diverse mineralization styles in a young sedimentary basin, in Sangster, D. F., editor, *Carbonate-Hosted Lead-Zinc Deposits: Society of Economic Geologists Special Publication Number 4, 75<sup>th</sup> Anniversary Volume*, p. 218-229.

Lakatos, S., and Miller, D.S., 1983, Fission-track analysis of apatite and zircon defines a burial depth of 4 to 7 km for lowermost Upper Devonian, Catskill Mountains, New York: *Geology*, v. 11, no. 2, p. 103-104.

Leach, D.L., 1994, Genesis of the Ozark Mississippi Valley-type metallogenic province, in Fontbote, L., and Boni, M., editors, *Sediment hosted Zn-Pb ores*: Berlin, Springer-Verlag, p. 104-138.

Leach, D.L., and Rowan, E.L., 1986, Genetic link between Ouachita fold belt tectonism and the Mississippi Valley-type lead-zinc deposits of the Ozarks: *Geology*, v. 14, p. 931-935.

Leach, D.L., Viets, J.G., Kozlowski, A., and Kibitlewski, S., 1996, Geology, geochemistry, and genesis of the Silesia-Cracow zinc-lead district, southern Poland, in Sangster, D. F., editor, *Carbonate-Hosted Lead-Zinc Deposits: Society of Economic Geologists Special Publication Number 4, 75<sup>th</sup> Anniversary Volume*, p. 144-

- Lewchuk, M.T., and Symons, D.T.A., 1996a, Paleomagnetism and Mississippi Valley-type ore genesis in the Ordovician Know Supergroup of central Tennessee, *in* Sangster, D.F., editor, Carbonate hosted lead-zinc deposits: Society of Economic Geologists, Special Volume 4, p. 567-576.
- Lewchuk, M. T., Al Aasm, I. S., Symons, D. T. A., and Gillen, K. P., 2000, Late Laramide dolomite recrystallization of the Husky Rainbow "A" hydrocarbon Devonian reservoir, northwestern Alberta, Canada; paleomagnetic and geochemical evidence: *Canadian Journal of Earth Sciences*, National Research Council of Canada. Ottawa, ON, Canada, v. 37, no. 1, p. 17-29.
- Lindgren, W., 1919, *Mineral deposits*: New York, McGraw-Hill Book Company, Inc., 957 p.
- McCracken, S.R., Etminan, H., Copnnor, A.G., and Williams, V.A., 1996, Geology of the Admiral Bay carbonate-hosted zinc-lead deposit, Canning Basin, Western Australia, in Sangster, D. F., editor, Carbonate-Hosted Lead-Zinc Deposits: Society of Economic Geologists Special Publication Number 4, 75<sup>th</sup> Anniversary Volume, p. 330-349.
- McKenzie, M. C., 1999, Carbonates of the Upper Devonian Luduc Formation, southwestern Peace River Arch, Alberta; indications for tectonically induced fluid flow, Master's Thesis: Edmonton, AB, Canada. University of Alberta.
- Misra, K. C., Gratz, J.F., and Lu, C., 1996, Carbonate-hosted Mississippi Valley-type mineralization in the Elmwood-Gordonsville deposits, Central Tennessee zinc district: a synthesis, in Sangster, D. F., editor, Carbonate-Hosted Lead-Zinc Deposits: Society of Economic Geologists Special Publication Number 4, 75<sup>th</sup> Anniversary Volume, p. 58-73.
- Montgomery, S. L., Barrett, F., Vickery, K., Natali, S., Roux, R., and Dea, P., 2001, Cave Gulch field, Natrona County, Wyoming: Large gas discovery in the Rocky Mountain foreland, Wind River basin: *American Association of Petroleum Geologists Bulletin*, v. 85, no. 9, p. 1543-1564.
- Mountjoy, E. W., Green, D., Machel, H. G., Duggan, J., and Williams-Jones, A. E., 1999, Devonian matrix dolomites and deep burial carbonate cements; a comparison between the Rimbey-Meadowbrook reef trend and the deep basin of west-central Alberta.: In *Lithoprobe; Alberta Basement Transects; Synthesis Issue: Bulletin of Canadian Petroleum Geology*: Canadian Society of Petroleum Geologists. Calgary, AB, Canada.

v. 47, no. 4, p. 487-509.

Nakai, S., Halliday, A.N., Kesler, S.E., Jones, H.D., Kyle, J.R., and Lane, T.E., 1993, Rb-Sr dating of sphalerites from Mississippi Valley-type (MVT) ore deposits: *Geochimica et Cosmochimica Acta*, v. 57, p. 417-427.

Osberg, P.H., Tull, J.F., Robinson, P., Hon, R., and Butler, J.R., 1989, The Acadian Orogeny, *in* Hatcher, R.D., Jr., Thomas, W.A., and Viele, G.W., editors, *The Appalachian-Ouachita Orogen in the United States: The Geological Society of America, Decade of North American Geology, The Geology of North America Volume F-2*, p. 179-232.

Packard, J.J., and Al-Aasm, I., 2002, Dolomite discrimination in the D-1: round up the usual suspects: Canadian Society of Petroleum Geologists, Diamond Jubilee Convention, June 3-7, 2002, Calgary.

Packard, J. J., Al Aasm, I., Samson, I., Berger, Z., and Davies, J., 2001, A Devonian hydrothermal chert reservoir; the 225 bcf Parkland Field, British Columbia, Canada.: *American Association of Petroleum Geologists Bulletin*. Tulsa, OK, United States, v. 85, no. 1, p. 51-84.

Pan, H., and Symons, D.T.A., 1993, Paleomagnetism of the Mississippi Valley-type Newfoundland Zinc deposit: evidence for Devonian mineralization in the northern Appalachians: *Journal of Geophysical Research*, v. 98, p. 22,415 - 22,427.

Pan, H., Symons, D.T.A., and Sangster, D.F., 1990, Paleomagnetism of the Mississippi Valley-type ore and hosts rocks in the northern Arkansas and Tri-State districts: *Canadian Journal of Earth Sciences*, v. 27, p. 923-931.

Parrish, J.B., and Lavin, P.M., 1982, Tectonic model for kimberlite emplacement in the Appalachian Plateau of Pennsylvania: *Geology*, v. 10, p. 344-347.

Pferd, Jeffrey W., 1981, Geology, drill holes, and geothermal energy potential of the basal Cambrian rock units of the Appalachian Basin of New York State: Albany, NY, New York State Energy Research and Development Authority, ERDA Report 81-14, 53 p.

Qing, H., and Mountjoy, E.W., 1994, Origin of dissolution vugs, caverns, and breccias in the Middle Devonian Presqu'ile Barrier, host of Pine Point Mississippi Valley-Type deposits: *Economic Geology*, v. 89, p. 858-876.

- Qing, H., Mountjoy, E.W., and McQueen, R., 1995, Regional fluid flow in the Presqu'île Barrier and genesis of Pine Point MVT deposits based on host rock petrology and geochemistry: Extended Abstracts of the International Field Conference on Carbonate-hosted lead-zinc deposits, Society of Economic Geologists, St. Louis, Missouri, p. 243-244.
- Ragan, V.M., and Coveney, R.M., Jr., 1996, Migration paths for fluids and northern limits of the Tri-State district from fluid inclusions and radiogenic isotopes, in Sangster, D. F., editor, Carbonate-Hosted Lead-Zinc Deposits: Society of Economic Geologists Special Publication Number 4, 75<sup>th</sup> Anniversary Volume, p. 419-431.
- Randell, R.N., and Anderson, G.M., 1996, Geology of the Polaris Zn-Pb deposit and surrounding area, Canadian Arctic Archipelago, in Sangster, D. F., editor, Carbonate-Hosted Lead-Zinc Deposits: Society of Economic Geologists Special Publication Number 4, 75<sup>th</sup> Anniversary Volume, p. 307-319.
- Randell, R.N., Heroux, Y., Chagnon, A., and Anderson, G.M., 1996, Organic matter and clay minerals at the Polaris Zn-Pb deposit, Canadian Arctic Archipelago, in Sangster, D. F., editor, Carbonate-Hosted Lead-Zinc Deposits: Society of Economic Geologists Special Publication Number 4, 75<sup>th</sup> Anniversary Volume, p. 320-329.
- Rankin, D.W., Drake, A.A., Jr., Glover, L., III, Goldsmith, R., Hall, L.M., Murray, D.P., Ratcliffe, N.M., Read, J.F., Secor, D.T., Jr., and Stanley, R.W., 1989, Pre-orogenic terranes, *in* Hatcher, R.D., Jr., Thomas, W.A., and Viele, G.W., editors, The Appalachian-Ouachita orogen in the United States: Geological Society of America, The Geology of North America, volume F-2, p. 7-100.
- Reinhold, C., 1998, Multiple episodes of dolomitization and dolomite recrystallization during shallow burial in Upper Jurassic shelf carbonates; eastern Swabian Alb, southern Germany.: *Sedimentary Geology*, v. 121, no. 1-2, p. 71-95.
- Rickard, Lawrence V., and Fisher, Donald W., 1970, Geologic map of New York, Finger Lakes Sheet: New York State Museum and Science Service, Map and Chart Series no. 15, scale 1:250,000.
- Riley, R.A., Harper, J.A., Baranoski, M.T., Laughrey, C.D., and Carlton, R.W., 1993, Measuring and predicting reservoir heterogeneity in complex deposystems: the Late Cambrian Rose Run Sandstone of eastern Ohio and western Pennsylvania: U.S. Department of Energy, Contract No. DE-AC22-90BC14657, 257 p.

- Ryder, R.T., Burruss, R.C., and Hatch, J.R., 1998, Black shale source rocks and oil generation in the Cambrian and Ordovician of the central Appalachian Basin, USA: American Association of Petroleum Geologists, v. 82, no. 3, p. 412-441.
- Szatmari, Peter, 1989, Petroleum formation by Fischer-Tropsch synthesis in Plate Tectonics: American Association of Petroleum Geologists Bulletin, v. 73, no. 8, p. 989-998.
- Sangster, D. F., editor, 1996, Carbonate-Hosted Lead-Zinc Deposits: Society of Economic Geologists Special Publication Number 4, 75<sup>th</sup> Anniversary Volume, 664 p.
- Sass-Gustkiewicz, M., 1996, Internal sediments as a key to understanding the hydrothermal karst origin of the Upper Silesia, in Sangster, D. F., editor, Carbonate-Hosted Lead-Zinc Deposits: Society of Economic Geologists Special Publication Number 4, 75<sup>th</sup> Anniversary Volume, p. 171-181.
- Schochow, S. , 2000, Petroleum frontiers: a quarterly investigation into the most promising petroleum horizons and provinces: Published by IHS Energy Group, v. 17, no.1, p. 8.
- Scotese, C.R., Bambach, R.K., Barton, C., Van der Voo, R., and Ziegler, A.M., 1979, Paleozoic base maps: Journal of Geology, v. 87, no. 3, p. 217-277.
- Searl, A., 1989, Saddle dolomite; a new view of its nature and origin: Mineralogical Magazine, v. 53, part 5, no. 373, p. 547-555.
- Sevon, W.D., 1985, Nonmarine facies of the Middle and Late Devonian Catskill coastal alluvial plain: Geological Society of America Special Paper 201, p. 79-90.
- Sheppard, S.M.F., Charef, A., and Bouhlef, S., 1996, Diapirs and Zn-Pb mineralization: a general model based on Tunisian (N.Africa) and Gulf Coast (U.S.A.) Deposits, in Sangster, D. F., editor, Carbonate-Hosted Lead-Zinc Deposits: Society of Economic Geologists Special Publication Number 4, 75<sup>th</sup> Anniversary Volume, p. 230-243.
- Simmons, Gene, and Diment, W. H., 1972, Simple Bouguer gravity anomaly map of northern New York: New York State Museum and Science Service, Geological Survey, Map and Chart Series No. 17A, scale

1:250,000.

Smith, Taury, personal communication 2002, diagrams and text of poster session: New York State Museum, Albany, NY.

Swan, Monte M., and Keith, Stanley B., 1986, Orogenic model for “anorogenic” granitoids in North America; product of oblique subduction at 1.4 Ga, *in* *Frontiers in Geology and Ore Deposits of Arizona and the Southwest*: Arizona Geological Society Digest, v. 16, p. 489-498.

Symons, D.T.A., and Sangster, D.F., 1991, Paleomagnetic age of the central Missouri barite deposits and its genetic implications: *Economic Geology*, v. 86, p. 1-12.

Symons, D.T.A., and Sangster, D.F., 1992, Late Devonian paleomagnetic age for the Polaris Mississippi Valley-type Zn-Pb deposits: *Canadian Journal of Earth Sciences*, v. 30, p. 1028-1036.

Symons, D.T.A., Sangster, D.F., and Leach, D.L., 1996, Paleomagnetic dating of Mississippi Valley-type Pb-Zn-Ba deposits, in Sangster, D. F., editor, *Carbonate-Hosted Lead-Zinc Deposits: Society of Economic Geologists Special Publication Number 4, 75<sup>th</sup> Anniversary Volume*, p. 515-526.

Taylor, W.R., and Green, D. H., 1988, Measurement of reduced peridotite-C-O-H solidus and implications for redox melting of the mantle: *Nature*, v. 332, no. 24, p. 349-352.

Terra Graphics, 1977, Natural gas map of the United States, December 31, 1978: Potential Gas Committee, Colorado School of Mines, Golden, CO, 80401, 303-279-4320.

Thomas, W.A., 1977, Evolution of Appalachian-Ouachita salients and recesses from reentrants and promontories in the continental margin: *American Journal of Science*, v. 277, p. 1233-1278.

Thomas, W.A., 1991,

Tissot, B.P., and Welte, D.H., 1984, *Petroleum formation and occurrence*: New York, Springer-Verlag, 699 p.

Tobin, K. J., Walker, K. R., and Goldberg, S. G., 1997, Burial diagenesis of Middle Ordovician carbonate buildups (Alabama, USA); documentation of the dominance of shallow burial conditions.: *Sedimentary*

Geology. Elsevier. Amsterdam, Netherlands., v. 114, no. 1-4, p. 223-236.

Torok, A., 2000, Formation of dolomite mottling in Middle Triassic ramp carbonates (southern Hungary): In Muchez, P. and Bechstaedt, T., editors, *Paleofluid Flow and Diagenesis During Basin Evolution: Sedimentary Geology*. Elsevier. Amsterdam, Netherlands., v. 131, no. 3-4, p. 131-145.

Tritlla, J., Cardellach, E., and Sharp, Z. D., 2001, Origin of vein hydrothermal carbonates in Triassic limestones of the Espadan Ranges (Iberian Chain, E Spain): *Chemical Geology*, Elsevier. Amsterdam, Netherlands, v. 172, no. 3-4, p. 291-305.

Vandrey, M. R., 1991, Stratigraphy, diagenesis, and geochemistry of the Middle Ordovician Glenwood Formation, Michigan Basin, Master's Thesis: Madison, WI, University of Wisconsin.

Vearncombe, J. R., Chisnall, A.W., Dentith, M.C., Dorling, S.L., Rayner, M.J., and Holyland, P.W., 1996, Structural controls on Mississippi Valley-type mineralization, the southeast Lennard Shelf, Western Australia, in Sangster, D. F., editor, *Carbonate-Hosted Lead-Zinc Deposits: Society of Economic Geologists Special Publication Number 4, 75<sup>th</sup> Anniversary Volume*, p. 74-95.

Viets, J.G., Hostra, A.F., and Emsbo, P., 1996, Solute compositions of fluid inclusions in sphalerite from North American and European Mississippi Valley-type ore deposits: ore fluids derived from evaporated seawater, in Sangster, D. F., editor, *Carbonate-Hosted Lead-Zinc Deposits: Society of Economic Geologists Special Publication Number 4, 75<sup>th</sup> Anniversary Volume*, p. 465-482.

Weary, D.J., Ryder, R. T., and Nyahay, R., 2000, Thermal maturity patterns (CAI and %R) in the Ordovician and Devonian rocks of the Appalachian basin in New York State: U.S. Geological Survey Open-file Report 00-496, 19 p.

Wendte, J., Qing, H., Dravis, J. J., Moore, S. L. O., Stasiuk, L. D., and Ward, G., 1998, High-temperature saline (thermoflux) dolomitization of Devonian Swan Hills platform and bank carbonates, Wild River area, west-central Alberta.: *Bulletin of Canadian Petroleum Geology*. Canadian Society of Petroleum Geologists. Calgary, AB, Canada., v. 46, no. 2, p. 210-265.

Wendte, J., Stasiuk, V., Snowdon, L., and Ward, G., 1999, Geopressured Devonian limestone reef reservoirs in the Wild River area, west-central Alberta.: *Annual Meeting Expanded Abstracts - American Association of*

Petroleum Geologists., p. A147.

White, T., 1995, Hydrothermal dolomitization of the Mississippian upper Debolt Formation, Sikanni Field, Northeast British Columbia., Windsor, ON, Canada, University of Windsor.

White, T., and Al-Aasm, I. S., 1997, Hydrothermal dolomitization of the Mississippian upper Debolt Formation, Sikanni gas field, northeastern British Columbia, Canada.: Bulletin of Canadian Petroleum Geology. Canadian Society of Petroleum Geologists. Calgary, AB, Canada. v. 45, no. 3, p. 297-316.

Wilt, J.C., 1993, Geochemical patterns of hydrothermal mineral deposits associated with calc-alkalic and alkali-calcic igneous rocks as evaluated with neural networks: Tucson, AZ, University of Arizona, Ph. D. dissertation, 721 p.

Wilt, J.C., 1995, Correspondence of alkalinity and ferric/ferrous ratios of igneous rocks associated with various types of porphyry copper deposits, in Pierce, F. W., and Bolm, J. G., editors, Porphyry copper deposits of the American Cordillera: Arizona Geological Society Digest, v. 20, p. 180-200.

Yoo Chan, Min, and Gregg, J. M., 1997, Dolomitization of the Trenton and Black River limestones (Middle Ordovician) in northern Indiana.: Abstracts With Programs - Geological Society of America (GSA). Boulder, CO, United States, v. 29, no. 6, p. 269.

Yoo Chan, Min, Gregg, J. M., and Shelton, K. L., 2000, Dolomitization and dolomite neomorphism; Trenton and Black River limestones (Middle Ordovician) northern Indiana, U.S.A.: Journal of Sedimentary Research, Section A: Sedimentary Petrology and Processes, Society of Economic Paleontologists and Mineralogists. Tulsa, OK, United States., v. 70, no. 1, p. 265-274.

Zeeh, S., and Kappler, P., 2000, Timing of cement precipitation and fault activity in the Eastern and Southern Alps (Austria, Germany, Italy and Slovenia): In Pueyo, J.J., Cardellach, E., Bitzer, K., and Taberner, C., editors, Proceedings of Geofluids III; Third International Conference on Fluid Evolution, Migration and Interaction in Sedimentary Basins and Orogenic Belts: Journal of Geochemical Exploration, v. 69-70, p. 585-588.

Zerrahn, Gregory J., 1978, Ordovician (Trenton to Richmond) depositional patterns of New York State, and their relation to the Taconic orogeny: Geological Society of America Bulletin, v. 89, no. 12, p. 1751-1760.







APPENDIX A: MAGMA-METAL SERIES MODELS USED IN THIS REPORT

**MAGMA-METAL SERIES MODELS USED IN TEXT OR LISTED ON PLATE 2 - MISSISSIPPI VALLEY TYPE  
AND RELATED MODELS.**

Mega Series (alum. cont.) <sup>1</sup>	Series (alkalinity) <sup>2</sup>	Sub-series (H <sub>2</sub> O content)	Mini-series (F-Cl content) <sup>4</sup>	Micro-series (Oxid. State) <sup>3</sup>	Sort Code <sup>6</sup>	Model Code(*) <sup>7</sup>	Model Description <sup>8,9,10</sup> Nanoseries (Emplacement Level/Tectonic Setting)	DEPOSIT TYPE/ZONE - MAGMA METAL SERIES MODEL (*) <sup>11</sup> ; Examples <sup>12</sup> MODEL TERMINOLOGY OF OTHER WORKERS <sup>13</sup>
M	M	ah	N	r	500520	5O	Methane-hydrogen seeps from magnesian peridotite in ophiolite complexes. Causative mechanism may be peridotite hydration by low-rank metamorphic fluids generated by dewatering in the ophiolite complex.	<b>ZAMBALES TYPE - MAGNESIAN METHANE-HYDROGEN GAS DEPOSITS</b> Methane-hydrogen gas seeps in peridotite near Mount Lanat within the Zambales ophiolite complex, Phillipines; serpentines(?) in Germany; methane, ethane, and hydrogen in Semail ophiolite, Oman; Moncheheysk ultramafic pluton(?), Kola Peninsula, Russia.
M	M	ah	N	rss - r	500525	5P	Metagenic, oil and/or gas-bearing, hydrothermal dolomite reservoirs. Source may be strongly reduced to reduced, mafic to ultramafic magnesian (komatiitic and peridotitic), subcrustal lithospheric mantle beneath cratons and Proterozoic craton margins. Komatiitic and peridotitic components of greenstone belts may also be sources within the crust above the lithospheric mantle. Depositional sequence features early dolomitization (Mg metasomatism) of pre-existing CaCO <sub>3</sub> limestones; followed by sulfide deposition (marcasite, pyrite, and trace sphalerite) coincident with bitumen, oils, methane; followed by late calcite +/- bitumen deposition. Paragenetic sequence is very similar to MVT (MAC34B model). Dissolution, crystal volume reduction, accompanied by permeability/ porosity enhancement and solution collapse, is coincident with early stage dolomitization, along with extensive hydrothermal 'karsting'. Ultimate source may be associated with devolatilization, serpentinization, and metagenic fluid generation of a high C-Mg, olivine-rich source (e.g. peridotite). The fluid generation may occur during continental assembly events (in the same setting as MVT (MAC34B model). Metagenically derived fluids then may ascend a high-angle fault and/or thrust framework and become entrained in first permeability calcium limestone reservoir permeability at or near the base of the local Paleozoic cover sequence. Field/reservoir setting is commonly foreland of the collisional suture within the craton.	<b>TRENTON-BLACK RIVER TYPE – HYDROTHERMAL OIL AND GAS HOSTED IN HYDROTHERMAL DOLOMITE RESERVOIRS</b> <b>Hosted in hydrothermal dolomite in Trenton-Black River group: deep gas fields (Gloades Corner) in Steuben County?, New York; deep gas in Kankakee Arch between Illinois and Michigan Basins?, northern Indiana; Albion-Scipio gas field, Stoney Point oil and gas field, Deerfield oil and gas field, Mich.; Lima-Indiana trend, OH-IN; southern Ontario oil and gas pools (Hillman pool in Essex County and Dover oil and gas fields, southern Kent County, Ont., Canada.</b> <b>Oil and gas reservoirs hosted in hydrothermal dolomite and/or chert of the Wabamun reservoir trend, Peace River, Alberta: Tangent, Teepee, Royce, Oak, Normandville, Peoria, Eaglesham, and Gold Creek hydrothermal dolomite-hosted oil and gas fields in the Peace River block of western Alberta; Parkland hydrothermal chert reservoir in Parkland gas field, northwestern Alberta.</b>

Mega Series (alum. cont.) <sup>1</sup>	Series (alkalinity) <sup>2</sup>	Sub-series (H <sub>2</sub> O content)	Mini-series (F-Cl content) <sup>4</sup>	Micr o-series (Oxid. State) <sup>3</sup>	Sort Code <sup>6</sup>	Model Code(*) <sup>7</sup>	Model Description <sup>8,9,10</sup> Nanoseries (Emplacement Level/Tectonic Setting)	DEPOSIT TYPE/ZONE - MAGMA METAL SERIES MODEL (*) <sup>11</sup> ; Examples <sup>12</sup> MODEL TERMINOLOGY OF OTHER WORKERS <sup>13</sup>
							Oil- and gas-bearing and/or inorganic carbon-bearing (CO, H <sub>2</sub> CO <sub>3</sub> , fluids may accompany the metagenic fluids to the emplacement site and/or be generated by carbon monoxide?/carbonic acid reduction during deposition of the early stage, rhombic/ saddle/baroque dolomite. Model is actively being researched and validated.	<b>Hosted in hydrothermal dolomites Slave Point and Keg River Platform areas, northeast BC (gas) and northwest Alberta (oil and gas): Helmet, Tsea, Cabin, Kotcho Lake, Kotcho East, Yoyo, Junior, Clarke Lake, Klua, and Adsett gas fields, BC; Otter Park Basin, Cordova Embayment, Shekile sub-basin, Zama, Amber, and Rainbow oil and gas fields, Comet Platform Alberta; Slave Point and Cranberry fields, northwest Alberta.</b> <b>Hosted in hydrothermal dolomite in Mississippian Debolt reservoirs of the Sikanni-Grassy-Pocketknife Trend, northeastern BC: Debolt Sikanni field, NE BC;</b> <b>Hosted in 'caprock-destroying' hydrothermal dolomite in Jurassic and Cretaceous limestone reservoirs in 2 zones peripheral to the Gatnia Salt Basin, Saudi Arabia.</b>
M	C	ah	M	rvs-r	500945	5X	<b>Methane-rich fluid plumes derived from prograde metamorphism (especially dewatering at greenschist-amphibolite transition of harzburgitic peridotite complexes.</b>	<b>ALPINE PERIDOTITE TYPE - CALCIC SERPENTINITE-RELATED METHANE PLUMES</b> <b>Central Alpine harzburgitic peridotites?</b>
M	C	ah	N	Rs	500950	5Y	<b>Methane-HC gas-rich fluid plumes derived from hydrous metamorphism at greenschist transition of olivine in harzburgitic portion of mélange wedge. Serpentinization may be accompanied by subsequent cold diapirism (protrusion) of the serpentinite through overlying mélange wedge material.</b>	<b>OPHIOLITE/FOREARC TYPE – CALCIC SERPENTINITE-RELATED METHANE PLUMES</b> <b>Serpentine diapir cores to mounds and seamounts with methane-HC gas in pore space and methane in fluid inclusions from associated carbonate chimneys in the Mariana forearc; serpentinite-hosted oil fields in Cuba (e.g. Jarabucca).</b>
M	AC	an	AN-R	r	1700070	17N	<b>Vanadium-rich (Ti, Fe) spinel (mainly titaniferous magnetite) magmatic segregations within clinopyroxene labradoritic anorthosite differentiates of quartz alkaline, clinopyroxene high-alumina ferronorites and gabbros (leucotroctolite). Compared to similar 34P model, Ti-V rich magnetite is main opaque oxide (contrasted with Ti-rich ilmenite in MQA34P model. Proximal relationship to gabbro-ferrodiorite is more frequent in MAC17N model compared to 34P model. Differentiation may be dominated by laterally pressure-</b>	<b>BUSHVELD (MAIN ZONE) TYPE - ALKALI-CALCIC MAGMATIC IRON-VANADIUM (TITANIUM) OXIDE SEGREGATIONS*</b> <b>Vanadiferous and titaniferous magnetite 'seams' in upper zone of Bushveld complex. Other labradoritic anorthosite massifs: Michigamu and Nain Massifs (e.g. Harp Lake complex), Grenville Province, Quebec-Labrador; Lofoten massif, Norway; Angola massif, Angola. <u>Ferrogabbro-anorthosite</u> hosted: Newboro Lake, Ontario, <u>Magpie</u></b>

Mega Series (alum. cont.) <sup>1</sup>	Series (alkalinity) <sup>2</sup>	Sub-series (H <sub>2</sub> O content)	Mini-series (F-Cl content) <sup>4</sup>	Micr o-series (Oxid. State) <sup>3</sup>	Sort Code <sup>6</sup>	Model Code(*) <sup>7</sup>	Model Description <sup>8,9,10</sup> Nanoseries (Emplacement Level/Tectonic Setting)	DEPOSIT TYPE/ZONE - MAGMA METAL SERIES MODEL (*) <sup>11</sup> ; Examples <sup>12</sup> MODEL TERMINOLOGY OF OTHER WORKERS <sup>13</sup>
							driven flow differentiation (unmixing) under non-equilibrium conditions. Formation of compositional layers is due to liquid-liquid fractionation induced by flow differentiation followed by within-layer, gravity-driven, crystal-liquid settling/fractionation.	<u>Mtn., St. Charles, Lac Dore, Quebec; Kiglapait, Labrador; Smaalands-Taberg, Sweden; Kachkanar and Kusinkoye, former U.S.S.R.; San Gabriel and Orocopia (San Gabriel Complex), CA; Iron Mtn., WY; titaniferous lunar anorthosites.</u>  <b>MAGMATIC VANADIUM; TABERG TYPE, GABBRO ANORTHOSITE-HOSTED IRON-TITANIUM; MAGMATIC-MAFIC, FE THOLEIITE IRON-VANADIUM-TITANIUM</b>
M	AC	h	N	os	3100400	31D	Epithermal, Fe (polymetallic, Sc,Y,F,P) fluorapatite veins, massive replacement, or immiscible oxide magma (IOS) associated with hypabyssal, oxidized, alkali-calcic, quartz latites (Kiruna/Pea Ridge type). Stage 3 in MACHos serial sequence. Similar to MAC27H model, but lacks fluorite and barite. Unlike similar style IOS magnetite deposits of MC7H model, 31D model contains fluorapatite (rather than chlorapatite) and is associated with K-rich quartz latitic rhyolitic volcanism (rather than low-K diorites).  Associated with alkali-calcic portion of hydrous magmatic arcs emplaced into tectonically mature, oxidized crust in compressive/transpressive tectonic settings.	<b>KIRUNA TYPE - ALKALI-CALCIC IMMISCIBLE IRON OXIDE (FLUORAPATITE,SCANDIUM,Y</b>  <b>Intrusive magma/replacements: <u>Cerro Mercado, Sierra Encinillas, and La Perla, and El Volcan, Mex.;</u> El Carmen, Chile; <u>Kiruna</u> (Henry, Rektorn, Kirunavoara, Luossavaara, Haukivaara, and Nukutusvaara), Sweden; Modarelli, NV; Pea Ridge, MO; Aunik (Bingol), SE Turkey; Bafq, Mishdovan, Chador Malu, Zaragan, and Kushk, central Iran. Glacier Lake?, Contact Lake? Terra?, Blanchet Island? Labelle Peninsula?, and Regina Bay?, NWT  Magnetite-apatite flows: El Laco, Magnetita Pederrales?, El Carmen, and Hermitita?, Chile <b>KIRUNA TYPE, PEA RIDGE TYPE, VOLCANIC-HOSTED MAGNETITE; IRON OXIDE BRECCIAS AND VEINS; OLYMPIC DAM TYPE</b></b>
M	QA	h	N	ow	3400600	34A*	Epigenetic and metagenic(?), telethermal, Cu (PGE-Au-Ag-Co-Bi, Pb [Zn], Ni, U, HC), hosted in anoxic marine rocks. Can be associated with extensive Na-Ca propylitic and/or early(?) hematitic (Rotliegendes) alteration. Pb-Zn-Ag zones may be developed distal to Cu-U-PGE (Co, Ni) zones. Methane gas zones may develop in outermost distal zones. May be metagenetically derived(?) from dewatering of Cu-(PGE, Au, U, Co, Bi, Ni, C) rich, weakly oxidized, MQA basement sources (e.g. shoshonitic volcanism in basement	<b>KUPFERSCHIEFER TYPE - QUARTZ ALKALIC BLACK SHALE-SILTSTONE HOSTED COPPER-PGE (GOLD-SILVER-COBALT-BISMUTH)*</b>  Copper portion: <u>Lubin (Kupferschiefer), Poland; Blackbird?, ID; Tar Sands?, Alberta; Redstone, NWT; White Pine?, MI; Creta?, OK; upper Windsor Group, Nova Scotia, New Brunswick; Lady Annie?, Mt Isa (Cu)?, N. Australia; Redstone, June Creek, and Hottah Lake, NWT; Lochaber Lake, Nova Scotia; Seal Lake area,</u>

Mega Series (alum. cont.) <sup>1</sup>	Series (alkalinity) <sup>2</sup>	Sub-series (H <sub>2</sub> O content)	Mini-series (F-Cl content) <sup>4</sup>	Micr o-series (Oxid. State) <sup>3</sup>	Sort Code <sup>6</sup>	Model Code(*) <sup>7</sup>	Model Description <sup>8,9,10</sup> Nanoseries (Emplacement Level/Tectonic Setting)	DEPOSIT TYPE/ZONE - MAGMA METAL SERIES MODEL (*) <sup>11</sup> ; Examples <sup>12</sup> MODEL TERMINOLOGY OF OTHER WORKERS <sup>13</sup>
					3400600 .2	34A.2	beneath Lubin) and Eastern Creek shoshonitic volcanics in basement beneath Mt. Isa, and Keweenaw high-K volcanics in basement beneath Black Pine), which have experienced greenschist/ amphibolitic facies metamorphism). Compared to similar 39 – Zambian type red bed copper model, Kupferschiefer type is suggested to be related to ascending hydrothermal fluids metagenically derived from underlying shoshonitic, MQA volcanic terranes in basement beneath typically reduced silici-clastic cover sequences. In contrast, Zambian type is envisioned to be deposited from descending meteoric waters utilizing permeability and oxidized continental red bed sequences and may be derived from surficial MQA basaltic sources lateral to the red bed sandstone facies.	Labrador; Kurpandzha, eastern Russia.  Pb-Zn-Ag distal(?) to Cu: Lady Loretta, Mount Isa (Pb)?, N. Australia; copper occurrences in the Pictou Group (e.g. Canfield, Oliver, Limerock, McClellan Brook, Rights River, Yankee Line Road, and Frenchvale), Nova Scotia; Lubin NE and Rudna SE at Lubin, Poland.  With hydrothermal hydrocarbon product(s): Lubin, Poland; extensive gas deposits upsection from Lubin, Poland, may have been produced by hydrocarbon synthesis during deposition of underlying Lubin deposits (especially the PGE component).  SEDIMENT-HOSTED STRATIFORM COPPER, KUPFERSCHIEFER TYPE; AGUA-REDOX (SUBHYDROTHERMAL) COPPER?; SEDIMENT-HOSTED COPPER
M?	AC?		N-R?	R-o	3400500  3400500 .1	34B  34B.1	Epigenetic and metagenic(?), Pb-Zn (Cu, Cd), +/- F, Ba, Co, Ni, Mg, Sr, HC, telethermal, replacements commonly in karstic, lower Paleozoic carbonate/clastic sequences (Mississippi Valley Type or MVT). Metals were released? from underlying?, rapakivine?, metaluminous?, peraluminous?, and alkalic-calcic?, granitoid? basement as metagenic fluids generated by dewatering at chlorite-stable greenschist-amphibolite facies metamorphism during crustal thickening episodes related to late collisional orogenic events. Low silver contents distinguish MVT type from all other MAC and PAC Pb-Zn-Ag-bearing models (except for similar 25GG model). Zn-Fe-rich character (relative to silver and, to a lesser extent, lead) may be related to selective release of Zn and Fe from destabilization of greenschist facies minerals (e.g. chlorite) in contrast to feldspar (a lead-silver sink), which is stable across most steps in metamorphic grade. Low silver content makes MVT model less economic compared to other giant sized Pb-Zn-Ag models, such as the 24, 24D, 24J, and 25 models. These models typically are	MISSISSIPPI VALLEY TYPE - ALKALI-CALCIC LEAD-ZINC TELETHERMAL REPLACEMENTS (MVT)* Stratabound replacements: Tri-state (Joplin, MO; Baxter, KS); Rosiclaire, IL); Racine, WI; Galena (Missouri Lead), MO; Gayna River and Pine Point, NWT; Irish lead-zinc deposits (Navan, Silver Mines, and Tynagh)?; Upper Silesia Zn-Pb deposits (Boleslaw, Pomorzony, and Trezbionka), Poland; <u>Polaris</u> , NWT; Robb Lake, BC; Nanisivik, Baffin Island; Gays River, Quebec; Newfoundland Zinc, NF; <u>East Tennessee</u> (Mascot-Jefferson City, Copper Ridge, Sweetwater areas), <u>central Tennessee</u> ; Hansonburg, NM; Mibladen?, Morocco; Bov Beker-El Abed, Morocco-Algeria; Wagon Pass, Twelve Mile Bore, Cadjebut, and Blendevalle, NW Australia; Coxco, Cooley and Ridge, HVC? (McArthur River), N. Australia; Pearyland, Greenland; Dairi?, Sumatra; San Vicente, Central Peru; Timberville, VA; Freidensville, PA; Nitalany Arch, PA; Shawangunk, NY.

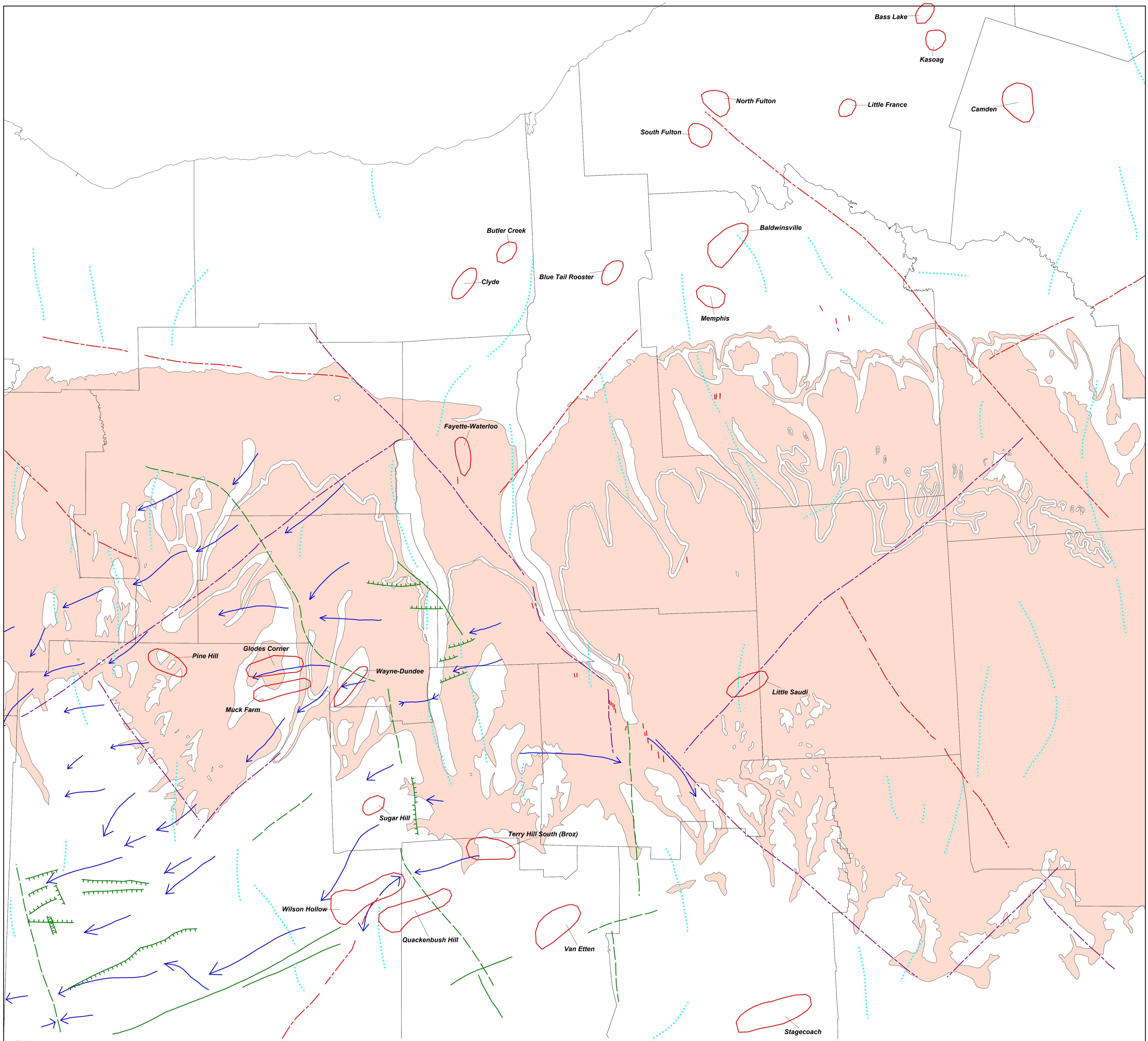
Mega Series (alum. cont.) <sup>1</sup>	Series (alkalinity) <sup>2</sup>	Sub-series (H <sub>2</sub> O content)	Mini-series (F-Cl content) <sup>4</sup>	Micr o-series (Oxid. State) <sup>3</sup>	Sort Code <sup>6</sup>	Model Code(*) <sup>7</sup>	Model Description <sup>8,9,10</sup> Nanoseries (Emplacement Level/Tectonic Setting)	DEPOSIT TYPE/ZONE - MAGMA METAL SERIES MODEL (*) <sup>11</sup> ; Examples <sup>12</sup> MODEL TERMINOLOGY OF OTHER WORKERS <sup>13</sup>
					3400500 .2 3400500 .3	34B.2 34B.3	associated with higher temperature, intrusive-related carbonate replacements. All deposits contain an early phase of low-temperature (mainly 100-200 degrees C) hydrothermal, rhombic, saddle, or baroque dolomite. 12% decrease in volume during early dolomitization may enhance permeability and induce locally extensive hydrothermal 'karst'. Deposit type shares many similarities with hydrothermal dolomite-hosted oil and/or gas deposits (e.g. Railroad Valley, NV of the 45M model, and Gloades Corner, Steuben County, NY of the 5P model), implying similar processes of formation.	Veins: Navarana Fjord Zn-Ba (Pb-F) deposit, north Greenland With hydrothermal humate/ hydrocarbon (HC) product(s): methane in East Tennessee, Timberville, VA and Gays River, Nova Scotia; humates in the Upper Silesian Pb-Zn deposits, Poland; San Vicente (pyrobitumen and extrinsic HC), central Peru; Navarana Fjord (bitumen), north Greenland.  MISSISSIPPI VALLEY TYPE (MVT); HYDRO-MESOTHERMAL LEAD-ZINC; SE MISSOURI LEAD-ZINC
M?	AC?		N-R?	r-o	3400510	34BA	High temperature, mesothermal, early 'rhombic' dolomitization of footwall carbonates. Predates Pb-Zn sulfide deposition of 34B model.	SOUTHEAST MISSOURI ZONE of the MISSISSIPPI VALLEY TYPE - EARLY RHOMBIC DOLOMITIZATION of FOOTWALL CARBONATES within the MISSISSIPPI VALLEY TYPE All deposits in 34B model (see above).
M	QA	an	AN-R		3400700 .1 3400700 .2 3400700 .3	34P* 34P.1 34P.2 34P.3	Magmatic, Ti-Fe-V(P, U, Co, S), immiscible oxide segregates (IOS) (ilmenite-apatite magma), in and near the base of ferro syenogabbro-diorite (jotunite) intrusions, and as dike-like bodies in or near massif-type katazonal to mesozonal, hypersthene andesine anorthosite bodies or rutile-apatite dikes (nelsonite) in or adjacent to andesine anorthosites. Compared to similar 17N model, principal oxide mineral is ilmenite, compared to vanadiferous, titaniferous magnetite in MAC 17N model.  Differentiation is dominated by laterally pressure-driven flow differentiation (unmixing) under non-equilibrium conditions. Formation of compositional layers is due to liquid-liquid fractionation induced by flow differentiation followed by within layer, gravity-driven, crystal-liquid/settling/fractionation.	ALLARD LAKE TYPE - QUARTZ-ALKALIC ANDESINE ANORTHOSITE-RELATED IMMISCIBLE TITANIUM-IRON-VANADIUM-APATITE MAGMA* Immiscible oxide segregates in anorthosite : <u>Lake Sanford</u> , NY; <u>Allard Lake</u> (Lac Tio); Degrosbois Lac des Pins Rouges, Ivry, (Morin anorthosite) and St. Urbain, Que.; <u>Egersund</u> (Tellnes, Storgangen, Bjafjell, <u>Aana-Sira</u> ) and Lofoten, Norway; Kunene, Namibia-Angola; Ilmen Mountains, former U.S.S.R.; Nelsonite dikes: Roseland, VA Nelsonite segregations: Labrieville and St. Urbaine Quebec; Bogidenskoe, Gayumskoe, Maimkanskoe, and Dzhanskoe, Far Eastern Russia. ANORTHOSITE TITANIUM; MAFIC INTRUSIVE-HOSTED TITANIUM IRON; ALLARD TYPE; MAGMATIC-MAFIC, IRON THOLEIITE TITANIUM; ANORTHOSITE APATITE Ti-P; MAGMATIC FR-TI±V



Mega Series (alum. cont.) <sup>1</sup>	Series (alkalinity) <sup>2</sup>	Sub-series (H <sub>2</sub> O content)	Mini-series (F-Cl content) <sup>4</sup>	Micr o-series (Oxid. State) <sup>3</sup>	Sort Code <sup>6</sup>	Model Code(*) <sup>7</sup>	Model Description <sup>8,9,10</sup> Nanoseries (Emplacement Level/Tectonic Setting)	DEPOSIT TYPE/ZONE - MAGMA METAL SERIES MODEL (*) <sup>11</sup> ; Examples <sup>12</sup> MODEL TERMINOLOGY OF OTHER WORKERS <sup>13</sup>
								<b>OXIDES DEPOSITS</b>
M	QA	h	N	os	3900000	39*	Epithermal, Cu-Ag(Au, As, Na-Ca) deposits in oxidized trachybasalts (commonly native Cu in amygdule spaces). 1st? stage in hypabyssal MQAhos serial sequence. Shoshonitic host rock-specularite-copper 'oxide' assemblage distinguishes 39A, 39, and 36 model from all other models. Associated with trachybasalt shoshonitic volcanism and syenodioritic hypabyssal intrusions in quartz alkalic portions of transpressive arcs or transtensional cratonic or rift volcanism emplaced into deep-seated, strike slip faults within tectonically mature, oxidized to strongly oxidized crust.	<b>KEWEENAW TYPE - QUARTZ ALKALIC EPITHERMAL NATIVE COPPER (SILVER) VEINS and AMYGDULE FILLINGS*</b>  <u>Keweenaw</u> Peninsula basalt (conglomerate) copper deposits (Mohawk, Baltic, Isle Royal, Allouez, Pewabic, Kingston, Mt. Bohemia, Kearsarge, Osceola, Calumet-Hecha), MI; Karmutsen basalts (Vancouver Island), Nicola Basalts, Purcell basalts, Natkusiak basalt (Victoria Island), Hazelton-Takla basalts, and Sustut, BC; La Colorada, AZ; Coppermine River, (Copper Lamb, Jack Lake, Coppercorp, 47 zone, and Mamainse Point) NWT; Sierra Ancha basalts, AZ; Boyer (Table Mtn.), NV; White River, Yukon; Northstar, BC; Cu (Ag) deposits in Jurassic La Quinta Formation (Sebuco-El Cobre, Cano Tigre, El Rincon, and El Tuto Casacajales), Columbia-Venezuela <b>KEWEENAW TYPE COPPER; VOLCANIC REDBED COPPER; BASALTIC COPPER; METAMORPHIC-HYDROTHERMAL COPPER</b>
M	QA	h	N	o-os	3900100  3900100 .1  3900100 .2	39A  39A.1  39A.2	Epithermal, Cu-Ag-Fe (as specularite) deposits in or near quartz alkalic, mafic dikes or mantos in oxidized, mafic/intermediate, high-potassium, shoshonitic volcanics. 2 <sup>nd</sup> stage in hypabyssal, MQAho serial sequence. Chlorite-albite alteration is common. Lack potassium metasomatism compared to similar-appearing volcanic-hosted mantos of Candelaria type MQA44J model. Shoshonitic host rock-specularite-copper 'oxide' assemblage distinguishes 39A, 39, and 36 model from all other models. Associated with trachybasalt shoshonitic volcanism and syenodioritic hypabyssal intrusions in quartz alkalic portions of transpressive arcs or transtensional cratonic rift volcanism emplaced into tectonically mature, oxidized to strongly oxidized crust.	<b>KENNECOTT TYPE (VEINS) and MANTOS BLANCOS TYPE (MANTOS) - QUARTZ ALKALIC EPITHERMAL COPPER-SILVER SPECULARITE MANTOS, VEINS, and FRACTURE FILLS</b>  Mantos: Matamoros, El Grullo, and Jimulco?, Mex.; Bueno Esperanza, Santo Domingo, and Mantos Blancos, Ivan, Sierra de Valenzuela, Sierra del Ancha, Mantos de la Luna, Michilla, northern Chile; Abbas-Abad?, Iran; Bleida, Morroco; Northstar, BC  Veins and Fracture Fills: Kennecott (Erie, Jumbo, Bonanza, Mother Lode, Green Butte, Westover), AK; Humo SE Jecacahui, Guadalupana?, Santo Nino, NW

Mega Series (alum. cont.) <sup>1</sup>	Series (alkalinity) <sup>2</sup>	Sub-series (H <sub>2</sub> O content)	Mini-series (F-Cl content) <sup>4</sup>	Micr o-series (Oxid. State) <sup>3</sup>	Sort Code <sup>6</sup>	Model Code(*) <sup>7</sup>	Model Description <sup>8,9,10</sup> Nanoseries (Emplacement Level/Tectonic Setting)	DEPOSIT TYPE/ZONE - MAGMA METAL SERIES MODEL (*) <sup>11</sup> ; Examples <sup>12</sup> MODEL TERMINOLOGY OF OTHER WORKERS <sup>13</sup>
					3900100 .3	39A.3		<b>Mexico; El Barqueno?, and Ayutla?, central Mexico; Lobo Muerto, Estacion Varillas, El Desesperada, Ivan, Emperatariz, Sierra de Valenzuela, Porte Zuelo, Sierra del Ancha, Sierra la Sardena, Michilla, Palmira?, Santo Domingo (Africa), and Caturra?, El Soldado, northern Chile; Great Bear Magmatic Zone (Sue-Dianne); Van Horn (Hazel, Black Shaft, Sancho Panza, Hackberry, St. Elmo, Mohawk, and Pecos)?, west Texas; Huehuetenango?, Guatemala</b> <b>Near dikes: Ajo Cornelia, Cardigan, Dunns Well, Swansea, Clara, Cleopatra, and Mineral Hill, AZ; San Mateo, Guatemala; Cerro Cobre?, Guatemala.</b> <b>VOLCANIC REDBED COPPER, KENNECOTT TYPE, BASALTIC COPPER; METAMORPHIC-HYDROTHERMAL COPPER</b>
M	QA	h	N	o	3900180	39B	<b>Epigenetic U,V, continental redbed-hosted, 'Red Bed' Cu-Ag-Co-Mn (+/- Cl), distal to MQA basaltic/latitic system volcanics of 39A model or syenodiorite/monzonitic intrusions. 'Roll front' meteoric mechanisms similar to 40E model may also be involved. In the roll front scenario, copper (cobalt-silver) would be leached from oxidized MQA basalt (absarokite) sources up meteoric gradient (and commonly slightly up-stratigraphy) and transported along hydrologic pathways (commonly paleostream channels in fluvatile sandstone sequences) to the red-bed host. Sulfate reduction probably attends deposition of chalcopyrite-pyrite assemblage.</b>  <b>Associated with trachybasalt-shoshonitic volcanism and syenodioritic hypabyssal intrusions in transpressive arcs or transtensional cratonic rift volcanism emplaced into deep-seated, strike-slip faults within tectonically mature, oxidized crust.</b>  Compared to similar 36B – Kupferschiefer type, Zambian type is envisioned to be deposited from descending meteoric waters utilizing permeability and oxidized continental red bed sequences	<b>ZAMBIAN TYPE - QUARTZ ALKALIC EPIGENETIC 'REDBED', SANDSTONE-HOSTED COPPER (SILVER, COBALT) DEPOSITS*</b>  <i>Dzhezkazagan</i> and Chu River; northern Kirgizia and Pzheval, Kazakhstan; <i>Tenke Fungurume</i> , Kanshanshi, Chibuluma, Roan Antelope, Konkola, and <i>Musoshi</i> , Zaire (Zambian 'redbed' Cu belt); Vigas?, Cuehillo Parado, La Vibora?, Miquihuana?, Samalayuca?, northern Mexico; Mt. Gunson, S. Australia; Kalihari Copper Belt (Ngwako Pan, Klein Aub, and Witvlei), Namibia-Botswana; Paoli, OK; Lisbon Valley, Pilot, UT; Nacimiento and Eureka (Cuba), NM; Dorchester, New Brunswick; Firth of Forth, Drumshantie and Larkfield, Great Britain; southern end of Teniz Basin, Russia; Mogollon Rim, AZ; Hot Brook Canyon, WY?; Desbaret, Ontario; Richmond Gulf, Quebec; Rae Group, Green Hills, and Hurwitz group, NWT; Dorchester, Midway, and Goshen, New Brunswick; Searston, Bald Mountain, Boswartos, etc., Newfoundland. Yalaguina(?), Nicaragua <b>SEDIMENT-HOSTED COPPER, KUPFERSCHIEFER TYPE; SEDEX COPPER, SABKHA TYPE COPPER,</b>

Mega Series (alum. cont.) <sup>1</sup>	Series (alkalinity) <sup>2</sup>	Sub-series (H <sub>2</sub> O content)	Mini-series (F-Cl content) <sup>4</sup>	Micro-series (Oxid. State) <sup>3</sup>	Sort Code <sup>6</sup>	Model Code(*) <sup>7</sup>	Model Description <sup>8,9,10</sup> Nanoseries (Emplacement Level/Tectonic Setting)	DEPOSIT TYPE/ZONE - MAGMA METAL SERIES MODEL (*) <sup>11</sup> ; Examples <sup>12</sup> MODEL TERMINOLOGY OF OTHER WORKERS <sup>13</sup>
							and may be derived from surficial MQA basaltic sources lateral to the red bed sandstone facies. In contrast, Kupferschiefer type is suggested to be related to ascending hydrothermal fluids metagenetically derived from underlying shoshonitic, MQA volcanic terranes in basement beneath typically reduced siliciclastic cover sequences.	REDBED COPPER, ZAMBIAN TYPE COPPER; AGUA-REDOX (SUBHYDROTHERMAL) COPPER-COBALT
M	QA	h	r	o	4500400	44L	<p><b>Mesothermal, Cu-U-Au-REE(Ag-F-Co) iron oxide porphyry deposits in or near epizonal, moderate-F, high-K, alkali, rapakivine granites. Stage 3 of MQAhRow-o crystallization sequence.</b></p> <p><b>Associated with mesozonal to epizonal, rapakivine, quartz-alkalic magmatism emplaced in away-from-trench, quartz alkalic portions of transpressive magmatic arcs emplaced into deep-seated, strike-slip fault regimes within reduced, fluorine-rich, tectonically mature, oxidized crust.</b></p>	<p><b>OLYMPIC DAM TYPE - RAPAKIVINE QUARTZ ALKALIC COPPER (URANIUM-GOLD-REE-IRON) PORPHYRIES*</b></p> <p><u>Olympic Dam</u> (Roxby Downs), Prominent Hill (Uranus)?, and Mt. Painter, S. Australia; Carrizallo de las Bambas?, N. Chile; Great Bear Magmatic Zone (Damp, Fab, and Mar)?, NWT KIRUNA-TYPE</p>



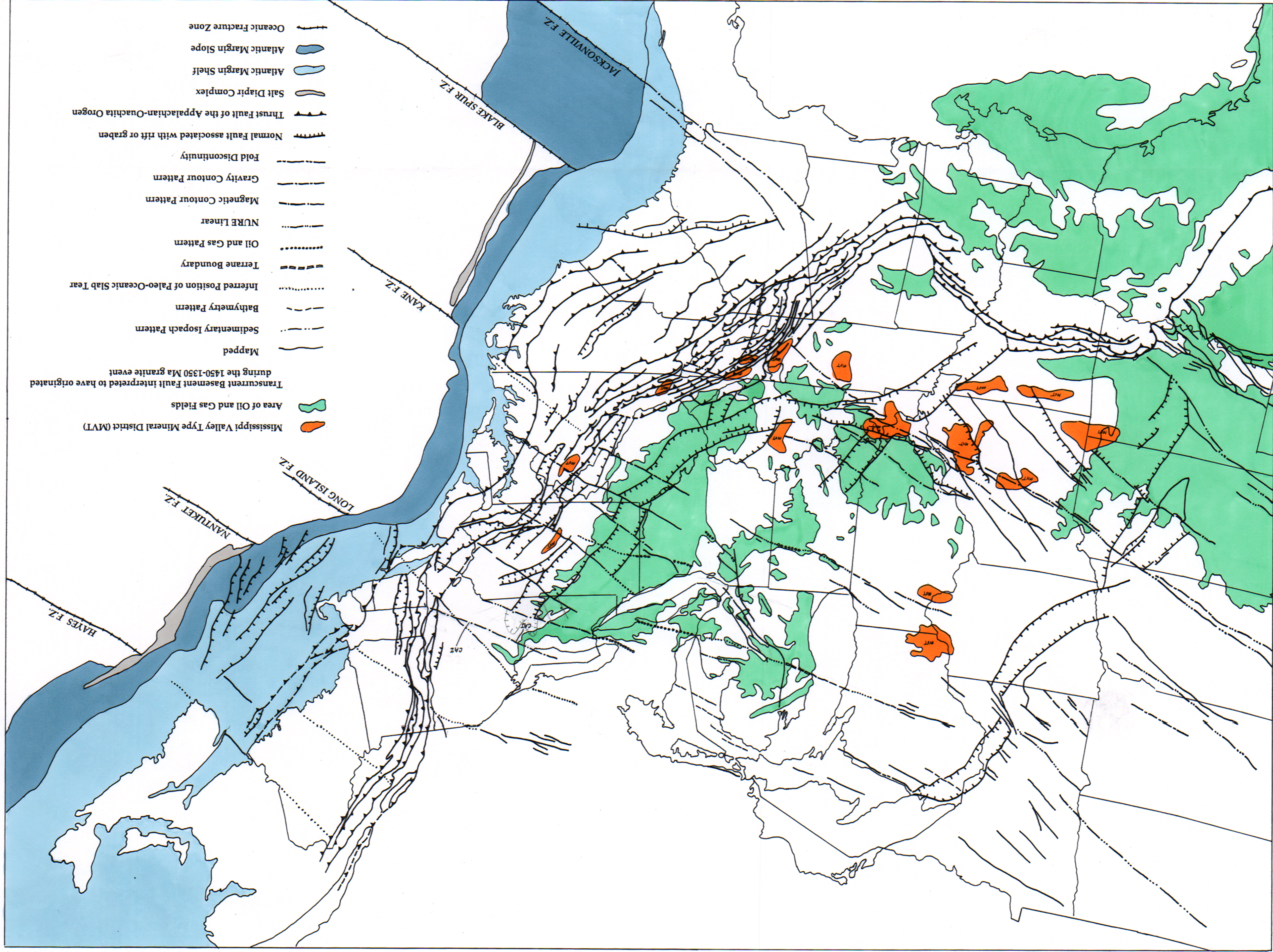
**Structural Interpretation of the Finger Lakes region 1:250,000 scale**

**Explanation**

- |   |                          |   |   |
|---|--------------------------|---|---|
| * Drill Hole (Trenton/Black River test)         | ← Syncline               | ⋯ Potassium Low (trend of elongation)                   | - - - Fault (based on outcrop patterns) |
| ○ Gas Field with Trenton/Black River production | — Ordovician CAI isograd | — Fault (mapped on surface - teeth on downthrown block) | - - - Fault (based on magnetic data)    |
| ■ Middle Devonian Sedimentary rocks             | — Devonian CAI isograd   | - - - Fault (based on subsurface data)                  | — County boundary                       |
| Kimberlite dike                                 | ○ Magnetic High          |   |   |



# Oil and Gas Fields, MVT Mineral Deposits, and 1400 Ma Transcurrent Basement Faults of the Eastern U.S.





# Oil and Gas Fields, MVT Mineral Deposits, and 1400 Ma Transcurrent Basement Faults of the Eastern U.S.

